REFERENCE ONLY

UNIVERSITY OF LONDON THESIS

Degree PhD Year 2006 Name of Author TSCHENKUTTEN, A

Gene Therapy for Retinal Degeneration due to a Defect in the Retinal Pigment Epithelium

Marion Tschernutter

A thesis submitted for the degree of
Doctor of Philosophy
2006

Division of Molecular Therapy
Institute of Ophthalmology
University College London

ProQuest LLC
789 East Eisenhower Parkway
P.O. Box 1346
Ann Arbor, MI 48106-1346

Abstract

The Royal College of Surgeons (RCS) rat is a well characterised model of autosomal recessive retinitis pigmentosa (RP) due to a defect in the retinal pigment epithelium (RPE). It is homozygous for a null mutation in the gene encoding *Mertk*, a receptor tyrosine kinase found in RPE cells, which is required for phagocytosis of shed photoreceptor outer segments. The absence of *Mertk* results in accumulation of outer segment debris. This subsequently leads to progressive loss of photoreceptor cells. Recently, *MERTK* has been established as a human retinal dystrophy gene. Retinal dystrophies are the most common cause of visual impairment in the Western World, for which no effective treatment exists.

In order to evaluate the efficacy of virus mediated gene replacement therapy in the RCS rat, we produced recombinant adeno-associated viruses (AAV) and lentiviruses containing murine *Mertk* cDNA. Vectors were subretinally injected into the right eye of 10 day old RCS rats; the left eye was left untreated as an internal control. Animals were examined at various time points by light and electron microscopy, electroretinography, and ophthalmoscopy. A detailed assessment of the duration and extent of the morphological rescue and the resulting functional benefits is presented in this thesis.

AAV-2-mediated gene therapy resulted in preservation of retinal function for more than 9 weeks, when there is no activity in untreated eyes. Photoreceptors were still present at this time point and debris layer thickness was reduced. After subretinal delivery of human immunodeficiency virus type 1 (HIV-1) based lentiviral vectors carrying a functional copy of *Mertk* to the RCS rat eye, correction of the phagocytic defect, slowing of photoreceptor cell loss and preservation of retinal function was observed for up to 7 months, the latest time point evaluated. Whilst this was an improvement of the rescue compared to that achieved with AAV-2, lentiviral vectors raise more safety concerns regarding clinical application. Due to these biosafety issues, gene therapy vectors based on non-human lentiviruses and integration-deficient vectors have been

developed. As part of this project, the potential of equine infectious anemia virus (EIAV) and non-integrating HIV-1-based vectors for the management of retinal degenerative disorders has been evaluated. The results presented in this thesis support the use of viral vectors for the treatment of retinal dystrophies. However, the development of an efficient therapy depends on the identification of patients and characterisation of pathological changes. Therefore, a panel of DNA samples from patients with autosomal recessive and sporadic forms of RP was screened for mutations in the *MERTK* gene. A new homozygous frame-shifting deletion was identified in four affected members of a family with RP. Clinical examination of these patients showed distinctive clinical signs that may improve the chances of identifying further patients and families in the future.

Table of contents

Figures

Tables

Acknowledgements

I would like to thank Robin Ali for giving me the opportunity to do my PhD in his group as well as for his encouragement, enthusiasm and support during the last four years. My thanks go to Sander Smith for all his advice and his help with cloning; Jim Bainbridge for the injections; Frank Schlichtenbrede for his help with ERGs; Peter Munro and Robin Howes for teaching me everything about histology; Naushin Waseem for answering all my questions and for her help with the patient screen; Andrew Webster for the clinical examinations. I am also grateful to everyone else in the group, especially Cathryn for her aid and all those kind words.

Von ganzem Herzen möchte ich mich bei meinen Eltern, Großeltern und Geschwistern für all ihre Hilfe und Unterstützung bedanken. Ein großes Danke auch an meine Freunde, die mir trotz der Entfernung immer unterstützend zur Seite gestanden sind. Besonderer Dank gilt Martina und Conny für ihre zahlreichen Ratschläge und ihre ausdauernde Hilfe.

Τάσο, δεν ξέρω από που να πρωταρχίσω να σε ευχαριστώ. Για να μην το παρατραβώ λοιπόν απλά, σ' ευχαριστώ από καρδιάς για τα πάντα.

Danke

1

1 Introduction

Gene technology is one of the key technologies of the 21st century and it will soon have an influence on virtually all sectors of our lives. Basic research in biomedical sciences has already been revolutionised. In particular the vast potential of gene therapy is prized because it establishes a promising tool for the development of new and effective treatment strategies for numerous, so far incurable diseases, such as cancer, different infectious diseases, inherited disorders of the nervous system, or inherited retinal degenerations. It may be possible, in near future, to use gene therapy to treat various diseases whose genetic defects have been identified. However, the capacity and efficiency for gene therapy in the treatment of ocular diseases has just recently been explored.

Since we perceive approximately 85 % of information about our environment with our eyes, the human eye can be regarded as our major sense organ by far. Inherited retina degenerations are one of the most common causes of blindness in the western world, for which currently no efficient therapy exists. The best characterised form of inherited retinal degenerations is retinitis pigmentosa (RP) with prevalence up to 1:3500 [1]. So far many genes responsible for inherited eye disorders expressed within the retina have been identified, a pre-requisite for the development of efficient therapies. Furthermore, diseases of the eye are prime candidates for gene therapy approaches because the eye has the advantage of being highly accessible with altered immunological properties, important considerations for easy delivery of virus and avoidance of systemic

immune responses (for more details on immunological properties and the eye as a target for gene therapy see chapters 1.3.4.1 and 1.3.4.2).

1.1 The eye

1.1.1 Eye development

The eyes of all vertebrates develop in a pattern which produces an inverted retina, in which the photoreceptor cells are orientated in a way that their sensory ends, the outer segments, are directed away from incident light. The differentiation of the retina during development reflects the close interaction between two cell types: the photoreceptor cells and the retinal pigment epithelium (RPE) cells. Both cell types are alternately dependent on each other during different developmental stages, for example, they provide each other with different survival, growth and differentiation factors. This close interaction is not only seen during development but also in the adult eye. Retinal physiology and morphology depends on the close interaction and communication of these two cell types and involves complex, cellular signaling pathways, the most important of which will be discussed in more details in the following chapters.

Embryonically, the vertebrate eye develops from an outgrowth of the developing brain, the optic vesicle, which invaginates into the optic cup (see [2] for a review). It is derived from three types of embryonic tissue: the neural tube (neuroectoderm), from which arise the neuroretina and the RPE; the mesoderm, which produces the corneoscleral and uveal tunics; and the surface ectoderm, from which the lens is derived. In the optic cup the RPE gets thinner, while the neural retina thickens into a multicellular epithelium due to its high proliferation rate. The rim regions develop at a slow proliferation rate into the iris and the ciliary epithelium of the ciliary body. Furthermore, it has been known since the beginning of this century, that tissues surrounding the optic vesicle are crucial

for the eye development. Whilst the developing RPE lies next to the extraocular mesenchyme, the neural retina forms from the distal portion of the optic vesicle. During development there is an active signalling between the ectoderm adjacent to the distal part of the eye that promotes the neural retina fate [3]. Members of the fibroblast growth factor (FGF) family [8, 9] and activation of the mitogen-activated protein (MAP) kinase signalling pathway [10] have been shown to be involved in this signal cascade. Retinal cell types are generated in un-equivalent manner in all vertebrates. Cone, ganglion, amacrine and horizontal cells arise before bipolar, rod and Müller cells [11]. The ciliary epithelium and the iris derive from the rim region of the optic cup [12]. Recently it has also been suggested that the RPE and other cell types within the retina might be a source of retinal regeneration.

1.1.2 Anatomy and physiology of the mammalian eye

The vertebrate eye is designed to focus light onto specialised receptors that respond to light and therefore provides the ability to interact with the environment. A schematic overview of the human eye as an example for mammalian eye anatomy is shown in figure 1.1.

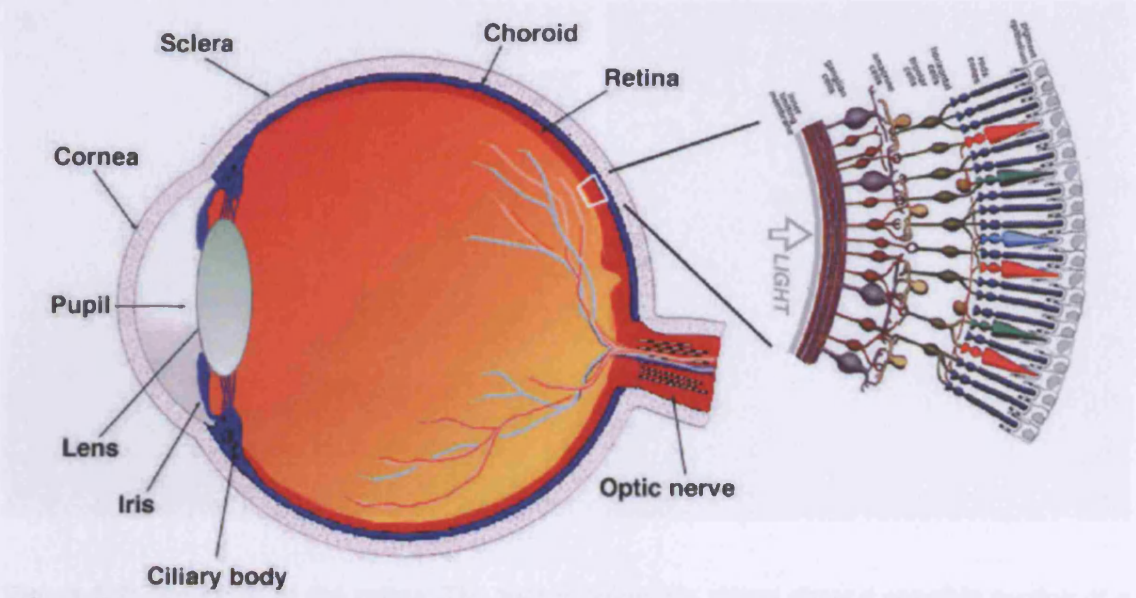

Figure 1.1: Anatomy of the human eye. A schematically cross-sectional view of a human eye (left of figure) shows that it is composed of three different layers: the outer layer consists of the sclera, and the cornea (white); the middle, vascular layer called uvea (blue), which itself is divided into the choroid, the ciliary body and the iris; and the inner neuronal layer (red) including the retina. The cellular organisation of the retina is projected to the right showing inter-retinal connections of different cell types involved in the first steps of light perception. (http://webvision.med.utah.edu)

The retina is the innermost layer of the eye. The retina can be divided into two areas, the neuroretina, which includes the photoreceptor cells as well as other retinal neurons and the RPE. The neuroretina itself is composed of ten layers, which are shown in figure 1.2 (A).

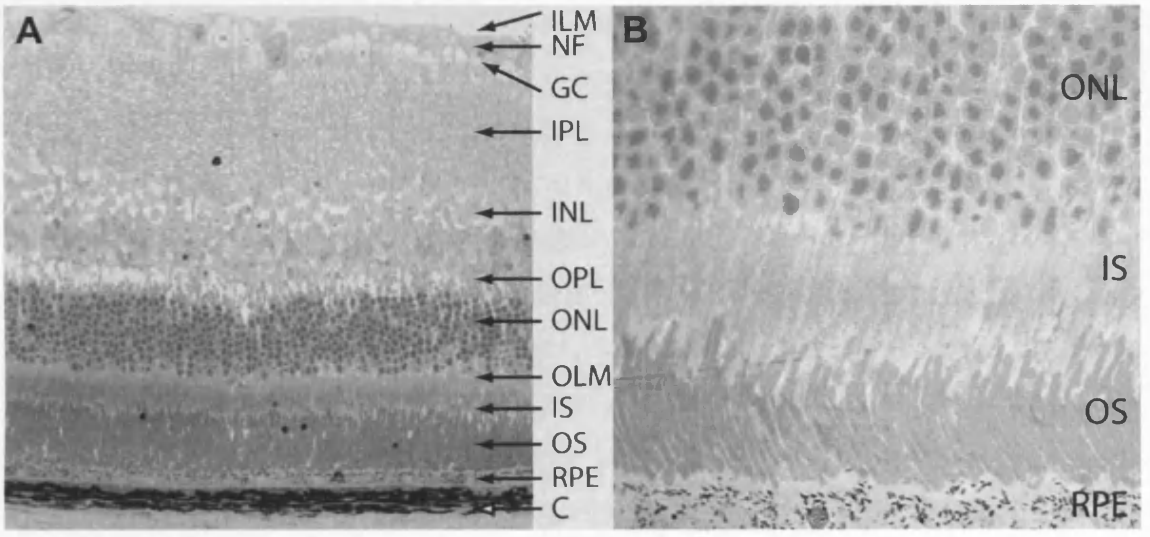

Figure 1.2: Structure of the retina. The light micrographs above show a semithin section of a mouse retina. **(A)** Outside the retina lies the vascular choroid (= C), which connects the outer retina with the vascular system. **(B)** The picture on the right was taken at higher magnification to give a closer view of cell types, namely photoreceptor and RPE cells, involved in the initial processes of vision such as the visual cascade.

Retinal layers:

- Retinal pigment epithelium (RPE), a pigmented monolayer, basally attached to the Bruch's membrane and appically surrounding photoreceptor outer segments
- Layer of photoreceptor outer segments (OS)
- Layer of photoreceptor inner segments (IS)
- Outer limiting membrane (OLM) which gives structural support to photoreceptor cells as well as it forms a barrier
- Outer nuclear layer (ONL) consisting of nuclei and cell bodies of photoreceptors
- Outer plexiform layer (OPL) which contains the synaptic connections between photoreceptor cells and nerve cells
- Inner nuclear layer (INL) which is composed of the nuclei of nerve and support cells
- Inner plexiform layer (IPL) which is build up of synapses of nerve cells
- Ganglion cell layer (GC) consisting of ganglion cells
- Nerve fibre layer (NF) which is composed of the axons of the ganglion cells and astrocytes
- Internal limiting membrane (ILM) which forms the border between the retina and the vitreous.

1.1.3 The neuroretina

The differing sensory demands of using light to detect environmental space and time appear to have provided the selection pressure for the evolution of different photoreceptor systems in the vertebrates. Photoreceptor cells exist as two different types, the rods and the cones, which share the same basic structure (figure 1.3) and are one of the most highly metabolic cell types in the body. All photoreceptor cells have light-sensitive pigments in their membranes, which after the absorption of a photon change their structure and thereby initialise the phototransduction cascade (see chapter 1.1.4).

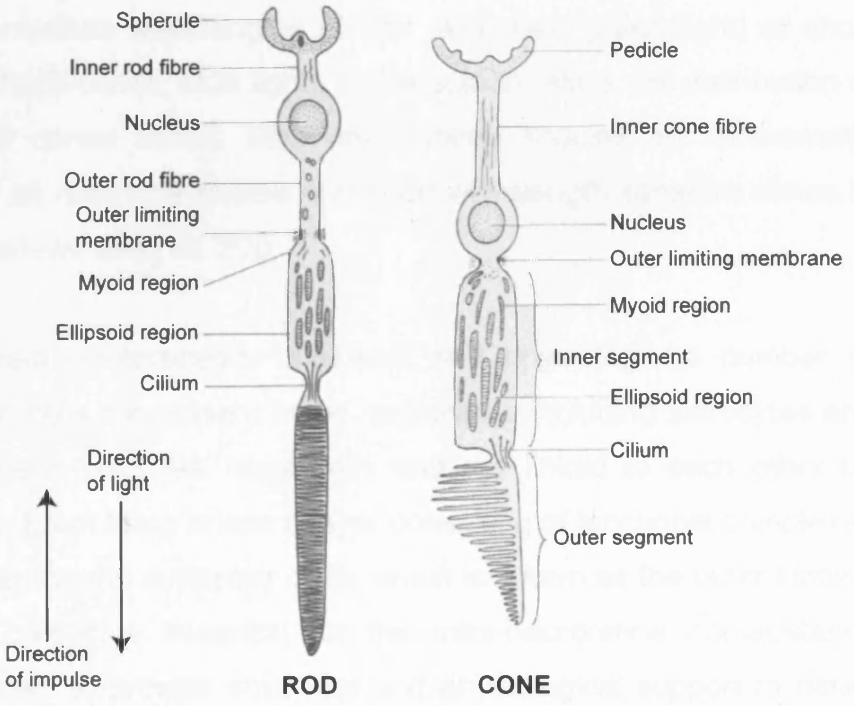

Figure 1.3: Structure of photoreceptors. Although generally similar in structure, rods and cones differ in their size and shape, as well as in the arrangement of the membranous discs in their outer segments.

The light sensitive structures of the photoreceptors are the outer segments, that lie in the inter-photoreceptor matrix (IPM) between the apical microvilli of the RPE cells. Rod outer segments contain a dense network of membranes, the discs, which are formed constantly and act to enlarge the sensory surface. Incorporated into the disc membrane is the light sensitive pigment rhodopsin. The cilium connects the outer segment with the inner segment which contains a large number of mitochondria. The synapses hold vesicles, which distribute neurotransmitters after light excitement of the photopigment, thereby passing the signal on to associated nerve cells. The rod system has a low spatial resolution but is extremely sensitive to light; it is therefore specialised for sensitivity at the expense of resolution. In contrast, the cone system has a high spatial resolution but is relatively insensitive to light; it is therefore specialised for acuity at the expense of sensitivity. In cones, discs are infolds of the cell membrane and do not form free discs as they do in rods. Cones contain cone opsins as their visual pigments and, depending on the exact structure of the opsin molecule, are maximally sensitive to either long wavelengths of light (L-cones, red light), medium wavelengths of light (M-cones, green light) or short wavelengths of light (S-cones, blue light). In the human retina, the distribution of spectrally different cones varies. Most mammalian species are dichromatic containing as well as rods only middle and short wavelength sensitive cones in their retinae (for reviews see [19, 20]).

In order to maintain photoreceptor structure and physiology, a number of different supporting cells are present in the neuroretina including astrocytes and Müller's cells. Müller's cells are large cells that are linked to each other by adherent junctions. From them arises a layer consisting of junctional complexes between photoreceptor and supporter cells, which is known as the outer limiting membrane. This barrier is essential for the intra-neuroretina homeostasis. Astrocytes are known to provide structural and physiological support to nerve cells throughout the nervous system [21]. Furthermore, there are several classes of neuronal cells in the retina which are responsible to modulate and forward the signal received from photoreceptor cells.

After light excitement of photoreceptors, the signal is first passed on to bipolar cells, which themselves pass the signal on to ganglion cells. Ganglion cells send their axons from the eye to the brain via the optic nerve. Whereas the above mentioned neuronal cells are directly involved in the visual signaling pathway, horizontal cells, amacrine cells and interplexiform cells on the other hand modulate the passage of impulses on their way from the photoreceptors to the ganglion cells.

The mammalian retina is divided into specialised areas. The axons of the optic nerve exit from the retina in an area called the optic disc where no photoreceptor cells are present and therefore a blind spot in the visual field is produced. Furthermore, the central artery and vein supplying the inner retina exit the retina at the optic disc. In humans and primates, laterally of the optic disc is the macula, which is rich in cones (figure 1.4). The centre of this region – the fovea centralis – consists only of cones. Rods are absent in the fovea but dense elsewhere. In the human retina, there are approximately 120 million rods and 6 to 7 million cones.

Figure 1.4: Distribution of rods and cones in the human retina. In the human retina, cones are concentrated in the macula whereas only few are found outside this region. The fovea is the central area of the macula and consists only of cones. Rod concentration peaks in a submacular ring approximately 20° around the fovea and decreases fast towards the fovea and slowly towards the periphery. Rods are absent in the fovea itself (http://hyperphysics.phy-astr.gsu.edu/hbase/vision/rodcone.html).

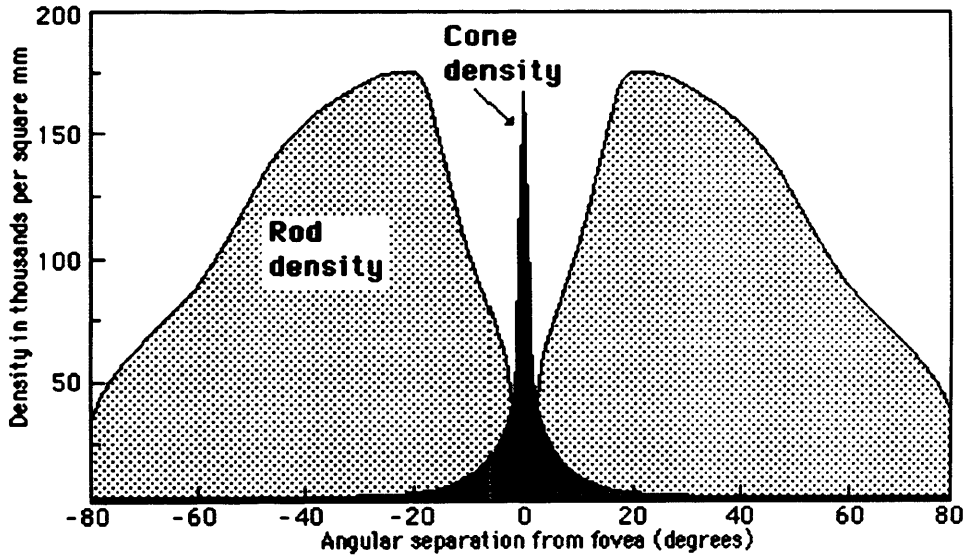

1.1.4 Visual cycle and cascade

Vision is a process triggered by the absorption of photons by photosensitive pigments integrated into the membranous photoreceptor outer segment discs. The absorption of a photon results in a conformation change of the photopigment. This conformation change initiates a complex intra-photoreceptor signaling pathway, the phototransduction cascade, which is finally converted and amplified into an electrical response that is passed on to retinal neurons which sent their axons to the brain via the optic nerve.

Unstimulated photoreceptor cells have open cation channels that allow sodium and calcium to enter and potassium ions to exit the cell. The steady influx of sodium ions maintains an electrical membrane potential of -40 mV on the inner cell membrane. At this membrane potential the photoreceptor cell is continually releasing neurotransmitters to bipolar cells. Light stimulates the photoreceptors to trigger a sequence of biochemical events that change this membrane potential and results in a hyperpolarisation of the receptor. Changing the membrane potential reduces the amount of transmitters, that is set free into the postsynaptic space causing the photoreceptor cell to initiate a neural message that is sent to the brain via other neuronal cells of the retina. By this means, the photopigments in rod and cone outer segments transduce light into electrical signals in the visual cascade.

Even though generally similar in structure and physiology, rods and cones differ in their photopigments and enzymes involved in the phototransduction cascade. It has been shown that cones express counterparts of many of the phototransduction enzymes found in rods [36]. It has also been suggested that cones may have an alternative system for generation of their photopigments during the visual cycle [37]. Since rod function is better characterised than cone function, the following description of the phototransduction cascade and the visual cycle will focus on the physiology of rods.

The light absorbing photopigment of rod photoreceptors, rhodopsin, consists of the vitamin A-derived chromophore 11-*cis* retinal, and the protein opsin, which

is inserted into the plasma membranes of the rod outer segments. The phototransduction cascade is initiated when a photon strikes the 11-*cis* retinal. This causes the isomerisation of 11-*cis* retinal to all-*trans* retinal, which leads to a configuration change of the photopigment to metarhodopsin II [23, 24]. Metarhodopsin II is the binding site for regulator proteins such as rhodopsin kinase, arrestin and transducin [25]. Each light-excited photopigment binds several molecules of transducin which results in a 10^2 to 10^3 amplification of the visual cascade (see figure 1.5 for an overview of the visual cycle). Transducin is a member of the guanosine-5'-triphosphate (GTP) binding protein (G protein) family that connect receptors with their second messenger pathway. On interaction with excited photopigment, transducin molecules exchange bound GDP for GTP, forming an active transducin-GTP complex. The transducin-GTP complex on one hand passes a greatly amplified signal on to another protein, cGMP phosphodiesterase (PDE).

During light, active PDE hydrolyses cGMP to 5'-GMP and this results in the closing of cGMP-gated calcium channels. These channels are composed of transmembrane guanylate cyclase proteins (retGC). Their activity is regulated by calcium sensitive guanylyl cyclase activator proteins (GCAPs) [26]. The closing of cGMP-gated calcium channels on one hand interrupts the flow of cations into the cell (reviewed in [27]) and on the other hand causes a hyperpolarisation of the surface membrane along the entire cell. The interruption of the ion flow through the membrane decreases the intracellular calcium concentration. At low calcium levels GCAPs bind to the intracellular domain of retGC and thereby stimulating the resynthesis of cGMP which is used to keep cationic channels open.

During dim light and in the dark, metarhodopsin II is phosphorylated at its C-terminus by protein kinase C, which decreases the affinity of metarhodopsin II to transducin while it increases the affinity to another protein, arrestin. Arrestin prevents further interactions between metarhodopsin II and transducin completely. The inactivated photopigment exchanges all-*trans* retinal to 11-*cis* retinal and releases arrestin. All-*trans* retinal enters the visual cycle to be resynthesised to its photosensitive isoform, 11-*cis* retinal. The synthesis and

recovery of 11-cis retinal during the visual cycle is important to maintain sensitivity of the visual system. The visual cycle takes place within photoreceptor and RPE cells and the recovered rhodopsin starts the visual cascade again after light stimulation (see [28, 29] for reviews).

The supply of retinoids to the photoreceptors is one of the crucial steps for retinal physiology. Retinoids are supplied as vitamin A (all-*trans* retinol), which is taken up from food in the small intestine by cellular retinol-binding protein 2 (CRBP2) and delivered by serum retinol-binding protein (SRBP, RBP4) to the target cells via a specific surface receptor. All-*trans* retinol is then bound to the intracellular transporter protein CRBP1. In the RPE cell, all-*trans* retinol is esterifyed to form retinyl ester by lecithin-retinol acyltransferase (LRAT). The all-*trans* retinyl ester is converted to 11-*cis* retinyl ester by the isomerohydrolase RPE65 [30, 31]. In this form vitamin A is stored within the RPE cells. In further steps the 11-*cis* retinyl ester is converted into 11-*cis* retinal which is oxidised by 11-*cis* retinal dehydrogenase (RDH) to its aldehyde. In RPE cells, 11-*cis* retinal is carried by cellular retinaldehyde-binding protein (CRALBP). In order to cross the subretinal space, 11-*cis* retinal is bound to interphotoreceptor retinoid-binding protein (IRBP) and transported to photoreceptors. There it is bound to the photopigment apoprotein in the membrane of rod outer segments where it forms part of the visual pigment. Photons lead to isomerisation of 11-*cis* retinal to all-*trans* retinal that changes the inactive form of rhodopsin to the active metarhodopsin II form. For recovery of the chromophore, all-*trans* retinal is released from metarhodopsin II to all-*trans* RDH which catalyses the reduction of all-*trans* retinal to all-*trans* retinol using NADPH as a cofactor. All-*trans* retinol is bound to the ATP-binding cassette transporter ABCA4 and transported through the cell membrane to the interphotoreceptor matrix [32]. There it is picked up by IRBP, which shuttles the chromophore to the RPE cells. In the dark it undergoes isomerisation within the RPE cell to form 11-*cis* retinol [33, 34].

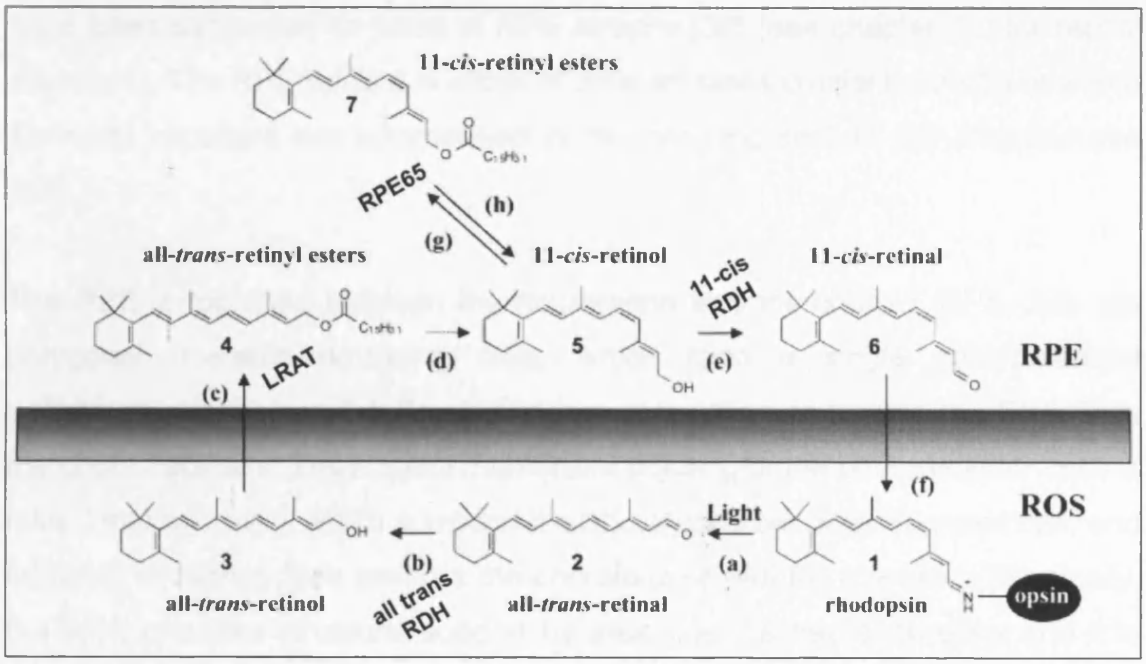

Figure 1.5: Visual cycle. The capture of a photon causes the isomerisation of the chromophore 11-*cis*-retinal to all-*trans*-retinal (reaction a) of the photosensitive pigment rhodopsin in rod outer segment (ROS). All-*trans*-retinal is hydrolysed and reduced to all-*trans*-retinol (reaction b) by all-*trans*-retinal specific dehydrogenases (RDH). The all-*trans*-retinol then diffuses to the RPE where it is esterified to all-*trans*-retinyl esters (reaction c) by LRAT. These esters can be hydrolysed to 11-*cis*-retinol (reaction d). 11-*cis*-retinol is isomerised to 11-*cis*-retinal in a reaction (reaction e) that is catalysed by an isomerohydrolase, the RPE-specific RPE65 protein. 11-*cis*-retinal diffuses across the subretinal space to be incorporated in ROS membranes (reaction f). In the dark, under conditions of low 11-*cis*-retinal utilization, 11-*cis*-retinol can also be esterified to 11-*cis*-retinyl esters by LRAT (reaction g). With insufficient chromophore levels the hydrolysis of 11-*cis*-retinyl esters occurs (reaction h) (picture taken from Kim et *al* [35]).

1.1.5 Retinal pigment epithelium

The physiological events in the eye depend on the cooperation of the neuroretina and the RPE. The importance of this interaction is reflected in different retinal disorders. For example, mutations in the RPE-specific protein RPE65 cause an early onset type of retinal degeneration, known as Leber's congenital amaurosis (LCA), and vice versa, gene defects in photoreceptor-specific genes, such as the peripherin/*rds* gene that is associated with RP,

have been suggested to result in RPE atrophy [38] (see chapter 1.2 for retinal disorders). The RPE fulfils a number of different tasks crucial for vision of which the most important are summarised in the following section (for a review see [39]).

The RPE is localised between the neuroretina and the choroid. RPE cells are polygonal, melanin-containing cells, which form a single cell polarised epithelium attached to the Bruch's membrane, which separates the RPE from the choriocapillaris. Their apical membrane pointing at the photoreceptor cells is folded into microvilli, which surround the photoreceptors outer segment tips, and its basal infoldings face towards the choroid (see [40] for a review). Physically, the RPE provides structural support by attaching the neuronal retina and it is involved in the interphotoreceptor matrix (IPM) production that fills the narrow subretinal space between the RPE and the photoreceptors. The IPM mediates adhesion between the RPE and photoreceptors, RPE phagocytosis and nutrients exchange (reviewed in [41]). It also contains factors important for vision, such as IRBP, FGF-2 and matrix metalloproteases (for example the tissue inhibitor of metalloproteinase 3, TIMP3) [42, 43]. During embryonic development the RPE also provides trophic factors necessary for the correct morphogenesis of the retina (see section 1.1.1). Furthermore, the RPE is known to produce a variety of growth factors necessary for photoreceptor survival and factors for the maintenance of structural integrity of the retina, such as TIMP3. Growth factors secreted by the RPE include ciliary neurotrophic factor (CNTF), FGF-2, members of the interleukin family (IL) and pigment epithelium derived factor (PEDF) [43-47]. The characteristics of some neurotrophic factors are discussed in section 1.3.2 in more detail. The RPE also acts as a blood-retina barrier for choroidal blood circulation, which is necessary to regulate the environment and homeostasis of the neurosensory retina. The blood-retina barrier is maintained by tight junctions which exist between the endothelial cells of the retinal vessels and similar tight junctions in the RPE (see [48] for a review).

The RPE increases the optical quality and maintains high visual acuity by forming a pigmented barrier that absorbs scattered light. Light is focused onto

the retina by the lens. The outer retina is exposed to an oxygen rich environment [49]. This combination is ideal for photo-oxidation and oxidative damage, consequently. The amount of reactive oxygen is further increased by disc shedding and phagocytosis (see chapter 1.1.6) [50]. The RPE has essential defence mechanisms against this damage and toxic substances. RPE cells contain various pigments – the main one of these is melanin – that are specialised to absorb light of different wavelengths and supplement light absorption of photoreceptors (reviewed in [51]). Melanin is a heterogeneous polymer and serves a photoprotective role by absorbing radiation, scavenging free radicals and reactive oxygen molecules, which arise during light excitement. In aged cells, however, melanin is known to be phototoxic because it interacts with oxygen and thereby leads to increased reactive oxygen amount within the cells. It has been shown that in aging RPE cells, melanin forms aggregates, which increase the production of radicals. Consequently, a chemical toxic cellular environment is created which results in RPE cell death, a major role in the pathenogenesis of age-related macular degeneration (AMD), the leading cause of blindness in the population over 60 years of age [51]. Photoreceptors contain carotinoids as the most important pigments, which mainly absorb blue light [52]. Blue light is in particular dangerous for the RPE because it leads to the oxidation of lipofuscin to cytotoxic substances. Lipofuscin is another RPE pigment that is beneficial for visual function at first but it accumulates during life and in older eyes it can reach toxic levels and results in a reduction in the ability of the RPE to absorb light [53]. This is an important factor in the development of AMD.

The RPE transports nutrients and ions between the photoreceptors and the choroid. Each RPE cell is firmly attached to surrounding RPE cells by adherent junctions. These junctions limit any transport across this cell layer [54]. Since there is no direct blood supply, the RPE is responsible for regulation of traffic between the choroid and the photoreceptors. Thus, the RPE cell actively and passively has to manage the bidirectional flow of fluids, molecules and ions into and out of the photoreceptor layer of the retina. This includes supplying nutrients to maintain the high metabolic rate of the photoreceptors, the removal of waste material, and maintaining ionic gradients essential for

phototransduction. The RPE cells, which surround the outer segments with their apical microvilli, supports photoreceptor function by the removal of metabolic end products, such as lactic acid [55]. Photoreceptor cells are among the most highly metabolic cells. Extensive protein and lipid synthesis ensures a continuous turnover of new outer segment membranes at the junction with the inner segment. The tips of the outer segments contain the oldest discs, which are phagocytosed as small packets of about 200 discs by the RPE cell, a process that occurs in a diurnal manner. Photoreceptors shed approximately 10 % of the length of their outer segments daily (reviewed in [40, 56]). The waste material is cleared by RPE cells making them one of the most efficient phagocytes in the body (the process of phagocytosis is described in detail in sections 1.1.6 and 1.1.7). TIMP3 is a regulatory protein controlling tissue degradation in the eye by inhibiting proteases, that breakdown proteins from ingested outer segments in the RPE. TIMP3 is also a potent angiogenesis inhibitor that has been shown to inhibit vascular endothelial growth factor (VEGF)-mediated angiogenesis. Mutations in *TIMP3* cause Sorsby fundus dystrophy, a macular degenerative disease with submacular choroidal neovascularisation [57] (see section 1.2.4).

The RPE also stabilises the ion composition in the subretinal space which is necessary to maintain high excitability of photoreceptors. RPE cells are apical to basolateral polarised cells which are connected to each other via tight junctions. The tight junctions between RPE cells make the RPE layer a polarised barrier between the subretinal space and the choroid. This polarity makes transepithelial transport of molecules through RPE cells necessary. The polarity is also reflected in RPE cell morphology, in the distribution of organelles and membrane proteins [40]. The Na^+-K^+-ATPase is located on the apical surface and provides energy for the transepithelial transport [59]. The high metabolic activity of retinal neurons and photoreceptors results in the production of large amounts of water that needs constant removal. In the inner retina, this is accomplished by Müller cells and the RPE eliminates water from the subretinal space [58]. The water transport is mainly driven by a transport of Cl^- and K^+ ions and results in an apical positive membrane potential. The Na^+-K^+-ATPase, furthermore, establishes a Na^+ gradient that facilitates the uptake of

HCO_3^- via a Na^+- HCO_3^- cotransporter and K^+ and Cl^- via the Na^+-K^+-$2Cl^-$ cotransporter, which in turn regulates of intracellular Cl^- concentration. This is important for the regulation of intracellular pH (reviewed in [60]). In order to increase the intracellular Cl^- concentration the Cl^-/ HCO_3^- exchanger on the basolateral membrane extrudes HCO_3^-. K^+ is transported from the IPM to the RPE via Na^+-K^+-ATPase and Na^+-K^+-$2Cl^-$ cotransporter and can leave the cell via K^+ channels. In the dark, there is a higher transport rate of K^+ at the basolateral membrane that is leading to the K^+ flow from the subretinal space to the choroid [61].

The transepithelial transport is important to maintain the homeostasis in the subretinal space. The RPE is also able to compensate for fast occurring changes in the ion composition that takes place during light activation of photoreceptor cells. Therefore, the electrical activity of the retina depends on the RPE. In the dark, there is a constant influx of Na^+ via open cGMP gated cation channels in the outer segments and efflux of K^+ via K^+ channels in the inner segment [24]. During light activation the efflux of K^+ is reduced resulting in a decrease of subretinal K^+ concentration. This change is compensated by the RPE. The low K^+ subretinal concentration leads to the hyperpolarisation of the apical membrane of the RPE [62]. This causes the activation of inward rectifier K^+ channels resulting in change of the transport ratio between apical and basolateral membrane. The increased K^+ transportation on the apical surface results in an increased K^+ amount secreted from the RPE to the subretinal space [63]. The decrease in subretinal K^+ also decreases the uptake of Cl^- via the Na^+-K^+-$2Cl^-$ cotransporter in the late stage of the apical membrane hyperpolarisation. Consequently, the intracellular Cl^- concentration decreases and this causes a change in the Cl^- transport through the basolateral membrane, which normally is high. The result is a hyperpolarisation of the basolateral membrane that further reduces the extruding rate of Cl^- to the choroid [64]. This mechanism can be monitored by the electroretinogram (ERG) as the c-wave (see chapter 3.6 for more details on ERG). Light activation closes cationic channels in the photoreceptor outer segments and thereby increases the subretinal Na^+ amount, which is compensated by the Na^+/H^+ exchanger and the Na^+-K^+-$2Cl^-$ cotransporter in the apical membrane of the RPE.

Consequently, the Na^+ concentration decreases in the subretinal space after the opening of cationic channels in the dark. This is compensated by the Na^+-K^+-ATPase in the inner segments and the RPE [65].

The RPE also transports glucose and other nutrients from the blood to the photoreceptors [55]. Glucose transporters, GLUT1 and GLUT3, are localised on the apical as well as the basolateral membrane [66]. Another important function of the RPE is the uptake of all-*trans* retinal (vitamin A) from the bloodstream. The continuous process of light activation and the consumption of 11-*cis* retinal during the visual cycle (see section 1.1.4) requires constant regeneration of 11-*cis* retinal from all-*trans* retinal. The regeneration takes place in the RPE, where all the necessary enzymes to catalyse this reactions are located. Furthermore, the RPE is the major storage place for vitamin A [67].

1.1.6 Disc shedding and phagocytosis

Because of their close interaction with photoreceptors, RPE cells play a critical role in vision. One of the RPE's most important tasks is the phagocytosis and the recycling of used rod and cone outer segment membranes [68]. Disruption of this phagocytic function may result in clinical disorders leading to blindness, which is the case in RCS rats and autosomal recessive RP patients both of whom carry mutations in the *MERTK* gene, a key regulator protein of RPE phagocytosis [69].

The high level of activity within rod and cone outer segments requires a continual renewal of their photoreceptive membranes [70, 71]. The renewal process occurs in a light-dependent manner at an impressive pace because the rate of disposal must equal the rate of disc synthesis since outer segments maintain a relatively uniform length throughout life [71]. A normal rod cell sheds around 10 % of its oldest outer segment discs daily at its distal ending and the outer segment lengthens from the cilium. This process effectively maintains the high sensitivity of photoreceptors. The renewal process can be divided into several main steps and involves the synthesis of new membranes to form photopigment containing discs by the inner segment. These newly formed discs displace older discs outwards, towards the tip of the outer segment. The oldest discs are disposed by detachment at the tip, a process termed disc shedding, and are phagocytised by the adjacent RPE cells. The initial step in phagocytosis is the recognition of shed outer segments and the binding to the RPE's apical microvilli, which surround the outer segment tips (figure 1.6). In the following step, the plasma membrane of the RPE cell invaginates the waste material into the extensive RPE phagolysosomal system. Finally, the waste material is transported to the choriocapillaries.

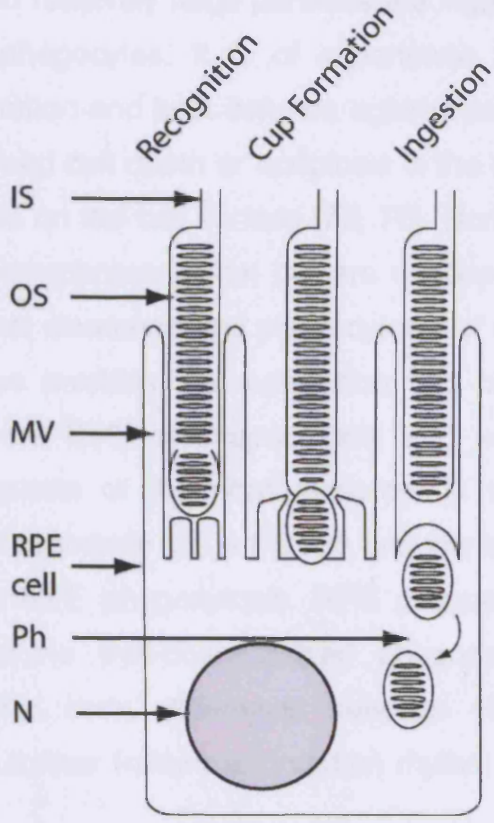

Figure 1.6: Schematic diagram of phagocytosis. The apical microvilli of RPE cells surround rod outer segment tips, which are phagocytosed by the pigment epithelium in a diurnal cycle. There is a burst of disc shedding at light onset in the morning, judged by increased numbers of phagosomes in the pigment epithelium shortly thereafter. After recognition the RPE cells internalise shed discs into phagosomes which are transported through the cytoplasm and degraded. IS=inner segment, OS=outer segment, MV=microvilli, Ph=phagosome, N=nucleus.

Disc shedding is a lighting cycle dependent process that follows a circadian rhythm [71, 72]. A burst of rod disc shedding occurs soon after onset of light in the morning. Apical processes of the pigment epithelium also phagocytise chunks of cone outer segments but at a different time in the diurnal cycle compared with rods at light off-set rather than light-onset [73, 74]. The picture of RPE phagocytosis is not complete yet. There are still many open questions and the distinct role of many factors involved is theoretical and needs still to be elucidated.

1.1.7 Phagocytosis and MERTK function

Phagocytosis is the process in which relatively large particles are ingested into vacuoles by specific cells called phagocytes. It is of importance in tissue remodeling, wound healing, inflammation and host defence against pathogens. One of the key features of programmed cell death or apoptosis is the exposure of phosphatidylserine (PS) molecules on the cell surface [75, 76]. Normally PS residues are localised in the inner membrane leaflet but are exposed on the exterior of dying cells. It is known that clearance and phagocytosis of apoptotic cells by different phagocytes always involves the recognition and binding to these PS molecules. In the eye, the RPE cells specifically and selectively remove the daily shed outer segments of the photoreceptors in a diurnal manner. The membrane of the outer segments tips is PS rich and this is thought to be one of the main triggers for RPE phagocytosis. RPE phagocytosis is poorly understood compared with the well-characterized phagocytosis by monocytes and macrophages. The main difference between RPE and phagocytosis elsewhere is that the former follows a circadian rhythm in many species [72].

The binding and the ingestion of the waste material are independent processes in which distinct receptors are involved. Receptor tyrosine kinases have been shown to play a central role in the transduction of extracellular signals into cells and thereby enable them to respond to their environment by a variety of cellular actions. So far four plasma membrane receptors of RPE cells have been described to participate in outer segment phagocytosis: a mannose receptor [77], MERTK which is a receptor tyrosine kinase [69], $\alpha v\beta 5$ integrin [78-80], and the type B scavenger receptor CD36 [81]. Little is known about the function of the mannose receptor. There is, however, evidence that it is involved in the internalisation process, even though neither the RPE receptor nor the outer segment ligand have been identified [77]. Two animal models – the RCS rat and the *mer*^{kd} mouse [69, 82] – carry mutations within the *MERTK* gene. Both animal models are deficient in photoreceptor phagocytosis, demonstrating the crucial role that MERTK plays in the removal of shed outer segments. A

schematic diagram of phagocytosis and the different signaling pathways is shown in figure 1.7.

Figure 1.7: Signal pathways during phagocytosis. Phagocytosis starts with the recognition of different rod outer segment (ROS) membrane molecules, mainly phosphatidylserine residues (PS), by four RPE receptors, namely MERTK, αvβ5 integrin receptor, CD36 and a mannose receptor. The activation of these receptors results in a variety of intracellular signalling pathways leading to cytoskeletal changes necessary for the ingestion and transportation of the waste material.

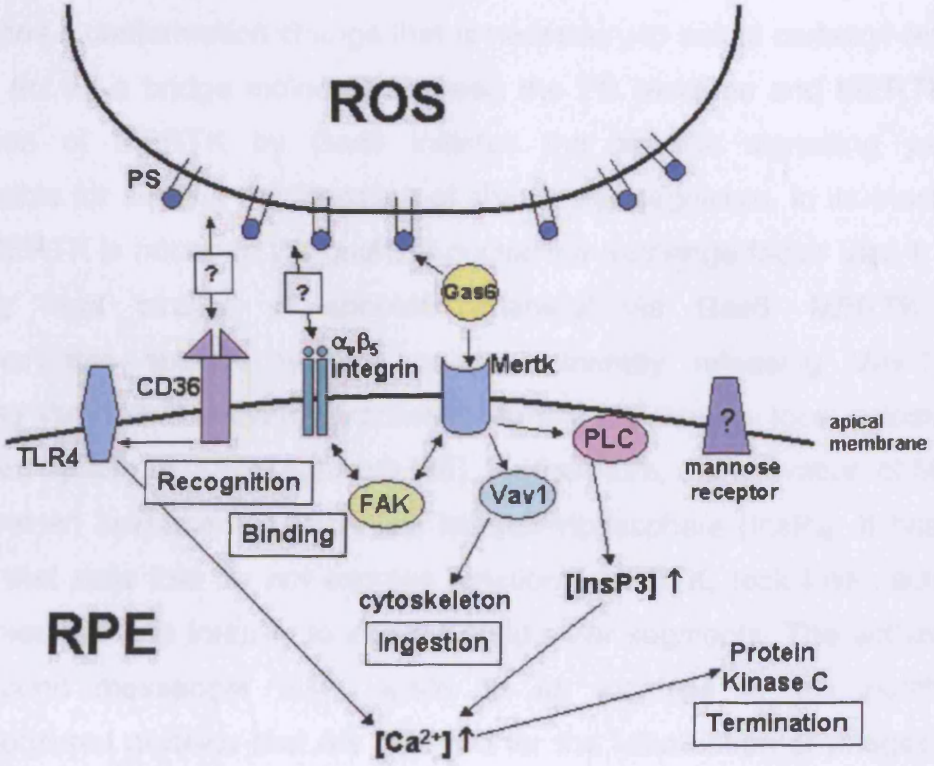

The initial step in phagocytosis, in which probably several RPE receptors are involved, is the recognition and binding of the shed outer segment by the RPE. In monocytes the αvβ3 integrin receptor recognises apoptotic cells during the early phase of phagocytosis. RPE cells express another member of this family of receptors, the αvβ5 integrin receptor [79]. They differ in the following signaling pathways that are activated upon receptor binding to its ligand. αvβ5 integrin forms complexes with the cytoplasmatic tyrosine kinase, FAK, at the

apical surface of the RPE [83]. Activation of FAK seems to be critical for the integrin function involved in cytoskeletal reorganisation necessary for the cup-formation. Furthermore, FAK signalling upon outer segment binding has been suggested to be required for the phosphorylation of MERTK to activate the engulfment machinery. That means that the functional interaction between αvβ5 integrin and MERTK is via FAK.

Growth arrest specific factor 6 (Gas6) specifically binds PS molecules exposed on the outer membrane of the outer segments via its amino-terminal domain in a calcium dependent manner. After binding to the outer segment Gas6 undergoes a conformation change that is necessary to set its carboxyl-terminus free to act as a bridge molecule between the PS residues and MERTK [84]. Activation of MERTK by Gas6 initiates the specific signalling pathway responsible for starting the ingestion of shed outer segments. In its inactivated state MERTK is bound to the guanine nucleotide exchange factor Vav-1. When sensing local binding of apoptotic material via Gas6, MERTK auto-phosphorylates specific tyrosine residues thereby releasing Vav-1. The released Vav-1 then activates processes leading to selective, local cytoskeletal-mediated uptake of outer segments [85]. Furthermore, the activation of MERTK results in an increase in intracellular inositol-triphosphate ($InsP_3$). It has been shown that cells that do not express functional MERTK, lack $InsP_3$ activation which results in the inability to ingest bound outer segments. The activation of the second messenger $InsP_3$ leads to an increase in the number of phosphorylated proteins that are required for the initialisation of phagocytosis. The increase in $InsP_3$ also increases the concentration of intracellular free Ca^{2+}. Both the increase in $InsP_3$ and in Ca^{2+} regulates phagocytosis. Whereas the increase in $InsP_3$ on its own activates phagocytosis, the increase in Ca^{2+} consequently results in an activation of protein kinase C which is thought to be a shut-down signal for phagocytosis [83, 86, 87].

Another receptor involved in phagocytosis is a transmembrane glycoprotein, the macrophage scavenger receptor CD36 [81]. CD36 was found to regulate the rate of outer segment internalisation. Since CD36 is expressed on the apical as well as on the basal membrane of RPE cells, it is likely that its function includes

signalling during phagocytosis. Activation of CD36 by its ligand leads to its dimerisation. The ligand has recently been suggested to be the toll-like receptor TLR4. The dimerisation activates a cellular signalling pathway, the target of which is the internalisation mechanism of the RPE [88]. A second messenger system that acts as a modulator of the rate of phagocytosis is cAMP [87]. An increase in cAMP reduces the phagocytic activity of the RPE. The $InsP_3/Ca^{2+}$ and the cAMP second messenger pathway can interact. It has been shown that the two systems are coregulated by serotonin via protein kinase C [89].

1.2 Inherited retinal disorders

Processes that enable us to see are complex and involve a number of proteins encoded by a variety of different genes. Inherited retinal disorders are a group of heterogeneous diseases and are a major cause of blindness in the Western world. The visual deficits are caused by progressive dysfunction and degeneration of photoreceptor cells, which are triggered by mutations in one of over 150 so far identified genes. Of those, over 110 genes have been cloned (table 1; RetNet, up-date September 2005, http://www.sph.uth.tmc.edu/Retnet). Many mutations affect proteins that are specifically expressed in photoreceptor cells or RPE cells. These proteins are involved in a wide range of functions including the phototransduction cascade, the structure of photoreceptors, retinal metabolism, and photoreceptor cell-specific transcription factors (table 2). A mutation in the same gene, can cause a variety of different diseases. Even though retinal disorders have been known since the 19th century, the heterogeneity of the diseases and their complexity present a problem for those involved in counselling patients, and for the development of efficient therapies (for reviews see [1, 90, 92,93]).

This large and diverse group of visual disorders affects patients of all ages. There are many types of inherited retinal degenerations. Their differentiation is not always easy since many of them share clinical features. The conditions are grouped into a number of broad categories, such as RP, cone and cone-rod dystrophies, macular degenerations, and Leber congenital amaurosis (for reviews see [92, 94, 95]). All these diseases are characterized by degeneration of the photoreceptor cells of the retina, resulting in a loss of vision. The mechanisms by which these mutations lead to death of photoreceptor cells are not completely understood. However, it is thought that in all forms of retinal degeneration, photoreceptors die via apoptosis (see [96] for a review).

Table 1: Number of retinal dystrophy genes by disease category. The table summarises the number of identified and cloned genes that are associated with different types of retinal disorders (RetNet, up-date September 2005).

Disease	Number of loci	Number of cloned genes
Macular degeneration autosomal dominant	13	6
Macular degeneration autosomal recessive	1	1
Leber's congenital amaurosis autosomal recessive	8	6
Usher syndrome autosomal recessive	11	8
Cone and cone/rod dystrophies autosomal dominant	6	4
Cone and cone/rod dystrophies autosomal recessive	2	0
Cone and cone/rod dystrophies x-linked	2	0
Retinitis pigmentosa autosomal dominant	13	13
Retinitis pigmentosa autosomal recessive	16	11
Retinitis pigmentosa x-linked	5	2
Other retinopathies	84	60
Total number of genes	161	111

Currently, there are no effective treatments for RP. One of the strategies under development is gene therapy, which will be discussed in more details in section 1.3.4. Generally, recessive diseases are easier to approach with gene therapy strategies because they "only" require the addition of a functional copy of the mutated gene. Monogenic dominant diseases are more complicated to treat. In many cases (for example peripherin/*rds*) the mutation leads to a gain of function that often has cytotoxic effects. Therefore, the disease causing allele needs to be removed from the affected cell type and a functional allele added. For several reasons, defects in genes specifically expressed in the RPE have proven to be more amenable to effective gene therapy compared to photoreceptor-specific defects. Therefore, the following section will focus mainly on diseases arising from RPE-specific gene defects.

1.2.1 Leber's congenital amaurosis

Leber's congenital amaurosis (LCA) is one of the most frequent causes of severe early onset retinal degeneration with a prevalence of 3 in 100000 newborn babies. It is a clinically and genetically heterogeneous retinal dystrophy presenting in infancy. Classical features of LCA include severe visual loss, nystagmus (involuntary eye movements) and pigmentary retinopathy. In the majority of patients, the inheritance pattern of LCA is recessive autosomal and only a few cases of autosomal dominant inheritance have been reported. The appearance of the retina is initially normal in fundus examinations, however little if any retinal activity can be measured by ERGs early in the disease process. Later various changes, including narrowing of retinal blood vessels, pigmentary changes of the RPE, and intraretinal pigment migration, can be found [97]. To date eight different genes are known to be associated with autosomal recessive LCA, one of these is also associated with autosomal, dominant LCA. The clinical heterogeneity of LCA is reflected by the genetic heterogeneity of this disorder [92, 98, 99]. The genes are predominately expressed in the neuroretina and the RPE. Their functions are diverse and include phototransduction (*GUCY2D*), vitamin A metabolism (*RPE65*, *RDH12*), retinal embryonic development (*CRX*), protein trafficking (*RPGRIP1*, *AIPL1*, *TULP1*), and photoreceptor cell structure (*CRB1*).

Mutations in the *RPE65* gene account for 2 % of recessive RP and 15 % of LCA cases [100]. RPE65 is an RPE-specific microsomal protein that in its membrane bound form binds all-*trans*-retinyl esters, allowing their entry into the visual cycle for processing into 11-*cis*-retinal (for details on vitamin A metabolism see section 1.1.4) [101-103]. A naturally occurring animal model, the $Rpe65^{-/-}$ dog, suffers from early and severe visual impairment similar to that seen in human LCA [104]. This dog model has been used to develop an effective treatment for LCA. Using a recombinant adeno-associated virus (rAAV) carrying wild-type *Rpe65,* it was possible to restore visual function over a long period of time (see chapter 1.3.4.4.3) [105].

1.2.2 Cone and cone-rod dystrophies

The cone–rod dystrophies (CORDs) are a clinically and genetically heterogeneous group of progressive retinal disorders. The CORDs usually present with cone dysfunction related symptoms, including photophobia, poor colour vision, and reduced central visual function. Night and peripheral vision are preserved at the beginning but as the disease progresses rods degenerate, causing poor night vision, defective dark adaptation and peripheral vision loss. The onset and the degree of visual impairment is variable. The inheritance pattern of cone-rod dystrophies is complex and includes autosomal recessive, autosomal dominant as well as X-linked types. So far 15 genes with different functions (RetNet, up-date Sep 2005) have been shown to be associated with CORDs including *AIPL1* (retinal development [106]), *GUCY2D* (phototransduction [107]), *CRX* (transcription factor [108]), *ABCA4* (protein trafficking [109]), and *RDH5* (vitamin A metabolism [110]).

It has been shown that mutations in the 11-*cis* retinol dehydrogenase 5 (*RDH5*) gene are associated with recessive fundus albipunctatus (a type of congenital stationary night blindness characterized by delay in the regeneration of photopigments, see section 1.2.5) and recessive cone dystrophy [111, 112]. *RDH5* is specifically expressed in the RPE and has an important function in the visual cycle (see section 1.1.4). After light excitement, the all-*trans* retinal of rod and cone photopigments is recycled to 11-*cis* retinal in RPE cells. It has been suggested that RDH5 catalyses the conversion of 11-*cis* retinol to 11-*cis* retinal [110].

1.2.3 Retinitis pigmentosa

The term retinitis pigmentosa (RP) includes a group of inherited genetic diseases leading to progressive photoreceptor degeneration and finally to blindness. Worldwide approximately 1.5 million people suffer from this retinal disorder, making RP one of the most common causes of visual impairment [1].

The clinical features observed in RP patients are variable and are reflected by its genetically heterogeneous basis. The inheritance patterns are autosomal dominant, autosomal recessive, X-linked, mitochondrial and digenic (for reviews see [1, 113]). RP may also be either familial (multiplex), affecting multiple family members, or isolated (simplex), affecting one individual only (see [114] for a review). Furthermore, RP can be classified as non-syndromic, not affecting other organs or tissues, syndromic, affecting other systems such as hearing (for example Usher syndrome, see also section 1.2.5); or systemic, affecting multiple tissues. Further allelic heterogeneity arises from different mutations in the same gene. The first mutation identified as a cause of an autosomal dominant form of RP was a mutation within the rhodopsin gene. Mutations in the rhodopsin gene account approximately 25% of cases and therefore represent the most common cause of RP [115].

Patients with RP may present with varying symptoms (see [94, 116] for reviews). The onset is often gradual and many patients fail to recognize the manifestations of this condition until it has progressed significantly. In typical cases, the rods are predominantly affected. The initial clinical symptoms include a defective dark adaptation leading to night-blindness at an early age and loss of mid-peripheral vision causing tunnel vision. Usually the central, macular vision is preserved in the beginning of the disease with normal central vision acuity and colour vision. As the degeneration progresses, cone photoreceptors are also affected and day vision and central vision are compromised. These symptoms reflect early loss of rod photoreceptors, followed by a slower degeneration of cones.

Electron microscopy studies show that in earlier stages of the disease the only remaining photoreceptor cells are the cones in the posterior pole and these are atypical and fewer in number. The outer segments are connected to abnormally wide and shortened inner segments via apparently normal cilia and the nuclei of these cone cells appear to be 30% larger than their normal counterparts. Degenerative changes in the neural retina are very variable, with structurally well preserved ganglion cells and nerve fiber layers in some patients and

complete degeneration of these in others. Additional changes include an increase in the size of Müller fibers and migration of these cells between the inner nuclear layer and the RPE (reviewed in [117]).

Commonly reported by many RP patients are flashes of light and a twinkling, shimmering sensation in the mid-peripheral or peripheral field, which are hypothesised to be aberrant electrical impulses generated by the degenerating retina. Fundus appearance is dependent on the stage of retinal degeneration. The earliest observed change in the fundus is the narrowing or attenuation of the retinal arterioles. Retinal pigmentary changes occur in form of fine spotting or granularity with surrounding areas of atrophy. Later, star-shaped pigment formations may be noted at perivascular locations in the mid-peripheral retina. These hyperplastic formations are often referred to as "bone spicules" (reviewed in [94]).

As the disorder progresses, general atrophy of the RPE and choriocapillaries ensues, exposing the larger choroidal vessels (see figure 1.8). The optic nerve head is often normal in early RP but may demonstrate a waxy yellow or pale appearance later. RP has a strong correlation with acquired optic disc drusen. The macula, like the optic nerve, is usually unaffected in the early stages but in some forms of RP may demonstrate preretinal gliosis ("cellophane maculopathy"), cystoid macular edema or focal RPE defects. Additional findings in RP include pigment cells in the vitreous ("tobacco dust sign"), posterior vitreous detachment and posterior subcapsular cataracts.

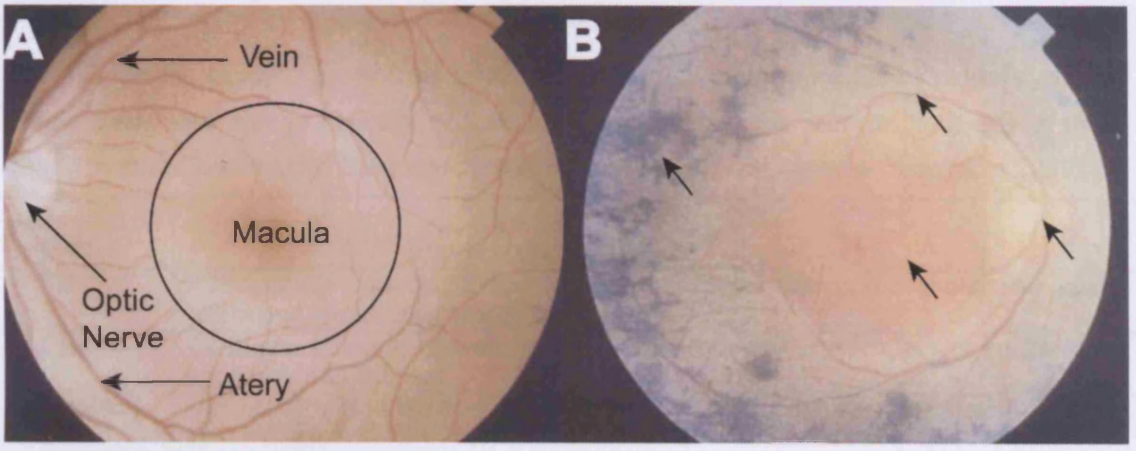

Figure 1.8: Fundus images. **(A)** Fundus image of a normal subject and **(B)** of a patient diagnosed with RP. Changes include narrowing of blood vessels, intraretinal accumulation of melanin (bone spicule), hypopigmentation in the macula area, pallor of the optic disc (changes indicated by arrows).

Findings on ophthalmoscopy include intraretinal pigment around the mid-peripheral retina for which this condition is named. Histopathological examinations of eyes with advanced stage of RP have shown that loss of vision is due to degeneration of both rod and cone photoreceptor cells. Retinal function is abnormal as determined by light evoked electrical response from the retina that is measured by electroretinography. This abnormality reflects the loss of photoreceptor function. Patients with early stage of RP show ERGs with reduced amplitude. ERG amplitudes diminish as the disease progresses (see [118] for a review).

To date, five genes associated with autosomal, recessive RP have been identified that are primarily expressed in the RPE, namely *RPE65* (see sections 1.1.4 and 1.3.4.4.3) [103, 119], *LRAT* (see section 1.1.4) [120, 121], *MERTK* (see sections 1.2.5, 1.2.6.1 and 5.2) [69, 122], *RGR* [123, 124] and *CRB1* [125] (genes associated with autosomal recessive RP and their function are summarised in Table 2). The later is also expressed in photoreceptor inner segments [125]. Recent success in the treatment of the *Rpe65*$^{-/-}$ dog suggests that these genes are prime candidates for the development of gene therapy approaches [105].

Table 2: Genes causing autosomal recessive RP. The proteins encoded by retinal dystrophy genes show wide spread diversity of function. Nevertheless, the interruption of any of these genes by mutations leads to the same clinical phenotype (RetNet, up-date September 2005).

Gene	Protein function
ABCA4	ATP binding cassette transporter, retina specific, transport of molecules across extra- and intracellular membranes
CERKL	Ceramide kinases, convert sphinglipid metabolites which are key mediators of apoptosis and survival
CNGA1	Rod cGMP-gated channel α subunit, important role in neuronal function
CNGB1	Rod cGMP-gated channel β subunit, see CNGA1
CRB1	Crumbs homolog 1 protein, localized to RPE and inner segments, possibly involved in cell-cell interactions and cell polarity
LRAT	Lecithin retinol acyltransferase, visual cycle, transformation of vitamin A into 11-*cis*-retinol
MERTK	Receptor tyrosine kinase, involved in phagocytosis of shed outer segments by the RPE
NR2E3	Nuclear receptor, ligand dependent transcription factor, possibly involved in development and maintenance of proper cell function
NRL	Neural retina lucine zipper, promotes rhodopsin and other genes transcription, required for rod development
PDE6A	Rod cGMP phosphodiesterase α subunit, expressed in rod outer segments, regulates cGMP concentrations and thereby membrane current
PDE6B	Rod cGMP phosphodiesterase β subunit, see PDE6A
RGR	RPE-retinal G protein coupled receptor, in RPE and Müller cells, bind all-*trans* retinal which light converts to 11-*cis* retinal
RHO	Rhodopsin, transmembrane photosensitive protein of rods
RLBP1	Cellular retinalaldhyde-binding protein, possible functional component of the visual cycle
RP1	Important but unknown role in photoreceptor biology
RPE65	RPE specific protein, necessary for production of 11-*cis*-vitamin A
SAG	Arrestin, involved in desensitization of the photoactivated transduction cascade
TULP1	Tubby-like protein 1, involved in rhodopsin transport from inner to outer segment, also expressed during development
USH2A	Basement membrane associated, important for development and homeostasis of inner ear and retina

1.2.4 Macular degeneration

Macular degeneration (MD) is a term used for different types of retinal disorders that are characterised by a degeneration of the macula and a progressive loss of central vision (reviewed in [126]). The macula is a small, highly sensitive part of the retina temporal to the optic nerve and is required for central vision. It is the area that provides the most distinctive vision due to its higher concentration of cones compared to other parts of the retina. The centre of the macula is called fovea. Here, there are only cones present making it the area of the highest visual acuity. To date, 14 genes associated with this condition have been identified (RetNet, up-date September 2005). The inheritance pattern of MD is autosomal (apart from mutations in *RPGR*, which is located on the X-chromosome) and may either be dominant or recessive.

Age related macular degeneration (AMD) is the most common cause of vision loss in the elderly. The term refers to a group of late onset conditions that affect the macula. AMD has been clinically recognised since more than 100 years but since the clinical characteristics of AMD only partial overlap, there is no satisfying definition for this group of retinal degenerations. However, all types of AMD have the accumulation of proteins, lipids, and cellular debris between the RPE and the Bruch's membrane in common. These accumulations are called drusen. Further classical features of AMD are the patchy loss of RPE cells, known as geographic atrophy, and an abnormal distribution of the pigment in the RPE. Common is the growth of blood vessels through the Bruch's membrane into the subretinal space. AMD has been shown to be hereditary in about one fourth of the cases. There are factors that increase the risk of developing AMD, such as hypertension, high cholesterol, smoking, and high exposure to sunlight. The complement factor H (*CFH*) gene – a serum glycoprotein that controls the function of the alternative complement pathway – has been determined to be strongly associated with the risk of developing MD at older age. A substitution of tyrosine to histidine at codon 402 of CFH is resulting in variant of CFH that accounts for up to 50% of the append risk of AMD [127, 128].

Sorsby's fundus dystrophy (SFD) is a late-onset, autosomal dominant inherited form of macular dystrophy whose pathological phenotype arises from mutation in the tissue inhibitor of metalloproteases 3 gene (*TIMP3*) [57]. The clinical characteristics are similar to those found in AMD patients, including drusen, accumulation of extracellular matrix material (including collagen, elastin, and glycoaminoglycans) and lipids at the level of Bruch's membrane, and colour vision deficits. Most commonly, patients suffer from a sudden acuity loss, which manifests in the third to fourth decades of life and that is due to submacular neovascularisation [57]. *TIMP3* encodes an RPE endopeptidases which is involved in retinal extracellular matrix remodelling and a component of the Bruch's membrane. TIMP3 is an inhibitor of matrix metalloproteinases that breaks down connective tissue material in the extracellular matrix [129]. The mechanisms that lead to SFD phenotype are not completely understood yet. However, it has been suggested that mutant TIMP3 forms a dimer which is not degraded as quickly as normal TIMP3 and may accumulate in the Bruch's membrane. Because the mutant TIMP3 is able to inhibit metolloproteinase activity, it might have an increased inhibition of protease activity, which in turn leads to an increased accumulation of extracellular material. The altered elastic fibers in the Bruch's membrane might lead to choroidal neovascularisation (CNV) [130].

The most common form of juvenile macular degeneration is called Stargardt's disease and the onset of the disease is between 5 and 20 years of age. Stargardt's disease is mainly inherited recessively but rarely dominant inheritance patterns can be found. The clinical features are similar to those observed in AMD and SFD patients. Lipid rich deposit accumulates underneath the RPE, mainly in the macula area, and subsequently causes atrophy of the macula and the RPE, thereby creating a central blind spot in the visual field that increases in size as the disease progresses (reviewed in [131]). The phenotype is due to mutations in the retinal specific ATP-binding cassette transporter gene (*ABCA4*, *ABCR*) [109]. The product is a transmembrane protein localised to the rim of rod outer segments where it acts as an ATP dependent flippase for N-retinylidine-phosphatidylethanolamine (N-retinylidine-PE) [132]. ABCA4 is thought to translocate N-retinylidine-PE across the membrane. In the

intracellular space, N-retinylidine-PE is hydrolysed causing the release of all-*trans* retinal. All-*trans* retinal is then isomerised to all-*trans* retinol by retinal dehydrogenases (see section 1.1.4). In the absence of ABCA4, N-retinylidine-PE and all-*trans* retinal accumulates within the outer segment. After phagocytosis, the outer segment discs undergo enzymatic digestion resulting in the generation of N-retinylidine-N-retinylethanolamine (A2-E), a major component of lipofuscin. The accumulation of high levels of lipofuscin has a cytotoxic effect and results in apoptosis of RPE cells [109, 133].

Best's vitelliform macular dystrophy, is an autosomal dominant disorder, which classically presents in childhood with the appearance of lesion in the macula [134]. Abnormalities result from a disorder in the RPE. Accumulation of lipofuscin within the RPE cells and in the sub-RPE space, particularly in the foveal area, is most commonly found in patients. The RPE appears to have degenerative changes and secondary loss of photoreceptor cells has been noted. In early stages, visual acuity is good but the advancing RPE atrophy and possible development of choroidal neovascularisation results in reduction in visual acuity (reviewed in [135]). The gene mutated in Best's disease has been identified as the retina-specific *VMD2* gene that encodes for a protein termed bestrophin. The protein localises to the basolateral plasma membrane of the RPE and functions as a transmembrane, oligomeric ion channel protein. *VMD2* mutations have been suggested to result in reduced or abolished membrane current [134, 136]. Lipofuscin accumulation may be a secondary change to abnormal ion flux. Even though most of the cases have an early onset of degeneration, 1 to 2 % of *VMD2* mutations might lead to AMD.

1.2.5 RPE defects

The previous section shows that mutations in many RPE-specific genes result in different types of retinal degeneration. Diseases caused by alterations of the retinoid cycle in the RPE share characteristics in their fundus such as the appearance of yellow to white spots (reviewed in [137]). Such disorders include

the previously mentioned Stargardt disease (*ABCA4* gene; see section 1.2.4) [109], the retinol binding protein deficiency syndrome (*RBP4* gene) [138], fundus albipunctatus (*RDH5* gene) [112] and retinitis punctata albescens (*CRALBP* gene) [139]. Retinol binding protein deficiency syndrome [138] arises from mutation in the *RBP4* gene. RBP4 is produced in the liver, mobilises and transports vitamin A to the basolateral membrane of the RPE. The fundi of patients are characterised by small yellowish to white dots in the periphery and severe atrophy of the RPE. The impairment of vitamin A uptake and transport to the photoreceptors results in reduced dark adaptation and scotopic ERG is unrecordable. In fundus albipunctatus, white to greyish dots are initially apparent as a ring around the macula and spread towards the equator as the disease progresses (see [137, 140] for reviews). Although the dots are in discrete areas, functional testing reveals global rod dysfunction. This disorder is associated with mutations in *RDH5* (see chapter 1.2.2), the product of which is involved in the conversion of 11-*cis* retinol to 11-*cis* retinal in the RPE [112]. Retinitis punctata albescens is characterised by a progressive rod and cone degeneration. The fundus typically shows distinct dots that sometimes invade the macula, as well as bone spicule. In late stages the dots disappear and RPE atrophy, pigmentary changes and attenuated vessels develop. This disease has been linked to defects in the cellular retinaldehyde binding protein (CRALBP), which is found in RPE and Müller cells. CRALBP carries 11-*cis* retinol and 11-*cis* retinaldehyde. In the absence of functional CRALBP all-*trans* retinyl ester accumulate in the RPE [124, 141, 142].

Retinal and RPE dystrophies display heterogeneity of genotype and phenotype. Variations have been observed on inter- and intrafamilial level and mutations within the same gene can result in different phenotypes. Besch *et al* [143] have suggested several mechanims that might contribute to this heterogeneity, including the non-homogeneous shape and density of RPE cells, regional differences in the photoreceptor ratio per RPE cell, the uneven distribution of rod and cone photoreceptors, accumulation of lipofuscin, and variation in the Müller cell distribution.

Another RPE defect is ocular albinism. Albinism is a disorder of amino acid metabolism that results in a congenital hypopigmentation of ocular and systemic tissues. Cellular pigmentation is dependent upon the ability of specialised cells, called melanocytes, to manufacture melanin. This is accomplished within organelles called melanosomes. Inside the melanosome, melanin is synthesised from the amino acid tyrosine through the actions of the enzyme tyrosinase [144]. Albinisms are characterized by a reduction or total absence of pigment in the hair, skin, and eyes. Ocular albinism is a subgroup of disorders arising from a reduction of melanin pigment in the RPE (reviewed in [145]). The disease phenotype has been associated with mutations in the *OA1* gene. Retinal morphogenesis depends on the organising influence of the adjacent RPE. The insufficient uveal pigmentation and poor development of the RPE in the albinotic patient provides a developmentally unstable substrate for normal retinal organisation. Hence, the albinotic macula is always hypoplastic and the albinotic patient has secondarily reduced acuity. Pigment deficits in the RPE also lead to a reduction in the number and distribution of photoreceptors and other retinal cells by affecting the mechanisms controlling cell proliferation during the early development of the retina.

Failure of outer segment phagocytosis by the RPE results in retinal degeneration, as it is the case in animal models and patients that carry mutation in the *MERTK* (see sections 1.2.6.1 and 5.2) and *Myo7A* genes. Usher syndrome is an inherited condition resulting in hearing loss as well as loss of vision (see [146, 147] for reviews). It is the major cause of deaf-blindness in the world. The clinical features of the visual impairment are the same as in RP (see chapter 1.2.3). Depending on the hearing at birth three types of Usher syndrome are distinguished, with type 1 being the most severe one (born deaf) and type 3 the mildest type (born with good hearing). All three types of Usher syndrome are inherited in an autosomal recessive manner. Mutations in the myosin VIIa gene (*Myo7A*) are associated with Usher syndrome type 1 (USH1). The absence of functional MYO7A results in cytoskeletal abnormalities including abnormal organisation of microtubules in the connecting cilium of photoreceptor cells, nasal cilia cells, and sperm cells, as well as by the widespread degeneration of the organ of Corti that is responsible for deafness.

It has been reported that *Myo7a*-null mice show abnormalities in the phagocytosis of photoreceptor outer segment discs by the RPE [148]. RPE cells display a reduced ability to ingest bound outer segments, probably due to the disturbed vesicle trafficking and fusion between phagosomes and lysosomes. This suggests that the primary defect responsible for the visual deficits in USH1 patients is in the RPE rather than in the photoreceptors.

Changes in the secretory activity of the RPE are associated with proliferative disorders of the retina. An example of a disease in which proliferation is one of the key factors is AMD (see chapter 1.2.4). A complication in patients with AMD is the development of choroidal neovascularisation (CNV). The initial mechanisms leading to CNV are not completely understood but are thought to involve local hypoxia, RPE cell loss and growth factors. In all cases the major angiogenetic factor, VEGF, causes the development of neovascularisation. In the eye, VEGF is mainly produced by the RPE and it has been shown that VEGF secretion from RPE cells is up-regulated in AMD patients with neovascularisation. Many extracellular factors, such as insulin-like growth factor 1 (IGF-1), have been suggested to be involved in the higher production of VEGF [149, 150]. IGF-1 is exclusively produced by photoreceptor cells in healthy eyes but by RPE and photoreceptor cells in eyes with AMD. Therefore, it might contribute as a stimulus for the increased VEGF production.

1.2.6 Animal Models for inherited retinal dystrophies

Inherited retinal degenerations are the most common cause of blindness. However, the mechanisms that lead to photoreceptor cell loss are still not well understood. Hence, a suitable and efficient treatment for most of these diseases has yet to be found. For some types of retinal degeneration natural occurring animal models exist (see [151] for a review). Over the past few years, the identification of gene loci for inherited retinal degenerations and the progress in genetic engineering have led to the development of numerous transgenic animals. The successful development of transgenic animal models for human

diseases was a remarkable breakthrough and had a significant impact on the development of approaches to diagnosis, treatment, and intervention of human diseases. Additionally, the models have clarified our understanding of disease mechanisms and the onset and course of pathology associated with disease. These animals, mainly rodents, carry constructs that result in the disruption or overexpression of specific candidate genes for retinal degenerations that mimic the human disease. Animal models are crucial to understand the processes involved in retinal degeneration and have been widely used in visual research. They represent a powerful tool to investigate the role of specific gene mutations and the resulting cellular defects that finally lead to photoreceptor cell death and are required for the development and testing of new treatments. All vertebrate eyes are similar in structure and function. There are, however, some differences depending on the life style of different species that play a decisive role, particularly when selecting the best qualified animal model for experiments. The choice of an appropriate animal model is crucial for the validity of an experiment. Whilst animal models are often very valuable they should only be seen as an approximation to the morphological, physiological and pathophysiological conditions of humans.

For various reasons, mice and rats have been used most extensively of all species, including their short gestation time, their small size, the existence of several readily available retinal degeneration mutants, multiple inbred and congenic strains with genetic controls, and different eye pigmentation types. However, initial findings need to be validated in larger animal models with eyes that more closely resemble human eyes. Any new developed treatment must be evaluated for its therapeutic value as well as for its safety before it is applicable for clinical trial. Treatment doses, duration, and timing must be assessed thoroughly.

In most experiments, rodents are the animals of choice. However, there are differences between rodent and human eyes that sometimes make an interpretation of results obtained from the animal difficult. In both humans and rodents, light passes through the cornea, which allows both visible and ultraviolet light down to 300 nm to pass through. Then the light passes through

the pupil, which in rodents like in humans is highly variable in size. The lens acts as a filter to block certain wavelengths of light and it is not equally transparent to all colours. Which colours are allowed through differs between species. Whilst only visible light can pass through the lens in humans, rodent lenses allow all visible light plus almost 50 % of ultraviolet A light to pass through. Once the light hits the retina it is detected by the photoreceptor cells. Humans have in addition to rods three different types of cones. Rodents on the other hand have only two types of cones, green and blue, and are therefore unable to see longwave light. The distribution of rods and cones varies within the retina in humans. At the periphery of the retina are more rods which respond to light intensity and cones are concentrated in the optical centre of the retina. The ratio of rods and cones varies between different species of all vertebrate families. In humans, 5 % of the photoreceptors are cones compared to only 1-2 % in rats and mice (There are however exceptions [152]. Other rodents such as the African mole-rat have despite of its subterranean, nocturnal mode of life a high proportion (~ 10 %) of cones). Each neural cell in the rodent retina is responsive to a larger number of photoreceptors than those of the human retina, which increases sensitivity at the expense of acuity. In humans and primates, laterally of the optic disc is the cone-rich macula, whereas cones are evenly distributed over the entire retina in rodents.

The small size of the mouse eye, combined with a relatively large lens, makes intraocular procedures and accurate delivery of therapeutic substance extremely difficult. The rat eye is several-fold larger than the mouse eye, which simplifies intraocular procedures and electroretinographic evaluation. In addition, rats breed as rapidly as mice, generating large litters in a short gestational time.

To date, there are a large number of mouse models, both naturally occuring and transgenic (see [151, 153, 154] for reviews). The first natural occurring animal model was discovered 1923 by Clyde E Keeler. He discovered a mouse strain that has no photoreceptor cells but a lack of interest in the research community made him abandon his work on this mouse strain. Almost 30 years later Brückner and colleagues reported severe retinal degeneration in a wild mouse

strain and named it retinal degeneration (*rd*) mouse, which later became one of the most studied animal models for inherited autosomal recessive retinal degeneration. Seventy years after Keeler discovered his mouse strain, Pittler and co-workers identified the genetic defect underlying photoreceptor degeneration in the *rd* mouse and demonstrated by polymerase chain reaction (PCR) that the defects in Keeler's mouse and the *rd* mouse were identical [155]. The gene mutated in the *rd* mouse encodes the β-subunit of the rod cGMP phosphodiesterase (β-PDE), an enzyme of the visual cascade specifically expressed in photoreceptors (see chapter 1.1.4) [96, 156].

The retinal degeneration slow (*rds*) mouse is a mouse model for inherited autosomal dominant RP [157]. This mouse carries an insertional mutation in the *rds*/peripherin gene encoding for a photoreceptor-specific structural protein expressed both in rods and cones. Peripherin is located in the rims of photoreceptors and has an important role in disc morphogenesis. It is hypothesised that peripherin stabilises the membrane fold at the edge of outer segments and that lack of peripherin in *rds* mice disrupts these folds and thus proper disc function (reviewed in [91]). *Rds* mice fail to develop photoreceptor outer segments and undergo degeneration of both types of photoreceptors.

The Royal College of Surgeon (RCS) rat, first described in 1938 [158], is an example of a natural occuring model for autosomal recessive RP caused by RPE dysfunction. The gene that is disrupted in RCS rats is the receptor tyrosine kinase *MERTK* [69, 159]. RPE cells in RCS rats have lost their ability to phagocytise shed outer segments, resulting in the accumulation of waste material between the RPE cell layer and the photoreceptor cells. The two cell types lose contact and the RPE cells are unable to provide nutrients and oxygen to the photoreceptors. The result is a progressive loss of photoreceptor cells, which starts at two weeks of age and is completed around three months. The RCS rat has been used extensively to assess different treatment strategies for photoreceptor degeneration (for more details see chapters 1.2.6.1, 1.3.2 and 1.3.4.4.2).

The pig eye is anatomically human-like, and unlike rodents, its retina has many cones. The transgenic pig model of RP expresses a rhodopsin mutation that causes retinal degeneration [160, 161]. Like RP patients with the same mutation, transgenic pigs have early and severe rod loss. Initially, cones are relatively spared but degenerate over time. By the age of 20 months, there is only a single layer of morphologically abnormal cones left and the cone-specific ERG is markedly reduced, resembling the pathological phenotype in RP patients with rhodopsin mutations. Even though the pig retina lacks a foveal-macular region, the retina has a significant higher amount of cones than the rodent retina. Therefore, the pig eye resembles the primate eye more closely. Given the strong similarities in phenotype to that of RP patients, the transgenic pigs provide a large animal model for study retinal degeneration (especially cone degeneration) found in RP.

In comparison with other animal models of photoreceptor degeneration, the dog model offers some advantages. In the dog, more autosomal gene loci causing photoreceptor degeneration have been identified than in any other species. The canine retina has a similar composition and distribution of cones, which apart from the fovea resembles that of humans. The large size of the dog eye allows intraocular procedures to be carried out more easily than in rodents and it also permits examination of different retinal regions of the same eye. The Briard dog (*Rpe65*$^{-/-}$ dog) is a canine model of a recessively inherited retinal disorder characterized by congenital night blindness with various degrees of visual impairment under photopic illumination [104]. Along with the visual impairment, affected dogs have an abnormal ERG trace and electron microscopy studies of the retina demonstrate large, lipid inclusions in the retina as well as disorientation of outer segment disc membranes. In Briard dogs a homozygous 4-bp deletion within the *Rpe65* gene was identified. The gene encodes a microsomal protein expressed exclusively in the RPE (see sections 1.1.4 and 1.3.4.4.3). Clinical features of the canine disease are similar to those described in human. Therefore this form of canine retinal dystrophy provides an attractive model of severe early onset retinal degeneration [104, 162, 163]. There are also two mouse models that carry mutations in the *Rpe65* gene: the *Rpe65*$^{-/-}$ knockout mouse and the natural occurring *Rd12* mouse [164, 165]. Both

models have severely reduced photopic and scotopic ERG responses as a result of low levels of photopigment. Functional and biochemical studies have confirmed that vitamin A metabolism and visual processing are disrupted. These mouse models can be used as initial templates for the development of therapies, that can be further evaluated in the Briard dog.

Primate eyes are the most similar to those of humans. Like humans, monkeys have a macula that is rich in cones. It has been shown that diurnal species, such as the rhesus monkey, have a fovea that consists of all three types of cones (red, green and blue). Macular changes that are similar to that in age-related macular degeneration in humans have been reported in the rhesus monkey. Because of the similarity to humans, monkeys would be the animal model of choice to investigate such disorders. However, due the long lifespan of monkeys, retinal degenerations occur over a longer period of time compared to the short-living mice and rats, making experiments long lasting. Further disadvantages are the small litter size, long gestational time, high costs, great housing requirements (space) and ethical problems (see [151] for a review).

1.2.6.1 The Royal College of Surgeon's rat

The main interest in the Royal College of Surgeon's (RCS) rat and its pathological condition relates largely to its potential value as an investigative model of human autosomal recessive retinal degeneration. In RCS rats the RPE fails to phagocytose shed outer segments due to a mutation in the *MERTK* gene and photoreceptor cells eventually die [68].

The RPE of RCS rats is unable to remove the outer segment material, which accumulates within the subretinal space. As a result RPE and photoreceptor cells lose contact and photoreceptor cells do not get any nutrients or oxygen. Consequently, photoreceptor cells undergo apoptosis which finally leads to progressive thinning of the neuroretina over time. An unusually phenomenon that is not seen in any other model of inhered retinal degeneration is the presents of a great number of pyknotic nuclei [166]. It is therefore likely that the

delayed clearance of pyknotic nuclei is a direct consequence of the phagocytic defect in this animal model. Some hemispheric differences and gradients of photoreceptor degeneration have been found between the superior and inferior hemisphere, with ONL cell loss in the inferior hemisphere occurring more rapidly than in the superior half. RCS rats also show a distinct central-peripheral gradient of cell loss. Degeneration of the peripheral retina is slowed by approximately 10 days compared with the degeneration in the posterior pole [167]. Similar observations have been made in the mer^{kd} mouse, a generated mouse model that carries a mutation within *MERTK* [82]. Before photoreceptor cell death during retinal degeneration, RCS rats show failure to phagocytise rod outer segments. This deficit leads to the formation of membranous whorls adjacent to the RPE surface. Furthermore, longer than normal outer segments are present and the rhodopsin content in the eye increases in the beginning of degeneration [82, 168, 169]. The membranous whorls consist of disorganised outer segment membranes and RPE cell processes. Phagosomes are absent in the RPE of the RCS rat providing direct evidence of the phagocytic defect [82, 167]. Another characteristic feature of the degeneration is the presence of vacuoles throughout the retina. They are thought to result from interphotoreceptor abnormalities either in osmotic composition or in abnormal transport and recycling of fatty acids [170]. However, it remains to be determined how the gene defect leads to vacuoles in the outer retina and if the vacuoles play a role in photoreceptor cell death.

In RCS rats, retinal abnormalities are first detected at two to three weeks of age. Photoreceptor cell loss is detectable histologically and electroretinographically from postnatal day 18 (P18) onward and subretinal accumulation of debris is apparent at that time [167, 169, 171]. Both scotopic a- and b-waves and photopic b-wave amplitudes decline rapidly over time. Usually after P40 neither scotopic nor photopic b-waves are recordable in response to bright stimuli. From P25 onwards invading macrophages and microglia are found in retinal sections [167, 172]. By P45 the whorls, abnormal outer segments and debris layer disappears and only a few pockets of debris membranes are found. At late stages of retinal degeneration the RPE shows small focal regions of thinning, although some regions of RPE appear thicker

than normal [167]. Depending on pigmentation of the animal the degeneration is virtually complete after 2 to 3 months.

Figure 1.9: **Time course of retinal degeneration in the RCS rat**. The pictures show semithin sections of a normal rat eye (8 weeks old; **9A**) and RCS rat eyes at the age of 4 **(9B)**, 6 **(9C)**, and 8 **(9D)** weeks. The loss of photoreceptor cells can be seen in the reduction of nuclei in the ONL. In normal rat eyes, 12 rows of nuclei are found. After the onset of degeneration the loss of photoreceptors is rapid. At the age of 4 weeks only 8 rows of nuclei remain and the formation of a debris layer in the subretinal space can be seen. Two weeks later only 4-5 rows of nuclei remain until at the age of 8 weeks almost all photoreceptors died (size bar = 50 µm).

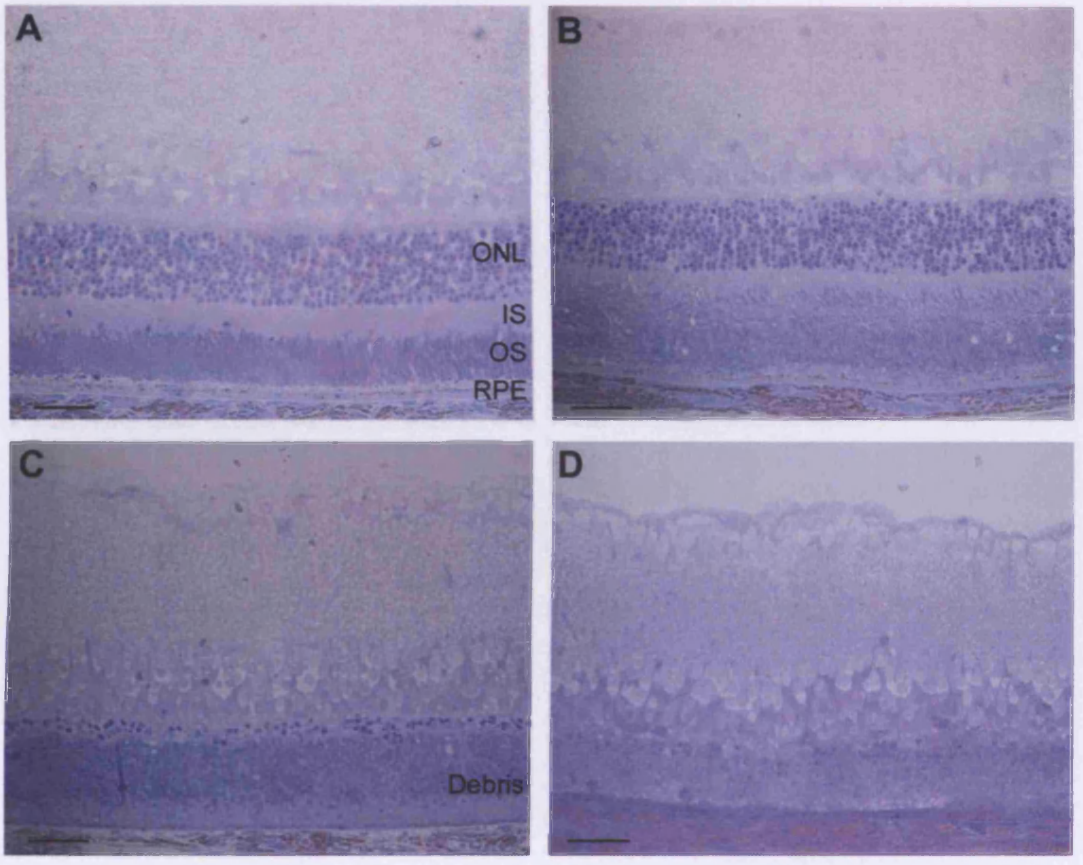

Using a positional cloning approach and sequence analysis D'Cruz and collegues identified the gene defect in RCS rats as the epithelial expressed receptor *MERTK* that is located on chromosome 3 in rodents [69]. *MERTK* is a member of a family of receptor tyrosine kinases, which also include Ax1, Sky, and Tyro3. All these molecules play an important role in the development and physiology in mammals and are proto-oncogenes, which are involved in several

types of malignancies (reviewed in [173]). In RCS rats there is a small deletion (409 bp) of genomic DNA that includes the splice acceptor site next to the second coding exon. This deletion results in the production of an aberrant mRNA in which the second coding exon has been skipped, leading to a frameshift and a stop signal only 20 codons after the start of the open reading frame. The aberrant mRNA is incapable of encoding a functional protein [69].

1.3 Therapies for retinal dystrophies

The clinical features observed in patients with retinal degenerative disorders reveal a large amount of heterogeneity. The complexity of the diseases makes it difficult to counsel patients or to develop efficient therapies. Currently strategies for retinal degenerations therapies include pharmacological treatments, intraocular injections of factors that prolong photoreceptor survival, transplantation of normal photoreceptors, RPE cells and stem cells, and gene therapy.

1.3.1 Pharmacological agents

Pharmacological strategies have the advantage that the treatment can be stopped at any time. Pharmacological agents can compensate for a biochemical defect and enhance or inhibit the activity of various effectors. Pharmacological agents usually can be taken orally or applied by injections. However, they need to be constantly administered. Since their effects are not targeted to a specific tissue, they might result in systemic toxicity and other long-term negative side effects.

It has been suggested that some types of Ca^{2+} channel blockers, such as nilvadipine, are able to preserve photoreceptor cells in the *rd* mouse model and the RCS rat and can potentially be used to treat some RP patients [174]. However, caution needs to be exerted in extrapolation to the comparable human forms of RP, as was highlighted by D-*cis*-diltiazem, another calcium channel blocker, that was successfully used to slow degeneration in the *rd* mouse but failed to show any effects in the *rcd1* dog – animal models for RP due to mutations in the PDE gene [175, 176]. RPE cells and choroidal endothelial cells are important cell types in the process of choroidal neovascularisation in AMD. It has been shown that the antiproliferative and antimigratory abilities of drugs modulating calcium-dependent signal

transduction (carboxyamido-triazole) on RPE cells and choroidal endothelial cells inhibit important substeps of choroidal neovascularisation. Therefore, they may be of value for the treatment of choroidal neovascularisation in AMD [177, 178].

Vitamin A has been used as a therapeutic and chemopreventive agent for some types of cancer and for the degenerative eye disease such as RP [179, 180]. Patients supplemented with a daily oral dose of vitamin A have shown a slightly slower rate of deterioration of retinal function, if the intervention is continued over several years. Up to 12 years of follow-up in these patients did not reveal any signs of liver toxicity as a result of excess vitamin A intake [181]. However, it is important to note that treatment with high doses of natural or synthetic retinoids overrides the body's own control mechanisms, and therefore carries with it risks of side effects and toxicity. Additionally, all of these compounds have been found to cause birth defects.

1.3.2 Neurotrophic factors

An alternative strategy to treat retinal dystrophies and a type of pharmacological treatment involves the use of neurotrophic factors. In all types of retinal degeneration, photoreceptor cell loss is caused by apoptosis. Apoptosis can be manipulated by a variety of different neurotrophic factors implicating that photoreceptor cell death can be delayed or even - to a certain degree – prevented by the delivery of different neurotrophic factors. This form of treatment has the advantage that it may be effective in disease with unknown genetic mutation. Since neurotrophic factors promote photoreceptor survival in general, this approach can be used not only for a specific form of retinal degeneration but for a wide range of disorders. To date many neurotrophic factors have been tested and their effects investigated in different animal models. Neurotrophic factors have also been delivered by viral vectors (see section 1.3.4.4) in order to achieve long-term expression and beneficial effects.

The first evidence that neurotrophic factors might be an efficient approach to treat retinal dystrophies, was the demonstration that injection of FGF-2 into the eye results in long-term survival of photoreceptor cells in the RCS rat [182]. It has been reported that FGF-2 slows the loss of rod photoreceptor cells in other animal models for RP including the *rd* mouse [183]. However, despite of the morphological preservation, FGF-2 treatment did not result in a functional improvement. FGF-2 is a widely distributed heparin-binding growth factor with a diverse range of actions critical in normal development, reproduction, angiogenesis and response of the nervous system to injuries. A potential disadvantage of FGF-2 is its lack of specificity and its angiogenic activity which results in neovascular complications.

Another neurotrophic factor with similar effects to FGF-2 is interleukin 1 beta (IL1-β). IL1-β has been tested in the RCS rat and has been shown to rescue photoreceptor cells from degeneration [184]. In addition to preserving photoreceptor cell number, IL1-β treatment also results in a preservation of rod inner and outer segments. Rescued photoreceptors have been shown to be functional and capable of conveying stimulus information. A problem associated with IL1-β is its dose dependent effect: beneficial effects on photoreceptor survival were retained at low dosage over a period of a few weeks. However, at high dosage this cytokine has been shown to be associated with extensive disruption of the retinal cytoarchitecture probably due to its proinflammatory actions.

Glia cell derived neurotrophic factor (GDNF) is a neurotrophic factor that is synthesized in the retina. Initially, it has been found that GDNF stimulates survival of mice photoreceptors suggesting possible beneficial effects in *vivo*. This theory has been proven true by the intraocular delivery of GDNF into eyes of different animal models of retinal degeneration, such as the *rd* mouse [185, 186]. GDNF delivery results in a significant morphological and physiological rescue of photoreceptor degeneration.

A drawback of this strategy is that the effect of the neurotrophic factors is relatively short lived, lasting only about a month in animals, although the effect may be much longer in humans considering the different life span. Delivery of drugs is one of the most significant problems to be solved when contemplating survival factor therapy. The survival promoting factors are peptides that do not cross the blood-retina barrier. This barrier must be bypassed, which can be accomplished with intraocular injection. Repeated injections are not only expensive and time consuming but also raise the risk of retinal detachment and endophthalmitis. In some studies significant proliferative response, including epiretinal membrane formation has been reported. This observation of toxicity caused by different survival factors pose another issue that has still to be investigated in more detail and has to be resolved before an efficient treatment can be realised. Yet, this problem can be solved by the delivery of growth factors via viral vectors (see section 1.3.4.4) or other biological and biochemical delivery systems.

Different neurotrophic factors have been delivered to animal models via adeno-associated virus (AAV) vectors [186, 231, 232, 244, 245]. CNTF was expressed intraocularly using AAV-mediated gene delivery in the *rds* mouse. It has been shown that CNTF reduces the loss of photoreceptor cells. Visual function, however, was significantly reduced compared with untreated controls [231, 232]. In summary, it has been demonstrated in different studies that the delivery of neurotrophic factors via viral vectors can result in a significant delay in retinal degeneration. Whereas FGF2 and CNTF result in long-term morphological protection they did not result in a functional improvement. In contrast, GDNF did lead to morphological as well as functional improvement [186, 245].

The effects of SIV-mediated subretinal transfer of pigment epithelium derived factor (PEDF) has recently been evaluated in RCS rats [246]. Significant delay of retinal degeneration up to 24 weeks and functional preservation but not prevention of photoreceptor loss could be shown by SIV-mediated delivery of PEDF in RCS rats. This result suggests the therapeutic value of PEDF. Even though the retinal protection might not be sufficient in humans, an additional delivery of PEDF in combination with other strategies, such as gene

replacement therapy or transplantation, might result in additional beneficial effects on photoreceptor survival.

Despite the encouraging aspects of these results in animal models, their clinical usefulness may be limited, because rescue effects are partial and transient and the mechanisms by which they occur are not well known and understood. Yet, they might be an useful tool in combination with other approaches. Perhaps survival factors together with other agents that exhibit protective effects on photoreceptor cell survival in retinal degeneration like antioxidants or anti-inflammatory agents might be more powerful and/or longer lasting than either agent on its own. Another possible use for growth factors is in combination with gene transfer approaches. Many specific mutant gene targeted therapies do not result in a permanent rescue and often the expression of the transgene is in therapeutical inappropriate levels. In both cases survival factors may provide a better protection due to their cell death inhibiting effects when co-delivered to the specific transgene.

1.3.3 Cell therapy for retinal dystrophies

The ultimate goal of cell therapy as a therapeutic strategies for different degenerative retinal diseases is either to replace lost photoreceptors with healthy ones and to re-establish the cellular connections with the inner nuclear layers or to successfully transplant RPE cells.

1.3.3.1 Transplants

Retinal transplantation was first performed in 1946 by Tansley *et al* [190] who transplanted embryonic ocular tissue into the brain of young rats and demonstrated retinal differentiation of the transplanted tissue. However, significant interest in retinal transplantation was not generated until the mid-

1980s when del Cerro *et al* [191] transplanted full-thickness strips of retina into the anterior chamber of a mouse and demonstrated survival of both allografts (donor and host from the same species) and xenografts (donor and host from different species). These original animal experiments involved transplantation of full-thickness retina. Over the last 15 years, many animal experiments have been carried out to improve transplantation protocols of different cell types into the eye and to prolong their life span in the host [192, 193]. A main problem, that still has to be overcome, is that transplants have a limited ability to integrate into the host retina. Animal experiments suggest that visual information may be received and transmitted by transplanted retinal tissue to the host brain but the quality of the transmitted information is undefined, and vision beyond simple light perception has not been demonstrated in patients.

Different retinal degenerations affect different layers of the retina. Mutations of the *MERTK* gene for example lead to a malfunction of the RPE and to degeneration of this cell layer. The loss of photoreceptor cells is secondary. The development of techniques to transplant retinal epithelium cells that remain viable and functional for relatively long periods of time has opened up the possibility of correcting such genetic defects by transplantation. In the past decade, the idea of replacing aged and/or diseased RPE with healthy RPE allograft or xenograft has been extensively investigated in the RCS rat [194-196]. It has been demonstrated that it is possible to transplant normal retinal epithelial cells into the subretinal space of dystrophic, congenic RCS rats. The host retina re-attaches over the transplant and host photoreceptor shed outer segments are phagocytosed by the transplanted RPE cells, thereby locally correcting the genetic defect. RPE transplants have been shown to survive in the subretinal space and prevent photoreceptor degeneration to some extent. These results raise the possibility that some blinding disorders in humans may be amenable to treatment by RPE transplantation. However, currently there is a major problem with rejection of transplanted cells. In most animal studies either immune suppression or congenic cells are required for long-term survival.

A number of clinical trials involving transplantation of either RPE or photoreceptor cells have been carried out. A patient suffering from non-

neovascular AMD received healthy fetal RPE cells as a suspension infused into the subretinal space with the aim of preserving photoreceptor cells. The patients vision, however, remained unchanged and fluorescein angiography showed leakage and staining at the level of the outer retina. Furthermore, there was an immune response against proteins associated with photoreceptors [197]. In another study, eight patients with RP and one patient with advanced neovascular AMD received subretinal transplants of fetal retinal photoreceptor suspensions. Even though light responses improved initially, visual improvement disappeared between 3 and 13 months [198].

For transplantation to become a viable therapeutic option for patients with retinal degenerations, a number of different problems will need to be overcome. New techniques are likely to be required to allow larger quantities of tissue to be transplanted into the subretinal space in the proper orientation. Approaches to enhance long-term survival of grafted tissue have to be developed. To develop a useful transplantation strategy for AMD and some forms of RP the survival of transplanted photoreceptor cells has to be ensured. This will require, among other things, healthy cells forming a layer between the remaining retina and the RPE. More reliable and reproducible methods of measuring visual function in patients with low levels of vision are essential. However, the largest hurdle is the establishment of functional connections between the graft and the host retina. Currently, experiments are carried out to replace lost or damaged photoreceptor cells by implanting sheets of photoreceptor cells grown in tissue culture onto the retina of animals [199, 200]. However, the transplanted cells have not yet successfully integrated effectively with the cells of the host retina. In other approaches, stem cells are being placed in the retina in an attempt to form functioning photoreceptors.

1.3.3.2 Stem cells

Recently, stem cell implantation as a regenerative strategy for treating retinal disease has become the object of extensive investigation. Stem cells are cells

that self renew and give rise multiple mature cell types. Many experiments have employed stem cells or neural precursor cells derived from the developed retina or brain [201-204].

Embryonic stem cells (ES) are pluripotent and can be induced under specific conditions to differentiate into almost any cell type including neurons (reviewed in [205]). ES have been shown to cause tumours when introduced into animals [206] and therefore it is important for clinical applications that ES undergo a certain degree of differentiation before introduced into the target tissue. ES can be induced to generate neural progenitor cells in *vitro* that can be used as therapeutic agents. These cells have been injected intravitreally into *rd* mice, a model for autosomal recessive RP that carries a mutation in the β-PDE gene (see chapter 1.2.6.). Cells have been shown to migrate to the inner retina, integrate into the neuroretina and develop neuron like processes. However, donor cells did not differentiate into photoreceptors, a potential limitation of this approach [203].

An alternative to embryonic stem cells are retinal stem cells, which are multipotent precursors that give rise to the retina during development (see chapter 1.1.1) [207]. While retinal stem cells are present throughout life in lower vertebrates, they have little activity after the eye cup formation in mammals [18]. However, it is possible to isolate retinal stem cells from postnatal mouse retina and culture them. Stem cells that are derived from the central nervous system (CNS) have been injected into the vitreous of RCS rats. This resulted in cells integrating into the degenerating retina and there was some suggestion of differentiation into neurons [204]. However, there is little evidence to suggest that the cells had differentiated into retinal neurons in this or in any other study involving transplantation into animal models of retinal degeneration [201, 208].

A major issue facing stem cell therapy for retinal dystrophies is the question of functional integration of grafted cells. Furthermore, experiments need to be extended to larger animal models, such as the pig, the dog and monkeys, to demonstrate efficiency in settings more closely to humans. Studies of larger

animal models will allow a more accurate assessment of functional relations and facilitate the development of applicable cell delivery strategies. Furthermore, retinal stem cells of humans need to be isolated and characterised. However, stem cells have a promising potential and play an important role in the development of strategies directed towards retinal dystrophies.

1.3.4 Gene therapy

Gene therapy may be one of the most important developments in medicine. Since gene therapy may be able to correct the underlying genetic defect rather than just focusing on symptoms it might be able to provide an effective treatment for otherwise incurable diseases. Nevertheless, before this can be realised certain technical problems common to all methods of gene delivery must be overcome.

Gene therapy for other diseases has already moved from the laboratory into the clinic. Severe combined immune deficiencies (SCIDs) is characterised by a disturbances of lymphocyte development and function resulting in immune system disfunction [209]. Affected individuals are inclined to infections and without treatment do not survive beyond the first year of life. SCIDs comprise a group of monogenic diseases of which the main two disorders are X-linked SCID (SCID-X1) and adenosine deaminase-deficient SCID (ADA-SCID) [210]. General treatment options for the latter disorder include transplantation of bone marrow, injections of synthetic ADA and gene therapy. Bone marrow transplants from normal, histocompatible, donors would ideally give the child a continuous source of ADA^+ T and B cells. However, even though the child cannot reject the transplant because the child has no immune system, T cells in the transplant (unless the donor was an identical twin) can attack the cells of the child producing graft-versus-host disease. ADA injections have been tested in clinic and have shown to keep patients healthy. ADA is currently conjugated with polyethylene glycol (PEG) to delay its breakdown in the blood but, as it is

the case with diabetic patients and insulin injections, injections of PEG-ADA must be repeated frequently [211]. Virus-mediated gene therapy on the contrary would not result in an immune response and does not require constant treatment. The first clinical trial was started in September 1990 when scientist treated 4-year old Ashanthi DeSilva who was born with ADA-SCID. Ashanti carried a defective version of the gene that encodes ADA. In the first attempt to treat the disorder, her own T cells were stimulated to proliferate, infected with retroviral vectors that carried a functional copy of ADA and then injected. The treatment resulted in an improved immune function but the injections had to be repeated because T cells live for only 6–12 months in the blood. However, she was treated with PEG-ADA for additional benefits. Therefore, it is not certain whether the introduction of the therapeutic gene into her white blood cells deserves the credit (reviewed in [212]). In 2002, the first successful gene therapy treatment of two young ADA-SCID patients was reported. They were treated with their own blood stem cells that had been transformed in *vitro* with the ADA gene. After a year, both children had fully-functioning immune systems and were able to live normal lives without any need for additional treatment such as ADA-PEG [213].

SCID-X1 is due to a mutation of the γ-c chain gene encoding a number of multiple cytokine receptors including interleukin-7 (IL-7). IL-7 is essential for converting blood stem cells into the progenitors of T cells. Boys with SCID-X1 can make normal B cells but because B cells need T-helper cells to function, these boys had neither cell-mediated nor antibody-mediated immune responses and had to live in a sterile bubble before their treatment. In October 2002 it was reported that 3 out of 15 children suffering from X-linked SCID showed the first symptoms of a leukaemia like syndrome, 30 months after receiving genetic treatment [215, 216]. Later insertional mutagenesis of the viral vectors into the oncogene LMO2 has been framed to be the cause of the T cell leukaemia [217]. However, now four years after the treatment the other 12 children live normal lives at home instead of inside a sterile "bubble", they have normal T cell numbers, and their antibody production is sufficiently good so that they have no need for frequent injections of immune globulin.

The incidence was taken seriously by the scientific world and dramatic progress has been made in the basic science of viral and non-viral vector development used to transfer genes into patients over the last few years [218]. In order to further develop this technology it is necessary to identify genes involved in diseases, to improve the regulation of the transgene expression and to upgrade gene delivery systems. Frequencies and mechanisms of vector integration into the host genome have to be understood better in order to seek a way to gain accurate control over the integration process.

Figure 1.10: Clinical trials. (a) Number of clinical trials world wide. **(b)** Clinical trials by diseases (http:// 217.215.32.12/trials).

(a)

Continent	Number
America	662 (67.1 %)
Europe	277 (28.1 %)
Asia	19 (1.9 %)
Australia	17 (1.7 %)
Africa	1 (0.1 %)

(b)

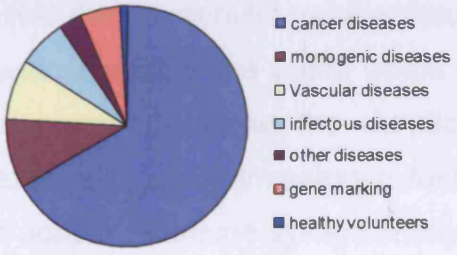

Indications	Number	Percent
cancer diseases	656	66.5
monogenic diseases	93	9.4
Vascular diseases	80	8.1
infectious diseases	65	6.6
other diseases	29	2.9
gene marking	52	5.3
healthy volunteers	12	1.2
total	987	100

1.3.4.1 Gene therapy and the immune system

One of the main challenges of gene therapy is to circumvent the host immune system. When pathogens enter the body an innate immune response develops quickly and causes the generation of cytokines and an influx of non-specific inflammatory cells such as macrophages and dendritic cells. These non-specific cells recognise pathogenic epitopes in the viral capsid or bacterial membranes via specific receptors. The recognition results in the production of proinflammatory cytokines and a stimulation of the adaptive immune system. The adaptive immune system is activated later on by antigen-presenting cells (APCs) that carry antigens from pathogens to the lymph nodes. There they evoke a lymphocytes response of $CD4^+$ and $CD8^+$ T cells which consequently leave the lymph nodes. Via specific T cell receptors the specific, APC-presented, pathogenic epitopes are recognised and the production of proinflammatory cytokines (such as IL-1 and TNF) is stimulated. $CD8^+$ T cells eliminate the infected cell by secreting cytotoxic substances like INFγ. The interaction of the pathogen with B cells results in the production of antibodies (ABs), which are able to bind to the pathogen and thereby launch a chain of reactions that ultimately neutralise the microorganismus. The final success of each gene therapy approach depends in large part on the ability of the vector to deliver the therapeutic gene without evoking an immune response. An immune response against the vector would eliminate the vector and the transfected cells and hence decrease the duration and intensity of transgene expression. Additionally, proinflammatory cytokines have a cytotoxic effect. The activation of the adaptive immune system finally results in the generation of a "memory" that renders re-administration of vectors difficult.

Strategies to circumvent immunity of vectors, including vector alterations, pseudotyping, immunosuppression, the generation of "tolerant" APCs and alteration of the vector structure, have been developed to increase safety of gene therapy approaches (see [219-221] for reviews). One of the main advantages of retro- and lentiviral vectors for gene therapy is that they generally

do not induce an immune response. Immunity is usually targeted against the transgene rather that the recombinant virus. However, retro- and lentiviruses can be inactivated in the serum by the complement system and a cytotoxic response [222, 223]. Immune responses to other vectors are various and depend on the vector's characteristics (see chapter 1.3.4.4), the dose, route of administration, the transgene and host related factors. One possible way of a non-viral gene therapy approach employs plasmid derived from bacteria. These plasmids can – when delivered on their own or in combination of liposomes or electroporation – evoke an innate immune response. It has been demonstrated that bacterial DNA includes CpG motifs more frequently than eukaryotic DNA. The CpG motifs have an immune stimulating character and induce cytokine production as well as an activation of the adaptive immune system. The level of immune stimulation is dependent on the level of methylation of the CpG motifs. Strategies to avoid an immune response against bacterial plasmids include the elimination or methylation of these motifs [224, 225].

Another problem is the immune response against the transgene itself. Gene replacement therapy introduces a gene that is normally not expressed in the patient. If APCs present this unknown gene to $CD4^+$ T cells they might respond with the production of cytokines. An activation of B cells might result in the production of ABs against the therapeutic gene and $CD8^+$ T cells might develop a cytotoxic response. Therefore a specific tolerance has to be induced prior to any contact with the transgene. This is possible by the administration of the gene of interest without any non-human sequences that could boost the immune system. Without these costimulatory signals the transgene is introduced to T cells making them "unresponsive" to the specific transgene. In this state T cells would not be activated by this specific transgene even with costimulation of a virus.

1.3.4.2 The eye as a target for gene therapy

Inherited retinal dystrophies comprise a large number of disorders characterised by a slow and progressive retinal degeneration. There is currently no treatment by which the primary disorder can be modified. To date much work has been – and still is – done to develop different therapeutic approaches to solve this problem. These approaches are based on the possibility of modulation of cell death by pharmacological substances, growth factors, transfecting photoreceptor and RPE cells with functioning genes, or transplanting photoreceptor, RPE cells or stem cells into the subretinal space. Most of the strategies so far have been limited in success. Gene therapy appears the most promising approach to date. Conditions or disorders that arise from mutations in a single gene are the best suited candidates for gene therapy and there are many monogenic disorders leading to retinal degeneration.

The eye is an attractive target for gene therapy because of its accessibility that facilitates an in *vivo* examination by ophthalmoscopy. Another advantage is the immune privilege of the eye, which reduces the risk of stimulating immunocytes and therefore enhances the effectiveness of gene therapy approaches. The blood-retina and the blood-aqueous barrier concentrate the vectors and reduce their spread out of the eye. Since the eye consists of a variety of tissues, for example endothelium, epithelium, muscle and neurons, it might be used to test and investigate the delivery of transgenes to different cell types [226].

The delivery of the transgene to a specific tissue is of significant importance. There are several possible sites for introducing genes into the eye. Intravitreal injection is a relatively safe and easy method of approach but potential complications such as vitreous haemorrhage, retinal detachment, and endophthalmitis cannot be ignored. Furthermore, studies using animal models have found that while intravitreal injections result in efficient AAV-mediated ganglion cell transduction, transduction efficiency is lower for outer retinal layers [227]. Therefore, it is important to deliver the vector as close as possible to the target cell type. The retina-blood barrier restricts the permeation of large

molecules and there is evidence that neural retina is also a diffusional barrier for macromolecules. The neural retina is a multilayer consisting of various cell types. Among these layers, the internal and external limiting membranes and the interphotoreceptor matrix, which is rich in glycosaminoglycans, might have barrier properties. Therefore, subretinal injection, which produces a local and often transient detachment of the retina, has so far been the most favoured means of accessing the photoreceptor layer and the RPE [228, 229].

Recently significant progress regarding in *vivo* gene transfer to photoreceptors using viral vectors to delay photoreceptor loss and prolong and improve retinal function has been achieved in different animal models of retinal degeneration [105, 230-233].

1.3.4.3 Therapies for monogenic dominant disorders

Monogenic recessive diseases require the functional gene to be expressed in therapeutically useful levels in order to alter the patho-physiological state. Replacing or augmenting a defective gene by delivering its wild-type counterpart, thus offers a potential means to correct the pathogenic basis of the disease (see section 1.3.4.4). Monogenic dominant diseases are more complicated to treat, since the addition of a healthy allele may not be enough because its disease causing, malfunctioning counterpart may have a toxic effect on the cell. Therefore, the aberrant gene needs to be silenced.

Antisense oligonucleotides have been used to demonstrate downregulation of the expression of a photoreceptor-specific protein, *rds*/peripherin in *vitro*. However, oligonucleotides are poorly stable in *vivo*, have a low intracellular penetration and are quickly eliminated form the vitreous. Administration of oligonucleotides are therefore repeated. Although, antisense oligonucleotides that target VEGF delivered via intravitreal injection have been shown to reduce iris neovascularisation in a non-human primate model [234], to date there have

been no successful in *vivo* treatments for dominant retinal degenerative diseases.

Another approach to address dominantly inherited diseases is the use of ribozymes, small RNA molecules that cleave mutant transcripts in an allele-specific manner while leaving wild-type transcripts intact [235]. Twentyfive percent of all RP cases are due to mutations in the rhodopsin gene. The inheritance pattern is autosomal dominant. The most common mutation is a substitution of histidine for proline at codon 23 (P23H), resulting in photoreceptor cell death from the synthesis of the abnormal gene product. Ribozymes can discriminate and catalyse the in *vivo* destruction of P23H mutant mRNAs in a transgenic rat model of autosomal dominant RP. Recombinant adeno-associated virus (rAAV) vectors were used to deliver ribozyme genes to photoreceptors. Expression of the ribozyme, slowed the rate of photoreceptor degeneration for at least 8 months and resulted in significantly greater (93 %) electroretinogram amplitudes in comparison to untreated control animals [236, 237].

The most effective way of ablating mRNA is through the use of small interfering RNA (siRNA). siRNAs are small double stranded RNA molecules, which, when inserted into a cell, interfere with post-transcriptional processing of the endogenous mRNA and thereby specifically turn off the expression of a certain gene. siRNA targeted against VEGF has been shown to effectively inhibit laser-induced choroidal neovascularisation in a mouse model and in non-human primates [238, 239]. These results show the potential value of RNA interference for the treatment of retinal diseases that involve abnormal blood vessel growth and is now being tested in patients with AMD [240]. In *vitro*, siRNA has been used to target rhodopsin in a mutation independent approach. Degeneracy of the genetic code was used to engineer a codon-exchanged mRNA. In these experiments, native transcripts are suppressed by a single RNAi molecular species, whereas transcripts from genes engineered at degenerate third-codon wobble positions are resistant to suppression. Suppression levels of the native transcript were up to 90 %. The result was confirmed in retinal explants [241, 242].

These technologies are however limited by the large number of dominant mutations in different genes and by the accessibility of the ribozyme or siRNA to the transcript [243]. In order to overcome this problem, strategies to deliver neurotrophic factors that promote photoreceptor survival have been developed (see chapter 1.3.4.4).

1.3.4.4 Virus-mediated gene transfer for retinal degenerations

The ideal vector should fulfil different requirements that are necessary for an efficient treatment. Preparation of this vector would be relatively simple (e.g. not involving multiple steps such as attachment of a ligand targeting a particular cell type) and result in high vector concentrations. The ideal vector should be able to deliver the transgene to a specific target cell type without it spreading elsewhere. Many viruses have preferences for specific cell types, for example the natural tropism of HIV-1 to $CD4^+$ cells, or they infect a wide range of cell types, like adenoviruses. However it is possible to change this tropism by pseudotyping. Another regulatory element for tissue specificity is the choice of the promoter. The most frequently used promoters are viral in origin, often derived from a different virus than the vector backbone, for example the cytomegalovirus (CMV) promoter has been used in all vector systems. Viral promoters have the advantages of being smaller, stronger and better understood than most eukaryotic promoter sequences. One of the drawbacks of viral promoters is their tendency to be silenced when there is an immunological response and that many of them are ubiquitously active in all tissue types [247]. A temporal expression of the transgene can be controlled by inducible promoters such as the tetracycline promoter, which has been shown to lead to sustained inducible transgene expression in retinal ganglion cells in mice and rats [248-250]. Expression of the transgene should be in appropriate therapeutical levels and over a designated period of time, which in case of monogenetic inherited disorders would mean permanent expression. To successfully achieve this, efficient uptake of the virus into the target cell has to

be ensured. The transgene should be expressed without inducing harmful side effects. To allow subsequent re-administration and avoid undesired host reactions there would be no significant immune response to any component of the vector. The lack of an immune response may allow transgene expression to be sufficiently prolonged from episomal systems, such that re-administration is not necessary. Alternatively, integration into the host genome, preferably in a site-specific location, would ensure that the transgene is not lost during the lifetime of the cell. Furthermore, endocytosis and lysosomal degradation of the virus must be avoided [46].

Viruses can be regarded as highly developed biological machines that have successfully evolved a way to gain access to eukaryotic cells. Once they have entered into the host cell they use the host's innate cellular machinery for their own replication. For most gene therapy applications the optimal virus-based vector employs the viral infection pathway but at the same time avoids the negative effects of a viral infection such as viral replication of the virus and toxicity. To accomplish this, coding regions that are normally necessary for viral replication and packaging are deleted from the viral genome. Instead of these viral sequences, a transgene of choice is cloned into the viral backbone. The recombinant vector particles are then produced in packaging cell lines, in which the vector genome and the packaging construct are co-transfected. The complementing packaging plasmid delivers genes necessary for replication and packaging in *trans*. Normally, vectors are designed in a way that they share no homologous sequence, thereby reducing the risk of generating replication proficient wild-type virus by homologous recombination. For gene therapy approaches, four main classes of viruses have been used. These can be separated into two groups: retroviruses including the family of lentiviruses which integrate their genome into their host's whereas the genome of adeno-associated viruses, adenoviruses, herpes viruses persists as extrachromosomal episome. Initially, gene therapy was only targeted against monogenetic inherited defects but to date acquired disorders, such as cancer or infectious diseases, form the main field of gene therapy research. The diversity of the diseases makes clear that no single vector is suitable for all applications. Each

of these viruses has advantages and disadvantages as vectors for gene therapy (reviewed in [251]).

Gene therapy approaches for ocular diseases have relatively recently started to develop. However, many different types of vectors have been successfully used to deliver reporter genes and therapeutical transgenes into different animal models of ocular disorders, suggesting the potential for targeting the eye. To date, experiments have shown that non-neuronal cells of the retina and in particular RPE cells are efficiently transduced by different viral vectors. This data suggests that retinal degenerative disorders, which arise from mutations within genes specifically expressed in the RPE, are most suitable for gene therapy approaches. A major challenge which still needs to be addressed is to further improve the efficiency of transduction of photoreceptor cells and other neuronal cell types in the retina and to reduce immune responses against different viruses in order to prolong transgene expression.

1.3.4.4.1 Herpes simplex virus-based vectors

Herpes simplex viruses (HSV) are a family of large, complex viruses; of which several are known to be human pathogens. The viral genome is a linear, double stranded DNA molecule of approximately 152 kb. Since most of the viral genes are dispensable for viral growth in tissue culture, more than half of the viral genome can be deleted allowing the insertion of large transgenes including complex regulatory elements. Further advantages are the easy manipulation and the production of high titre viral suspensions. Their episomal nature in the latent state also avoids problems of disruption or activation of cellular genes that could occur with vectors, which integrate into the cellular genome such as retroviruses. To minimise the risk of cytotoxicity all viral gene expression must be abolished and the possibility of generating wild-type virus avoided.

Wild type HSV enters its host via epithelia and spreads to neuronal cells where latency, in which the virus persists as an intranuclear episome, is established.

Interest has mainly focused on HSV-1, a neurotropic human virus, as a vector for gene transfer to the nervous system. Two main types of HSV-based vectors have been reported in gene delivery approaches - recombinant viruses and amplicons [252]. Spencer and colleagues [253] used a replication competent, attenuated HSV virus. The virus is deleted for essential in *vivo* virulence genes but retains the ability to be propagated in *vitro* and limited replication capacity in *vivo*. Therefore, the virus can be easily grown to high titres without helper cell lines or viruses. The virus was tested in rats and mice in *vivo* and the transduction pattern was evaluated after different application routes. The authors suggested that after topical delivery to the cornea, transgene expression in the corneal epithelium was apparent with occasional cells expression in the iris pigment epithelium, trabecular meshwork, and the ciliary body. They also claimed that intracameral and intravitreal injections resulted in transduction of approximately 75 % of the RPE and weak transduction of the ciliary body and cells of the trabecular meshwork as well as the corneal endothelium [253].

While gene transfer to the eye using recombinant HSV have been evaluated in several studies [253, 254], the potential of amplicons has only recently been explored [255]. The HSV amplicon contains bacterial and viral origins of replication, to allow easy manipulation in E. coli, and a viral packaging signal. After infection of the amplicon and HSV helper virus in eukaryotic cells, the amplicon is amplified and packed into virions. Hybrid vectors, which incorporate the AAV inverted terminal repeats (ITR) into the amplicon plasmid have been generated to increase the target cell spectrum. If in addition the AAV *rep* gene is present the virus gains the ability to integrate into the host genome. It has been demonstrated that HSV/AAV hybrid vectors can be packaged into HSV-1 virions, thereby exploiting the large transgene capacity of HSV-1. Moreover, upon infection of human cells, the hybrid vector genome directs the integration of transgenes into the AAVS1 locus. However, the AAV *rep* gene inhibits HSV-1 DNA replication, which drastically reduces the titres of HSV/AAV hybrid vectors, compared to that of standard HSV-1 amplicons [256-258].

Amplicons, in which the AAV ITRs but not the *rep* gene have been included, have been tested in *vitro* and in *vivo*. In these vectors the *gfp* gene was either under the control of the CMV promoter or the RPE-specific *rpe65* promoter. Transduction profiles of HSV amplicons after subretinal delivery into rat eyes have been evaluated. Efficient transduction with both vectors, which was restricted to RPE cells was observed. However, transgene expression was apparent as early as 24 hr after delivery but was transient and undetectable 6 weeks after injection [255]. Therefore it was concluded that HSV amplicons allow early onset and efficient transfer to the RPE. The transient nature of gene expression, however, limits the usefulness for gene replacement therapy and is probably due to an immune response to the HSV capsid.

1.3.4.4.2 Adenoviral vectors

Adenoviruses (Ad) are non-enveloped viruses, which contain a linear, non-segmented double stranded DNA genome. Many Ad serotype strains, even though not highly pathogenic, are associated with infections in humans, in particular of the respiratory tract. The lifecycle of Ad normally does not involve integration in the host genome but they replicate as episomal elements in the nucleus of the host cell and therefore there is no risk of insertion mutagenesis. DNA fragments up to a size of 30 kb can be incorporated into these vectors. The production is easy and virus suspensions can be purified to high titres. Whereas Ad vectors have several advantages over other vector systems, limitations have become apparent with their use in *vivo* (reviewed in [259]).

First generation Ad vectors carry deletion of the E1 and/or E3 regions, viral genes that are involved in modulation of the cell cycle, viral DNA replication, and invasion of the host immune system [260, 261]. The major disadvantage of the first generation of Ad is that they evoke immune responses against the viral vector capsid proteins and infected cells expressing viral antigens. Therefore transgene expression in *vivo* is transient and disappears 1 to 2 weeks after delivery. To circumvent this problem, second generation Ad vectors have been

constructed by further deletion of additional early genes necessary for viral DNA replication [262, 263], in order to minimise the immune response, abolish the potential oncogenicity, to make vector replication deficient as well as to expand the cloning capacity of adenoviral vectors. Since E1 proteins are essential for viral replication, they need to be delivered in *trans* (helper dependent Ad vectors). The third generation Ad vectors, also called gutless or mini Ad vectors, are deleted of more viral genes. They only retained the viral ITR and packaging sequences and required helper virus and appropriate complementing cells for propagation, followed by careful purification. Nevertheless, there were problems associated with these techniques, mainly due to contaminating helper virus and vector instability [264-267]. They have been shown to give less immune response and hence resulting in longer transgene expression. Encapsidated Ad mini-chromosomes (EAM) contain only the ITR and five *cis*-acting Ad encapsidation signals necessary for packaging but no viral coding sequences. These vectors can accommodate up to 36 kb of exogenous DNA and are unable to express viral proteins [268, 269]. EAM vectors are produced by replication in the presence of a helper virus, which provides all necessary viral proteins in *trans*. Thereby cytotoxic effects due to *de novo* synthesis of Ad proteins of earlier generations of Ad are reduced [270]. It has been shown that EAMs can transduce retinal cells. EAM-mediated delivery of the β-PDE to *rd* mice resulted in a prolonged photoreceptor survival up to 12 weeks post injections [271].

The ability of Ad vectors to deliver and express genes at high levels, especially in *vitro*, has been demonstrated over the last two decades. However, the immune response in *vivo* has been a limiting factor in the development of vectors for human applications. It is critical to control or to suppress the immune response to the vector and the transgene where persistent expression is needed in the case of supplementing the activity of a faulty gene. However, the first lifetime phenotypical correction of a gene defect using Ad vectors has been reported recently [272]. Safe and permanent correction of a liver-based genetic, autosomal recessively inherited disease (Crigler–Najjar (CN) disease type I) has been demonstrated in rats for more than 2 years after the delivery of the therapeutic gene via helper dependent Ad.

Ad vectors have also been extensively studied for in *vivo* gene transfer to the eye. The virus is able to transduce a wide range of different cell types in the eye but favours transduction of the RPE as well as Müller cells of the neuronal retina following subretinal injections into the adult mammalian eye [273]. However, even in the immune privileged retina, immune reaction to Ad vectors appear to limit its effectiveness to 3 to 8 weeks in mice, suggesting that vectors antigens are recognized and responded to relatively normally in the subretinal space [274]. Photoreceptor cells are poorly transduced by the virus, but transduction efficiency is higher if the photoreceptor cell are in the process of development, as it is the case in neonatal mice shortly after birth or in the process of degeneration, for example in young adult *rds* mice. In these cases, photoreceptors are more accessible to virus. The former finding is of no clinical importance though, because photoreceptor cells in humans are fully developed at birth.

An example for the utility of Ads in ocular gene therapy is the rescue of the RCS rat. Recently it was shown by Vollrath *et al* [233] that 1 month after treating the RCS rat with rAd containing the *MERTK* gene, the number of photoreceptor cells was 2 to 3 fold higher in areas of injections and photoreceptor function was maintained. The authors show that the phagocytic function of the RPE was restored and that photoreceptor activity one month after injection was higher. In this study, however, the survival of the photoreceptors was not followed over time and it is therefore unclear how long the improvements lasted. These experiments provided the formal proof that the *MERTK* gene is the actual cause of the disease in these animals and indicated gene therapy for this form of RP may be possible [233].

1.3.4.4.3 Adeno-associated viral vectors

Adeno-associated viral (AAV) vectors have generated considerable interest recently. AAV belong to the family of parvoviruses, which are among the

smallest, simplest eukaryotic viruses. Essentially, they fall into two groups, defective viruses that are dependent on helper virus for replication and autonomous, replication-competent viruses. Their wild-type genome is a single stranded DNA molecule. AAVs are not associated with any human disease and therefore are considered to be safer than other viruses for the development of gene therapy approaches for human disorders. AAV exist in different serotypes. They differ in their cell surface receptors, heparin sulphate and sialic acids, which results in different cell tropism of viruses. Therefore, it is possible to use different serotypes to target specific cells in *vivo*. A number of serotypes are currently under development as clinical gene delivery vectors for the treatment of human diseases but AAV-2 is the most extensively studied and used (for a review see [275]). A route to alter the cellular tropism of rAAV is pseudotyping. Constructs are employed that encode *rep* from one serotype whereas the *cap* gene is derived from the serotype or another virus displaying the cell tropism of choice [221]. The cellular tropisms of different serotypes in the eye are discussed in more details in section 3.8.

The main advantages of AAVs are that they are capable to infect both, dividing and non-dividing cells and that the wild-type AAV integrates into a specific point on chromosome 19 of the host genome at a high frequency. However, rAAV lacks the ability to do this and only a small percentage integrates into the genome (1-5 %) whereas most of the virus remains in the nucleus as an episome. rAAV vectors (see figure 1.11) are deleted for all virally encoded proteins and these sequences are replaced by the transgene of choice. Since all viral proteins are missing, their immunogenicity is remarkably reduced. In contrast to Ad, AAV do not induce a innate immune response. However, they induce an adaptive immune response, even though it is much weaker than that evoked by Ads (see [276] for a review). A possible reason for this is that AAVs different than Ads are unable to infect mature APCs. AAVs can infect immature APCs, which would lead to a specific T cell response and in turn would decrease transgene expression. However, this immune response would only develop if enough immature APCs would be at the site of infection. Therefore, AAV usually does not induce a sufficient T cell response. In some cases however, a T cell response can occur against the transgene. Administration of

Ad and AAV vectors also results in a presentation of viral capsid antigens to B cells. This induces the production of neutralising antibodies (ABs) against the capsid, which can prevent infection by vectors and render readministration of the vector difficult. Another problem is the pre-existing immunity in humans against both Ad and AAV. A majority of the population has specific ABs against Ads and AAVs because of viral infections. These ABs are able to neutralise viral vectors, induce an inflammatory response and thereby reduce the efficiency of vector infection.

Figure 1.11: rAAV. (A) Schematic diagram of wild-type AAV genome and the rAAV production plasmid. ITR=inverted terminal repeats; rep=AAV replication and integration associated gene; cap=AAV capsid encoding gene; CMV=cytomegalovirus promoter; transgene=gene of interest. **(B)** Schematic diagram of rAAV production. The rAAV plasmid, which carries the gene of interest, and a helper plasmid providing the rep and cap genes in *trans* are co-transfected into BHK cells; the cells are subsequently infected with HSV (or another helper virus) and after 72 hr the rAAV particles are harvested.

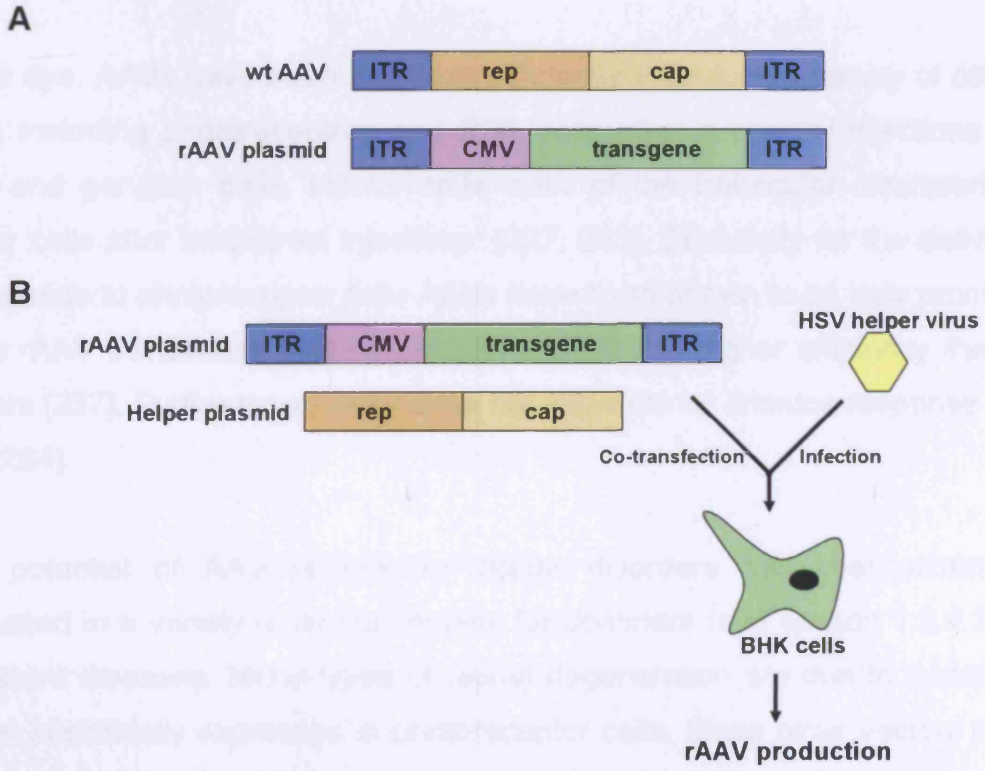

Transduction by AAV vectors results in an efficient expression of the transgene. Interest in AAV vectors has been due to the prolonged transgene expression compared to Ads. However, the total length of the insert is relatively small and cannot exceed ~5 kb, which is approximately the length of the wild-type genome. Another disadvantage of AAV is a delay in the onset of expression for most serotypes lasting between two and four weeks depending on the treated species (see also chapter 3.8).

Recently AAV has been used to specifically target genes [277-280]. This reduces the potential risk of disrupting essential genes or causing malignant transformation of the target cells and ensures long-term expression since the viral genome is integrated into the host genome. It can also be used to switch off the expression of certain genes. Gene targeting is the precise alteration of a specific chromosomal site by an AAV vector. Although this achievement is of minor importance for gene therapy applications in the eye, AAV gene-targeting vectors are promising vehicles for gene therapy in other disorders [278, 281].

In the eye, AAVs have been shown to efficiently transduce a variety of different cells, including photoreceptors and RPE cells after subretinal injections [228, 282] and ganglion cells, bipolar cells, cells of the trabecular meshwork and Müller cells after intravitreal injections [227, 283]. Especially for the delivery of transgenes to photoreceptor cells AAVs have been shown to be very promising, since rAAV transduces these cells with a 2000-fold higher efficiency than rAd vectors [227]. Furthermore, rAAV does not stimulate an immune response in the eye [284].

The potential of AAV vectors for ocular disorders has been extensively evaluated in a variety of animal models for dominant (see section 1.3.4.3) and recessive diseases. Many types of retinal degeneration are due to mutation in genes specifically expressed in photoreceptor cells. Since other vectors mainly transduce RPE cells, AAVs are a promising tool to deliver a functional copy of the mutated gene for this group of disorders.

Peripherin-2 (*Prph2*, *rds*) is a photoreceptor-specific glycoprotein that localises in the outer segments in a complex with rom-1. Peripherin-2 is necessary for the stabilisation of photoreceptor outer segments where the phototransduction cascade takes place. Mutations in *prph2* have been shown to result in a variety of photoreceptor dystrophies, including autosomal dominant or recessive RP and macular dystrophy. The retinal degeneration slow (*rds* or $Prph2^{Rd2/Rd2}$) mouse is homozygous for a null mutation in *prph2* and is characterised by a complete failure to develop photoreceptor outer segments. ERG recordings show diminished a- and b-wave amplitudes which decline to virtually undetectable levels by two months. It has been shown that after subretinal delivery of an AAV-2 vector expressing a functional copy of *prph2*, stable generation of outer segment structures occurs containing both peripherin and rhodopsin. Furthermore, ERG traces showed an improvement of retinal function for at least 2 months. That was the first successful in *vivo* gene therapy approach that aimed to correct a photoreceptor-specific defect [230, 285].

Retinitis pigmentosa GTPase regulator (RPGR) is a photoreceptor protein which is coupled to the connecting cilia via RPGR-interacting protein (RPGRIP) [286]. RPGR is thought to control the function and/or organization of the photoreceptor outer segment [287]. Mutations in *RPGRIP* are associated with LCA in humans [288]. The *RPGRIP* deficient $RPGRIP^{-/-}$ mouse has an early onset of photoreceptor degeneration that is virtually completed at the age of 3 months. The rapid course of the disease in this animal model corresponds with the course of the disease observed in LCA patients. Recently, it has been shown that AAV-2-mediated expression of a functional copy of the *RPGRIP* gene after subretinal delivery results in a restoration of retinal function and prolongation of photoreceptor survival in $RPGRIP^{-/-}$ mice for more than 5 months. These data demonstrated the value of AAV-mediated gene therapy for photoreceptor-specific defects [289].

Mutations in the human *Rpe65* gene are responsible for autosomal recessive early childhood blindness including LCA and early-onset RP [100]. Defects in the *Rpe65* gene, which is selectively expressed in the RPE, result in blindness and gradual photoreceptor cell degeneration [104]. The $RPE65^{-/-}$ Briard dog is a

naturally occurring animal model that carries a mutation within this gene and it has been used to develop an AAV-mediated gene replacement strategy. AAV.RPE65 vectors, in which expression of the canine *rpe65* gene was from a CMV promoter, have been subretinally injected into dog eye [105]. The gene transfer resulted in effective transduction of the RPE and reversed the disease-specific phenotype up to 3 years after treatment. ERG recordings demonstrated a remarkable improvement of retinal function, suggesting that a normal visual cycle was restored by the treatment [105, 290, 291]. However, in one study 75 % of the treated animals developed uveitis in response to the immunopathogenic character of the RPE65 molecule [290, 291], a serious complication which still needs further evaluation but may have been due to the quality of the viral preparation or surgical technique. These results laid the cornerstone for the approval of a clinical trial of human patients with retinal degenerative diseases that result from *Rpe65* gene defects. In order to further evaluate the benefits and study the effects and mechanisms of AAV-mediated gene replacement for *Rpe65* defects, this approach was also tested in the $Rpe^{-/-}$ knockout mouse. AAV-2/1-mediated gene delivery was used in an *in utero* approach in this animal model. *In utero* treatment has the advantage to correct the defect before significant damage to the retina has evolved [292]. The treatment showed beneficial effects on retinal function similar to those found in dogs. However, AAV-2/2-mediated gene therapy in adult $Rpe65^{-/-}$ mice has been reported to result in an improvement in retinal function but did not lead to a slow down of photoreceptor degeneration or apoptotic cell death [293].

AAV vectors have not only been used for gene replacement approaches but also to deliver neurotrophic and anti-apoptotic factors to the eye. These factors are molecules that promote survival of cells. Therefore, once their potential has been evaluated they can be used as a supplement for other approaches such as gene replacement therapy or transplantations, for a variety of disorders (see chapter 1.3.2).

1.3.4.4.4 Retroviral vectors

Retroviruses are a class of enveloped, small viruses containing 2 single stranded RNA molecules as the genome, which replicate through a DNA intermediate. Retroviruses comprise many different families but as a group they have been identified in virtually all organisms. Since retroviruses are highly pathogenic, particular attention to safety issues with regard to the development of retrovirus-based vectors for gene therapy should be paid. The general advantage of retroviruses for use as vectors is, that they can stably infect dividing cells by integrating into the host DNA without expressing immunogenic viral proteins. The disadvantage is that most retroviral vectors require cell division for stable infection, limiting the target tissues for which they can be used. Retroviral vectors can carry transgenes up to a 7.5 kb which is too small for some genes even if the cDNA is used (reviewed in [294]). The first problem can be overcome by the use of retroviruses from the lentivirus family. Lentiviruses are a subclass of retroviruses that are able to infect both proliferating and non-proliferating cells efficiently and permanently by integrating their genome into their host's. Since the discovery that lentiviruses, in contrast to retroviruses, are able to transduce non-dividing cells, vectors from a variety of members of this family have been developed, like feline immunodeficiency virus (FIV), the human immunodeficiency virus type II (HIV-2), equine infectious anaemia virus (EIAV), semian immunodeficiency virus (SIV) and bovine immunodeficiency virus (BIV) [246, 295-302]. The most commonly used lentiviral vectors, however, are based on the human immunodeficiency virus type I (HIV) and so far have dominated the research field of lentiviral-based gene transfer. Wild type HIV has a natural tropism for $CD4^+$ cells. To increase the range of cells, HIV has been pseudotyped with viral envelopes derived from a variety of different viruses. For gene therapy applications, HIV is most commonly pseudotyped with vesicular stomatitis virus G-protein (VSV-G) because of the broad cell tropism. VSV-G envelope protein recognises a ubiquitous phospholipid in the cell membrane that enables the virus to infect different cell types. Since it is possible to target HIV-vectors to a variety of cells, the potential use of HIV for different clinical protocols has been evaluated. Initial

problems with insufficient vector titres could be been overcome by the improvement of virus production protocols and the use of ultracentirifugation. During the clinical trial of SCID patients it became clear that insertional mutagenesis by the vector (in the case of the SCID trial, a retrovirus) as it integrates into the host genome is a main problem which needs to be addressed further, in order to increase the safety of integrating viruses in clinical applications. Another safety issue, that evokes serious considerations in particular when using HIV-based vectors, is the possibility of generating wild-type viruses. Increased safety is achieved by accurate analysis of virus preparations using long-term cultures and PCR assays to determine whether there is any contamination.

In the first generation of HIV-1 vectors, viral proteins such as the HIV core proteins, enzymes as well as accessory factors for transcriptional signals were delivered in *cis* [303, 304]. In the second generation HIV-derived packaging components were reduced to the *gag*, *pol*, *tat*, and *rev* genes of HIV-1 [305]. In either case, the vector itself carried the HIV-derived *cis*-acting sequences necessary for transcription, encapsidation, reverse transcription, and integration [304, 306-310]. The biosafety of a viral vector depends in part on how much segregation of the *cis*- and *trans*-acting functions of the viral genome is achieved by the vector design and is maintained during vector production. The possibility of generating replication proficient virus particles through replication has to be abolished because it presents a potential risk in *vivo*. The likelihood of this type of recombination is dependent on residual *cis*-acting sequences in the packaging plasmid, allowing some level of encapsidation, and on the extent of sequence homology between packaging and vector constructs. In the third generation of HIV-1 vectors, all HIV sequences required for encapsidation and reverse transcription [307, 308, 310, 311] are absent. Third generation vectors are packaged by three non-overlapping expression constructs: two expressing HIV proteins and the other expressing the envelope of a different virus (see figure 1.12). To abolish transcriptional activity of the 3-prime long terminal repeat (3' LTR) a major deletion is included in this region. Upon reverse transcription and integration the deletion is transferred to the 5' LTR. The resulting transcriptional inactive vector cannot be converted into a full length

vector RNA in transduced cells and thereby the risk of regenerating replication competent viruses is minimised. These vectors are also called self inactivating (SIN) vectors [312].

Figure 1.12: Schematic diagrams of wtHIV-1 genome and the 3 plasmids used in recombinant lentivirus production. LNT.SFFV.transgene, pCMVR8.91 and pMD.G plasmids are co-transfected onto 293T cells (human embryonic kidney cells) for the production of lentivirus. LTR=long terminal repeats; gag=capsid coding gene; pol=polymerase coding gene; cPPT=central polypurine tract; RRE=Rev-responsive element; env=envelope coding gene; 3'ΔLTR=deleted 3' LTR;

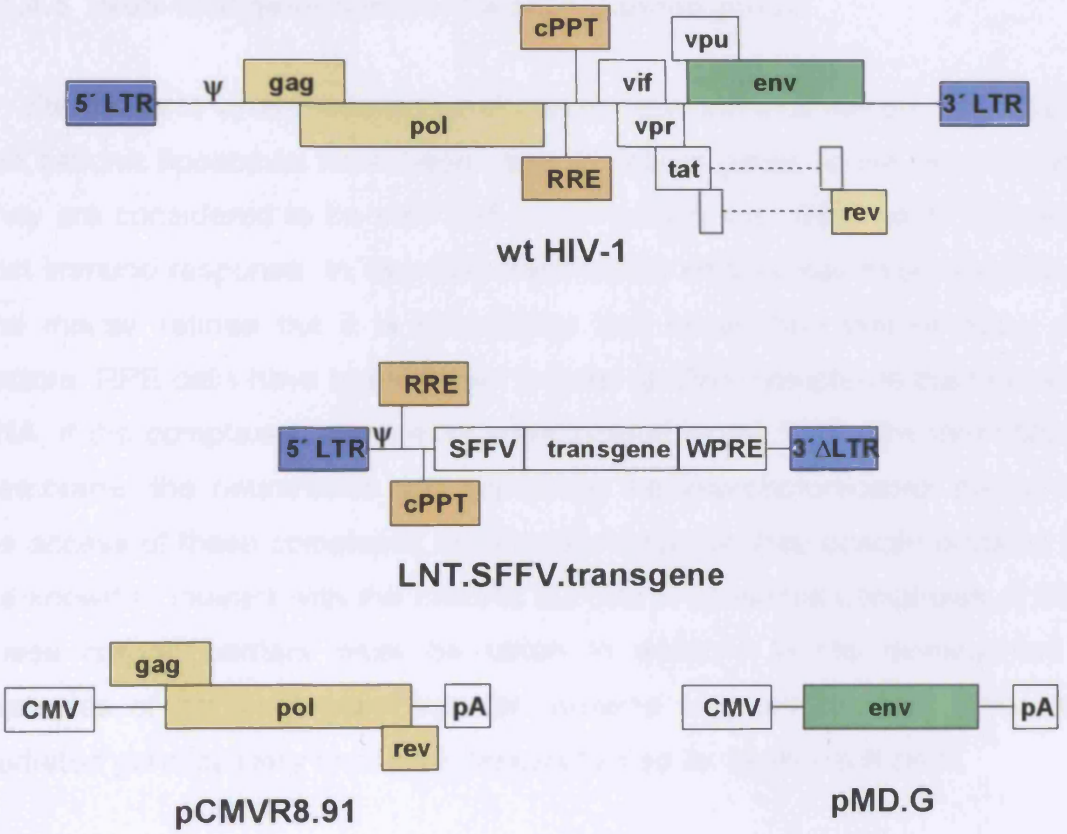

In the eye, HIV-mediated *gfp* expression has been shown to be limited to the RPE, if the virus is pseudotyped with VSV-G and the transgene is driven by a cytomegalovirus (CMV) promoter, or spleen focus forming virus (SFFV) [313]. However, reporter gene expression in photoreceptor cells has been reported if

injections are performed in neonatal mice [283, 314] suggesting that the tropism of of this vector depends on the age of the animal. *Gfp* expression in photoreceptor cells has been reported after subretinal injection into adult mice of HIV/VSV-G if the reporter gene is under the control of the photoreceptor-specific rhodopsin promoter. However, the level of expression is not adequate for efficient gene transfer to photoreceptors. SIV-, FIV- and BIV- mediated expression of reporter genes has also been reported to be restricted to the RPE in rodents [296, 299, 301].

1.3.4.5 Non-viral gene transfer for retinal dystrophies

An alternative to virus-mediated gene transfer are non-viral vectors. Naked DNA and cationic liposomes have been used to deliver genes to the retina in *vitro*. They are considered to be safe and biocompatible with little risk of inducing a host immune response. In *vivo* their transfection efficacy has been tested in rat and mouse retinae but it is inadequate and lower than that of many viral vectors. RPE cells have been shown to take up DNA complexes but not naked DNA, if the complexes are directly administered to the RPE. The inner limiting membrane, the neuroretina and especially the interphotoreceptor matrix limit the access of these complexes significantly because they contain proteins that are known to interact with the cationic surface of liposomal complexes of DNA. These natural barriers must be taken in account in the development of strategies of non-viral gene transfer systems targeted to RPE. Liposomal-mediated gene delivery to photoreceptors has so far been insufficient.

In *vivo* transfer and expression of a reporter gene into adult mammalian retina has been achieved using HVJ liposomes [315]. HVJ liposomes are a mixture of liposome and expressing plasmid complexed with high mobility group 1 (HMG1) chromosomal proteins, which are then coated with the envelope of Sendai virus (haemagglutinating virus of Japan, HVJ). The HMG1 proteins contain a nuclear localisation signal to facilitate nuclear uptake and may also protect the DNA from degradation. HVJ induces membrane fusion and cytoplasmic entry, the

encapsulated plasmid is thought to bypass endocytosis and lysosomal degradation by the host immune system. Expression up to 30 days could be detected in photoreceptor cells after subretinal injections, and neurons and glial cells in the ganglion cell layer after intravitreal delivery. However, the level of transgene expression is lower and the duration short compared to virus-mediated expression.

The therapeutic use of non-viral gene transfer is limited by poor transduction efficiency to viral vectors and the transient nature of expression compared. The blood-retinal barrier and the neural retina are diffusional barriers for macromolecules and decrease the penetration of these molecules. Therefore, different ways to improve transductions levels are under development and evaluation. Lipofectin has been mainly used for gene transfers in *vitro*. Recently, its ability to promote gene delivery in *vivo* has been tested. Cationic lipids condense DNA and thereby protect it from degradation and facilitate endocytosis. Electric fields alter the structure and permeability of cell membranes. Electroporation uses this phenomenon to facilitate penetration of macromolecules into cells. Both techniques have been used to increase the efficiency of non-virus-mediated gene transfer [316]. A non-viral plasmid containing the LacZ reporter gene under the control of either the RPE-specific VMD2 promoter or the ubiquitous CMV promoter was delivered to mouse eyes. After subretinal delivery, LacZ expression from the VMD2 promoter was exclusively detected in the RPE whereas staining was also observed in photoreceptors – even though predominately in RPE cells – when the reporter gene was under the control of the CMV promoter. Expression was evident up to 28 days after treatment and could be increased by repeated administration. These techniques hold promise for in *vivo* analysis of gene regulation or promoter analysis but are inefficient for clinical applications due to their transient effect.

In *vivo* electroporation has also been used to deliver the *gfp* reporter gene into neonatal mouse and rat retinae [317]. A solution of DNA plasmids was directly injected into the subretinal space of neonatal mouse and rat pups, and electric pulses were applied by electrodes. Five days after the treatment expression

was observed in the developing outer and inner nuclear layer. *Gfp* expressing cells were identified as rod photoreceptors, bipolar cells and Müller glial cells 2 weeks after injection. Even though expression levels were decreasing over time, expression was still detected at 50 days. The potential of electroporation techniques was further tested in gain and loss of function experiments. Rax is expressed by proliferating retinal progenitor cells and differentiating Müller glial cells, and its forced expression in the P0 rat retina with a Molony murine leukemia virus (MLV) vector leads to the generation of cells resembling Müller glia [108]. The same results were obtained by using a plasmid containing a rax expression cassette. For loss of function analysis, DNA-based RNAi vectors that produce siRNA against the transcription factors Crx and Nrl were used. In retinae transfected with the RNAi plasmids, the numbers of rhodopsin-positive cells were significantly reduced (~ 5 %) compared to control eyes (~ 60 %). Consistent with the reported phenotypes of knockout mice, photoreceptors did not have clear outer segment structures [317].

Recently the integrase from the bacteriophage phiC31 was used to confer long-term gene expression by means of genomic integration in the RPE of rats. PhiC31 integrase mediates integration in to the mammalian genome by recombination between a plasmid containing the attB sequence and pseudo-attP sites of the host. The potential of phiC31 integrase to mediate long-term expression has first been shown in mouse liver [318] and human skin grafted onto immune deficient mice [319]. A phiC31 expression plasmid carrying both reporter genes luciferase and *gfp* and the phiC31 integration sequence attB were generated and injected subretinally in rat eyes [320]. Reporter gene expression was confirmed in injected eyes and was approximately 1000 fold higher in eyes that were electroporated compared to eyes which only received subretinal injections but were not electroporated. In both cases expression was restricted to the RPE. If the phiC31 integrase was provided by another plasmid, expression levels were approximately 85 % higher than without integrase and was detected up to 4.5 months. These findings suggest that phiC31 integrase may be a simple and effective tool for non-viral long-term gene transfer in the eye [320].

The application of viral vectors involves problems, which can be partly circumvented by using non-viral methods of gene transfer. Most viral vectors induce an immunological response to some degree and have safety risks, such as insertions mutagenesis, toxicity problems, and the reversion to a disease causing virus inside a patient. Another problem of virus-mediated gene transfers is that the capacity of viruses is limited and large scale production is often difficult to achieve. Non-viral approaches, however, require only a small number of proteins, have a large capacity, are not infectious or mutagenic and large scale production is possible by using pharmaceutical techniques. The main disadvantage of non-viral gene transfer approaches, however, is the poor efficacy to date in *vivo*. A number of non-viral gene delivery methods into the retina have yet to be tested. One such strategy is transposon-based vector delivery system that represents a promising new tool for chromosomal transgene insertion and establishment of persistent gene expression in *vivo*. In a mouse model for hemophilia B it was possible to partially correct the pathogenic phenotype by delivering factor VIII with transposon-based vectors [321].

2

2 Materials and Methods

2.1 Cloning and plasmid construction

In order to create a recombinant virus, which fulfils the requirements of gene transfer, most of the viral genome must be replaced with a recombinant genome carrying the therapeutic gene under the control of an appropriate promoter to ensure its expression in the right cell type and at an efficient level. To avoid the attention of the immune system and as a result the removal of the virus or the transduced cell, viral capsid encoding genes and genes necessary for virus in-*vivo* replication should be deleted. Since recombinat viruses are produced in-*vitro*, possible issues regarding safety and purification need to be considered. There should be a minimal risk of the creation of replication competent viruses through recombination during production. In order to minimise toxicity, viral particles need to be thoroughly purified.

2.1.1 RNA isolation

RNA of rat retinae was isolated using Trizol reagent (Invitrogen Life technologies, Paisley, UK). Tissue samples were homogenised in 800 µl Trizol and incubated for 5 min at room temperature to disrupt cellular components and maintain RNA integrity. To separate nucleic acids from cellular components, 0.2 ml of chloroform was added and the sample was shaken for 15 sec. After a 3 min incubation step at room temperature, the sample was centrifuged for 15 min at 5000xg at 4°C. Following centrifugation the mixture separates into phases, in which RNA remains in the upper most aqueous phase. This phase was then transferred into a new tube and RNA was precipitated by adding 0.5 ml isopropyl alcohol. After 10 min incubation at room temperature, RNA was pelleted by centrifugation at maximum speed at 4°C. The supernatant was removed and the RNA pellet was washed with 1 ml of 75 % ethanol. The sample was mixed by vortexing and centrifuged again at maximum speed at 4°C. After removing of supernatant, the RNA pellet was air dried and resuspended in RNase free water. The concentration of RNA was measured by lightspectroscopy. Approximately 1 µg of total RNA was treated with RQ1 RNase free DNase (Promega, Madison, WI) to remove traces of genomic DNA that could function as templates in PCR reactions.

2.1.2 *MERTK* cDNA

The murine *MERTK* cDNA (see Appendix for cDNA sequence) was RT-PCR amplified in 2 fragments from mRNA isolated from total murine retinae. Both PCR fragments were sequenced after cloning into pGem-T (Promega, Madison, WI) and the 2 fragments were combined using a naturally occurring *EcoRV* site to give a full length cDNA clone ranging from nt –1 to nt 3037 in relation to the start codon .

2.1.3 Restriction enzyme digests

For cloning protocols, plasmid DNA that carried the sequence of interest was digested with appropriate restriction enzymes in accordance with the enzyme manufacturer's instructions (New England Biolabs Ltd., Herts, UK). In order to ascertain right orientation after integration of the transgene into plasmids non-complementary ends were created.

2.1.4 DNA electrophoresis

After the restriction digest DNA fragments were separated on a 1 % (w/v) agarose gel using 1x TBE buffer. Ethidium bromide (1 µl per 25 ml of gel) was added to visualise nucleic acid bands. Samples were loaded onto the gel using gel-loading buffer (6 x; 0.25 % (w/v) bromophenol blue and 30 % (v/v) glycerol in water and a 1 kb DNA ladder (Invitrogen Ltd.) was run at the same time to provide a size marker. The voltage was chosen considering the seperation time of fragments of the expected size. Gels were then photographed on an ultraviolet transilluminator.

2.1.5 Extraction of DNA fragments from agarose gels

The required DNA fragments were excised from the agarose gel and extracted using QIAquick™ Gel Extraction Kit (QIAGEN Ltd.) following the manufacturer's instructions. The concentration of the eluted DNA was measured by photospectroscopy using a Unicam UV 500 spectrometer. An absorbtion of 1 at OD_{260nm} was taken to equal the concentration of 50 µg/ml double stranded DNA.

2.1.6 PCR and sequencing

To ensure that the isolated fragments have the correct sequence they were amplified using appropriate primers and cycling conditions. PCR reactions were performed in a total volume of 20 µl. 0.2 mM dNTPs (Promega UK), 25 pM of each primer and 1 U of Taq polymerase (Promega UK), and 8 µl of buffer were mixed and DNA was added to a final DNA concentration of less than 10 ng/µl. The amplified fragments were then sequenced (MWG-Biotech).

2.1.7 Ligations

The ligation of gel purified DNA fragments was carried out at 25°C for 3 hr. T4 DNA ligase (New England Biolabs Ltd. UK), the supplied buffer, the viral vector backbone and the insert of interest were added in accordance with the manufacturer's instructions. To check whether the ligation was successful the ligated plasmid was transformed in bacteria. Newly cloned plasmid were isolated from bacteria and analysed by appropriated restriction enzyme digests and gel electrophoresis.

2.1.8 Transformation and recovery of plasmids

For transformations, DH5α™ competent cells (Invitrogen Ltd., UK) were defrosted on ice. After the bacteria suspension had thawed, the viral vector solution was added and the transformation mix was incubated on ice for 15 min. Samples were then heat shock treated for 90 sec at 42°C in a water bath, cooled down for 90 sec on ice, and 750 µl LB (Luria Bertani, Merck Ltd, Leics, UK) medium was added. All plasmids used included the ampicillin resistance gene as a selection marker for successfully transformed colonies. To ensure efficient expression of the resistance gene, transformed bacteria were incubated for 1 hr at 37°C before they were spread on LB agar plates. LB agar plates were prepared containing 14 g Bacteriological agar (Oxoid Ltd.) per litre

of water, 5 g/l yeast extract, 10 g/l tryptone (Oxoid Ltd.), 10 g/l sodium chloride, and 50 µg/ml ampicillin. Plates were incubated overnight at 37°C to allow resistant bacteria to grow.

Bacteria colonies were inoculated into 2 ml of LB medium containing 50 µg/ml ampicillin (1000x; Sigma Aldrich Company Ltd.) the following day and incubated at 37°C overnight to allow growth. For small scale preparations, plasmids were recovered using QIAprep® Spin Miniprep Kit (QIAGEN Ltd., Sussex, UK). For large scale preparation 200 µl of the 2 ml culture were used to inoculate 250 ml LB medium and bacteria were grow as described above. DNA was then recovered using a QIAGEN® Plasmid Mega Kit (QIAGEN Ltd.).

2.2 Tissue Culture

2.2.1 Cell lines and culture of cells

Baby hamster kidney (BHK) cells were grown in BHK-21 media. Ten percent heat inactivated foetal bovine serum (FBS), 5 % tryptose phosphate broth, 5 ml of antibiotic and antimyotic solution, 5 ml of 200 mM L-glutamine, and 4 ml of 50 mg/ml geneticin G418 were added to 500 ml of medium. 293T cells were cultured in Dulbecco's Modified Eagle's Medium (DMEM) supplemented with 5 ml/500 ml of antibiotic and antimyotic solution and 10 % FBS. HeLa cells were grown in DMEM. 5 ml of antibiotic and antimyotic solution, 4 ml of 50 mg/ml geneticin G418 and 10 % FBS were added to 500 ml of the medium (all reagents were purchased at Invitrogen Ltd.). Cells were grown in a Sanyo CO_2 incubator at 37°C with 5 % CO_2.

2.2.2 Passaging cells

In order to keep cells at an appropriate density, they were split every 2 to 3 days. The old medium was removed and cells were washed twice with 1x PBS (10 phosphate buffered saline tablets (Oxio Ltd.) dissolved in 1 l sterile ddH_2O) before trypsin-EDTA (Invitrogen, Ltd.) was added dropwise until all cells were covered. Plates were then incubated for approximately 10 min at 37°C to allow cells to dissociate. The process was stopped by adding FCS containing growth medium and cells were split onto new plates in an appropriate ratio, usually 1:6.

2.2.3 Long-term storage

For long-term storage cells were treated with trypsin-EDTA as explained above. Cells were pelleted by centrifugation and approximately 5 x 10^6 cells/ml were resuspended in growth medium with 20 % FCS and 10 % dimethylsulfoxide (DMSO; Invitrogen Ltd.). Tubes were pre-cooled on ice before cells were aliquoted. Tubes were then kept overnight at -70°C in a box containing isopropanol before transferring them to liquid nitrogen for long-term storage.

To re-culture cells, they were thawed in a water bath at 37°C. Cells were then pelleted by centrifugation, the DMSO containing medium was removed, and cells were resuspended in the appropriate medium and left to grow to the desired density in a CO_2 incubator at 37°C.

2.3 Adeno-associated viral vectors

The normal production method of recombinant AAV (rAAV) requires the cotransfection of two plasmids into a cell line in the presence of a helper virus. The vector plasmid carries the rAAV construct and the packaging plasmid provides the AAV rep and cap gene products in *trans* (see chapter 1.3.4.4.3 for more details) [322].

2.3.1 Constructs

The *MERTK* cDNA (see section 2.1.2) was cloned between the CMV promoter and the SV40 poly-adenylation site of construct AAV.CMV.GFP [323] to form construct pD10/CMV-Mertk. The RPE-specific *rpe65* promoter fragment (described in [324]) was amplified from murine genomic DNA (conducted by A. Smith) and cloned upstream of the *MERTK* transgene in construct pD10/CMV-Mertk replacing the CMV promoter. The new construct was termed pD10/RPE-Mertk. Constructs were used to generate rAAVs, AAV.CMV.Mertk and AAV.RPE.Mertk, as described [323]. As controls, the plasmids AAV.CMV.GFP and AAV.RPE.GFP were used (see chapter 3.2-3.4 for more details).

2.3.2 Production of rAAV

Prior the day of transfection BHK cells were split and plated at 1 x 10^6 cells/150 mm dish and incubated overnight so that they were approximately 70 % confluent the following day (1 x 10^7 cells). Recombinant AAV-2 particles were produced using the ITR bearing plasmids pD10/CMV-Mertk or pD10/RPE-Mertk, a replicating amplicon containing the *rep* and *cap* genes, pHAV7.3, and PS1 HSV helper virus. The pD10 construct and the pHAV7.3 amplicon were used to co-transfect BHK cells in a 1:1 ratio. The transfection solution for four 150 mm dishes was made by mixing 16 ml (0.1 mg/ml) Opti-MEM® (Invitrogen,

Ltd.) and 150 µl Lipofectin (Life Technologies, Paisley, UK). Cyclised integin targeting peptide 6 ((K16) GACRRETAWACG) - a β-integrin-targeting peptide used to improve the binding of the DNA-containing liposomes to the cells - was added to the same tube. In another tube 16 ml Opti-MEM®, 100 µg helper plasmid, and 100 µg plasmid DNA were mixed and this mixture was added to the transfection solution. Complexes were allowed to form by incubation at room temperature for 1 hr. Old medium was removed from plates and cells were washed twice with Opti-MEM®. For transfection, 10 ml of the transfection solution was added to each plate and cells were incubated for at 37°C for 4 hr. After incubation, the transfection solution was replaced by normal growth medium containing PS1 HSV helper virus at a MOI (multiplicity of infection = average number of particles that infect a single cell) of 10 to 20 infectious units per cell. Cells were incubated at at 37°C for 24 to 36 hr, to allow the completion of a lytic cycle, the cells were collected by scraping and pelleted by centrifugation at 3000xg for 10 min.

2.3.3 Purification of rAAV

Cells from ten 150 mm plates were harvested, resuspended in 10 ml DMEM, and were then lysed by three cycles of freeze thawing between –70°C and 37°C. Genomic DNA remaining in the lysate was degraded with 50 U of endonuclease benzonase per millilitre of lysate at 37°C for 30 min. To clarify the lysate cell debris was removed by centrifugation at 3000xg for 15 min. The supernatant was treated with 0.5 % deoxycholic acid for 30 min at 37°C and filtered through 5 and 0.8 µm syringe filters (Millipore, USA; SLSV R25 LS and SLAA O25 LS). After filtration the supernatant was transferred onto a heparin-agarose column (Sigma, USA) which was first pre-washed with PBS-MK (1 x PBS, 2.5 mM KCl, 1 mM $MgCl_2$) and then with 10 ml PBS-MK + 0.1 M NaCl. Viral particles were eluted with 6 ml PBS-MK + 0.4 M NaCl. The first 2 ml were discarded and the remaining suspension containing the purified virus was collected. The resulting virus suspension was concentrated by centrifugation at 5000xg for one hour using Centricon 10 columns (Millipore, USA). The flow-

through was discarded and the columns were washed with PBS-MK by a further centrifugation step at 5000xg for 10 min to dilute out remaining salt. For collection of the purified and concentrated virus suspension, columns were turned up side down and spun to elute the virus into a collection tube. A total volume of approximately 100 µl per 10 plates was collected [325].

2.3.4 Viral DNA extraction

To extract viral DNA from rAAV capsid proteins, 1 and 5 µl samples were treated with 100 µg (10 µl) proteinase K (Promega UK) with 100 µl 2 x proteinase K buffer (100 mM Tris (ph 7.4), 50 mM EDTA and 0.5 % SDS) and 100 µl dH_2O. After a 1 hr incubation step at 37°C, DNA was precipitated by adding 1/10 volume (20 µl) of 3M sodium acetate, 40 µg (2 µl) glycogen (Sigma-Aldrich Company Ltd.) and 2.5 volume (500 µl) of 96 % ethanol and left at -70°C for 30 min. DNA was pelleted by centrifugation at maximal speed for 30 min at 4°C. Each pellet was washed with 200 µl of 70 % ethanol, air dried and resuspended in 200 µl 0.4 M NaOH + 10 mM EDTA solution.

2.3.5 Titration with dot-blot analysis

The molecular titre of the concentrated virus was estimated by dot-blot analysis. A dilution series ranging from 10^9 to 10^{12} molecules of plasmid including a probe DNA of known concentration was used to produce a standard ladder. The samples were prepared with 0.4 M NaOH + 10 mM EDTA solution in a total volume of 200 µl. Samples from the dilution series and recombinant viral genome samples in alkaline solution were first denatured at 100°C for 2 min and then cooled for 2 min on ice to prevent re-annealing. Dot-blots were prepared on a pre-wet 0.45 µm Hybond^{TM}-N+ membrane (Amersham Pharmacia Biotech., Bucks, UK) - a positively charged nucleic acid binding membrane - in a dot-blot manifold (Bio-Rad Laboratories Ltd., Herts, UK). Each well of the manifold was pre-washed with 0.2 ml of dH_2O and vacuum dried

before denatured DNA samples were loaded. A vacuum was applied until wells were empty. Then 0.2 ml of 0.4 M NaOH and 10 mM EDTA was added to each well. Excess solution was removed by applying a vacuum and the membrane was air dried between blotting paper.

Meanwhile the probe DNA was excised from the plasmid with a restriction enzyme as explained in chapter 2.1.3. In order to label the probe radioactively, a Prime-It® II Randon Primer Labelling Kit (Stratagene Europe) was used. Following the manufacturere's instruction, 21 µl H_2O and 10 µl random oligonucleotide primer supplied by the manufacturer were added to the DNA probe and incubated at 95°C for 5 min. Samples were spun and 10 µl of 5 x Labelling buffer, 5µl ^{32}P-dCTP (3000 Curies/µl) labelled nucleotides, and 1 µl Exo-Klenow-enzyme (5 U/µl) were added and incubated at 37°C for 18 hr.

The membrane was then moistened with dH_2O, placed in a hybridisation tube and heated to 65°C in a hybridisation rotisserie oven. The water was replaced by Church buffer (0.5 M sodium phosphate buffer, 7 % w/v SDS, 0.01 M EDTA) and the membrane was incubated again for 30 min. The radioactively labelled DNA probe was denatured for 2 min at 95°C and immediately added to the membrane. The membrane was hybridised for 5 hr and washed twice with 50 ml of sodium phosphate buffer (0.05 M, pH 7.2) at 65°C. Excess liquid was removed and the membrane sealed in plastic. The membrane was then placed in a cassette with a Kodak Scientific Imaging BioMax™ MR-1 film. After an hour exposure, the film was developed in a Fuji RG II X-Ray Film Processor and the viral titre was estimated by comparison to the standard ladder (see chapter 3.2).

2.4 Lentiviral vectors

2.4.1 Constructs

The murine *MERTK* mRNA was isolated from murine total retinal RNA, RT-PCR amplified (see chapter 2.1.2) and cloned into a VSV-G pseudotyped HIV-1-based vector [313, 326]. The lentiviral *MERTK* expression construct, LNT.SFFV.Mertk, was generated by cloning the murine *Mertk* gene between the spleen focus forming virus (SFFV) promoter and the WPRE element of the pHR'SIN-cPPT-SEW lentivirus construct. The GFP control construct, LNT.SFFV.GFP, is identical to the construct pHR'SIN-cPPT-SEW as described by Demaison *et al* [326].

2.4.2 Production of recombinant lentivirus

Approximately 10^6 293T cells were seeded on 150 mm plates the day before transfection, in order to ensure efficient growth to sub-confluent level until the following day of transfection. Routinely, 12 150 mm plates were used for each preparation of lentivirus. Cells were transfected with 50 µg of the recombinant construct per plate in addition to the lentivirus helper constructs pMD.G (17.5 µg) and the packaging plasmid pCMVR8.91 (32.5 µg) [352]. Transfections were performed as described using 12 ml Opti-MEM® (Invitrogen, Ltd.) containing 75 µl Lipofectin (Life Technologies, Paisley, UK) and 400 µg peptide 6 [323]. After 5 hr incubation at 37°C the transfection mixture was replaced with complete DMEM. The following day, the medium was exchanged and plates were incubated. After 48 hr, the medium was collected and cell debris in the medium was pelleted by two 10 min centrifugation steps at 2000xg. The supernatant was filtered through a 0.45 µm filter (Millipore) and centrifuged for 2 hr at maximum speed to pellet the virus. The virus pellet was resuspended in Opti-MEM®, spun at 2000xg for 10 min to remove remaining debris and frozen in batches at -80°C. Vectors were titrated by infecting 293T and HeLa cells with

serial 1:10 dilutions of virus and analyzing for *egfp* expression at 3 to 5 days postinfection to estimate the transfectious titre (see chapter 1.3.4.4.4).

2.5 In *vivo* experiments

2.5.1 Animals

Dystrophic RCS rats and non-dystrophic RCS rats were used for this study. All animals were cared for in accordance with the Animal Scientific Procedures Act 1986 and procedures were in accordance with the ARVO Statement for the Use of Animals in Ophthalmic and Vision Research. To control for interanimal variability in the rate of degeneration, the right eye was treated whilst the left eye remained untreated in all animals. Therefore, the untreated eyes provided an internal control for all experiments. Each treated eyes received two injections of viral suspension or PBS. Subretinal injections were usually carried out in 10 day old animals. If not stated differently, animals were sacrificed by exposure to carbon dioxide.

2.5.2 Anaesthesia

For intraocular procedures animals were anaesthetised by intraperitoneal injections of anaesthetic solution (0.75 ml Ketamine, 0.5 ml Domitor, and 0.75 ml water). Adult rats between 250 and 300 g body weight received 0.25 ml of the anaesthetic solution. For 10 day old animals, the anaesthetic was diluted 1 in 20 with dH_2O and 0.15 ml were injected. To reverse the anaesthesia 0.2 ml of Antiseden and 0.8 ml dH_2O were injected intraperitoneal in adult animals and 0.05 ml of a 1:20 dilution in 10 day old rats.

For ERG recordings, rats were anaesthetised with a single intraperitoneal injection of ketamine (60 mg/kg), xylazine (8 mg/kg) and atropine (0.75 mg/kg).

2.5.3 Subretinal injections

If necessary the palpebral fissure was opened with a small scalpel blade and pupils were dilated with 1 % Tropicamide (Alcon Labs, Watford) topically administered. Surgery was performed under direct retinoscopy through an operating microscope. The eye was protruded by gentle pressure on either side of the eye and held in position by holding a section of the conjunctiva and extraocular muscle with a pair of forceps. The eye was then covered with 2 % hypromellose solution (Moorfields Eye Hospital, London, UK) and a cover slip was placed over it. The tip of a 1.5 cm, 34-gauge hypodermic needle (Hamilton) was guided underneath the cover slip to the sclera of the right rat eye (Figure 2.1) and then inserted tangentially through it, causing a self-sealing wound tunnel. The needle tip was brought into focus between the retina and the RPE. Approximately 4 µl virus suspension containing 4 x 10^7 particles of rAAV and 4 x 10^6 particles of lentivirus were injected to produce a bullous retinal detachment in the superior hemisphere. A second injection was performed subsequently to produce a similar detachment in the inferior hemisphere. Each injection covered approximately 25 to 30 % of the entire retina [313].

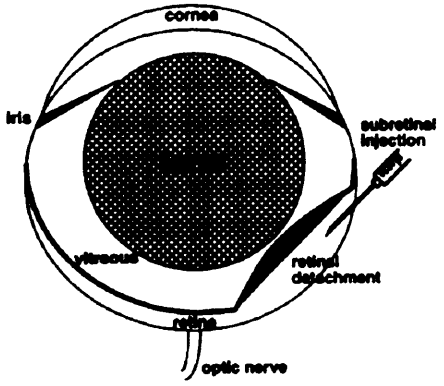

Figure 2.1: Schematic of a rodent eye. The route of subretinal injection is shown [228].

2.5.4 Electroretinography

ERGs from injected RCS rats were recorded in a standardised fashion at various time points. All animals were dark-adapted overnight (16 hr) and Ganzfeld ERGs were obtained simultaneously from both eyes of each animal in order to control for inta-animal variations. All procedures for recording were carried out under dim red light. After anaesthesia as described above the pupils were dilated using one drop each of 2.5 % Phenylephrine Hypochlorise and 1 % Tropicamide (both from Chauvin Pharmaceuticals Ltd.) to each eye. A single drop of 2 % hydroxy-propyl-methyl-cellulose was placed on each cornea to keep it moisturised after dilation. ERGs were recorded using commercially available equipment (Toennies Multiliner Vision, Jaeger/Toennies, Würzburg, Germany) after placing corneal ring-electrodes (type Henkes, Jaeger-Toennies, Germany) and midline subdermal reference and ground electrodes. Bandpass filter cut-off frequencies were 1 and 300 Hz for all measurements. Great care was taken to keep electrode impedances symmetrical and low (between 5 and 8 kOhm). Single flash recordings were obtained at light intensities increasing from 0.1 mcds/m^2 to 3000 mcds/m^2. Ten responses per intensity level were averaged with an inter-stimulus interval of 5 s (0.1, 1, 10, 100 mcds/m^2) or 5 responses per intensity with a 17 sec interval (1000 and 3000 mcds/m^2) to try and minimise the dark adapted conditioning flash effect. All data was analysed using the Toennies Multiliner Vision program.

2.6 Reverse transcription and PCR

RNA of injected and uninjected rat eyes was isolated using Trizol reagent (see chapter 2.1.1). Approximately 1 µg of total RNA was treated with RQ1 RNase free DNase (Promega, Madison, WI) to remove traces of genomic and viral DNA that could function as templates in the PCR reaction.

First strand cDNA production using random monomer primers was performed at 42°C for 30 min using M-MuLV reverse transcriptase (New England Biolabs, Beverly, MA). Reactions without RT were performed to confirm the complete removal of DNA. PCR reactions on single strand cDNA were done with the following primers: forward: 5'-TGCTCCATCAATATTCCTAACACA-3', nt 324 to 347 of the murine *MERTK* cDNA in relation to the start codon; reverse: 5'-GGAGGGGATTACTTTGATGTTGA-3', nt 833 to 855 of the murine *MERTK*. PCR reactions consisted of 35 standard cycles with an annealing temperature of 49°C. Both PCR fragments were sequenced after cloning into pGem-T (Promega, Madison, WI) and the 2 fragments were combined using a naturally occurring *EcoRV* site to give a full length cDNA clone ranging from nt –1 to nt 3037 in relation to the start codon (see chapter 3.4).

2.7 Histological analysis

2.7.1 Cryosections

At various time points, rats treated with viral vectors carrying the e*gfp* gene were anaesthetised with a single intraperitoneal injection of ketamine (see Chapter 2.5.2). The right atrium was opened with a single cut and periodate lysine paraformaldehyde (PLP; 2% paraformaldehyde, 0.05% glutaraldehyde) was injected into the left ventricle for pre-fixation of the tissue. PLP was injected until most of the blood was exchanged. Eyes were taken and immediately immersion fixed in PLP for 4 hr. After fixation the eyes were cryoprotected in 10% sucrose solution overnight at 4°C. Eyes were then embedded in O.C.T. (R A Lamb, E. Sussex, UK) and frozen in isopentane which had been pre-cooled in liquid nitrogen. Specimens were stored at -80°C and 12 µm thick sections were cut using a Bright cryostat. In order to visualise cell nuclei, sections were usually counterstained with propidium iodide.

2.7.2 Fixation of eyes for semithin and ultrathin sections

At various time points rats were sacrificed and their eyes were immediately removed and orientated with a nasal stitch. Then eyes were immersion fixed in 3 % glutaraldehyde and 1 % paraformaldehyde buffered to pH 7.4 with 0.07 M sodium cacodylate-HCl buffer (Karnovsky's; 0.2 M $(CH_3)_2AsO_2Na.3H_2O$ with 0.2 N HCl). After 12 hr the anterior part of the eye was removed by microdissection. The posterior segments were then osmicated for 2.5 hr in a 1% aqueous solution of osmium tetroxide, followed by a dehydration series through ascending alcohols (50 – 100%, 10 min per step). After 3 changes of 100% ethanol, specimens were passed through propylene oxide (3x 10 min) and left overnight in a 50:50 mixture of propylene oxide and araldite. Following a single change to fresh araldite (5 hr with rotation) the specimens were embedded in resin and cured for 48 hr at 60°C.

2.7.3 Semithin Sections

Semithin sections (0.7 µm) were cut using a Leica ultracut S microtome fitted with a diamond knife (Diatome histoknife). Sections were stained with toluidine blue stain (25 ml 2 % hydrated sodium borate, 25 ml 100 % ethanol, 0.5 g toluidine blue, SPI-Chem™) and slides were mounted with DPX after the sections had dried. Sections were analysed using a Leitz Diaplan microscope for observation and imaged with a Leica DC 500 digital camera.

2.7.4 Ultrathin sections

Ultrathin sections (50 nm) were cut using a Leica ultracut S fitted with a diamond knife for ultrathin sections (Diatome histoknife for ultrathin sections).

Sections were taken of treated areas of retinae and collected onto grids. Sections were stained with uranyl acetate for 10 min and lead citrate for 7 min and then washed with dH_2O. After the sections had dried they were analysed by electron microscopy (JEOL 1010 TEM).

2.8 Statistical analysis

The choice of an appropriate statistical method is important to draw conclusions from data that are subject to experimental error. Generally, statistics yield the probability value for a particular result. In science, a probability (p) of 0.05 or less is usually accepted as convincing evidence that a particular outcome is significant and not due to chance.

A "Student's t-test" can be performed knowing only the mean and standard deviation of two data sets. The Student's t-test determines a probability that two populations are the same with respect to the variable tested. The populations are assumed to follow a normal distribution (Gauss distribiution). For independent samples, as it was the case for most of the histological data presented in this thesis, an unpaired Student's t-test was used (unless stated differently). This test compares two small, independent sets of data that do not have to have the same number of data points in each group and are collected randomly. In order to evaluate the significance of the difference in number of surviving photoreceptor cells and retinal layer thickness between either non-dystrohic or dystrophic, treated or untreated animals, cell counts and thickness meassurements were carried out and on 10 sections per eye, in the middle of the superior injection site. Since the number of animals for each condition varied, the sets of data should to be regared as randomly collected and independent. Therefore an unpaired Student's t-test was applied.

For functional ERG results presented in this thesis, a paired Student's t-test was performed. A paired t-test can only be applied if the numbers of points in each

data set are the same, and if they are organised in pairs. Generally, it is used when measurements are taken from the same subject before and after manipulation, in this case the viral mediated expression of a transgene. Since ERG records electrical responses of both eyes simultanously, and recordings can be obtained at different time points over a period of time from the same animal, a paired Student's t-test was used. For each animal, the height of b-wave amplitude of the ERG recording obtained at a flash intensity of 100 mcds/m^2 was used for statistical analysis. The b-wave values (a-wave through to b-wave peak) of the treated (right) eye were paired with the untreated contralateral (left) eye to provide an internal control. A paired Student's t-test was used to evaluate significance ($p<0.05$). This method controls for interanimal variance and test-retest variance present in rodent ERGs.

2.9 Patient Screen

2.9.1 Patients

A panel of 96 patients with simplex and autosomal recessive retinal dystrophy were ascertained from the medical retinal clinics at Moorfields Eye Hospital. The study was conducted in accordance with the tenets of the Declaration of Helsinki and was approved by Moorfields Hospital Ethics Committee. All patients gave written informed consent to be included in the study and provided a blood sample for subsequent DNA extraction and DNA analysis.

2.9.2 DNA isolation

Blood samples were collected in EDTA tubes. DNA was extracted using a Nucleon Genomic DNA Extraction Kit (BACC2, Tepnel Life Sciences plc) following manufacturer's instructions. Solution A provided by thew supplier was

added to each sample and samples were shaken for 5 min. After centrifugation for 7 min at 5000xg the supernatant was carefully removed. Each pellet was then resuspended in 2 ml solution B, samples were transferred to a new tub and mixed with 450 µl of sodium perchlorate. Tubes were inverted several times in order to mix the samples and 1.5 ml chloroform was added. After mixing thoroughly 300 µl of Nucleon resin was added and samples were centrifuged for 5 min at 4000xg. The aqueous phase containing the DNA was transferred into a new tube and mixed with 6 ml 100 % ethanol. After a 5 min spin the supernatant was removed and DNA pellets were washed with 500 µl 70 % ethanol. Samples were centrifuged again at 4000xg for 5 min, the ethanol was removed and pellets were air dried. The DNA was resuspended in 400 µl dH_2O, rotated over night at 4°C to dissolve DNA, and stored at -20°C.

2.9.3 PCR

Primers were designed corresponding to intronic sequences for PCR amplification of all 19 exons of *MERTK*. Sequences of primers used are listed in Table 3 (see Appendix). All PCR reactions were performed in a total volume of 50 µl using 200 µM dNTPs (Promega UK), 0.5 µM of each primer, 2 µM DNA, magnesium containing Optimase reaction buffer (Transgenomic UK) and 2.5 U Optimase polymerase (Transgenomic UK). Reactions were cycled using a Techne Touchgene Thermal Cycler. The optimal annealing temperature for each primer set was calculated by using the program PrimerSelect™ (DNASTAR Inc.).

Cycling conditions were as followed:

Initial denaturation	5 min at 95°C	
Denaturation	1 min at 95°C	35 cycles
Annealing	15 sec at Ta	
Extension	1 min at 72°C	
Final extension	10 min at 72°	

Table 3: **Amplification of the human *MERTK* gene.** Primer pairs were designed to cover the entire coding sequence and important intronic sequences of the human *MERTK* gene (see also Appendix). Primer sequences and annealing temparatures for PCR are summarised in the table.

MERTK	Forward primer 5'-3'	Reverse primer 5'-3'	Ta [°C]
Exon 1	gacaggttcgggaggtccatctg	ccctgtggacgcgctccctccccag	60
Exon 2	ggacaccccagtgctctctcttc	gctacagaatgatactctgtctc	60
Exon 3	cacagcatatgacaaagaagttg	cagagttataaataggcaggc	59
Exon 4	ctttgggctctgtctctgtttt	ttgatcctgtccgctattagaga	52
Exon 5	tgtttctctgctgctggtctc	cctcaccagctcccagaac	65
Exon 6	gtagctgtagcctgtcatctataa	cccacagagagcaccaa	50
Exon 7	tgcctgacattcccaccac	tgggaagggtttgttgaatca	65
Exon 8	atgagaatacatctgtgtgtgcttt	agttgaaaggagatgactaatcg	50
Exon 9	ctgcagtttgcccagacctc	gaccatcacatcctatcagccc	50
Exon 10	tgactatttgttcttccctgttac	taacaaccttgtcaataccagtg	50
Exon 11	agtagccctgtttttatagtgaag	gtctattgatccttctttgttctc	48
Exon 12	caagtgaaagaaaacacgctg	aaactgctaccttcttatcccac	52
Exon 13	tggtcagggaagagtttgc	gcacccaatactgaagcaac	52
Exon 14	cccacccactcccctt	cacagagcagatcagcagag	60
Exon 15	tggtcacagtaacaaggactc	tcacataagccctgagaagt	42
Exon 16	cccccggcagaaact	tgcaaagaccaaacacca	58
Exon 17	gtgttttcacctgtgtctga	tatgccctcctctttgtg	48
Exon 18	gctttgtggaaaggcttg	tgtgtttccgaggtcagtg	50
Exon 19	ggcatggattgcacaaagagatgggtg	catcaggtacaattggattctc	60

2.9.4 Gel electrophoresis

Fragment size and purity of PCR reactions were controlled by gel electrophoresis. Samles were loaded onto a 2 % agarose gel made with 1% TBE buffer and 8 µl ethidiumbromide/200 µl total volume. The fragments were characterised under UV-light.

2.9.5 Sequencing

2.9.5.1 ExoSapIT treatment

Samples were processed for direct sequencing for characterisation. For each sample two reaction – one for the forward primer and one for the reverse primer – were set up. DNA fragments were purified by ExoSAP-IT® (Usb Corporation) treatment in a total volume of 18 µl using 2 µl (approximately 10 ng) of the amplified DNA fragment and 0.5 µl ExoSAP-IT enzyme with sterile dH_2O. The purification mix was incubated for 15 min at 37°C and then the enzyme was inactivated for 15 min at 80°C.

2.9.5.2 Big Dye

Samples were sequenced using a BigDye® Terminator v1.1 Cycle Sequencing Kit (Applied Biosystems). The Big Dye was diluted in 2.5 x Big Dye Buffer containing 200 mM Tris pH 8, 5 mM $MgCl_2$ with sterile dH_2O. To each ExoSAP IT treated sample 1 µl Big Dye v1.1 and either 1 µl (0.8 µM) forward or 1 µl reverse primer were added.

Cycling conditions were as followed:

30 cycles: 95°C for 30 sec
50°C for 30 sec
60°C for 4 min

2.9.5.3 Purification and sequencing

Samples were then purified using Millipore Montage™ Cleanup Kit (Millipore Corporation). The total volume of samples was transferred to a Millipore 96 plate and a vacuum (15 to 20 psi) was applied for 10 min. Each well was

washed twice with 25 µl injection solution supplied by manufacturer. Between and after the washing steps a vacuum was applied. Another 25 µl of injection solution was added to each well, the plate was sealed and shaken for 5 min to recover the purified PCR samples. Samples were then transferred onto an ABI® 96 plate (Perkin Elmer, Warrington, UK) for sequencing. Samples were run over night on an ABI Applied Biosystems 373A DNA Sequencer. Sequences were analysed using the DNASTAR software package (DNASTAR Inc.).

2.10 Clinical assessment

Affected individuals in whom a causative mutation in *MERTK* was identified underwent detailed phenotypic studies. Clinical investigations included assessment of visual acuity, colour vision assessment, Goldman field testing, slit lamp examination, funduscopy and retinal imaging, incuding fluorescein angiography (FFA), autofluorescent imaging with a confocal scanning laser ophthalmoscope (c-SLO-AF) and optical coherence tomography (OCT). Colour vision was evaluated using the Hardy, Randy, Rittler (HRR) plates (American Optical Company, NY, USA). Goldman kinetic visual fields were determined using the V4e and IIVe targets on a standard background. ERGs assessment included a full field electroretinogram (ERG) and pattern ERG (PERG), incorporating the protocols recommended by the International Society [327-330] for Clinical Electrophysiology of Vision Standard (ICSEV). Retinal autofluorescence was recorded using the Heidelberg Retina Angiography (HRA2; Heidelberg engineering, Heidelberg Germany). All clinical examinations were conducted by A. Webster, G. Holder and colleagues at Moorfields Eye Hospital.

2.11 Buffers and solutions

Ampicillin (1000 x): 50 mg/ml ampicillin (Sigma-Aldrich Company Ltd.) in dH_2O, sterile filtered, stored at -20°C

Big Dye Buffer (2.5 x): 200 mM Tris pH 8, 5 mM $MgCl_2$ with sterile dH_2O

Church Buffer: 21 g of NaH_2PO_4, 48.55 g Na_2HPO_4, 70 g of SDS, 0.5 M EDTA and dH_2O to 1 litre.

DNA loading buffer (6 x): 0.25 % (w/v) bromophenol blue and 30 % (v/v) glycerol in water

LB growth medium: 14 g Bacteriological agar (oxoid Ltd.) per litre of water, 5 g/l yeast extract, 10 g/l tryptone (Oxoid Ltd.), 10 g/l sodium chloride, and 50 µg/ml ampicillin

PBS (1 x): 85 g NaCl, 4.3 g KH_2PO_4, dH_2O to 10 litres, pH 7.2

PBS (tissue culture): 10 phosphate buffered saline tablets (Oxio Ltd.) dissolved in 1 l sterile ddH2O

PBS-MK: 1 x PBS, 2.5 mM KCl, 1 mM $MgCl_2$

Periodate lysine paraformaldehyde: 2% paraformaldehyde and 0.05% glutaraldehyde

Proteinase K buffer: 100 mM Tris (ph 7.4), 50 mM EDTA and 0.5 % SDS

Sodium cacodylate buffer (0.07 M): 0.2 M $(CH_3)_2AsO_2Na.3H_2O$ with 0.2 N HCl

Sodium phosphate buffer: 97.1 g Na_2HPO_4, 43.6 g NaH_2PO_4, pH 7.2

Toluidine blue stain: 25 ml 2 % hydrated sodium borate, 25 ml 100 % ethanol, 0.5 g toluidine blue (SPI-Chem™)

3

3 AAV-mediated rescue of the RCS rat

3.1 Introduction

AAV has nowadays reached the central point of prominence in the development of vectors for human gene therapy applications because of its structural simplicity and its non-pathogenic character in humans. Initial gene transfer studies to the eye showed that AAV-based vectors are the most efficient vectors to target photoreceptor cells after subretinal delivery and that long-term expression of reporter genes can be maintained [331]. Over the last few years AAV vectors were used to rescue different animal models of retinal degeneration due to photoreceptor-specific defects [105, 221, 228, 230, 231, 283, 285, 332]. However, several factors make retinal degenerations due to mutation within genes specifically expressed in the RPE a more attractive target for the development of novel gene therapy protocols. The RPE is a tissue that is relatively efficiently transduced by a variety of recombinant viruses including AAV [228, 273, 314]. A single RPE cell is in contact with a number of photoreceptor cells and therefore a single transduced RPE cell might protect or restore function to several photoreceptor cells. In conditions, in which there is an RPE-specific gene defect, photoreceptor cells are primarily both healthy and functional, and their function needs to be retained rather than restored. The ability of AAV to transduce RPE cells has also been evaluated in different

species including mouse, rat, and dog [105, 333, 334]. A recent study has shown the ability of AAV to restore vision in the *rpe65* null mutation dog, a model for retinal degeneration due to an RPE-specific defect [105]. Another gene specifically expressed in the RPE is the receptor tyrosine kinase *MERTK*, which is mutated in the RCS rat, a well studied animal model for retinal degeneration, and in patients afflicted with autosomal recessive RP [69, 72, 159, 335].

The aim of the work described in this chapter was to determine the potential value of AAV-2-based vectors for a gene therapy approach of retinal degeneration due to a defect in the *MERTK* gene.

3.2 Transduction of the RPE

Photoreceptor outer segment tips are shed daily to replace used photopigments and thereby maintain the high sensitivity of visual perception. The membranous waste material is phagocytised by RPE cells [68, 335]. Many proteins are involved in the recognition, binding and transportation of this waste material. As described in chapter 1.1.6 and 1.1.7, MERTK is one of the key-proteins involved in phagocytosis and mutations within *MERTK* are leading to the inability of RPE cells to remove the shed outer segments [71]. As a result the waste material accumulates in the subretinal space, photoreceptors and RPE cells lose contact, and the RPE cells cannot provide essential substances to the photoreceptors, which consequently die [68, 69, 159].

Since it was not known if RPE cells express a specific receptor necessary for the up-take of AAV or if AAV uses the phagocytosis machinery to enter the host cells, the first problem which needed to be addressed, was whether the phagocytotic defect of the RPE of RCS rats would affect the uptake of vectors. Therefore a recombinant AAV-2 (rAAV-2) vector containing the *gfp* marker gene under the control of a cytomegalovirus (CMV) promoter (the recombinant virus

was named AAV.CMV.GFP) was injected into the subretinal space of four 10-day old RCS rats. For the production of rAAV, BHK cells were co-transfected with HSV helper virus and two plasmids: the rAAV plasmid pD10 containing the reporter gene expression cassette and the replicating amplicon providing the rep and cap genes [323]. The rAAV plasmid is generally deleted of all viral genes and is comprised of the viral terminal repeats flanking the expression cassette (see p81, figure 1.11). The rep and the cap genes, necessary for virus replication and packaging [322], are usually delivered on a separate plasmid to increase safety [323]. Both constructs – the rAAV vector containing the expression cassette (the promoter of choice and the reporter gene or transgene of interest) and the complementing vector (containing the *cap* and *rep* genes) – are usually configurated in a way that they share no sequence homology. Hence, contaminating pseudo-wild-type virus can only arise via non-homologous recombination.

Twenty-four hours after infection BHK cells were assessed for e*gfp* expression (Figure 3.1) and harvested by centrifugation after the completion of the lytic cycle (24 to 36 hr).

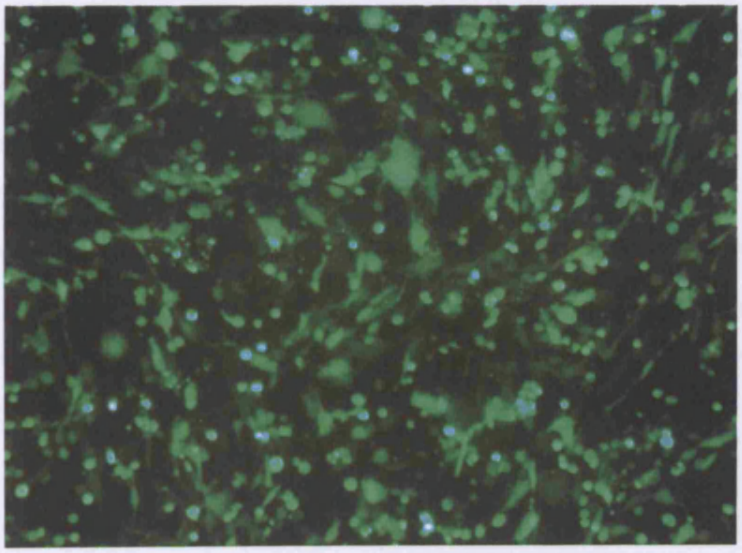

Figure 3.1: BHK cells expressing GFP. Twenty-four hours after infection cells were assessed for *gfp* expression to confirm that the transfection had been successful. The fluorescent image shows cells in which e*gfp* expression is under the control of the CMV promoter.

After purification, using a heparin column purification protocol [325] the molecular titre was estimated by dot-blot analysis (Figure 3.2). A serial dilution ranging from 10^9 to 10^{12} molecules of plasmid including a probe DNA of known concentration was used to produce a standard ladder. The dilution series was included in the blot. Usual titres ranged from 10^{11} to 10^{13} particles/µl.

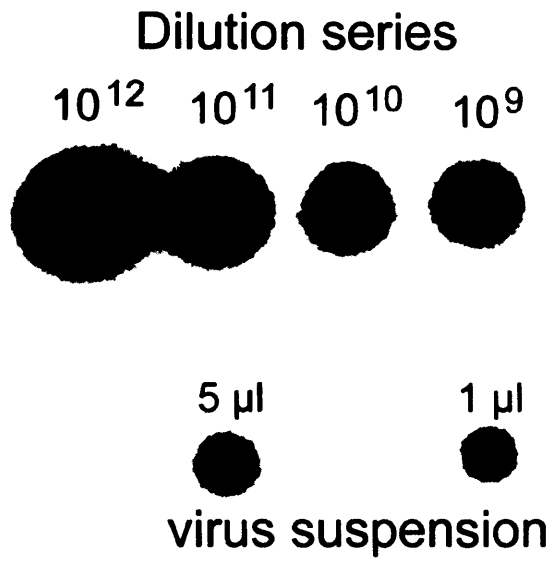

Figure 3.2: Autoradiogram of a dot-blot. The serial dilution of a DNA probe of known concentration serves as a standard ladder. 1 µl and 5 µl of the virus suspension were loaded and the concentration estimated by comparing the sample to the dilution series. In this case it was estimated that the virus suspension had a concentration of 10^{11} particles/ml.

We then injected 4 µl of virus suspension at a concentration of 4 x 10^7 rAAV particles/µl subretinally into each hemisphere of the right eye of four dystrophic RCS rats. The injections were performed under direct retinoscopy through an operating microscope [228]. The needle tip was inserted into the subretinal space causing a self-sealing tunnel and the virus solution was injected. The liquid causes a momentary detachment of the retina, which disappears steadily during the following 24 hr (see figure 3.3). The bleb size initially covers approximately one third of the retina.

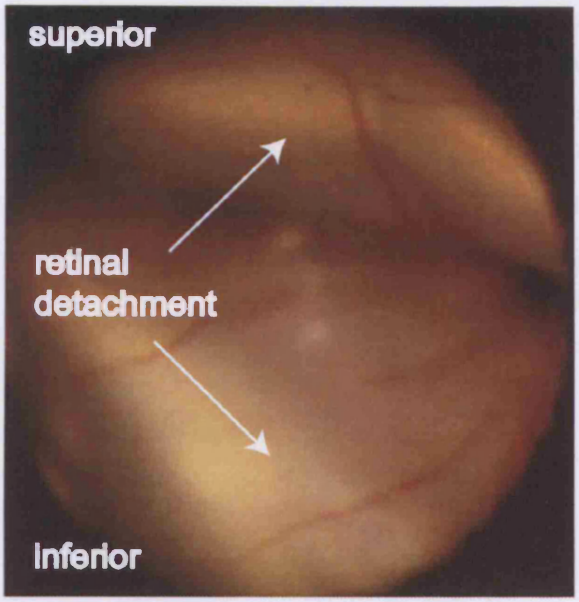

Figure 3.3: Rat fundus after subretinal injection. The injected virus suspension causes a momentary detachment of the retina. Detachments are seen in the superior and inferior hemisphere which together cover approximately two third of the retina.

Four weeks after injections, eyes were taken and prepared for cryosectioning. Sections were then analysed for GFP fluorescence. Propidium iodide was used as a nuclear counterstain for GFP fluorescence of transduced cells. The enhanced gfp (egfp) used in this project is known to give a brighter fluorescence compared to common *gfp*, and has a higher signal-to-noise ratio due to its shifted emission fluorescence. Therefore areas of maximal transduction rate and egfp expression, appear yellow in the fluorescent micrograph (figure 3.4). Efficient transduction of photoreceptor cells and RPE cells was observed in the treated areas, which covered approximately one third of the retina for each injection, of all animals. The size of the area, in which GFP fluorescence was observed, correlated with the bleb size generated by the injection of the virus solution. This result suggests that the phagocytotic defect of the RPE of RCS rats does not prevent the uptake of viral vectors.

Figure 3.4: AAV-mediated expression of e*gfp* in the retina. Four weeks after AAV-2-mediated delivery of the reporter gene e*gfp* under the control of the CMV promoter to the rat retina, efficient expression in photoreceptor and RPE cells is observed. Sections were stained with propidium iodide, a nuclear counterstain (red). Areas of maximal *egfp* fluorescence appear yellow. The size of the GFP fluorescent area correlates with the size of the momentary detachment of the retina generated by the virus suspension.

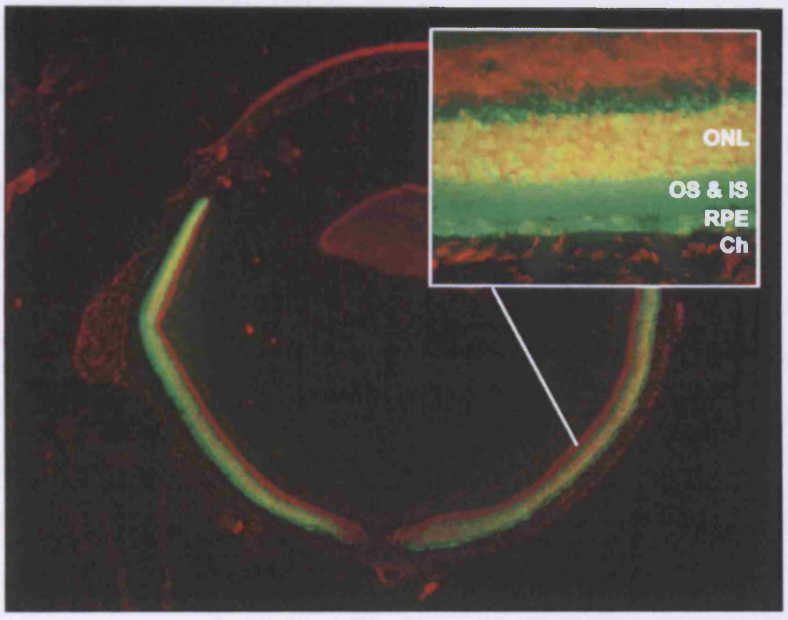

3.3 Expression pattern of different promoters

The choice of the promoter has an important role in location, strength and duration of expression. The CMV promoter has the advantage that it is considered to be a stronger promoter than other common promoters used in different vectors for gene therapy approaches and that it is highly active in a broad range of cell types.

In many gene therapy applications, however, a cell-specific promoter would be more appropriate because it provides the opportunity to restrict transgene expression to the cell type or tissue of interest. Hence, possible unwanted side

effects that might occur if the transgene is expressed in a non-native cell type are abolished and thereby safety of gene therapy increased. Since *MERTK* in the eye is predominately expressed in RPE cells, it was unclear if an additional expression of the therapeutic gene in photoreceptor cells - which would be the case if driven by the CMV promoter - would cause any unwanted effects. This problem can be circumvented by the use of an RPE-specific promoter. The *rpe65* promoter's activity is restricted to the RPE and therefore it can be used to target expression to the RPE [324]. However, the *rpe65* promoter is a mammalian promoter and therefore expression levels were expected to be lower than those of viral promoters such as CMV. In order to test the efficiency of the *rpe65* promoter's, another control construct was designed, in which the *egfp* marker gene is driven by the murine *rpe65* promoter. The approximately 650 bp RPE-specific *rpe65* promoter fragment described by Boulanger and collegues was amplified from murine genomic DNA [324] in our group. It contains an octamer (ATGCAAAT) and two protein-binding E-box sites which have been shown to be necessary for the RPE-specific activity of the promoter fragment.

The rAAV genome is generally comprised of the viral terminal repeats flanking the expression cassette of interest. The small size of the wild-type AAV genome (approximately 4.7 kb), however, limits the size of the fragment inserted into the rAAV plasmid. It has been shown that the optimal size of the rAAV vector, for high post-infection expression levels, lies between 4.1 and 4.9 kb. A possible reason might be that vectors in this size range are closer to the wild-type size of the AAV virus genome. Thus, whenever an expression cassette smaller than 4 kb is inserted into an AAV vector backbone – in this case the pD10 vector – a stuffer DNA sequence is cloned upstream or downstream to reach the optimal size range of 4.1 to 4.9 kb [323]. A stuffer DNA is a random sequence that is neither part of any promoter nor gene and does not contain long repeats to avoid non-specific transcription or intra-molecular recombination events, respectively. In this case, the *rpe65* promoter [324] and the reporter gene *gfp* were inserted in between the ITRs of the pD10 expression plasmid. In addition, a 2.3 kb stuffer sequence was inserted downstream the expression cassette because the total expression cassette size was only approximately 1.8 kb. The

construct was used to produce rAAV virus (AAV.RPE65.GFP). The virus suspension was then injected subretinally as described above into 10-day old non-dystrophic RCS rat eyes (4 µl of virus solution at a concentration of 4 x 10^7 particles/µl). Four weeks after injections the eyes were taken and analysed for GFP fluorescence (figure 3.5). Efficient RPE transduction was observed and the size of the area showing fluorescence was approximately the same size as the area covered by the bleb following injection. However, in contrast to the expression pattern of AAV.CMV.GFP, expression in photoreceptors was only found in areas of needle trauma. It is known that the damage to the neuroretina due to the surgical procedure including the degree of the needle trauma following subretinal injections and the speed of injection of vector suspension influences the efficiency of transduction. In these areas, transduction of photoreceptor cells by different viruses is commonly found. Our results suggest that the *rpe65* promoter is able to drive weak expression in photoreceptors and this only becomes in areas of needle trauma.

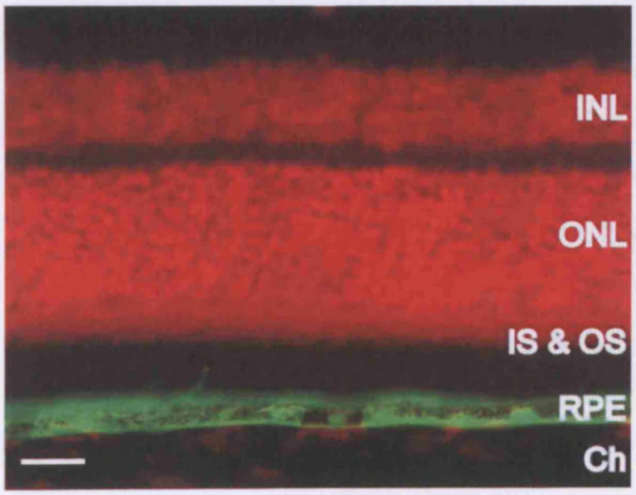

Figure 3.5: AAV.RPE65.GFP-mediated expression pattern. Four weeks after subretinal injection of AAV.RPE65.GFP eyes were analysed for *egfp* expression. Cryosections were counterstained with propidium iodide (red). GFP fluorescence was restricted to the RPE showing that the *rpe65* promoter is specifically active in the RPE. INL=inner nuclear layer, ONL=outer nuclear layer, IS & OS= inner and outer segments, RPE=retinal pigment epithelium, Ch=choroid, size bar=10 µm.

3.4 *MERTK* transgene expression

Having established that the cellular defect would not compromise transduction by AAV and that the *rpe65* promoter is functional, rAAV expressing the *MERTK* gene driven by either a CMV or an *rpe65* promoter were produced.

MERTK is a gene highly conserved between amniota. Comparison of the mouse and rat protein amino acid sequence shows that they are 91 % identical and therefore it was assumed that a murine copy of the *MERTK* gene would express a protein that would be functional in rats (for alignment of the amino acid sequences see Appendix). Rat eyes were collected and the cornea and lens were removed. The retina was immediately homogenised in Trizol reagent for total RNA extraction. Total RNA was then used to specifically amplify the *Mertk* cDNA by RT-PCR. Since it is difficult to amplify large fragments, 2 sets of primers were designed to cover the entire coding sequence of the approximately 3600 bp long *MERTK* mRNA. The two fragments obtained were combined using the naturally occurring *Eco*RV restriction enzyme site to give a full length cDNA clone of 3038 nucleotides. The *MERTK* cDNA was then cloned into the pGMT.Easy vector (Promega, Madison, WI). This plasmid contains a polylinker sequence that facilitates cloning since the PCR product is flanked by a variety of different restriction sites. The resulting plasmid was termed pGMT.Mertk and it was used to sequence the *MERTK* cDNA to ensure that no sequence changes occurred during the isolation and amplification of the fragment. After the sequence was confirmed, we used restriction enzymes *Sac*II and *Xho*I to excise *MERTK* (conducted by A. Smith).

After digestion, the sample was separated on a gel by electrophoresis, the fragment of the appropriate size was excised and gel extracted. The *MERTK* fragment was then ligated into the pD10 backbone, which was already digested at the same restriction sites. The *rpe65* promoter was already cloned into the gt-rpe65p2 plasmid. The restriction enzymes *Sal*I and *Sac*II were used to excise the promoter which was then ligated upstream of the *MERTK* gene in the pD10 backbone already digested with the same enzymes (figure 3.6). In this case, no

stuffer sequence was needed since the expression cassette size exceeded 4 kb. The resulting plasmid was named AAV.RPE65.Mertk (see figure 3.7 for the pD10 plasmid map).

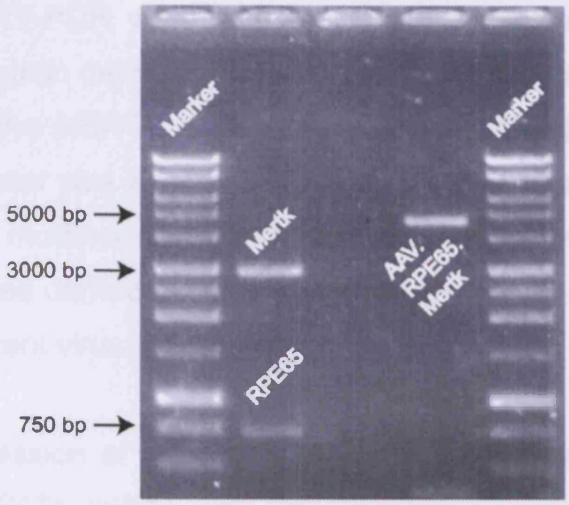

Figure 3.6: Restiriction enzyme digest. The ~3.1 kb *MERTK* fragment and the ~700 bp *rpe65* promoter fragment were isolated and cloned into the pD10 backbone to form the therapeutic construct AAV.RPE65.Mertk (~5 kb).

The same enzymes were used to excise the CMV promoter from the AAV.CMV.GFP construct. The *rpe65* promoter of the AAV.RPE65.Mertk construct was then exchanged against the CMV promoter fragment and the resulting construct was termed AAV.CMV.Mertk. Both constructs were used to produce rAAVs.

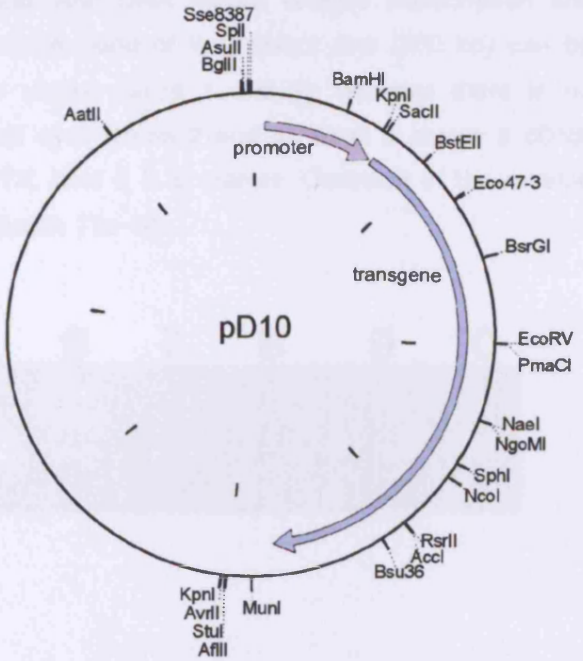

Figure 3.7: Map of the AAV-2 pD10 plasmid. The transgene (either *gfp* or *MERTK*) was cloned downstream of a promoter fragment (either CMV or *rpe65*). In case of the reporter gene *gfp* a stuffer DNA was additional included downstream the expression cassett to reach the optimal total vector size of 4.9 kb.

The two vectors carrying the therapeutic gene were then injected into the subretinal space of 10 day old RCS rats (3 animals for each construct). In order to demonstrate that the viruses are functional and the transgene is expressed, rats were sacrificed nine weeks after injection and RNA was isolated from the retina as described previously. RT-PCR was used to confirm expression of *MERTK*. In RCS rats, the phagocytotic defect is due to a premature stop codon shortly downstream of exon 2 of the *MERTK* gene. To prevent amplification of the endogenous mRNA, the 5' primer was located in the region of the gene that is deleted in the RCS rat by the mutation. The samples were DNase treated before the reverse transcription was carried out to avoid an amplification of the transgene present in the recombinant virus.

In eyes injected with rAAV, expression of the *MERTK* gene was detected by RT-PCR, whereas full length *MERTK* mRNA was not detected in uninjected control eyes (figure 3.8). Omission of reverse transcriptase resulted in the absence of signal in all eyes, confirming that the PCR product in the treated eyes was derived from mRNA rather than the recombinant gene.

Figure 3.8: RT-PCR amplification of *MERTK* from injected rat eyes. RNA was isolated from eyes injected with AAV.CMV.Mertk (lanes 1 and 7) and AAV.RPE65.Mertk (lane 3 and 9) and the uninjected control eyes (lanes 2 and 8 and lanes 4 and 10, respectively). Samples were treated with DNase to remove genomic and viral DNA before reverse transcription and amplification of the transgenic *MERTK* mRNA. A band of the correct size (500 bp) can be amplified from the eyes treated with either vector (lanes 1 and 3); whereas there is no transgenic mRNA detectable in the uninjected eyes (lanes 2 and 4). Lane 5 shows a cDNA positive control for the amplification of *MERTK*, lane 6 is a marker. Omission of the reverse transcriptase results in the absence of signal (lanes 7 to 10).

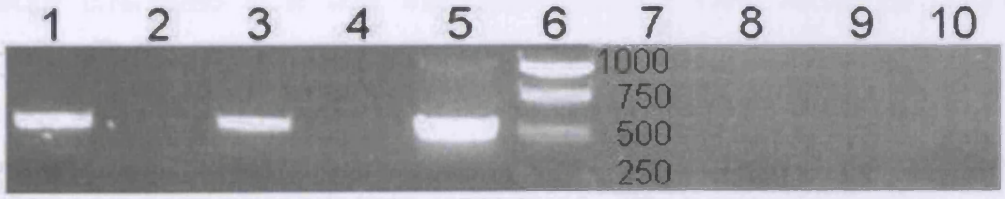

3.5 Effects of *MERTK* transgene expression on retinal morphology

Since expression of the *MERTK* transgene could be confirmed by RT-PCR we wanted to evaluate the effect of treatment on retinal morphology and to determine whether we would be able to delay retinal degeneration. For each vector, five RCS rats were injected subretinally. To increase the treated area and to maximise the number of RPE cells reached by the virus, the virus suspension was not only injected superiorly but the procedure was repeated in the inferior hemisphere. With this technique approximately 70 % of the retina is exposed to the virus. For each construct one eye of the animals was treated; the contralateral eyes were left untreated as internal controls. This was necessary because it is known that the pace of photoreceptor cell loss and the rate of retinal degeneration in the RCS rat is influenced by many factors and varies even between animals from the same litter. If only one eye of each animal is treated, the effect of a treatment can be estimated by comparing the treated with the untreated eye in each animal, thereby controlling for inter-animal variation. Since degeneration in RCS rats is rapid and starts at young age of the animals (approximately around postnatal day (P) 14 shortly after the palpebral fissure opens) injections were performed in 10-day old rats in order to achieve transgene expression at a time point when retinal degeneration is not yet too advanced [68].

Animals were sacrificed nine weeks after treatment and the eyes were taken and processed for semithin sections. Before fixation and embedding eyes were carefully orientated in a way that both injection sites would be present in sections taken in areas around the optic nerve head. For histological analyses sections were examined with light microscopy (figure 3.9). In treated eyes there appeared to be less debris deposited between the photoreceptor cell layer and the RPE than in untreated controls. This suggests that after treatment at least partial restoration of RPE phagocytosis was achieved. It is known that retinal degeneration in RCS rats is characterised by hemispheric differences in the

pace of photoreceptor cell loss, with an accelerated pace of degeneration in the inferior hemisphere. Furthermore, there is a gradient in photoreceptor loss from the posterior pole to the peripheral retina, with photoreceptors being preserved longer close to the ciliary body. Therefore, pictures of an area approximately in the middle of the injection site between the optic nerve and the ciliary body in the superior hemisphere were taken of each eye and the number of photoreceptor cell nuclei was counted over a 250 μm wide area of the outer nuclear layer (ONL). Pictures of untreated eyes were taken of analogous areas of the retina. To control for the inter-animal variation in the rate of degeneration, a paired t-test was performed between the number of photoreceptors in the treated and untreated eyes of each animal. In the eyes injected with AAV.CMV.Mertk, the number of photoreceptor cells was approximately 2.5 times higher at this time point than in untreated controls (85 ± 37 versus 33 ± 9; p=0.022). In eyes treated with AAV.RPE65.Mertk the number of photoreceptor cells was approximately 2 times higher at this time point compart to untreated controls (59 ± 28 versus 31 ± 7; p=0.05). The less efficient rescue achieved with AAV.RPE65.Mertk in comparison to AAV.CMV.Mertk was probably due to the difference in the promoter strength. The viral promoter CMV is a stronger promoter with higher expression levels than the mammalian *rpe65* promoter. The higher number of photoreceptor cells in treated eyes confirms that the photoreceptor loss was reduced. Furthermore, in both treatment groups a reduction in the debris layer thickness could be observed. This indicates that the phagocytic function of the RPE was at least partially restored after the treatment with the therapeutic constructs.

Figure 3.9: Histological analysis of AAV.CMV.Mertk treated eyes. Semithin sections of AAV.CMV.Mertk treated **(a)** and the contralateral untreated eye **(b)** were stained with toluidine blue 9 weeks after injection. The amount of debris deposited between the outer nuclear layer and the RPE is lower in the treated eyes than in the untreated eyes, indicative of a restoration of the phagocytic function of the RPE. Furthermore, the number of photoreceptor cell nuclei is higher after injection with therapeutic virus, confirming that the rate of photoreceptor cell loss in decreased (size bar = 10 µm).

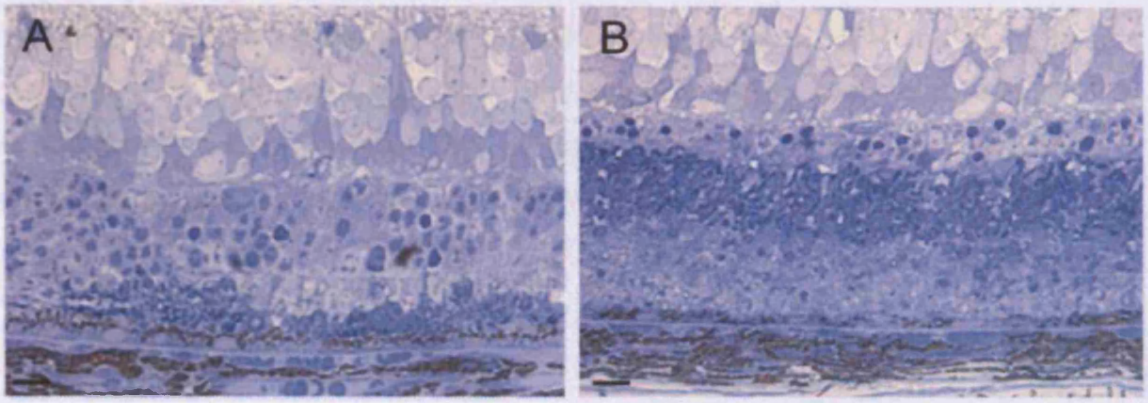

3.6 Effects of *MERTK* transgene expression on retinal function

After having established that the expression of the murine *MERTK* gene is delaying photoreceptor cell loss in the RCS rat, we then wanted to test if transgene expression would also increase and/or prolong retinal function. Photoreceptor cells are initially inherited healthy and functional in RCS rat, since the primary gene defect is in the RPE cells. Electroretinography (ERG) is a useful device to examine retinal activity and follow the progress of photoreceptor cell loss over time (see [336] for a review).

The electrical response of the retina over time can be separated in different parts (see figure 3.10). It begins with an a-wave, which polarity is negative relative to the cornea. This signal is interrupted by a large corneal-positive potential, the b-wave. The a-wave results from the closure of cyclic nucleotide

gated cation channels in the outer segment of photoreceptor cells in response to the capture of photons. The b-wave is generated in Müller and bipolar cells of the inner nuclear layer and its amplitude correlates with the number of functional photoreceptor cells in the eye. At the end of the trace another positive signal can be found, the c-wave. The c-wave is a sum of potentials generated by Müller and RPE cell which can be used to assess the functional integrity ot the retina. Oscillatory potentials (OPs) are a series of rapid low-amplitude potentials on the ascending limb of the b-wave of the ERG trace, usually comprising four or more wavelets (reviewed in [337]). OPs are sensitive to ischemia in the inner layers of the retina. Therefore OPs are useful indices for clinical application (for reviews see [327, 338]).

Figure 3.10: Electroretinogram sample trace. This is an example of an ERG trace. The main components are the cornea-negative a-wave and the cornea-positive b-wave. At the end of the trace another cornea-positive signel, the c-wave, is located. Not only the size of the b-wave amplitude is important but also the shape of the curve. Oscillatory potentials on the ascending limb of the b-wave are characteristic for normal ERG waves.

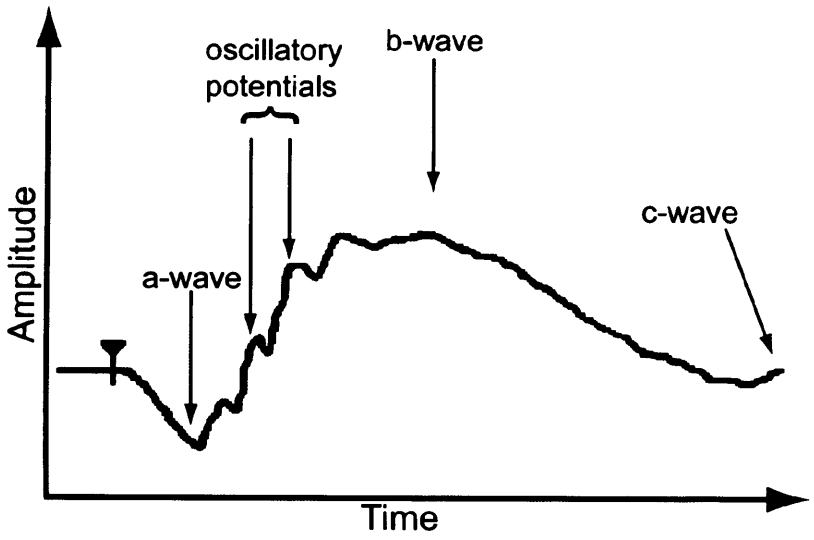

3.6.1 ERG intensity series

In this experiment both therapeutic vectors, AAV.CMV.Mertk and AAV.RPE65.Mertk, as well as the control vectors AAV.CMV.GFP and AAV.RPE65.GFP were used. For each vector the right eye of five dystrophic RCS rats was injected subretinally, whereas the left eyes remained untreated to control for inter-animal variations. After dark adaption over night, scotopic ERG recordings were obtained simultaneously from the injected, right and the control, left eye of all animals. Retinae were stimulated with bright light stimuli with increasing intensity. At an intensity of 10 mcd s/m^2, only rod responses are measured. At a flash intensity of 100 mcd s/m^2 the total response of both rods and cones was measured allowing us to analyse the overall rescue of photoreceptor cells. The response of cones is reflected in recordings at 1000 mcd s/m^2. Figure 3.11 shows ERG intensity series six weeks after treatment with therapeutic vectors and control injections with the AAV.CMV.GFP virus. At all flash intensities b-wave amplitudes were significantly higher (see section 3.6.2 for statistics) in eyes treated with with either AAV.CMV.Mertk (figure 3.11a) or AAV.RPE65.Mertk (figure 3.11b) than those measured in control eyes (figure 3.11c). Furthermore, there was an improvement in the shape of the ERG

trace after the treatment. A number of OPs are present on the ascending limb of traces from treated eyes. OPs cannot be seen in recordings taken from control eyes. The improvement was a direct consequence of the *MERTK* expression, since injections of GFP control vectors or (Figure 24c) or PBS did not alter the size of the ERG response or the shape of the trace.

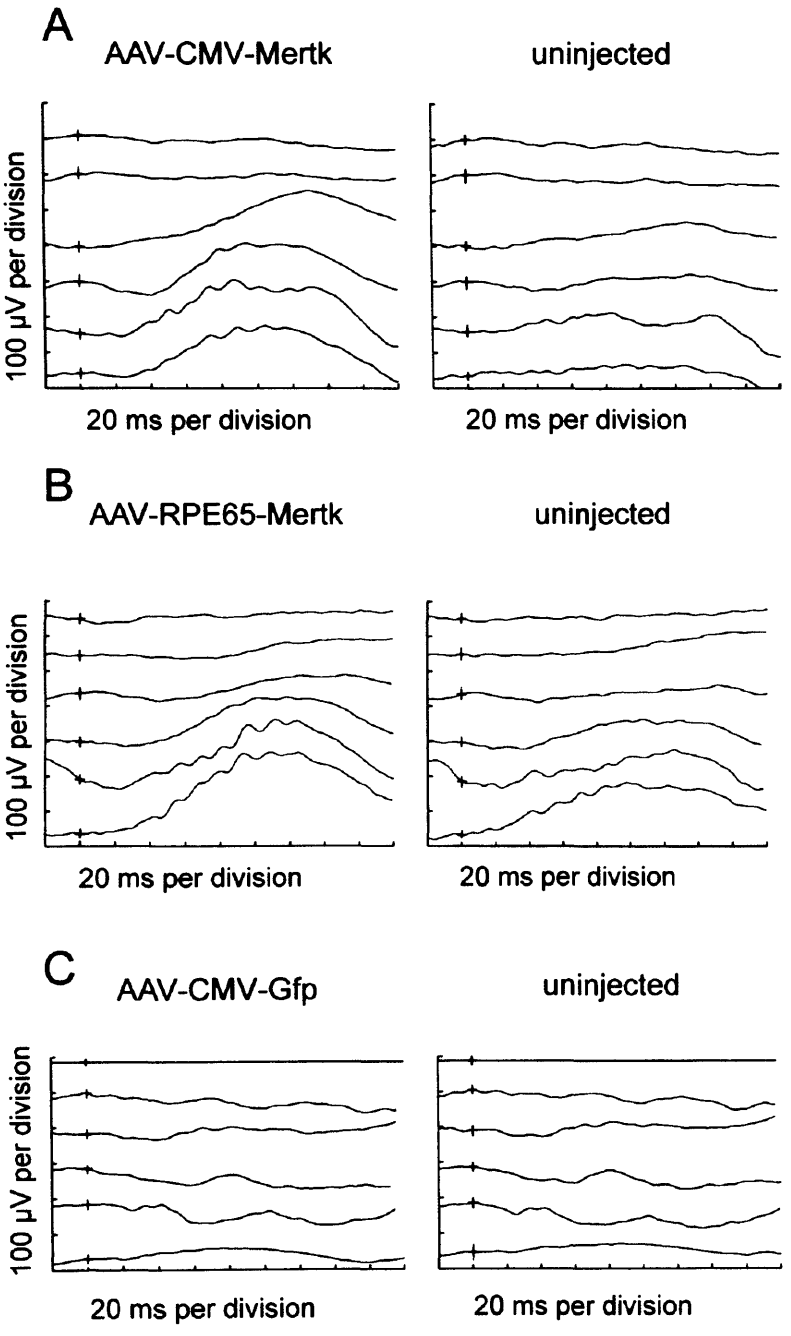

Figure 3.11: ERG recordings following gene delivery. A representative intensity series of right and left eyes is shown 6 weeks after various treatments. After treatment with AAV.CMV.Mertk **(a)** or AAV.RPE65.Mertk **(b)** an increased b-wave amplitude with OPs on the ascending limb of the b-wave was present in the treated eye. This indicates a prolonged photoreceptor function after the delivery of therapeutic vectors. Injection of control vector AAV.CMV.GFP **(c)** does not lead to altered traces at any time point suggesting that the improvement in treated eyes was due to the expression of the *MERTK* transgene. ERG traces shown in each chart were recorded at intensities of 0.1, 1, 10, 100, 1000, and 300 mcds/m^2.

3.6.2 ERG time course

ERG analyses are a non-invasive method and recordings can be obtained from individual animals at regular intervals, allowing the possibility of following the course of photoreceptor loss over time. Figure 3.12 shows ERG traces at a single flash intensity (100 mcd s/m^2) measured in the same animal at various time points after treatment with AAV.CMV.Mertk. This flash intensity was chosen for further analysis since electrical response of both rods and cones are measured. This allows the analysis of the overall rescue of photoreceptor cells. Five weeks after treatment, the b-wave amplitude in the treated eye was substantially higher than in the control eye (figure 3.12). This suggests that more photoreceptor cells were present in treated eyes compared with untreated, control eyes. In the untreated eye, the amplitude of the b-wave decreased rapidly over time reflecting the progressive loss of photoreceptor cells, until the trace was virtually flat after 6 weeks. At this time point there was still an ERG response present in the treated eye, suggesting that the degeneration of photoreceptor cells was slowed by the treatment.

Figure 3.12: ERG recordings. Recordings were taken from a single animal at various time points following gene delivery. Averaged responses at a flash intensity of 100 mcds/m^2 from one individual RCS rat are shown over 12 weeks following treatment with AAV.CMV.Mertk. The time course clearly reveals the improvement of b-wave amplitude and the shape of the trace. These effects are present for up to 9 weeks when the b-wave amplitude gradually declines on the treated side.

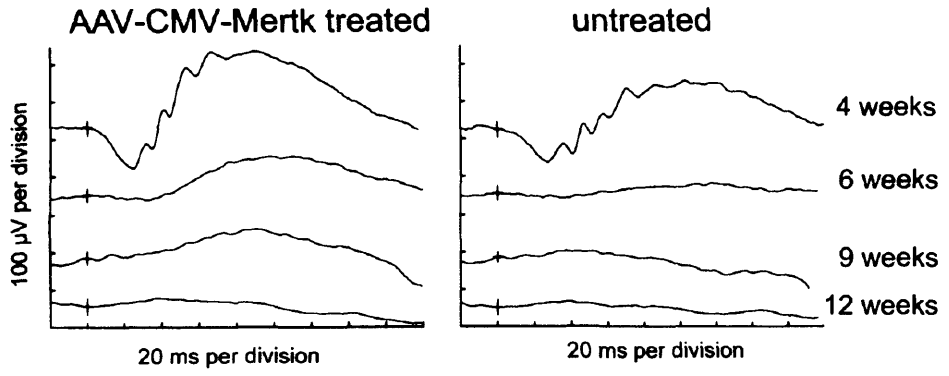

In order to show that the functional rescue we accomplished was significant, statistical analysis of the ERG recordings were carried out. Paired t-tests showed that the average b-wave amplitudes recorded from eyes treated with either AAV.CMV.Mertk or AAV.RPE65.Mertk were significantly higher than in the contralateral untreated controls at all time points examined up to 9 weeks after treatment (Figure 3.13). Maximal differences were obtained 7 weeks after treatment for both viruses. At that time point the average b-wave amplitude in the eyes treated with AAV.CMV.Mertk was 2.5 fold higher than in the untreated eye (76 ± 55 μV versus 29 ± 23 μV; $p = 0.011$). In the animals treated with AAV.RPE65.Mertk the average b-wave amplitude in the treated eyes after 7 weeks was 4 fold higher than in the control eyes (73 ± 36 μV versus 17 ± 13 μV; $p = 0.009$). In the control groups, injected with PBS or *gfp* expressing viruses, there was no significant increase in b-wave amplitude at any time point (Figure 3.13).

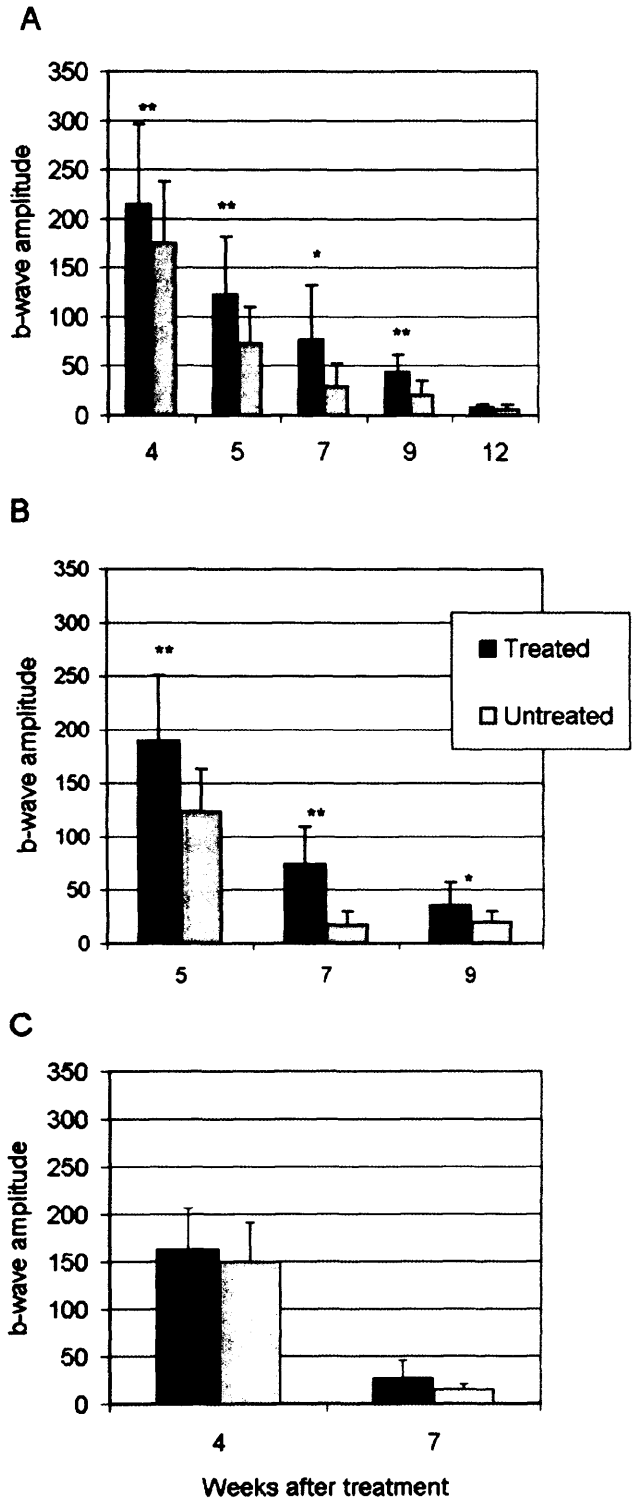

Figure 3.13: Mean ERG b-wave amplitudes after injection of recombinant AAV. The mean b-wave amplitudes and standard deviation (SD) of the treated and untreated eyes are shown at various time points after treatment with AAV.CMV.Mertk **(A)**, AAV.RPE65.Mertk **(B)** and AAV.CMV.GFP **(C)**. All measurements were performed at a flash intensity of 100 mcds/m^2. Statistical significance of the difference between the treated and untreated eyes was determined using a paired t-test (* = $p<0.05$, ** = $p<0.01$). After treatment with virus containing *MERTK* a significantly improved ERG response is present up to 9 weeks after injection, whereas injection of AAV.CMV.GFP did not increase the b-wave amplitude.

3.7 Effects of *MERTK* overexpression

AAV-2 is able to transduce photoreceptor cells and RPE cells in the eye [227] and thus transgenes would be expected to be expressed in both cell types when driven by a ubiquitous active promoter like the CMV promoter. Consequently, injections of AAV.CMV.GFP were leading to fluorescence in photoreceptor as well as RPE cells. Accordingly it can be assumed that *MERTK* is also expressed in both cell types after subretinal delivery. However, *MERTK* expression is normally restricted to the RPE cells. As mentioned previously the CMV promoter is a strong, viral promoter. Gene expression from this promoter is known to be at a higher rate compared to mammalian promoters. Virus-mediated expression of *MERTK* under the control of the CMV promoter is leading to higher expression levels than it would be expected when the transgene is driven by the endogenous promoter or other mammalian promoters. Therefore, it was necessary to establish if an additional expression of *MERTK* in photoreceptors and an overexpression in RPE cells would affect retinal function.

Therefore, AAV.CMV.Mertk was injected subretinally into four adult non-dystrophic rats and ERGs were recorded after the treatment with the therapeutic construct. In figure 3.14, a representative ERG intensity series of wild-type, non-dystrophic rats is shown, eight weeks after treatment with AAV.CMV.Mertk. The injection of the vector and the expression of *MERTK* in the photoreceptor cells did not affect the b-wave amplitude in these animals at this time point indicating that an additional *MERTK* expression in photoreceptor cells did not affect retinal activity.

Figure 3.14: ERG intensity series. Recording after injection of AAV.CMV.Mertk into normal, non-dystrophic rat eyes. No differences were found in b-wave amplitude or the shape of the trace. This shows that an additional expression of *MERTK* in photoreceptor cells has no effect on retinal function.

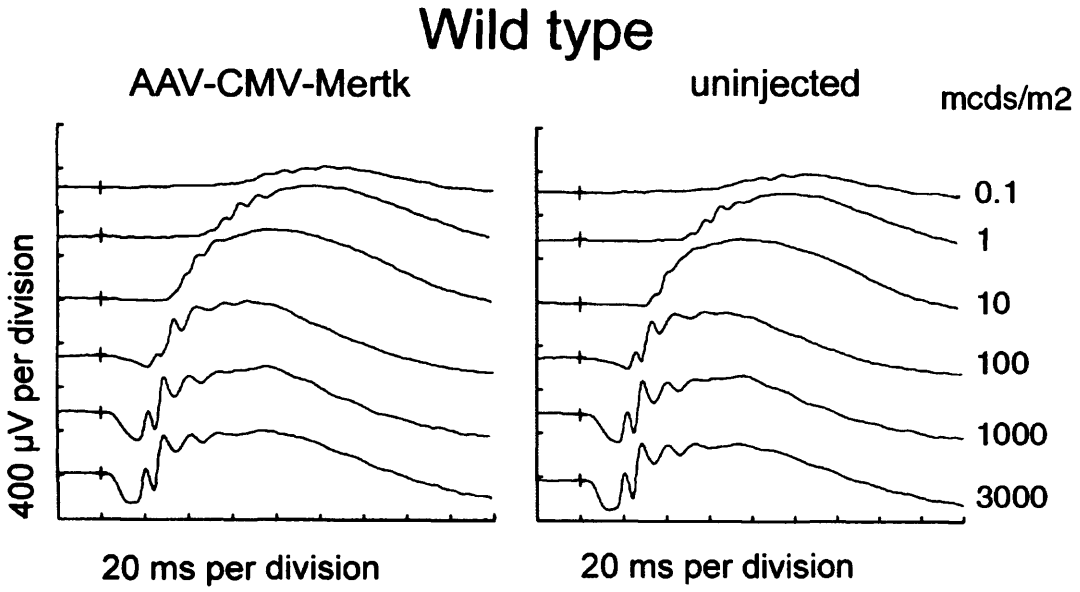

To confirm that the additional expression of *MERTK* in photoreceptor and RPE cells does not alter retinal morphology, which was already suggested by the ERG results, rats were sacrificed after the ERG recording and eyes were processed for semithin sections and light microscope analysis. Wild type eyes treated with the therapeutic vector did not differ from untreated eyes (figure 3.15) confirming that the additional *MERTK* expression had no effect on retinal morphology.

Figure 3.15: Light micrographs of a wild-type rat retinae. (A) Eight weeks after subretinal injections of AAV.CMV.Mertk into non-dystrophic rats, eyes were analysed histologically. The additional expression of *MERTK* in photoreceptor and RPE cells did not alter retinal morphology. **(B)** The contralateral untreated eye served as a control. INL=iner nuclear layer, ONL=outer nuclear layer, IS=inner segments, OS=outer segments, RPE=retinal pigment epithelium, size bars=50 µm.

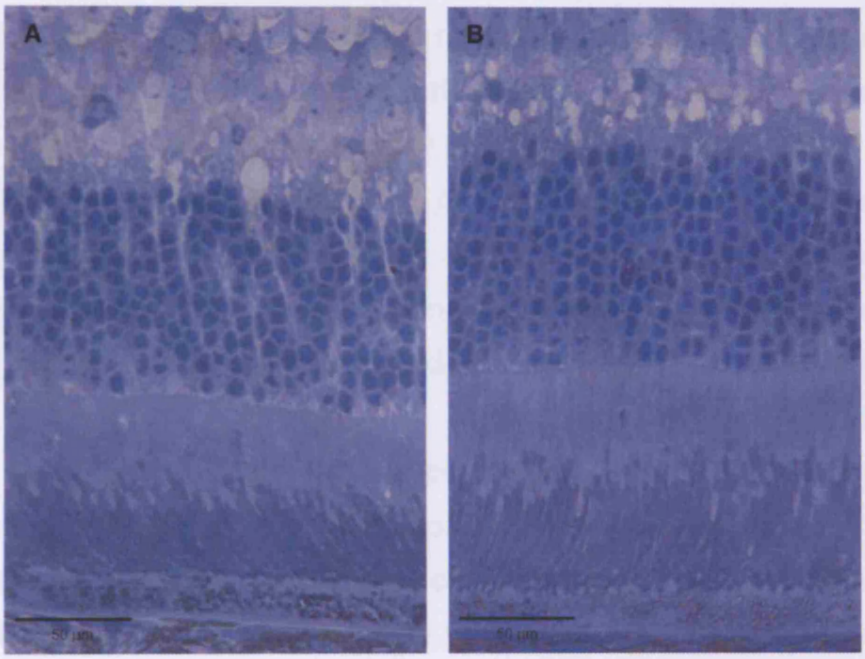

3.8 Discussion

In order to achieve successful gene therapy for RP a number of key requirements have to be fulfilled. The transgene should be expressed in the correct cell type and at an appropriate level. Another requirement is the long-term expression of the therapeutic gene to ideally allow a lifelong correction of the defect without the need of frequent follow-up treatments. The value of rAAV as a vector for gene delivery to the retina has become apparent over the last few years. Most of the studies however are targeted to photoreceptor cells. An example for the successful treatment of retinal degeneration due to a RPE-specific defect is the *rpe65*$^{-/-}$ dog [105]. This chapter describes the use of rAAV to treat retinal degeneration due to another RPE-specific defect, namely the phagocytic defect in the RCS rat caused by a mutation in the *MERTK* gene.

Recently, Vollrath *et al.* reported a temporary delay of retinal degeneration after rAd-mediated *MERTK* gene transfer into RCS rats. The authors could show that one month after injection, the number of photoreceptor cells in the area of the injection was 2 to 3 fold higher in the injected eye than in uninjected control eyes [233]. They also reported that they were able to restore the phagocytic defect of the RPE and that photoreceptor activity was improved one month after injection. However, they did not follow the survival of the photoreceptors over time and it is therefore unclear how long the improvements lasted although it is likely to be very short lived due to the host's immune response against Ad [233]. These experiments provided the formal proof that the *MERTK* gene is the actual cause of the disease in these animals and indicated gene therapy for this form of RP may be possible [233]. Ad vectors have several disadvantages for gene therapy approaches including the relatively short duration of transgene expression which has been ascribed to the immune responses generated against viral gene products [274, 339]. AAV-mediated gene transfer has the advantage over Ad vectors in that rAAV is able to transduce RPE cells with a high efficiency [227, 228] and in contrast to rAd vectors, transgene expression mediated by rAAV vectors is maintained over long periods. After injection into rodents, expression typically lasts throughout the lifetime of the animal [340].

AAV transgene expression studies in non-human primates have shown that there is still no notable decrease in transgene expression a year after treatment [341]. Therefore it is likely that transgene expression in humans will also persist for long periods of time.

The decrease in the debris layer thickness suggests that following transduction of RPE cells in the RCS rat with rAAV expressing *MERTK* the phagocytotic function of these cells is at least partially restored. In RCS rats, rod outer segment tips normally are not removed and accumulate in the subretinal space. The deposition of debris is slowed after treatment, even though it is not completely prevented. As a result of the treatment and the reversion of the phagocytotic defect the rate of photoreceptor cell loss and retinal degeneration is reduced and retinal activity prolonged. Photoreceptor function is still detectable in treated eyes 9 weeks after injection, whereas untreated eyes at the same time point provide no recordable activity, showing that retinal activity was improved after the treatment.

The effect of *MERTK* expression on photoreceptor survival does not last as long as *MERTK* transgene expression. This may be due to a number of factors. One factor might be the relatively late onset of AAV-mediated transgene expression (for a review see [275]). The animals were injected around postnatal day 10. By the time transgene expression started, 2 to 3 weeks later, there already is a substantial amount of debris deposited in the subretinal space. ERG recordings from one-month old RCS rats are already lower than in wild-type animals, suggesting that damage to photoreceptors has occurred by the time treatment with AAV vectors may take effect. The incomplete rescue in this model might also be explained by the fact that not all the debris between the photoreceptors and RPE is cleared. Not only has debris accumulated by the time AAV-mediated *MERTK* expression occurs, the level of transgene expression may not be sufficient to clear the backlog. Furthermore, only part of the retina is transduced. We estimate that the two subretinal injections in the rat cover roughly between 50 and 70 % of the retina. Even if the photoreceptor cells in these areas benefit from a reduction in debris, degenerating photoreceptors in other parts of the retina may have a negative impact on photoreceptor survival

in treated areas of the retina. This type of phenomenon has previously been described in chimaeric animals containing mutant and wild-type photoreceptor cells, in which the rate of photoreceptor cell death for both cell types was similar [342]. It was suggested that apoptosis of mutant cells generated a microenvironment that had a negative influence on the survival of healthy cells. Despite the partial nature of the rescue, loss of function in the treated rats was slowed by several weeks. In these experiments a murine *MERTK* cDNA was used to treat the RCS rat. Even though *MERTK* is highly conserved between species there are still some differences in the amino acid sequence. The rescue might be increased and photoreceptor survival and function maintained over a longer period of time by using the endogenous rat *MERTK* cDNA.

AAV exist in several serotypes, which differ in their cell surface receptors, heparin sulphate and sialic acids [221]. In the eye it has been established that rAAV-2 and AAV-2 pseudotyped with AAV-5 (AAV-2/5) efficiently transduce photoreceptor cells as well as RPE cells after subretinal delivery. Transgene expression has been shown to be restricted to the RPE for AAV-2/1 and AAV-2/4. Pseudotyping AAV-2 with either AAV-1 or AAV-4 gives another possibility to restrict transgene expression to the RPE independent of the promoter used. The advantage of AAV-2/1 is the early onset of expression which is only delayed by days compared to weeks if mediated by AAV-2/2. However, whereas RPE tropism for AAV-2/1 could only be shown in mouse, chimeric AAV-2/4 vectors result in a stable, RPE specific expression of the *gfp* reporter gene in a number of animal models including mice, rats, dogs and non-human primates. Since in particular AAV-4 has been shown to mediate high levels of transgene expression and that the onset of expression is faster in comparison to AAV-2/2 [343], in case of the RCS rat, which has a fast progressing retinal degeneration, AAV-2/4 might prove to be a better suited vehicle for efficient, long-term transgene expression. In the experiments presented in this chapter it was shown that transgene expression from a CMV promoter is higher than from a mammalian *rpe65* promoter. With AAV-2/4 transgene expression could be targeted to the RPE regardless from the promoter used. AAV-2/4 might be of particular relevance in terms of future clinical application since it is important to restrict expression of the transgene to a specific tissue or cell type, which in the

case of *MERTK* is the RPE. In addition, AAV-2/4-mediates higher levels of transgene expression compared to AAV-2/2. However, more experiments need to be carried out to define the realistic potential of rAAV-2/4 in gene therapy approaches.

4

4 Lentivirus-mediated rescue of the RCS rat

Retroviral vectors are becoming standard tools in cell biology as well as potential therapeutic agents for human diseases. Lentiviruses, a subclass of retroviruses, have the advantage over other viruses used for gene therapy approaches that they are capable to transduce a broad variety of different dividing and non-dividing cell types. Long-term expression is ensured because lentiviruses stably integrated their genome into their host's genome. Furthermore they have a relatively large cloning capacity, sufficient for most envisaged clinical situations. Illustrating these properties, vectors derived from HIV-1 allow an efficient in *vivo* delivery and stable expression of transgene in different tissues. Although this opens prospects for human gene therapy, the biosafety of HIV-based vectors requires a careful evaluation, considering also the pathenogenesis of the parental virus and the insertional mutagenesis induced by the random integration of the virus. The biosafety issues connected with HIV-based vectors have prompted the development of non-integrating and non-primate based lentiviral vectors as vehicles for gene therapy approaches [295, 298, 300, 301, 344, 345].

Using AAV-mediated delivery of *MERTK* we were temporarily able to restore photoreceptor function and improve retinal morphology (see chapter 3). The partial and temporary rescue we observed was probably due to a combination of factors, including insufficient transduction of the RPE, inappropriate

transgene regulation and, perhaps most importantly, the two- to three-week delay in onset of AAV-mediated transgene expression. The main potential advantage of using a lentiviral rather than AAV vector particularly in the RCS rat model, which has a rapid degeneration, is the much faster onset of lentivirus-mediated gene expression. In order to determine whether we would be able to prolong the rescue achieved with AAV-mediated gene delivery, we have constructed human immunodeficiency virus 1 (HIV-1) -based lentiviral vector carrying a *MERTK* cDNA and the long-term effects on retinal morphology and functions were evaluated in detail [283, 313, 314].

Lentiviruses have the ability of genome integration. Thereby the gene of interest is passed on by replication and long-term expression of the gene of interest is ensured. However, chromosomal integration has its disadvantages. Normally the insertion occurs randomly and as a result the location of the inserted gene varies enormously. This problem can be circumvented by the use of non-integrating lentiviruses. Thereofre, we aimed to assess the value of integration deficient HIV-1-based vectors for gene therapy approaches in the eye.

HIV-1-based vectors are the most thoroughly investigated lentiviral vectors for gene therapy. Over the last few years significant effort has gone into HIV vector development to maximise their biosafety and to minimize the possibility of generating replication-competent viruses. However, many questions about the biosafety of HIV-based vectors for use in human clinical trials remain to be answered. Due to the biosafety concerns, gene therapy vectors based on other, non-human lentiviruses have been developed. We wanted to examine the expression pattern and duration of equine infectious anemia virus (EIAV) based vectors [345, 346] after different routes of intra-ocular delivery and to evaluate their applicability as gene transfer vehicles for ocular gene therapy.

4.1 Treatment of retinal degeneration with lentiviral constructs

To determine whether we would be able to improve the rescue of retinal degeneration in the RCS rat model by using lentiviruses, we first produced VSV-G pseudotyped HIV-1-based lentiviruses containing the murine *MERTK* cDNA under the control of the ubiquitously active spleen focus forming virus (SFFV) heterologous promoter (figures 4.1 and 4.2) [312, 313, 326]. VSV-G envelope protein recognises a ubiquitous phospholipid in the cell membrane enabling for an extended viral host range and titres of up to 10^9 IU/mL (see page 87, figure 1.12) [303, 304].

In the third-generation self-inactivating (SIN) vector used in this experiment [347-349], the enhancer region of the 3' U3 of the long terminal repeat (LTR) bears a deletion, which is transferred to the 5' LTR of the proviral DNA upon reverse transcription and integration (see figure 4.2 for a vector map). This deletion abolishes the transcriptional activity of the LTR. The resulting transcriptional inactive vector cannot be converted into a full length vector RNA in transduced cells and thereby the risk of regenerating replication competent viruses is minimised [305, 312, 348]. This increases the safety of the virus as it renders vector mobilisation impossible even upon infection of replication competent HIV [350]. Furthermore, it reduces the likelihood that cellular coding sequences located next to the vector integration site will be expressed either due to the promoter activity of the 3' LTR or through an enhancer effect. The final advantage of using a SIN vector is that possible interference between the LTR and the internal promoter that drives the transgene is prevented by this design. Since any promoter activity seizes form the LTRs is abolished, an internal promoter is needed for the expression of the *MERTK* cDNA. As it is the case with all viral vector systems the choice of an appropriate promoter is important to achieve efficient transduction and expression. SFFV heterologous promoter is derived from a replication-defective retrovirus and allows transgene expression levels similar to that of a CMV promoter. Like the CMV promoter, the SFFV promoter is a strong viral promoter that is ubiquitously active. Since HIV-

1-based vectors have been shown to target the RPE specifically after subretinal delivery if pseudotyped with VSV-G and photoreceptor transduction is normally not found apart from areas of the needle trauma, it was not necessary to use an RPE-specific promoter in this experiment.

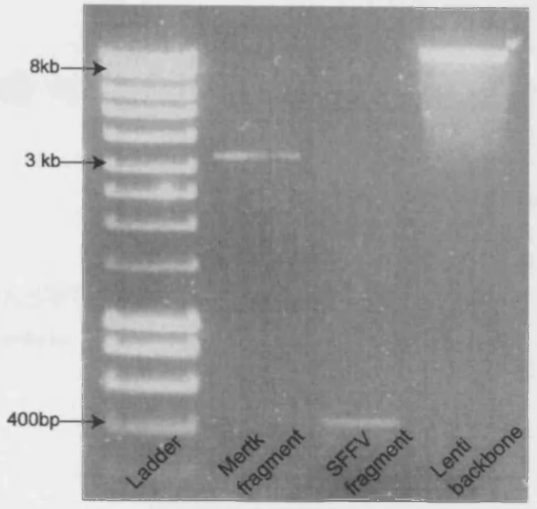

Figure 4.1: Restriction enzyme digest. The ~3.1 kb *MERTK* fragment was isolated from the pGMT.Easy vector and cloned into the pHR'SIN-cPPT-SEW backbone between the ~400 bp SFFV promoter fragment and the WPRE fragment of the vector backbone.

The central polypurine tract element (cPPT) is a *cis*-acting sequence that mediates the nuclear import of the viral genome (reviewed in [351]). Although not essential, the cPPT element increases the ability of the vector to infect non-dividing cells and thereby improving transduction efficiency. The *MERTK* cDNA was cloned in a way that its 3' end is followed by the Woodchuck hepatitis virus post-transcriptional element (WPRE). This *cis*-acting transcriptional regulatory element increases levels of transgene expression in the target cell up to 5-fold when included [352] and its action is independent of both the transgene and the host cell [351, 353, 354]. However, the full-length WPRE has promoter activity and the potential to express a 60 amino acid X protein-derived peptide. This peptide can activate or repress transcription of a number of cellular and viral genes. It has been suggested that X protein activity is associated with the generation of liver cancer, which is a common consequence of infection with hepatitis B virus in man [355, 356]. Therefore, we used the safer mutated form of WPRE to abolish any promoter activity and expression of the X protein. We termed the therapeutic recombinant viral vector LNT.SFFV.Mertk. As a control, a similar vector, LNT.SFFV.GFP, was constructed, which contained the reporter gene *gfp* cDNA instead of the functional copy of the *MERTK* gene.

Figure 4.2: Lentivirus vector map. The HIV-1-based vector pHR'SINcPPT-SEW was used to mediate the delivery of *MERTK* or *gfp* to the retina.

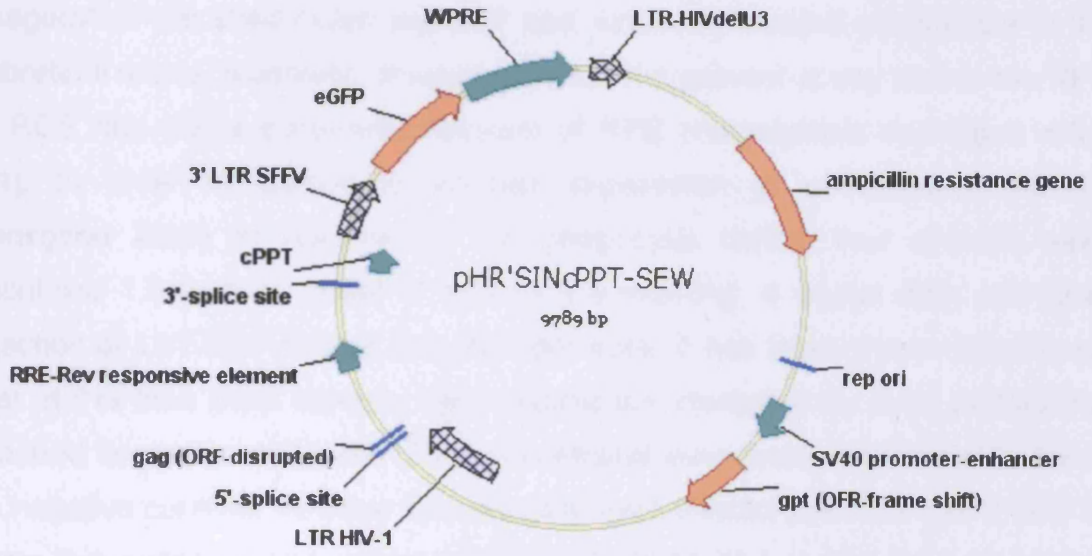

In order to optimise the effect of the treatment, the virus suspension was injected subretinally into the superior and inferior hemisphere of the eye to increase the size of the treated area [228]. For each injection 4 µl of virus suspension containing approximately 4 x 10^6 viral particles were used. RCS rats were treated at the age of 10 days to ensure transgene expression before the onset of degeneration and the appearance of a debris layer in the subretinal space. The right eyes of RCS rat were injected whereas the left eyes were left untreated as internal controls to balance inter-animal variations. Animals were examined histologically to investigate the effects of the treatment on retinal morphology over a period of seven months. To follow the course of retinal degeneration functionally, animals were examined by ERG at regular intervals over this period of time.

4.2 Restoration of the phagocytotic defect

Rod outer segment disc shedding follows a circadian rhythm in rats and is at its peak approximately 1.5 hr after onset of light in the morning [285]. Because of the mutation in the *MERTK* gene of RCS rats [69], the RPE is unable to phagocytise the shed outer segment tips, which as a result accumulate in the subretinal space. Normally, phagosomes are not present at any time in the RPE of RCS rats (for a schematic diagram of RPE phagocytosis see figure 4.3a) [71]. In order to determine whether expression of a functional *MERTK* transgene leads to reversal of the phagocytic defect, four animals were sacrificed 1.5 hr after onset of light in the morning, 4 weeks after subretinal injection of LNT.SFFV.Mertk into the right eyes. It has been shown previousely that at this time point reporter gene expression mediated by such vectors has reached its maximum levels. The contralateral eyes were not treated to serve as negative controls. Another four animals were treated with LNT.SFFV.GFP to show that possible improvements in LNT.SFFV.Mertk injected eyes are due to *MERTK* expression rather then induced by the surgical procedure or the virus itself. As positive controls 4 age-matched non-dystrophic rats were used. Eyes were taken, carefully orientate with a stitch through the conjunctiva and fixed in Karnovski fixative. Cornea and lens were removed the following day and the eyecups were processed for electron microscopy (EM). Semithin sections (0.7 µm thick) were taken and stained with toluidine blue. Treated areas were identified by light microscopy and 70 nm thick ultrathin section were then taken of these areas and corresponding areas of control eyes.

EM analysis of the retinae of wild-type rats shows that microvilli extend from the apical surface of RPE cells and surround the outer segment tips of photoreceptors. The recognition of shed outer segments, which express phosphotidylserine residues on their outer leaflet of the cell membrane, involves different receptors of the RPE cells. This recognition step leads to the activation of the receptor tyrosine kinase MERTK upon which the signal transduction cascade for the cytoskeletal changes necessary for the internalisation of the waste material into phagosomes is launched [84]. Figure 4.3a showes a

schematic diagram of phagocytosis. The first step is the cup formation, in which the RPE cell starts to surround the shed outer segment tip. After the up-take of the waste material in phagosomes it is transported through the RPE cell towards the choroid where they are conveyed to the circulation system. Numerous phagosomes containing outer segment debris are found in RPE cells of wild-type rats. There is no debris layer present between the RPE and the photoreceptors (4.3b). However, the mutation in the *MERTK* gene of RCS rats disables the RPE cells to internalise shed outer segments [69, 71]. The failure to phagocytise shed outer segment tips leads to an accumulation of membranous debris at the apical surface of the RPE. In untreated and LNT.SFFV.GFP (4.3c) injected controls, phagosomes cannot be found in any part of the eye [71]. In contrast, in the RPE of LNT.SFFV.Mertk treated animals we observed large round or oval phagosomes packed with structures resembling rod outer segment discs (4.3d). Whilst there were fewer phagosomes in the RPE of treated rats than in the RPE of normal rats, the phagosomes appeared to be morphologically very similar to that seen in wild-type animals (4.3b). This result indicates that we were able to at least partially reverse the phagocytic defect of RCS rats by delivering a functional copy of *MERTK* to the RPE cells.

Figure 4.3: EM analysis of the RPE. IS=inner segment, OS=outer segment, MV=microvilli, Ph=phagosome, N=nucleus, D=debris.

(a) Schematic diagram of phagocytosis. Phagocytosis begins with the recognition of shed outer segments by the RPE. This step is followed by the cup formation in which the microvilli surround the outer segment tips. After internalisation the waste material is degraded in the phagosomes and transported through the RPE cells towards the choroid.

(b) Non-dystrophic rat retina. Phagosomes are present in the RPE cytoplasm (indicated by arrows).

(c) LNT.SFFV.GFP injected RCS rat retina 4 weeks pi. No outer segments reach the apical surface of the RPE, instead a thick debris layer consisting of broken off outer segment tips and membranous waste material has built up due to the phagocytotic defect. The complete lack of phagosomes indicates that injections of LNT.SFFV.GFP have no therapeutic effect.

(d) LNT.SFFV.Mertk treated RCS rat retina 4 weeks pi. In some treated areas rod outer segment tips reach the surface of the RPE. In these areas no debris layer could be found due to the presence of numerous phagosomes. The morphology of treated retinae and RPE resemble that of normal, non-dystrophic animals.

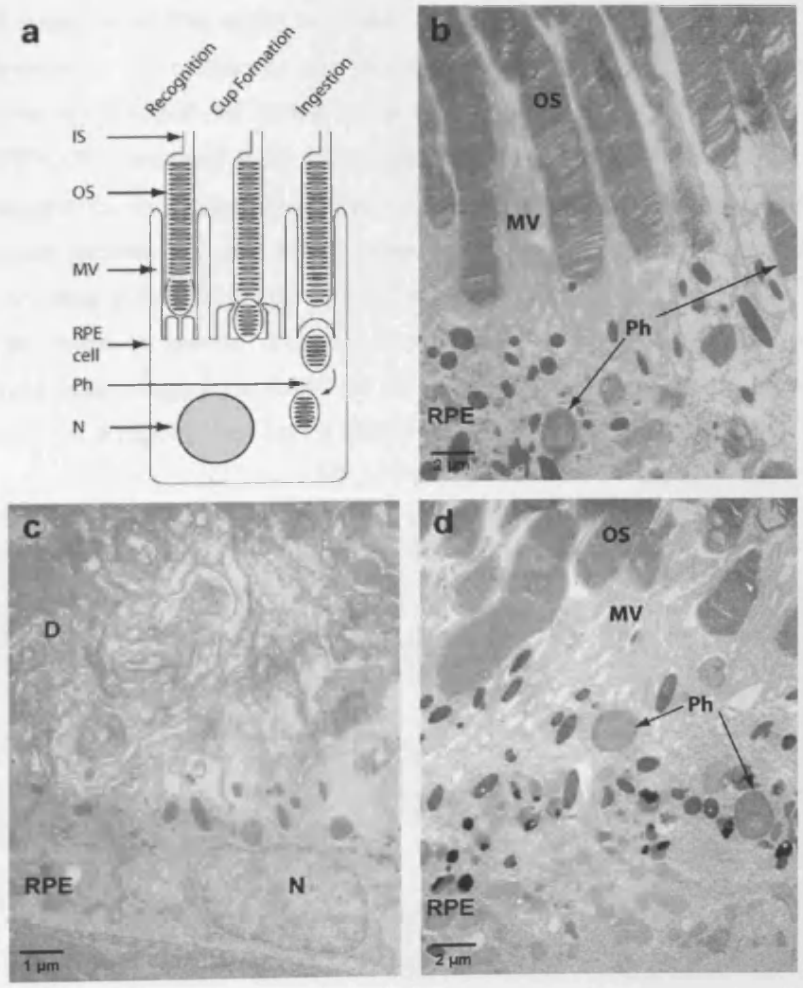

The restoration of the phagocytotic defect in RCS rats furthermore results in an improvement of photoreceptor morphology and a reduction of the debris layer. In untreated eyes, a thick debris layer is present and the RPE microvilli therefore cannot reach photoreceptor tips. The disruption of the nutrition-flow from the RPE to the photoreceptors and the transport of waste material towards the RPE caused by the presence of the debris layer induces apoptosis of photoreceptors. The degenerating retina in untreated animals has an unorganised appearance. Many abnormal short, whorl shaped, and broken off outer segments are found. In contrast, eyes treated with the therapeutic vector show a reduction of the debris layer thickness. The microvilli reach the photoreceptor outer segment tips, which are bound and internalised into phagosomes. Even though the total length of outer segments seems to be diminished compared to wild-type, the organisation and shape is similar (figure 4.4).

Figure 4.4: EM analysis of the outer segment layer (x2500 magnification).

(a) Non-dystrophic rat retina. In non-dystrophic animals there are well organised outer segments which reach the apical surface of the RPE.

(b) LNT.SFFV.GFP injected RCS rat retina 4 weeks pi. In LNT.SFFV.GFP treated retinae outer segments, that reach the RPE, could not be found. Due to the phagocytic defect, shed outer segments are not internalised and accumulate at the apical surface of the RPE, resulting in the formation of a debris layer.

(c) RCS rat retina 4 weeks after treatment with LNT.SFFV.MERTK. Areas with well organised outer segments could be found throughout the treated area indicating that restoration of phagocytosis has a beneficial effect on retinal morphology.

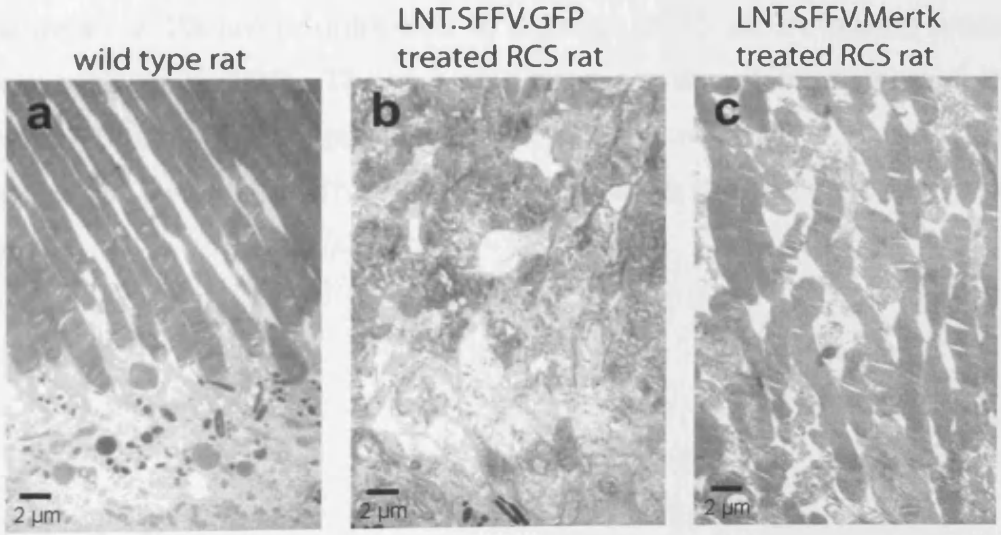

4.3 Thickness measurements of retinal layers

A characteristic feature of the RCS rat is the early accumulation followed by a slow disappearance of rod outer segment debris [71, 166, 357]. In RCS rats the debris begins to accumulate at the apical surface of the RPE at around postnatal day 14. The outer segment zone including rod outer segment and apical debris becomes thicker than in normal rats between day 14 and 20 and remains thicker for up to 2 months (18). To analyse the difference between treated RCS rat eyes in comparison to controls, thickness measurements of different retinal layers were performed on a number of semithin sections. Since the number of animals from different treatment groups varied, an unpaired Student's t-test was used to calculate the significance of results obtained (see chapter 2.8). Since the differences were most obvious 8 weeks after injection, all measurements were carried out at this time point. As the rate of degeneration is known to be slower in the extreme periphery, a picture of an area between the ora serrata and the optic nerve head, approximately in the middle of the superior injection site was taken and measurements were performed in a 250 µm area using Zeiss LSM 5 software. Figure 4.5 summarises the mean morphometric values of non-dystrophic, LNT.SFFV.Mertk injected and untreated RCS rat eyes. Consistent with the presence of phagosomes, which were packed with rod outer segment membrane waste material, in the treated areas we found a reduction in the debris layer thickness from a mean of 23 µm in untreated to a mean of 15 µm in treated areas from injected eyes ($p = 0.05$). There was also a significant improvement in RPE thickness - from a mean of 5 µm in untreated to 7 µm in treated areas of injected eyes ($p = 0.034$). The RPE is around 9 µm thick in eyes from wild-type animals.

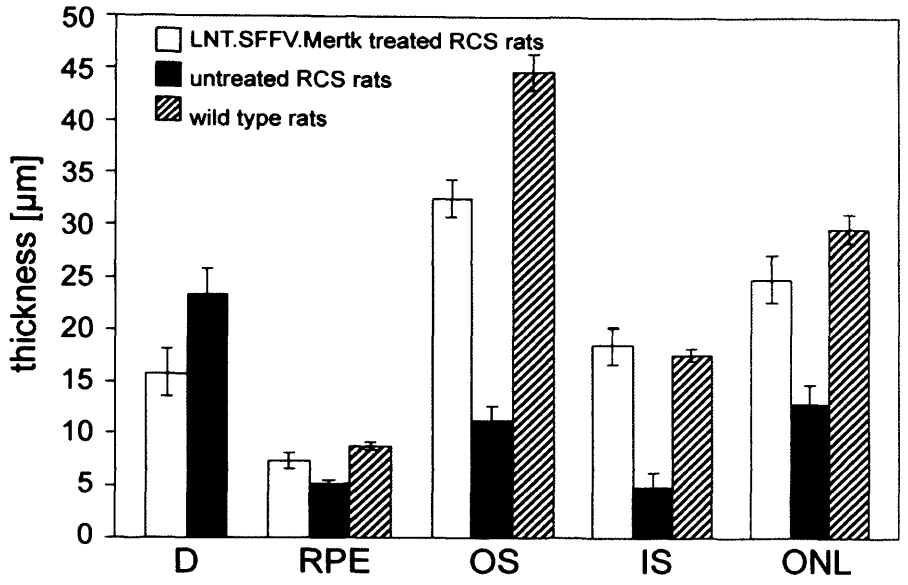

Figure 4.5: Measurements of the absolute thickness of retinal layers. Measurements were performed in 7 areas in the middle of the superior injection site in 4 treated animals 8 weeks after treatment with LNT.SFFV.Mertk and in corresponding areas of 3 untreated and 3 non-dystrophic rats. The SD is indicated for all the results. Significant differences in the thickness of all the measured layers could be found between untreated and treated areas, as determined with the help of an unpaired Student's t-test (indicates $p = 0.05$ or less). The reduction in the debris layer in treated eyes due to the presence of phagosomes indicates that we were able to partly restore RPE function in the RCS rat and reverse the phagocytotic defect. This results in an improvement in outer and inner segment morphology and ultimately in preservation of the outer nuclear layer. D=debris layer, RPE=retinal pigment epithelium, OS=outer segments, IS=inner segments ONL=outer nuclear layer.

The partial restoration of RPE function also resulted in an improvement in the morphology of the neuroretina (figure 4.6). In addition to an improvement in outer segment morphology (figure 4.4) we found a significant increase in outer segment length with a mean thickness of the outer segment layer of 25 µm in treated areas compared with 12 µm in untreated eyes ($p = 0.0074$). It is approximately 30 µm thick in wild-type rats. The degeneration also normally affects the inner segments. These are reduced by around 75 % ($p < 0.0001$) in dystrophic retinae but in treated areas the mean inner segment thickness was not significantly different from wild-type ($p = 0.35$). Finally, we found that the

ONL was around 3 times thicker in treated areas compared with equivalent areas from untreated eyes ($p = 0.0002$).

4.4 Retinal morphology

In order to analyse the effect of treatment on photoreceptor cell loss over time, animals were sacrificed at various time points over a period of 7 months and semithin sections were taken throughout the eye. For each time point and vector 3 to 5 animals were injected. Photoreceptor cells were found in treated areas of injected eyes for up to 30 weeks following treatment, whereas in equivalent areas from untreated eyes and in eyes injected with LNT.SFFV.GFP few, if any, photoreceptors remained at 12 weeks (figure 4.6). It has been reported previously that in the RCS rat the disappearance of debris is faster in posterior parts of the retina than in the periphery and it is therefore important to compare equivalent areas throughout the eye in order to assess the overall effect of treatment on the rate of degeneration [167].

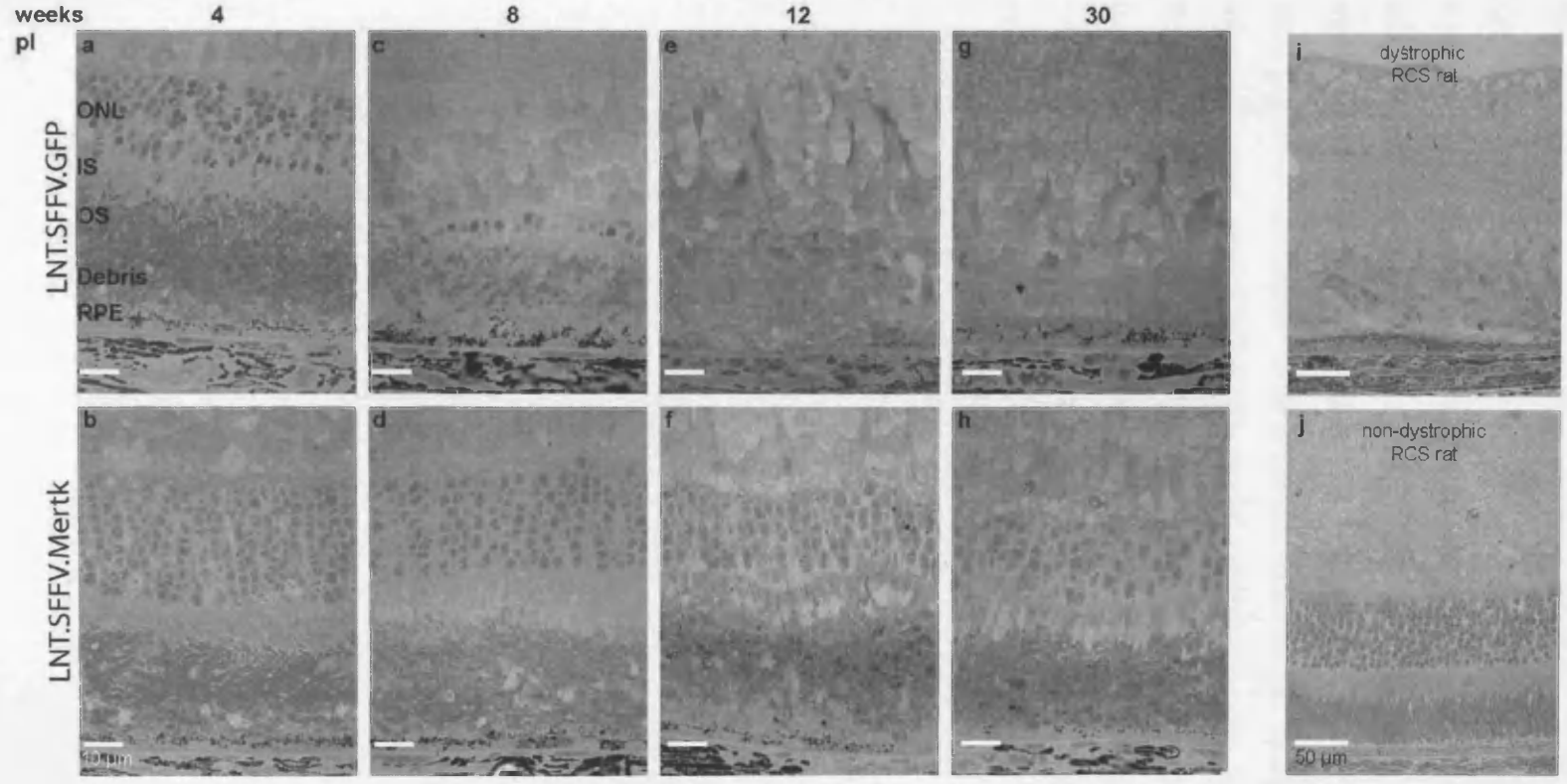

Figure 4.6: Light micrographs of RCS rat retinae. Serial sections were taken throughout the eyes of LNT.SFFV.GFP injected RCS rats (upper panel) and LNT.SFFV.Mertk treated rats (lower panel) at a number of different time points (4, 8, 12 and 30 weeks) after injection. Pictures were taken of treated areas between the optic nerve and the ora serrata of the superior hemisphere **(a-h)**. Photoreceptors were present in treated eyes up to 30 weeks pi indicating that the LNT.SFFV.Mertk construct reduces retinal degeneration, whereas no photoreceptor cells could be found in control eyes after 12 weeks. For comparison, an image of dystrophic RCS rat retina to compare to the GFP-treated panels **(i)** and a non-dystrophic rat retina to compare to Mertk-treated panels **(j)** are included. Control animals were 12 weeks of age. Size bars are 10 µm for (a-h) and 50 µm for (i and j).

Comparison of treated and control eyes showed a reduction in the loss of photoreceptor cells in treated eyes at different time points (figure 4.6). Whilst the number of photoreceptor cells in treated eyes was approximate 50 % greater in the middle of the treated area than in untreated ones 4 weeks after injection of LNT.SFFV.Mertk, this difference became more obvious at 8 weeks with a two- to three-fold increase in photoreceptor number. It remained significantly higher for the duration of the study which lasted 7 months. At all time points a significant difference between either uninjected or LNT.SFFV.GFP injected eyes and LNT.SFFV.Mertk treated eyes could be found (p-values between 0.004 and 0.0001). In contrast, no significant difference could be found between untreated and LNT.SFFV.GFP injected eyes at any time point, confirming that delivery of a non-therapeutic vector has no influence on photoreceptor survival beyond 4 weeks (figure 4.7).

Figure 4.7: Therapeutic effect. The number of nuclei in the ONL, which correspond to the number of photoreceptor cells, was determined at a number of points along the vertical meridian of eyes from the optic nerve head (ONH) to the ciliary body at different time points (4, 8, 12, and 30 weeks pi). The number of nuclei was counted in both LNT.SFFV.GFP or LNT.SFFV.Mertk injected eyes and the contralateral untreated eyes. For each treatment group and time point at least 3 animals were analysed. At all time points there was a significant difference between control eyes and LNT.SFFV.Mertk treated eyes (p values between 0.005 and 0.001). In LNT.SFFV.GFP injected and untreated eyes very few, if any, nuclei could be found at 12 weeks pi and time points thereafter, whilst there were still nuclei remaining in LNT.SFFV.Mertk treated eyes at 30 weeks pi.

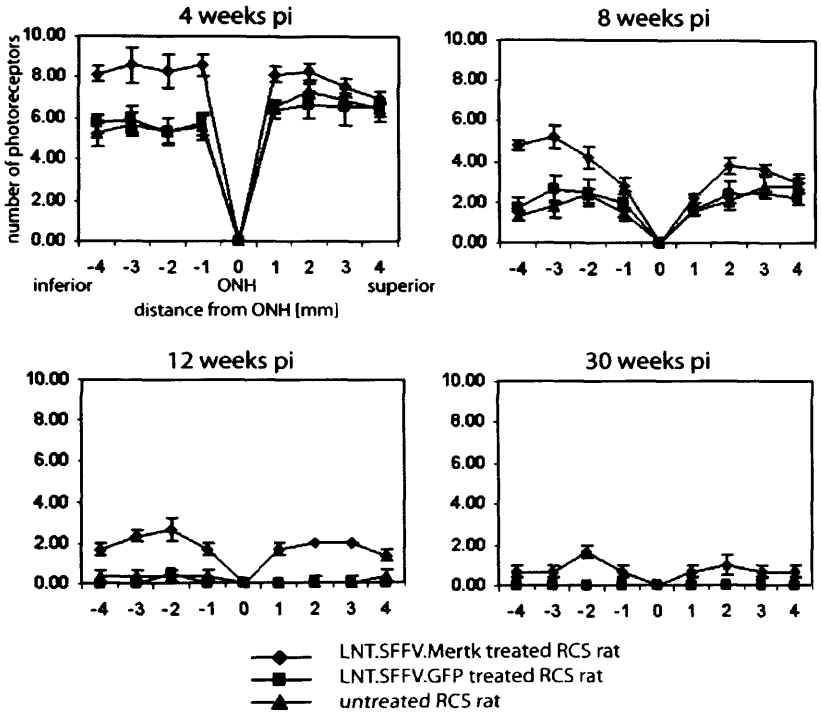

Even though there were still some photoreceptors remaining at 30 weeks after the injection of the therapeutic vector, the size of the area, in which photoreceptors were preserved, was reduced. It was shown that the size of the bleb generated by a subretinal injection correlates with the size of the transduced area and covers approximately 30 % of the retina. Thirty weeks after treatment photoreceptors, however, are only found in a small area around the injection site covering only about 15 % of the retina (figure 4.8). A possible explanation for this is that changes in dying photoreceptor cells in not treated areas generate a microenvironment that has a negative influence on the survival of healthy photoreceptor cells in treated areas [342]. This is known to be the case in animal models of retinal degeneration and RP patients.

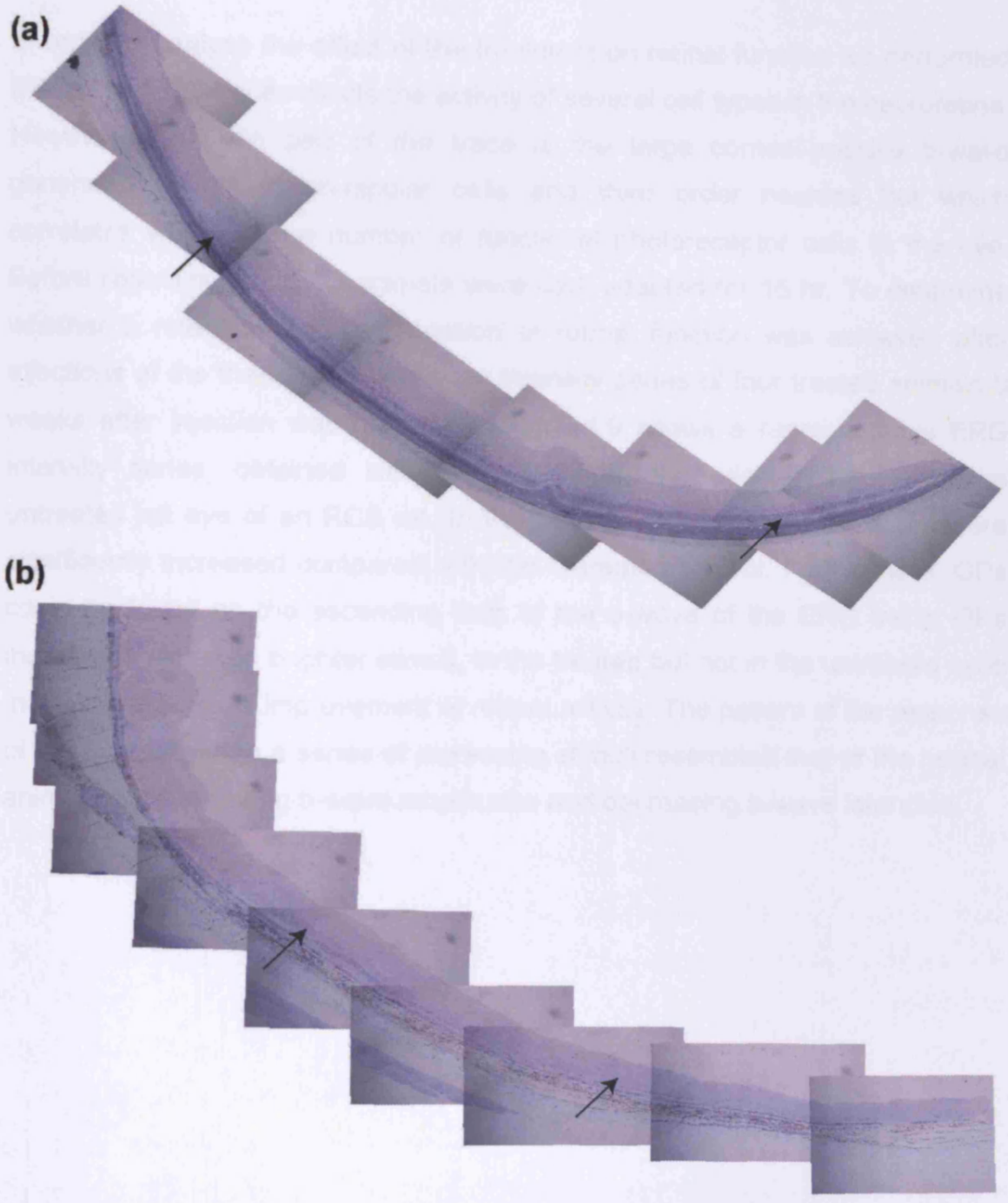

Figure 4.8: Light micrographs of the superior hemisphere of the retina. Pictures were taken 8 **(a)** and 30 **(b)** weeks after injection of LNT.SFFV.Mertk. The area of photoreceptor preservation (indicated by arrows) covers around 30 % of the retina at early time points but is reduced to 15 % at 30 weeks pi. Only a small island of surviving photoreceptor cell in the middel of the preserved area, which is assumed to be around the injection site, is found at this time point.

4.5 Effect of treatment on retinal function

In order to analyse the effect of the treatment on retinal function we performed ERG. The ERG trace reflects the activity of several cell types in the neuroretina. However, the main part of the trace is the large corneal-positive b-wave generated mainly in on-bipolar cells and third order neurons but which correlates well with the number of functional photoreceptor cells in the eye. Before recording the ERG animals were dark adapted for 16 hr. To determine whether a retention and prolongation of retinal function was achieved after injections of the therapeutic vector an intensity series of four treated animals 8 weeks after injection was recorded. Figure 4.9 shows a representative ERG intensity series, obtained simultaneously from the injected right and the untreated left eye of an RCS rat. In the treated eye, b-wave amplitudes were significantly increased compared with the untreated control. Furthermore, OPs could be found on the ascending limb of the b-wave of the ERG trace. OPs increase in size with brighter stimuli, in the treated but not in the untreated eyes indicating an overall improvement of retinal activity. The pattern of the response of the treated eye to a series of increasing stimuli resembled that of the normal animal, with increasing b-wave amplitudes and decreasing b-wave latencies.

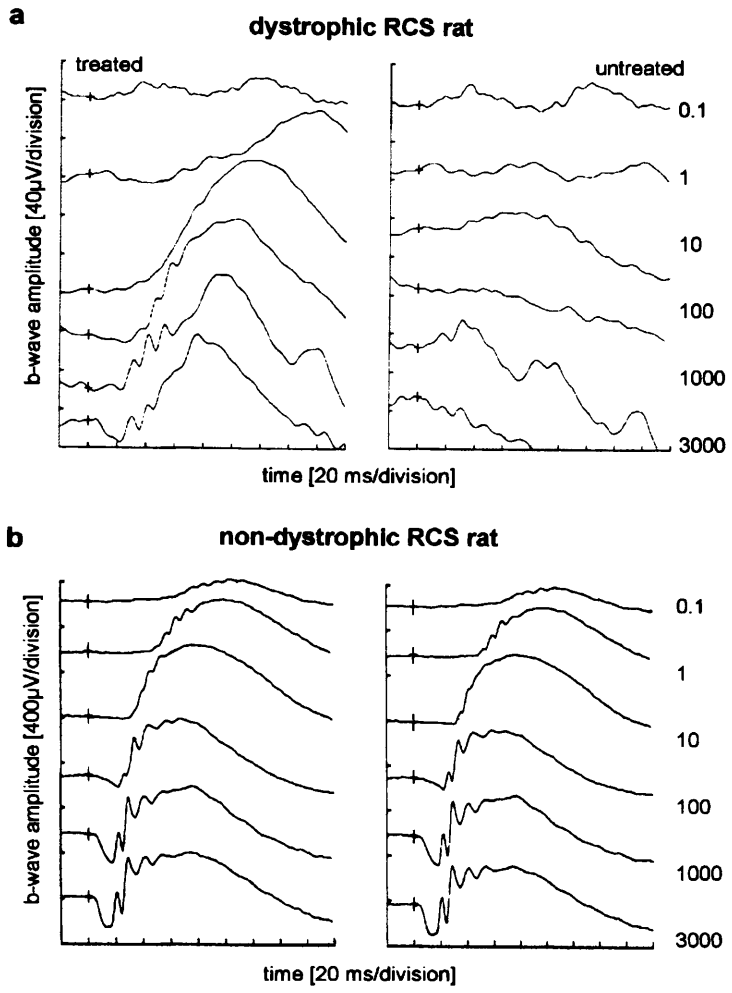

Figure 4.9: ERG intensity series. Eight weeks after treatment of a RCS rat with LNT.SFFV.Mertk an ERG with increasing flash intensities was recorded simultaneously of the treated, right and untreated, left eye. After treatment the b-wave amplitudes were significantly higher than those of untreated eyes, and the shape of the traces showed improvement, resembling the ERG traces of normal rats.

Since both rod and cone responses can be measured at an intensity of 100 mcd s/m^2, recordings of responses at this flash intensity were measured in five animals at weekly intervals over a period of seven months. Figure 4.10 shows ERGs at a single flash intensity of 100 mcd s/m^2 obtained from one animal treated with LNT.SFFV.Mertk at different time points. The traces were recorded simultaneously from the injected, right and the uninjected, left eye. In the untreated control eye, the b-wave amplitude decreased rapidly over time until it was completely gone after 8 weeks. In the treated eye, the ERG response was still present at this time and was observed for more than 18 weeks after treatment, suggesting that following treatment with LNT.SFFV.Mertk photoreceptor survival was prolonged. The difference between the untreated and treated eye was most obvious at 8 to 12 weeks.

Figure 4.10: ERG time course. ERGs were recorded of a single animal at various time points after LNT.SFFV.Mertk treatment at a single flash intensity of 100 mcd s/m^2. At this intensity both rod and cone responses are measured. The b-wave amplitude is substantially higher in the right, treated eye compared to the uninjected, contralateral eye. The difference is greatest at 8 and 12 weeks after treatment. Furthermore, OPs are present in treated eye up to 12 weeks after injection indicating proper retinal function.

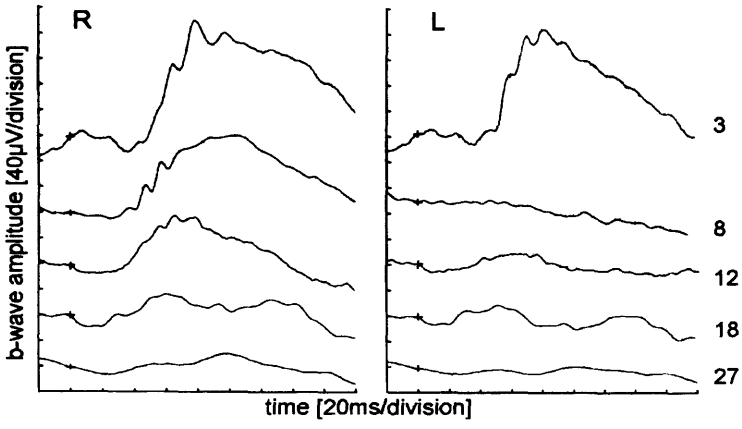

The average b-wave amplitudes of the ERG recordings were then evaluated statistically by using a paired Student's t-test (see chapter 2.8). The LNT.SFFV.Mertk treated eyes showed significantly higher b-wave amplitudes than the contralateral untreated eye at time points up to 27 weeks after injection ($p = 0.049$; figure 4.11a). Maximal differences were obtained 7 and 12 weeks after treatment. At these time points the b-wave amplitudes in the eyes treated with LNT.SFFV.Mertk were approximately four fold higher than in the untreated eye (median: 93.7 µV versus 22.5 µV; $p = 0.008$). In control animals injected with LNT.SFFV.GFP, no significant difference in b-wave amplitudes between treated and untreated eyes could be found at any time point (figure 4.11b). Results obtained with flash intensities of 10 mcds/m^2, and 1000 mcds/m^2 did not differ substantially.

Figure 4.11: Mean ERG b-wave amplitudes.

(a) The average b-wave amplitudes (and standard deviation) of LNT.SFFV.Mertk treated and contralateral, untreated RCS rat eyes are shown at various time points.

(b) The mean b-wave amplitudes of control animals injected with LNT.SFFV.GFP compared to untreated eyes are shown as well. All ERG recordings were performed at a flash intensity of 100 mcd s/m^2. After administration of the therapeutic vector, b-wave amplitudes were significantly increased between 6 and 27 weeks after treatment ($p < 0.05$), whereas injections of LNT.SFFV.GFP did not alter the electrical response of the retina. 3 weeks after treatment a non-significant reduction in b-wave amplitudes was found in treated eyes which was probably due to an immune response against impurities in the virus suspension.

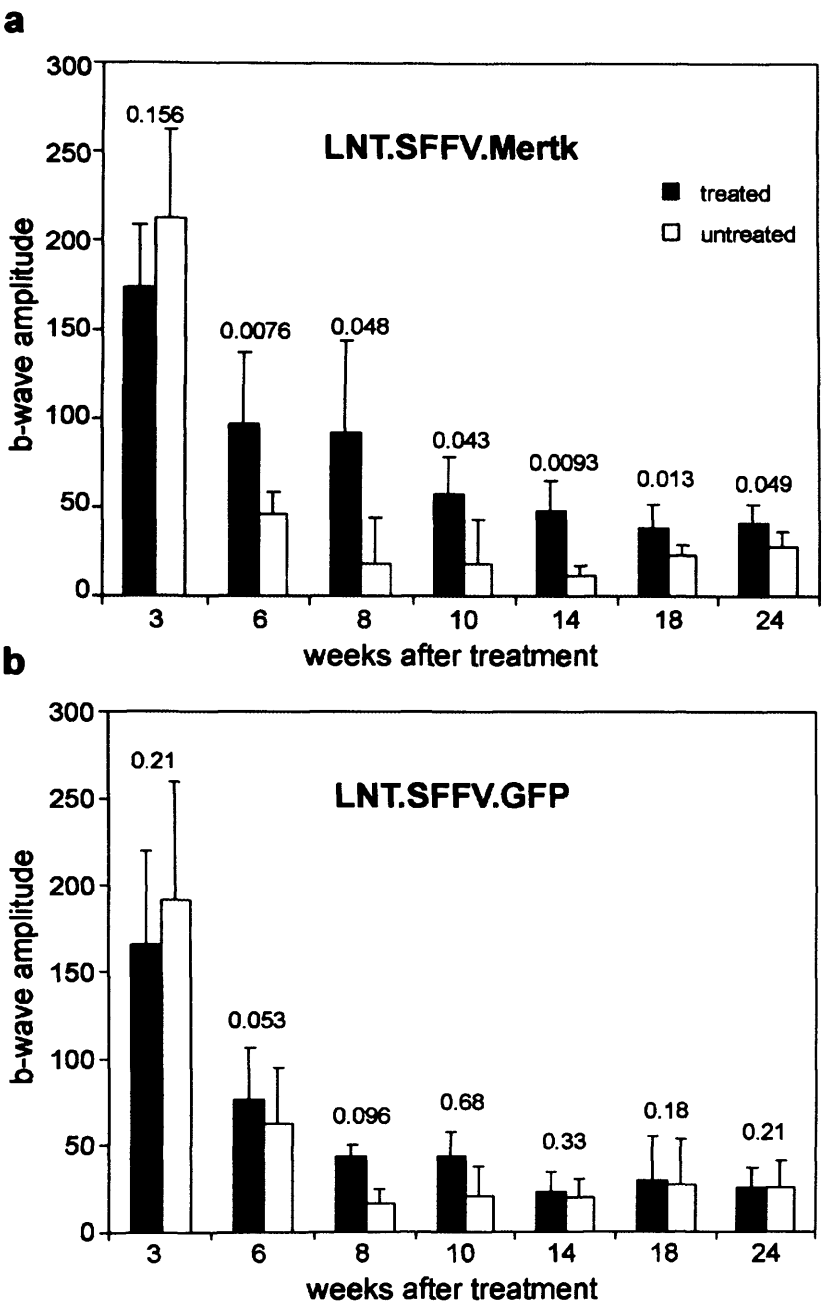

4.6 Overexpression of *MERTK*

Viral promoters are commonly used as regulatory elements in gene therapy vectors because they generally have strong activity in a wide variety of cells of different tissues and species. The SFFV promoter is a strong viral promoter. In order to determine if an overxpression of *Mertk* would affect retinal function, five non-dystrophic RCS rats were injected subretinally with the therapeutic vector. After dark adaption scotopic ERGs were recorded. A representative ERG intensity series from a wild-type rat seven weeks after injection of LNT.SFFV.Mertk is shown in figure 4.12. The b-wave amplitudes were normal indicating that the delivery of the therapeutic vector was not deleterious.

Figure 4.12: ERG intensity series. The ERG was recorded at different light intensities at a single time point of a non-dystrophic RCS rat after injection of LNT.SFFV.Mertk (right eye, R, treated and left eye, L, untreated). The traces shown are representative, average recordings. The b-wave amplitude and the shape of the trace were normal.

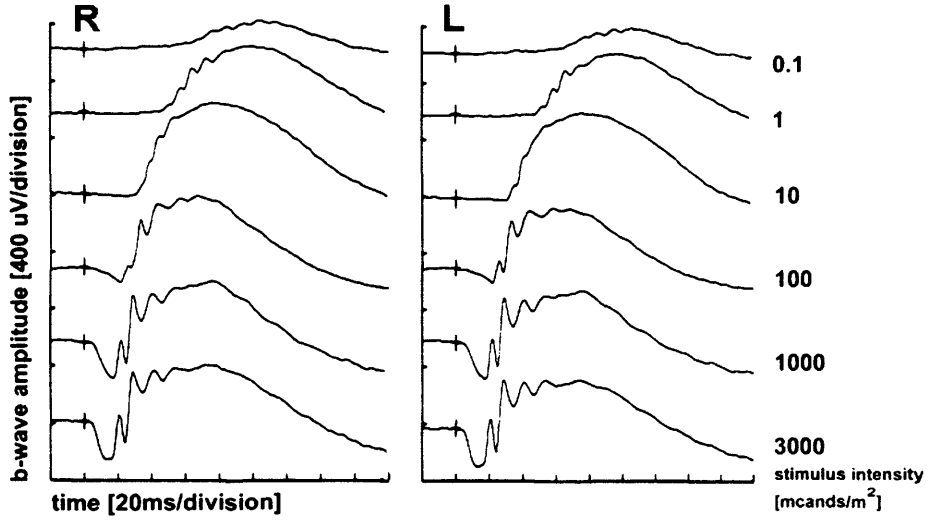

After ERG recordings some animals were sacrificed and their eyes processed for semithin sections. The sections were examined by light microscopy and pictures were taken (figure 4.13). Retinal morphology and histology was normal suggesting that the additional *MERTK* expression in RPE cells had no effects.

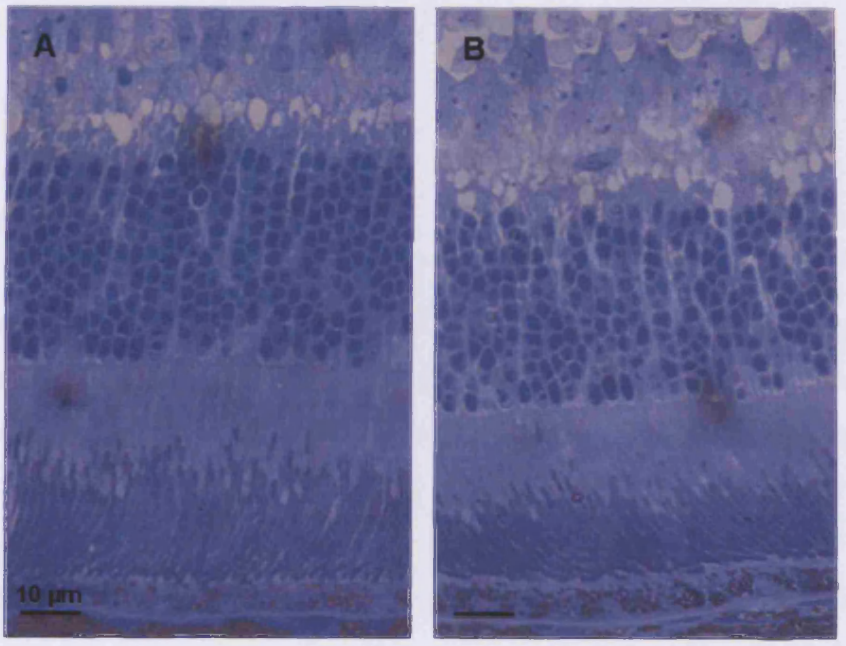

Figure 4.13: Light micrograph of a wild-type rat after LNT.SFFV.Mertk delivery. The pictures shows a treated eye 7 weeks after injection. Retinal morphology did not show any differences. INL=inner nuclear layer, ONL= outer nuclear layer, IS=inner segments, OS=outer segments, RPE=retinal pigment epithelium.

4.7 Non-integrating lentiviral vectors

4.7.1 Introduction

Lentiviruses can integrate their genome into the genome of dividing and non-dividing cells. Thereby the gene of interest is passed on by chromosomal replication following cell division to the progeny cells and long-term stable transgene expression is obtained. Hence, gene therapy using this approach may provide the possibility of a cure for some disorders. However, chromosomal integration has its disadvantages. Normally the insertion occurs randomly and as a result the location of the inserted gene varies enormously from cell to cell. An established complication of retroviral transduction in animal models and clinical trials is the insertional mutagenesis leading to cancer. An integration event in one of the many cells that are targeted could disturb the normal expression pattern of genes that control cell division or cell proliferation. For example, the integration can cause activation of an oncogene or it could inactivate a tumor suppressor gene or a gene involved in apoptosis. The necessity to overcome these drawbacks has been highlighted by reproducible induction of malignancy in murine models and the development of lymphoproliferative disease in SCID patients after treatment with retroviral vectors [217, 358]. Hence, it is crucial for successful clinical applications of lentiviral vectors to achieve stable long-term transgene expression and to minimise the risk of insertional mutagenesis. Mutations in the integrase coding sequence can result in integrase defective retroviral vectors. It has been demonstrated in *vitro* that prolonged transgene expression can be achieved using non-integrating lentiviral vectors provided that vector episomes are stably retained [359].

In consideration of the justified concerns regarding insertional mutagenesis, HIV-1 integration deficient vectors were produced to evaluate the efficiency of transduction in *vivo* (see figure 4.14a and b for vector maps). Initially integration

deficient vectors carrying a *gfp* reporter gene were tested in *vitro* (figure 4.14c). As for integration proficient vectors the peak of expression has been shown to occur at 3 days. In accordance with the loss of transgene during cell division, *gfp* expression declined rapidly in integrase deficient vector transduced cells between 3 and 10 days, whereas the integrase proficient vector-mediated expression remained stable (Cloning and in *vitro* studies were conducted by R. Yáñez-Muñoz and colleagues, Molecular Immunology Unit, ICH. In *vivo* experiments were performed by K. Balaggan, Div. of Molecular Therapy, IoO.).

Figure 4.14: Integration-deficient lentiviral vectors. (a) Schematic representation of HIV-1 vectors used in this study. Shown are the double-stranded DNA vector forms after completion of reverse transcription. Relevant features are named on L-cSegfpW, and only those differing are named on the other vectors. dLTR is the 5'-deleted LTR present in these self-inactivating vectors. Not drawn to scale.

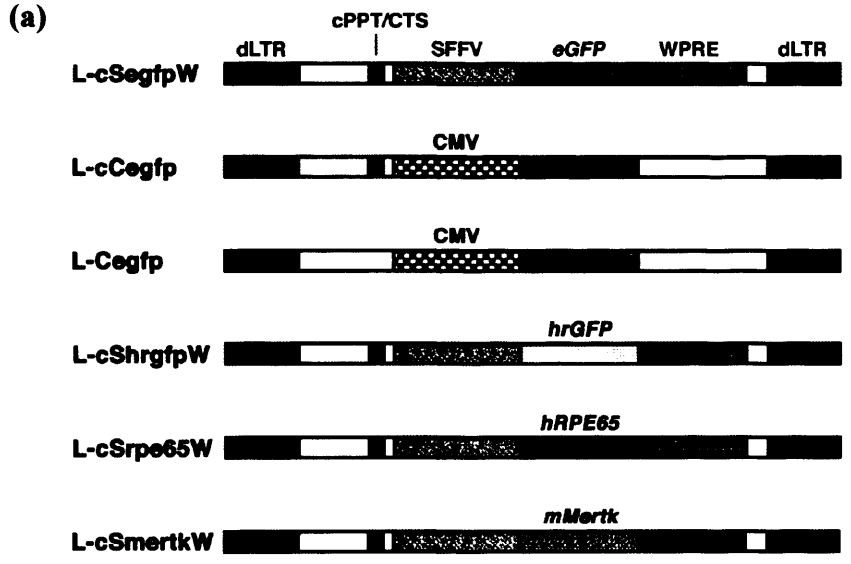

(b) Schematic representation of linear, integrated and circular forms of a generic lentiviral vector. Solid lines are vector DNA, discontinuous lines are genomic DNA and white boxes are dLTRs. Arrows represent the transgene cassettes in the corresponding vector forms.

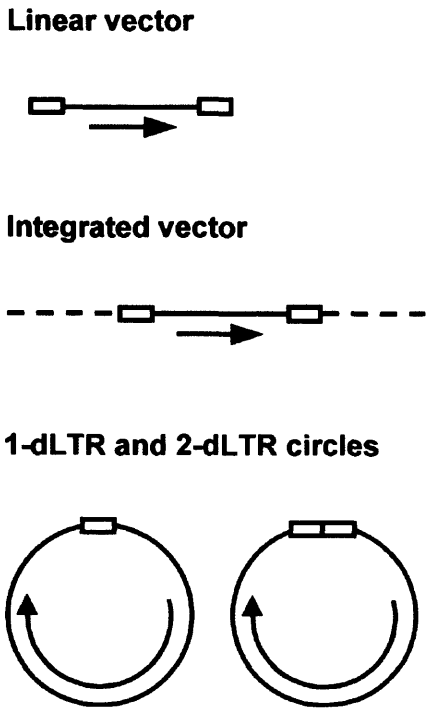

(c) Time-course of *eGFP* expression after transduction of HeLa cells with integration-proficient and deficient L-cSegfpW vector at the indicated multiplicity of infection (MOI). A representative experiment out of four performed is shown. Int- and int+ stand for integration-deficient and -proficient vectors, respectively.

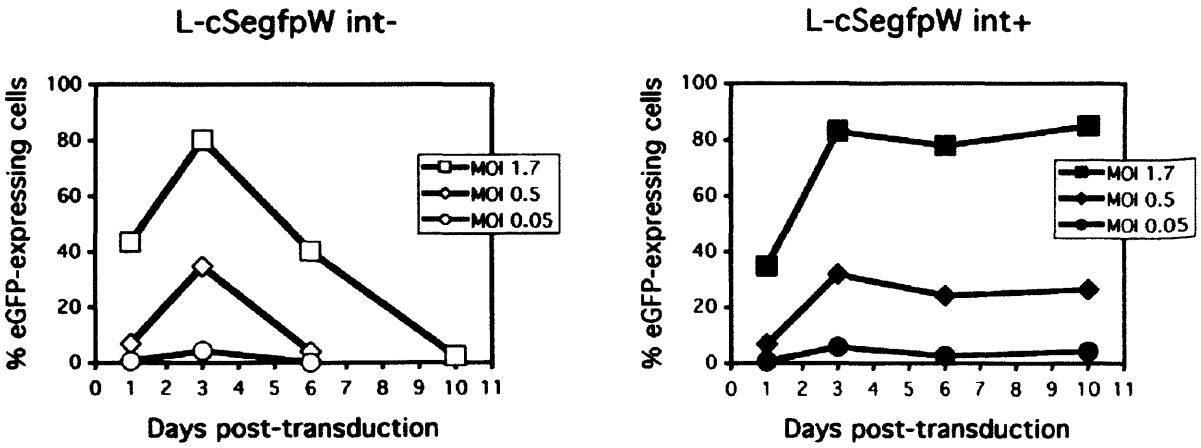

4.7.2 In *vivo* non-integrating HIV-1 vector-mediated expression

To determine whether long-term expression could be achieved in *vivo*, either integration deficient- or proficient vectors carrying the *gfp* transgene under the control of a SFFV promoter were delivered to mouse eyes by subretinal, intracameral, or intravitreal injections. Transgene expression was detected by in *vivo* fluorescence imaging and sections. With both types of vectors similar transduction pattern were found. Following subretinal injection *gfp* expression was found in the RPE. Intracameral injection led to expression in the corneal endothelium and limited expression in the trabecular meshwork. With either type of vectors no *gfp* expression could be found after intravitreal injections (figure 4.15). For both vectors, the earliest time point of transgene expression was 3 days after delivery. Seven days post injection the expression reached the maximum and remained so until the last time point studied, 9 months after injection. These results show that long-term expression can be achived with integration deficient HIV-1 vectors in *vivo*.

Figure 4.15: *Gfp* expression patterns in mouse ocular tissues. 6 month pi GFP fluorescence is detectable in mouse retina and cornea. The cryosections were counterstained with propidium iodide. In the retina, *gfp* is expressed within RPE cells. Fluorescence of the neuroretina originates from detached RPE microvilli. After intracameral injection of the vector GFP fluorescence is mainly present in the corneal endothelium and weak fluorescence is also dedected in the trabecular meshwork (gcl=ganglion cell layer, inl=inner nuclear layer, onl=outer nuclear layer, rpe=retinal pigment epithelium, cho=choroid, size bar=50 µm).

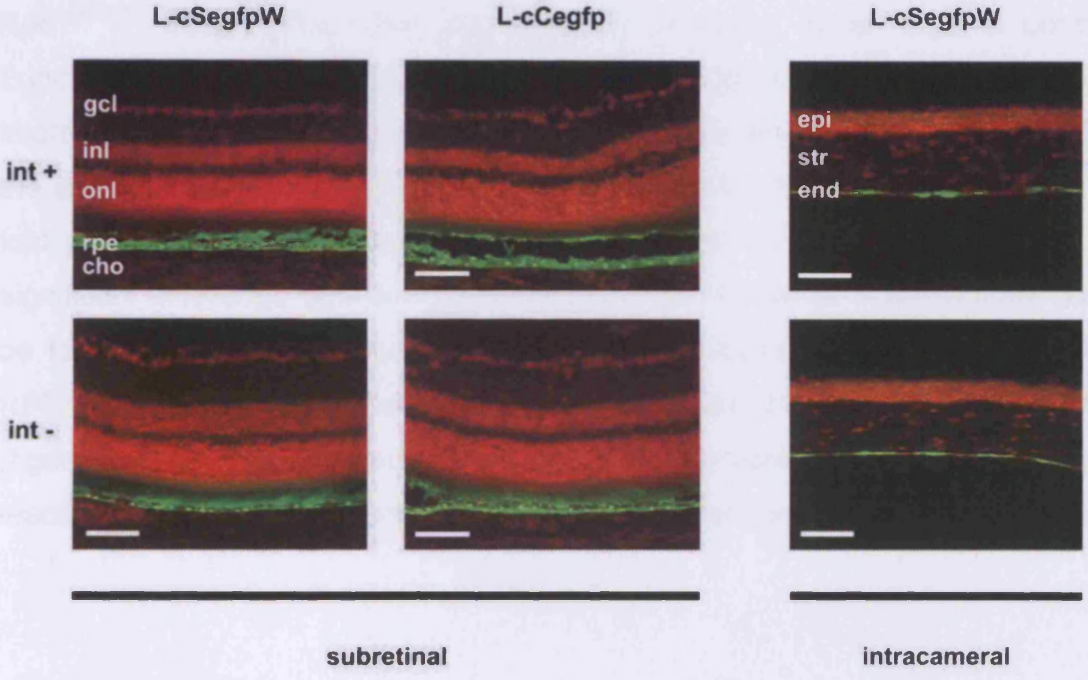

4.7.3 Gene therapy with non-integrating HIV-1 vectors

After it was established that non-integrating lentiviral vectors are able to mediate long-term transgene expression in *vivo*, we evaluated their potential for gene therapy approaches for retinal degeneration. Mutations in the human *rpe65* gene result in a severe form of early onset recessive RP, known as LCA [100]. RPE65 is an RPE-specific protein that is involved in the vitamin A metabolism [30, 31]. Patients with mutations in *RPE65* suffer of severe visual impairment from birth onwards. Mice homozygous for the rd12 mutation in the *rpe65* gene and the *rpe65*$^{-/-}$ dog have a similar phenotype. Recently, these

animal models for LCA have been used to successfully restore visual function by rAAV-mediated gene transfer [105, 165].

Since mutations that primarily affect the RPE are the most suitable for the development of gene therapy protocols involving lentiviral vectors, integration deficient vectors that carry a functional copy of the human *RPE65* gene were designed and injected into the subretinal space of one eye of 5 weeks old $Rpe^{rd12/rd12}$ mice. The other eye was left untreated as an internal control. Functional rescue was assessed by ERG (figure 4.16b). A significant improvement in retinal function was observed three weeks after injection of the therapeutic construct with b-wave amplitudes at 100 mcds/m^2 being almost 6-fold greater in treated eyes compared to untreated eyes. On the contrary, no significant difference between uninjected and control vector injected eyes could be found (figure 4.16c). Furthermore, *rpe65* expression was restricted to the RPE in mice after subretinal delivery as determined by immunohistochemistry (figure 4.16a). These results suggest that integration deficient viruses can mediate significant visual restoration in a clinical relevant animal model for LCA.

Figure 4.16: Rescue in RPE$^{rd12/rd12}$ mice three weeks after treatment. (a) Subretinal delivery of L-cSrpe65W results in efficient *rpe65* expression in murine RPE. Retinal cryosections were immunostained for RPE65 (green) and counterstained with propidium iodide (red). RPE65-positive immunohistochemical labelling in the RPE layer of wild-type mice (left) and in *Rpe65*$^{rd12/rd12}$ mice three weeks after subretinal injection of integrase-deficient L-cSrpe65W (centre left). RPE65 is not detected in sections from L-cSrpe65W-injected *Rpe65*$^{rd12/rd12}$ mice incubated without primary antibody (centre right) nor in uninjected *Rpe65*$^{rd12/rd12}$ mice (right). Some background fluorescence from the secondary antibody is visible in the choroid and sclera in all sections. (onl=outer nuclear layer, rpe=retinal pigment epithelium, size bar=10 μm)

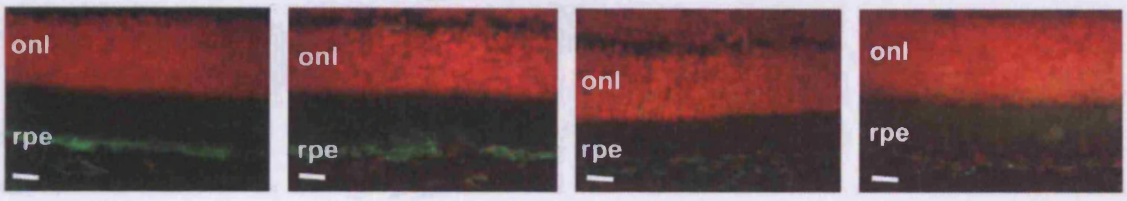

(b) Sample scotopic ERG traces at 10, 100, and 1000 mcds/m^2 flash intensities. Improvements in waveform are observed after treatment.

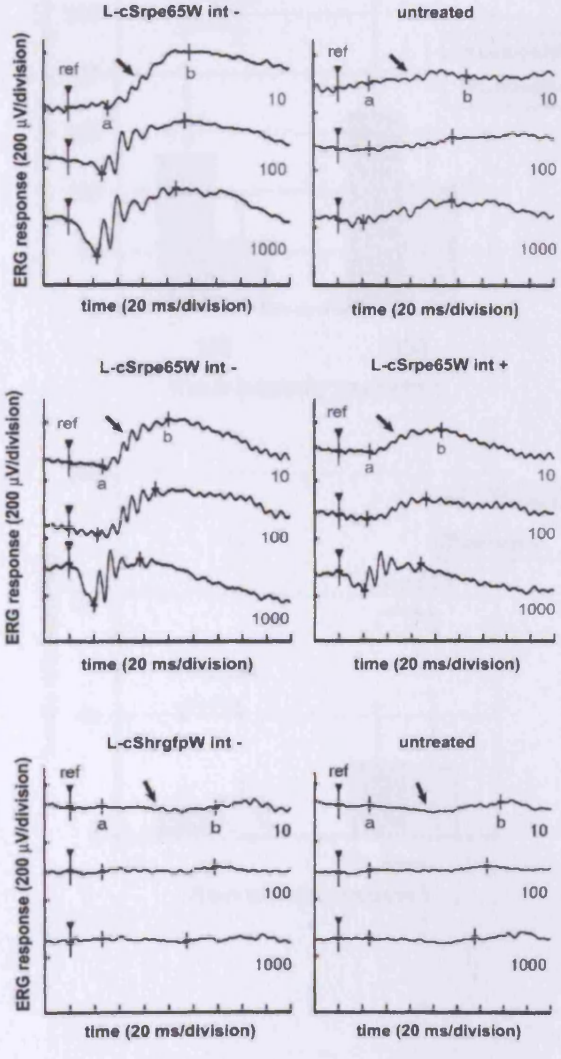

(c) Mean ERG b-wave amplitudes are significantly greater after the injection of the therapeutic construct.

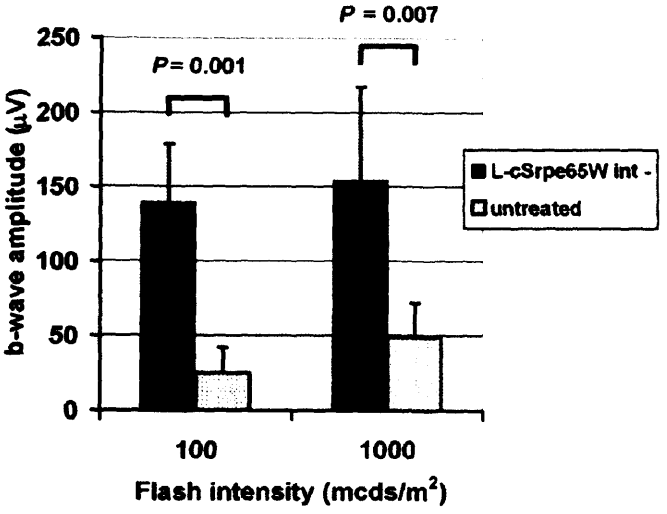

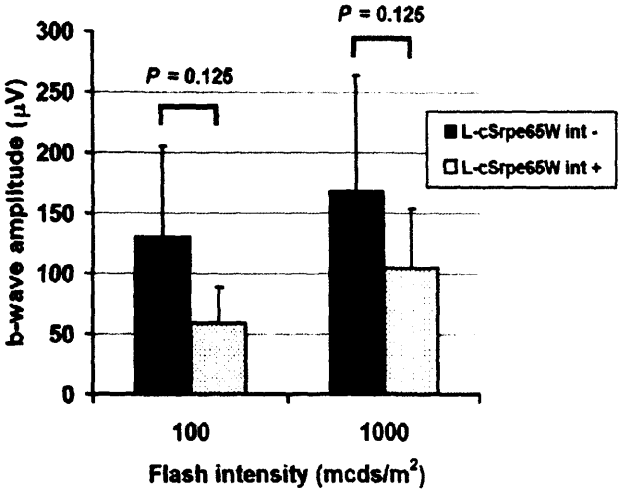

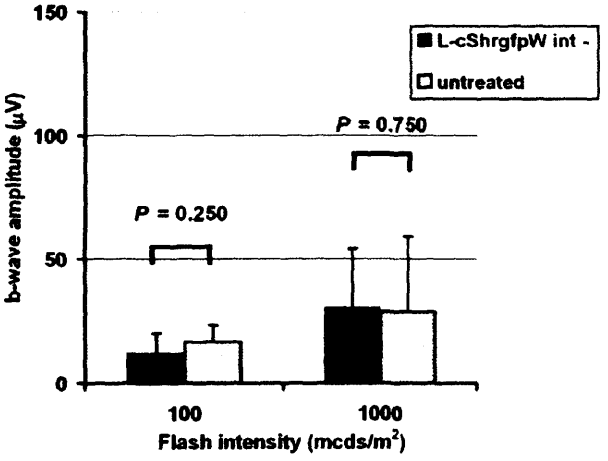

Lentiviral vectors are known to show variations in the cellular tropism after subretinal injections in different species. Like in patients and animal models carrying mutations in the *rpe65* gene, in humans and animals with mutations in the *MERTK* gene photoreceptor cells are initially inherited functional and morphological preserved. Therefore the RCS rat is another animal model to test lentivirus-mediated gene therapy protocols. To examine possible differences in the transduction patterns using integrase deficient vectors between species the mutant vector was also tested in RCS rats. Integrase deficient and proficient vectors that carry a functional copy of the murine *MERTK* gene were designed and injected subretinally into ten-day old rats. The functional rescue was assessed 6 weeks after treatment. With both vectors ERG waves showed an overall improvement in the shape form and b-wave amplitudes were 3-fold greater in integration deficient virus treated compared to untreated eyes (figure 4.17). The achieved rescue was comparable between integrase deficient and proficient viruses, whereas no significant rescue was observed after injection of control *gfp* vectors.

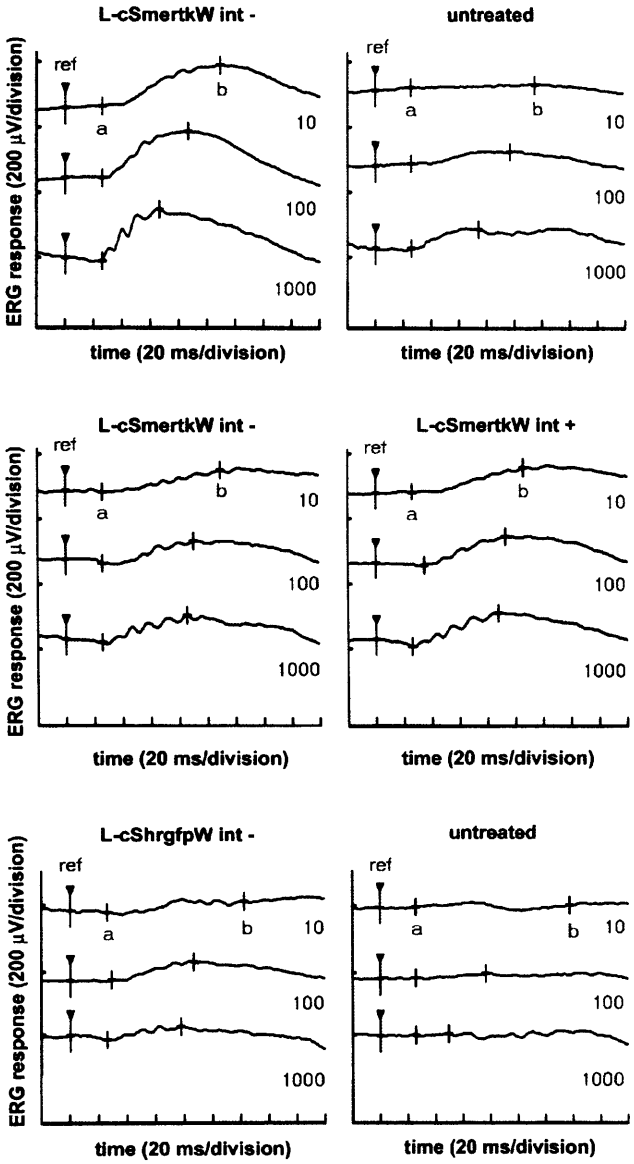

Figure 4.17: Functional rescue of the RCS rat. ERG recordings were carried out 6 weeks after treatment.

(a) Sample scotopic ERG traces at 10, 100, and 1000 mcds/m^2 flash intensities.

(b) Mean ERG b-wave amplitudes from control *gfp* virus, integration-deficient or -proficient virus treated eyes compared to the b-wave amplitudes of contralateral untreated eyes. There are improvements in waveform and mean b-wave amplitudes after the injection of the therapeutic constructs. No significant change in amplitudes is seen after control vector injections.

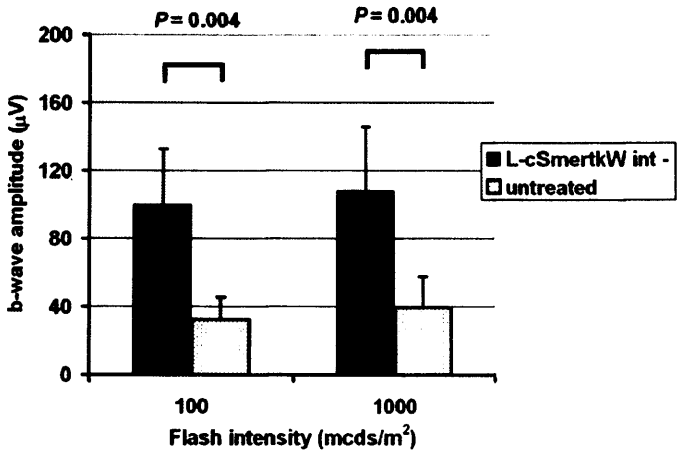

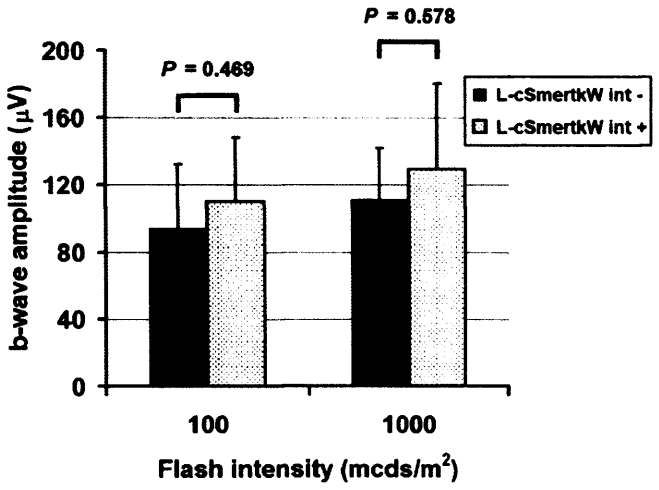

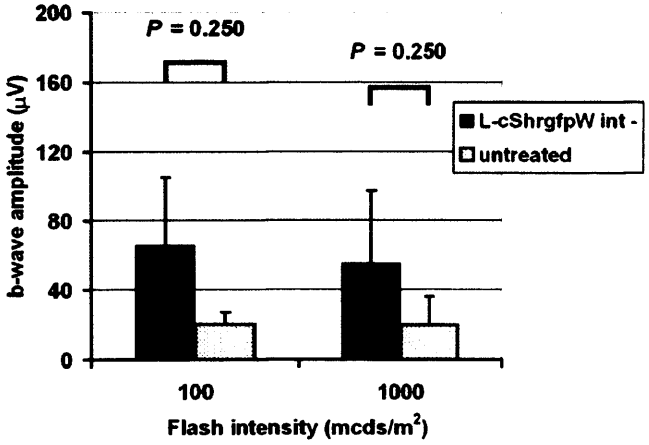

4.8 Equine infectious anaemia virus (EIAV) vectors

Biosafety concerns regarding HIV-based vectors for gene transfer have encouraged the development of vectors from lentiviruses that are not pathogenic in humans. Several studies in various animal models have demonstrated that, apart from HIV-based vectors, also simian (SIV), bovine (BIV) and feline (FIV) immunodeficiency virus-based vectors are able to mediate efficient and sustained transgene expression in a variety of ocular tissues after intraocular delivery [295, 300, 301, 360, 361]. The tropisms and expression patterns of these vectors are influenced by different factors including the natural tropism of the virus, vector pseudotype and genome configuration, the transgene promoter, and surgical technique. All lentivirus-based vectors have been shown to efficiently target RPE cells after subretinal injections, however reports about photoreceptor transduction rate and efficiency are variable [299, 313, 314, 362].

EIAV is another lentivirus that is not associated with any diseases in primates. EIAV causes a persistent non-fatal infection in horses, donkeys and mules but is non-pathogenic in humans (see [363] for a review). The cellular tropism and kinetics of EIAV-based vectors have been evaluated in the central nervous system of rodents [364, 365], and these vectors have been used to express therapeutic genes in experimental models of human disease [366-369].

We tested EIAV-based lentiviral vectors developed by Oxford Biomedica to evaluate their in *vivo* expression profiles in different ocular tissues and their utility in ocular gene therapy approaches. To investigate if different viral envelope proteins influence the cellular tropism of EIAV vectors, we tested VSV-G and rabies-G pseudotyped viruses. Three EIAV vector genomes were used in this study each containing a CMV promoter driven *gfp* expression cassette. The pONY8.0 genome has been described previously [16]. Furthermore, we defined the efficiency of a self-inactivating minimal EIAV vector

(pONY8.4) deleted for all EIAV sequences except essential *cis* elements, and a further minimal EIAV vector (pONY8.7) which also incorporates the central polypurine tract/central termination (cPPT) sequence and the woodchuck post-transcriptional regulatory element (WPRE) (figure 4.18). The expression pattern and transduction efficiency of all viruses was analysed by in *vivo* GFP imaging and histology after subretinal, intravitreal, and intracameral injections in adult mice (In *vivo* experiments were performed by K. Balaggan, Div. of Molecular Therapy, IoO.).

Figure 4.18: Vector maps. A schematic diagram of the genetic configuration of the EIAV pONY8.0, pONY8.4, and pONY8.7 expression cassette is shown. The pONY8.4 genome is self-inactivating, rev-independent and has been deleted for all EIAV sequences except essential *cis* elements, and is associated with higher expression levels *in vitro* than pONY8.0 vectors (Wilkes *et al.*, manuscript in preparation). The pONY8.7 genome also incorporates the cPPT sequence and the WPRE. These elements increase the efficiency of nuclear import of viral pre-integration complexes [349], and the export of the unspliced transcripts from the nucleus to the cytoplasm [352], respectively.

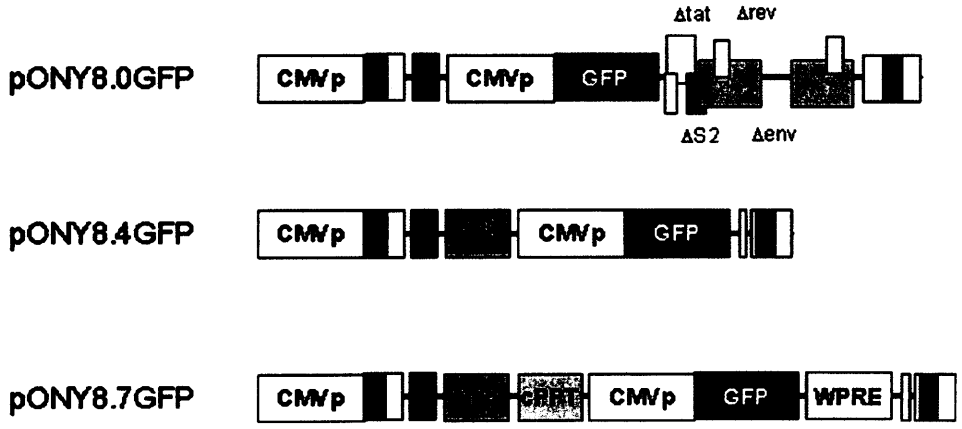

4.8.1 Subretinal injections

With in *vivo* GFP imaging *gfp* expression was detected first by 3 days after injection of EIAV vectors. Expression increased by 7 days and reached maximum levels at 14 days with all vectors tested. Higher expression levels could be found with pONY8.4 and pONY8.7 compared to pONY8.0 (figure 4.19).

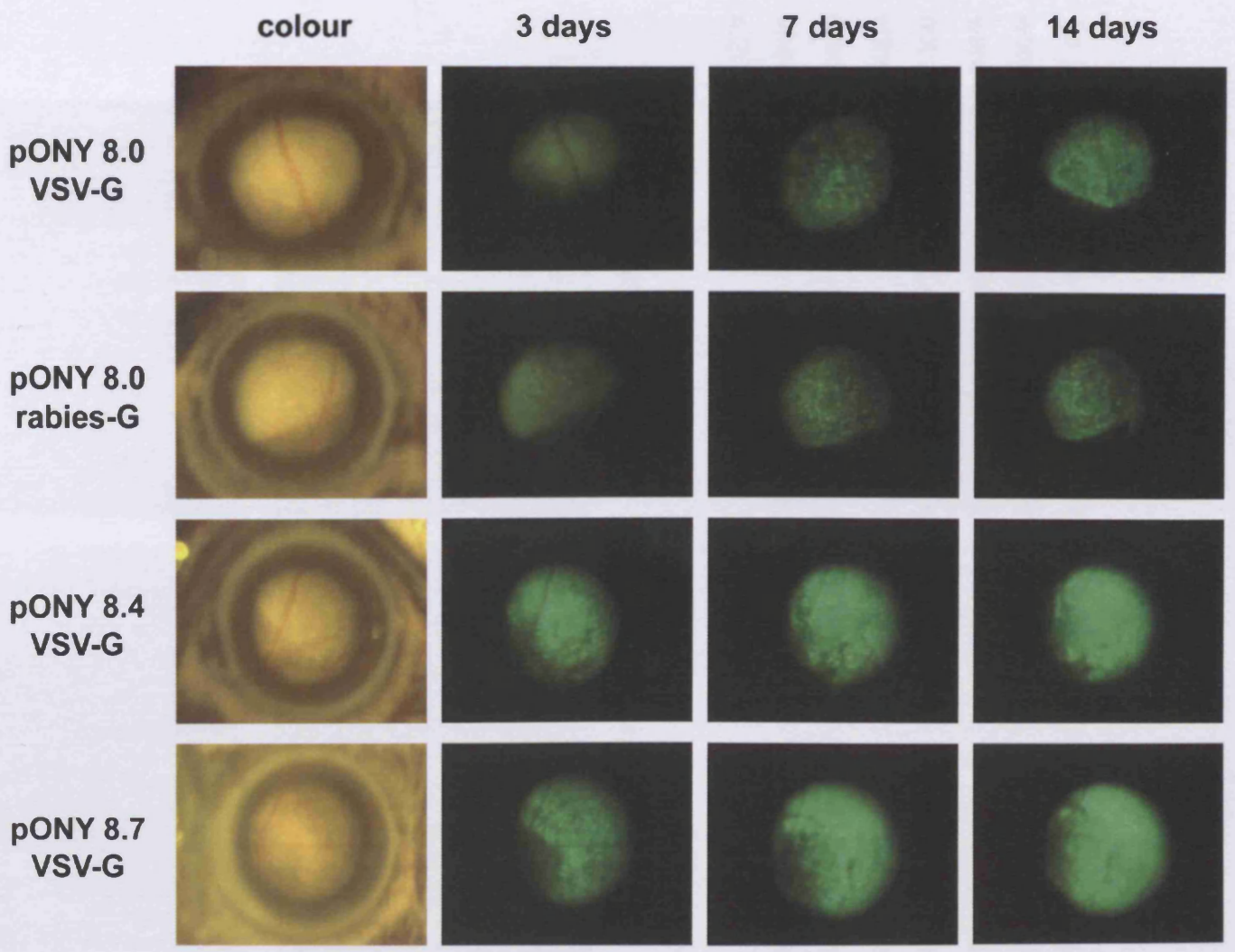

Figure 4.19: In *vivo* visualisation of retinal *eGFP* expression. Colour and fluorescent retinal images of eyes receiving subretinal injections of pONY8.0 EIAV.VSV-G (1.4×10^{10} TU/ml), pONY8.0 EIAV.rabies-G (1.0×10^{10} TU/ml), pONY8.4 EIAV.VSV-G (8×10^{8} TU/ml) or pONY8.7 EIAV.VSV-G (1.5×10^{9} TU/ml) vectors. The injected retina is clearly identifiable as a paler area using colour slit lamp biomicroscopy. eGFP fluorescence is detectable at 3 days post injection in pONY8.0 injected eyes and is already efficient at this stage in pONY8.4 and pONY8.7 injected eyes. Expression continues to increase with time achieving maximal levels between 7 and 14 days. Despite their lower titre, pONY8.4 and pONY8.7 vectors are able to mediate higher levels of *eGFP* expression than pONY8.0 vectors at all time points.

To investigate which cell types were transduced by EIAV vectors, cryosections were taken of eyes after injection. Sections revealed that up to 100% of RPE cells were transduced in injected areas. In addition, variable *gfp* expression, that was not restricted to the injection site, could be detected in photoreceptor cells with either pseudotype. The transduction pattern of RPE and neuroretina was irrespective of vector pseudotype, age of animals, and titre, and could be observed up to 10 months (EIAV.rabies-G) and 16 months (EIAV.VSV-G) (figure 4.20).

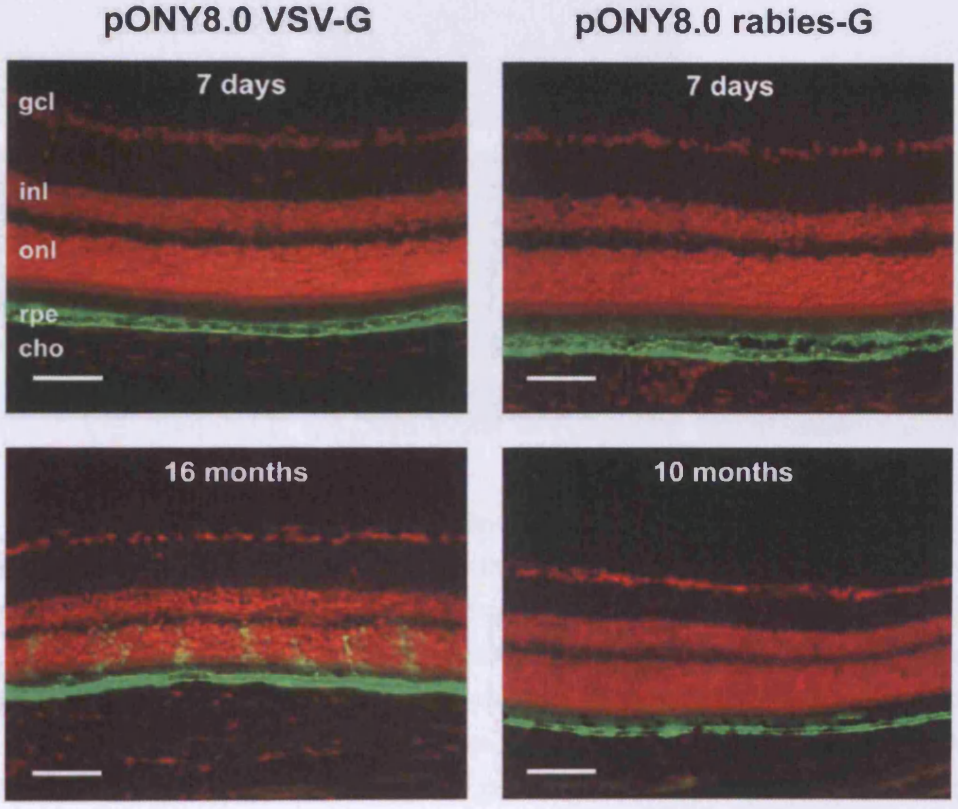

Figure 4.20: Cryosections of eyes after subretinal delivery of EIAV. In order to visualise cell nuclei, sections were counterstained with propidium iodide (red). In eyes injected with vectors pseudotyped with either VSV-G or rabies-G GFP fluorescence (green) is first observed at 7 days post injection and remains evident up to 16 months (gcl=ganglion cell layer, inl=inner nuclear layer, onl=outer nuclear layer, rpe=retinal pigment epithelium, cho=choroid, size bar=50 µm).

With pONY8.4 and pONY8.7, *gfp* expression was restricted to RPE cells in approximately half of the eyes treated. However, GFP fluorescence was observed in photoreceptor cells in the remaining eyes and with greater efficiency than with pONY8.0 vectors (figure 4.21). No *gfp* expression could be found in ganglion cells, optic nerve or brain following subretinal injection of EIAV vectors.

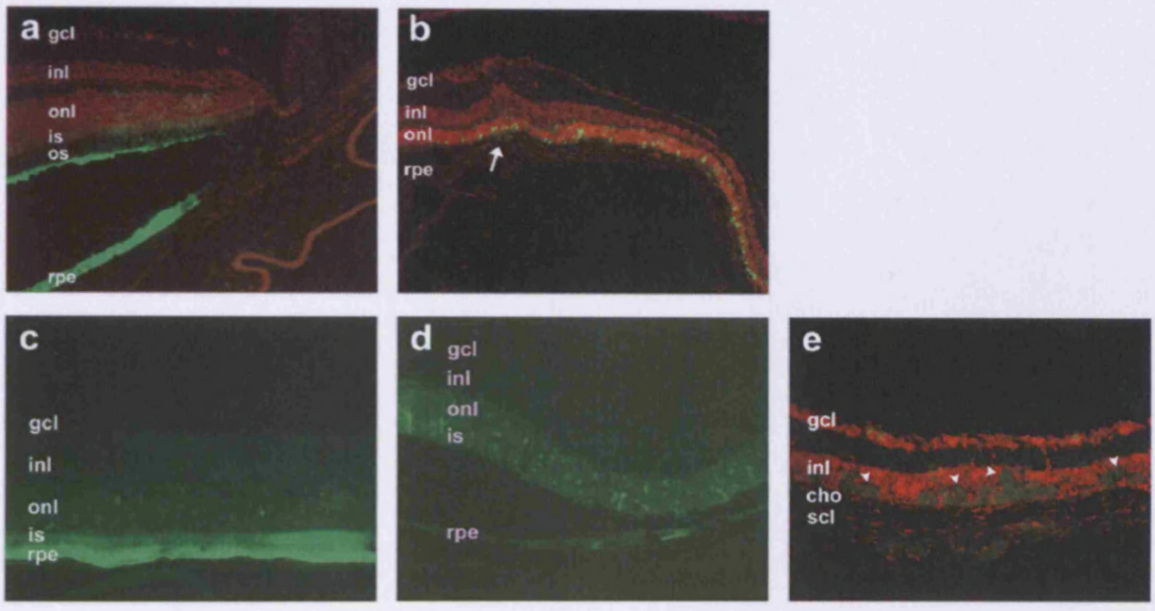

Figure 4.21: Retinal cross sections. (a) Limited photoreceptor cell transduction in the anterior retina is observed in eyes injected with pONY8.0. **(b)** The transduction is not limited to the site of injection trauma but extends across the injected area after injection of pONY8.4. Efficiency of transduction varied from occasional **(c)** to significant **(d)** proportion of photoreceptors within the injected area. **(e)** Long-term high levels of *gfp* expression lead to outer retina atrophy. At 6 months and later time points a loss of RPE and scattered areas of RPE hypertrophy (arrowheads) within the injected areas are observed. Following the loss of RPE cells, photoreceptor cells degenerate which is shown by the absent of the outer nuclear layer. (gcl=ganglion cell layer, inl=inner nuclear layer, onl=outer nuclear layer, rpe=retinal pigment epithelium, cho=choroid, scl=sclera).

Inflammatory infiltrates were observed in the subretinal space 1 week after injection but were not found at later time points. At 6 to 16 months following subretinal delivery of vectors carrying the *gfp* reporter gene, outer retinal atrophy was observed in approximately 70% of the treated eyes. These findings comply with previous reports of outer retinal atrophy after *gfp* administration due to the long-term high level *gfp* expression.

4.8.2 Intravitreal administration

EIAV vectors pseudotyped either with VSV-G or rabies-G were injected into the vitreous cavities of adult mice. No fluorescence was detected in any cell types after intravitreal delivery of vectors. There was no inflammatory cell infiltrate evident in the tissues examined at any time point.

4.8.3 Intracameral delivery

To investigate the transduction and expression pattern in the anterior chamber, EIAV vectors pseudotyped with either VSV-G or rabies-G were injected intracamerally in adult mice. Efficient expression levels were reached at 7 days post administration and were maintained up to 10 months. The cellular tropism of EIAV vectors was depended on the pseudotype. EIAV.VSV-G vectors mediated efficient *gfp* expression in corneal endothelium cells and limited expression in trabecular meshwork cells (figure 4.22). In contrast, no GFP fluorescence in corneal endothelium cells or trabecular meshwork cells was detectable in EIAV.rabies-G vectors injected eyes. However, this vector-mediated variable transgene expression in linear configurations. GFP fluorescence was found in radial orientation in corneal stroma and in an axial orientation in the epithelium consistent with the pattern of neuronal innervation in the cornea. Fluorescence was also present in the anterior iris and within the ciliary body in some eyes.

Figure 4.22: Croysections of eyes after intracameral injection. EIAV.VSV-G **(a, b)** and EIAV.rabies-G **(c-g)**. **(a)** GFP fluorescence is present in corneal endothelium cells 10 months post injection. **(b)** Cells of the trabecular meshwork and corneal endothelium are transducted. **(c-e)** Axial orientated fluorescence is observed in the corneal epithelium and in a radial orientation within the anterior and mid-corneal stroma after EIAV.rabies-G administration. Fluorescence is also observed along the anterior border of the iris **(e)** and within the ciliary body **(f)**. (epi=epithelium, end=endothelium, cor=cornea, cb=cliliary body, cep=cliliary epithelium, ac=anterior chamber, nr=neuroretina, str=stroma,

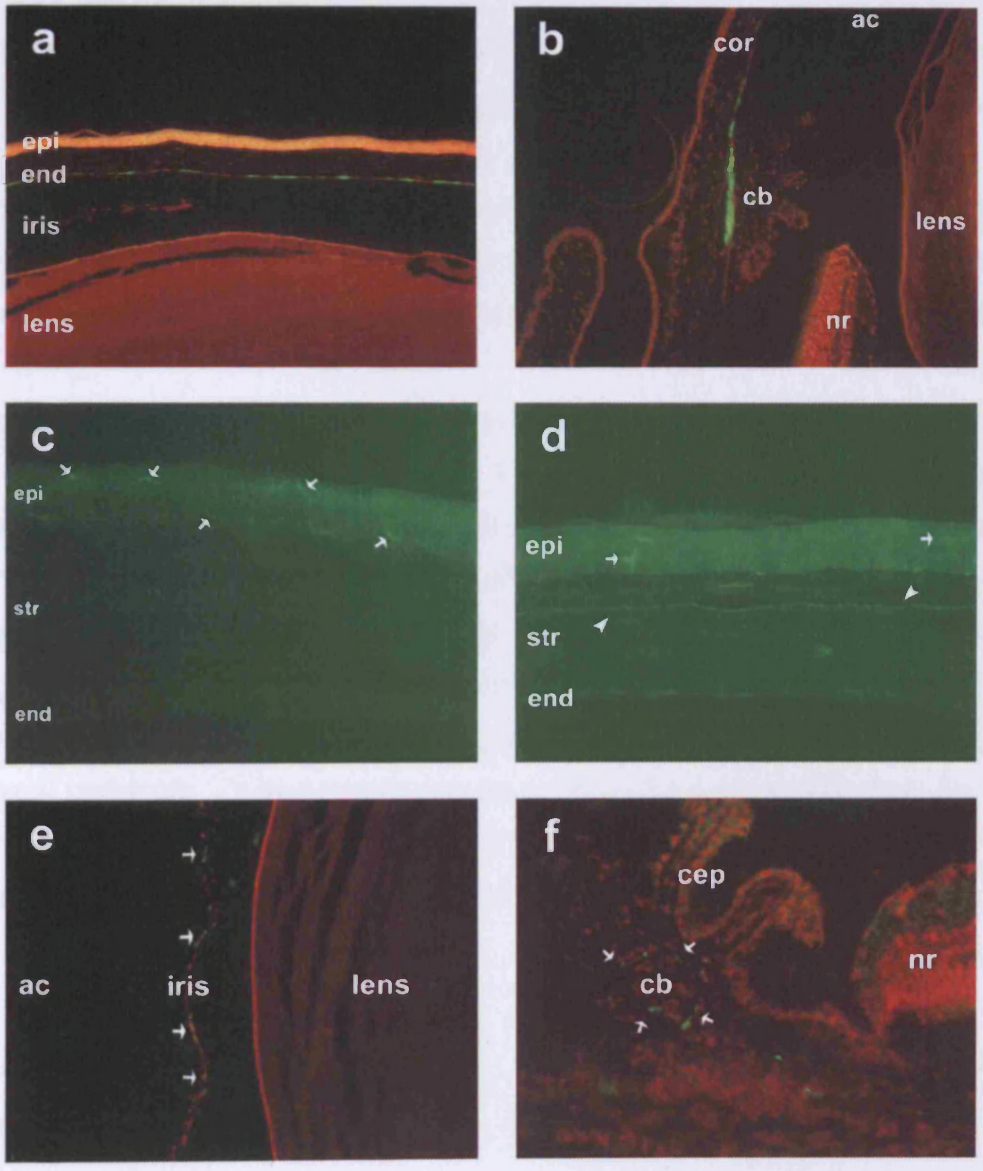

4.9 Discussion

In this chapter a detailed assessment of the duration and extent of the morphological rescue and functional benefit following HIV-1-mediated gene replacement therapy in the RCS was presented. The preservation of retinal function and morphology was observed up to seven months. This is the most significant rescue of a severe retinal degeneration to date. The results presented provide further evidence to support gene therapy approaches for the treatment of RP. For clinical protocols, however, HIV-based vectors have several disadvantages. Wild type HIV-1 is highly pathogenic in humans. A primary safety concern therefore is the generation of a replication-competent lentivirus by recombination events. To circumvent this risk we tested non-human lentivirus vectors, based on EIAV, and assessed the potential for gene therapy protocols.

The ability of lentiviruses to integrate their genome into their host's, implicate both asset and drawback. On the one hand, integration ensures long-term expression of the transgene, which is a prerequisite for successful gene therapy approaches to cure many genetic disorders. On the other hand, the integration events occur at random genomic locations and thus there is also the risk of insertion mutagenesis. Integration-deficient lentiviruses are unable to integrate into the host genome and therefore might be better gene transfer vehicles for the development of clinical protocols. To investigate transduction and expression profiles we tested integrase deficient HIV-based vectors. These vectors were also used to rescue two animal models of retinal degeneration.

4.9.1 Gene replacement in the RCS rat using HIV-1-based vectors

Gene replacement therapy using AAV-2 vectors is more effective in comparison to Ad vectors mainly due to their low immunogenicity. As described in chapter 3, photoreceptor degeneration could be delayed and retinal function improved in the RCS rat up to 9 weeks after treatment with AAV-based vectors. However, the late onset of AAV-mediated expression compromises its efficacy. Whilst AAV vectors are much less immunogenic than Ad vectors and AAV vector-mediated gene transfer is generally maintained over a long period of time, by the time maximal transgene expression is attained, retinal degeneration in the RCS rat is already well advanced [227, 275]. In RCS rats, retinal degeneration is rapid and starts around postnatal day 14 depending on the eye pigmentation [71, 167, 357]. Lentiviruses, as vehicles for transgene delivery, have the advantage that onset of transgene expression occurs within 24 hr after administration [313]. Therefore, they are more suitable for a gene replacement approach in the RCS rat than AAV-2-based vectors.

Following treatment with an HIV vector, an improvement of retinal function for up to 27 weeks after treatment was achieved, compared with treatment using an AAV-2 vector, which showed an improvement in the retinal response in treated eyes over a period of 9 weeks. b-wave amplitudes were significantly higher in eyes treated with LNT.SFFV.Mertk compared to untreated or LNT.SFFV.GFP injected eyes. The presence of OPs on ERG traces of treated eyes implies proper retinal function. After treatment with the therapeutic vector, the pattern of the ERG response to a series of increasing stimuli resembled that of normal animals, with increasing b-wave amplitudes and decreasing b-wave latencies indicating successful functional rescue at this time point. Since ERG recordings reflect changes in the inner as well as the outer retina that occur during retinal degeneration this data suggests an overall improvement of the retina. At 3 weeks b-wave amplitudes were lower in treated eyes than in untreated. However, this effect was only of short duration and disappeared at 6 weeks after the treatment.

Since purification protocols for lentiviruses are not optimal yet, this temporary decrease was probably due to an immune response against impurities of the virus preparation. The improvement in function did not last as long as the improvement in retinal morphology. Since an ERG is an average response from the whole eye, contributions to this response from a decreasing area of rescued retina will eventually be masked by the global response from areas that have degenerated. Treated areas covered approximately 50 to 70 % of the entire retina initially.

Whilst retinal degeneration was not completely prevented, photoreceptor loss was significantly delayed. Eight weeks after treatment, there were two- to three-fold more photoreceptor cells in treated areas than in equivalent untreated areas and photoreceptor cell survival was prolonged for up to 30 weeks after treatment, 23 weeks longer than that following treatment with an AAV-2 vector. One reason why treatment did not result in better photoreceptor cell protection might be that 50-70 % RPE transduction is insufficient to ultimately prevent degeneration in treated areas. Degenerating photoreceptor cells in other parts of the retina may have a negative impact on photoreceptor survival in treated regions [342]. Several studies have suggested that retinal metabolism is altered within the RCS rat retina and also in patients with RP [370, 371]. Changes in degenerating photoreceptors are likely to generate a microenvironment that has a negative influence on the survival of healthy cells [342, 372, 373]. Therefore it will probably be important to treat as much of the retina as possible in the RCS rat and eventually in patients.

4.9.2 Non-integrating HIV-1-based vectors

Lentiviruses, as vehicles for gene transfer, have the advantage of efficient cell transduction of a broad range of cell types including post-mitotic cells, the absent of an immune response, and long-term, high level transgene expression due to the integration of their genome into their host's. Integration events, however, are

random and bear the risk of insertional mutagenesis. This can be avoided by the use of gene therapy vectors that do not integrate. Existing non-integrating systems are often limited by inefficiency or immunogenicity. Lentiviruses can be altered to integration deficient by mutation of the viral integrase. Following reverse transcription, integration deficient vectors form stable episomal double stranded DNA genomes in the target cell nucleus [359]. In this study we tested non-integrating HIV-1-based vectors and defined their potential for gene therapy approaches for retinal degeneration. It was shown that these integration deficient vectors are effective templates for gene expression in *vivo* and that expression levels and the duration of transgene expression are similar to those achieved with integration proficient vectors. These results suggest that integration-deficient lentiviral vectors are attractive tools for human gene therapy approaches.

4.9.3 EIAV vectors

Different from HIV, EIAV is a non-human lentiviral pathogen and thus EIAV-based vectors might be more suitable for clinical gene therapy approaches than HIV-based vectors. The cellular tropism and kinetics of EIAV-based vectors have been tested in rodents CNS. In order to evaluate the potential of EIAV vectors for gene therapy in the eye, EIAV-based vectors with different expression cassettes and pseudotypes were designed and tested in *vivo* for their transduction and expression capability after different administration routes into the mouse eye.

In this study it was demonstrated that EIAV is able to mediate efficient and sustained transgene expression in different ocular tissues. After subretinal delivery GFP fluorescence in RPE cells was first detected at 3 days post injection and persisted until at least 16 months regardless of the vectors pseudotype. In contrast to HIV-mediated reporter gene expression, variable *gfp* expression was

also detected in photoreceptor cells and extended throughout the treated area. The persistence of *gfp* expression in photoreceptor cells for 16 months suggest that photoreceptor cells are indeed transduced by viral particles and that GFP fluorescence is not due to the transfer of GFP protein during vector manufacture (pseudotransduction). The transduction of photoreceptor cells was independent of the vector pseudotype or titers. However, it was influenced by the configuration of the EIAV genome with elevated expression levels after pONY8.4 and pONY8.7 administration compared to expression levels obtained with pONY8.0. The rate of photoreceptor cell transduction is often influenced by the stage of retinal maturation at the time of vector delivery. In this study, however, no age related effect was observed.

Intracameral administration of EIAV vectors resulted in a pseudotype-dependent *gfp* expression profile. Conforming with our experience with VSV-G pseudotyped HIV-1 vectors, VSV-G pseudotyped EIAV vectors transduce the corneal endothelium and trabecular meshwork. In contrast, vectors pseudotyped with the rabies-G envelope did not result in expression in the trabecular meshwork or corneal endothelium instead expression was detected in the corneal stroma consistent with the pattern of neuronal innervation and epithelium as well as in the iris and ciliary body. The ability of EIAV vectors pseudotyped with the rabies-G envelope to transduce corneal neurons is consistent with the enhanced neuronal tropism previously described for these vectors in other neuronal populations [364, 365]. Consistent with previous reports of HIV-based lentiviral vectors [313], intravitreal delivery of EIAV vectors, did not result in detectable transgene expression in any cells, irrespective of pseudotype.

We demonstrate that intraocular delivery of minimal non-primate EIAV vectors pseudotyped with either VSV-G or rabies-G envelope proteins can mediate rapid and stable highly efficient transgene expression in a variety of ocular cells. The favourable cellular tropism and expression kinetics of optimised EIAV vectors

make them attractive for delivering therapeutic genes in the management of inherited and acquired retinal and anterior segment disorders.

5

5 Screening retinitis pigmentosa patients for mutations in *MERTK*

5.1 Aim

The role of *MERTK* in human retinal disease has recently been established with the finding of mutations in autosomal recessive RP patients [122]. The results presented in chapter 3 and 4 suggest that defects within this gene are suitable targets for the development of gene therapy approaches in patients. However, the potential for an effective therapy in humans depends upon the identification of patients with *MERTK* mutations. Since the complexity of RP makes it difficult to counsel patients or to assess the effects of treatments, more about the specific clinical characteristics of this form of RP has to be established. To date, only four patients with mutation in the *MERTK* gene have been identified [122, 374]. In order to identify more patients and characterise the clinical features associated with this defect, a panel of 96 patients was screened for mutation in *MERTK*.

5.2 Patients with mutations in *MERTK*

To date, four unrelated patients with autosomal recessive RP and pathogenic mutations in the *MERTK* gene have been identified in two studies [122, 374]. Of these only one has been clinically characterised in detail. The mutations found in the first screen include a 5 bp deletion in exon 15, a splice acceptor site mutation in intron 10, and a premature termination codon in exon 14. All patients suffered from poor vision and night blindness since childhood. Over time visual acuities declined and peripheral vision was lost until only a small island of central vision remained [122]. In a second screen, another patient with *MERTK* mutations was identified. The patient was compound heterozygote for three sequence changes: a premature termination codon in exon 16 and two missense substitutions in exon 19 [374]. In *vitro* expression studies of the wild-type and *MERTK* variants showed a reduction in the level of mutant protein. It has been shown that the expression of mutant *MERTK* variants reduces the receptors autophosphorylation which is necessary for MERTK function [374, 375]. The patient suffered from visual problems from the age of three onwards and was diagnosed with advanced and progressive rod-cone dystrophy at the age of eight. At this age, the patient had no colour discrimination, the fundus showed disc pallor, macular atrophy and presence of bone spicule pigments. ERG showed a total loss of response to all rod and cone stimuli. At the age of fifteen both fundi showed a bull's eye like pattern of macular atrophy with widespread RPE thinning in the periphery [374] (All mutations found so far and their locations are shown in figure 5.3).

All four patients were reported to have relatively severe disease, with onset in early childhood and rapid progression to extensive peripheral visual loss by the late teenage years. However, a detailed clinical description of the phenotype has only been reported for the last identified of these patients. The recessive inheritance pattern of retinal degeneration associated with *MERTK* mutations in humans and in the RCS rat, suggests that pathenogenesis is due to a loss of

function [69, 122, 357, 374]. In contrast to the mutation in the RCS rat, however, the location of all mutations found in humans are within the region that encodes the cytoplasmatic domain of the protein. This leaves open the possibility that the human mutations do not result in a complete loss of MERTK function.

Table 4 summarises the identified disease causing mutations and common polymorphisms.

Table 4: Mutation and polymorphisms in the *MERTK* gene. The table summarises the known mutations and polymorphisms in *MERTK*. (adapted from Retina International's Scientific Newsletter)

Mutation Polymorphism	**Exon**	**Change**	**Remark**	**Ref**
ARRP	Intron 10	A → G	Aberrant splicing, homozygous	1,2
ARRP?	14	1951C→T, R651Stop	Premature termination , heterozygous, no 2nd mut found	1
ARRP	15	2070delAGGAC	Frameshift, premature termination, homozyous	1
ARRP	16	2164C→T, R722X	Nonsense mutation, Together with R844C and R865W	3
ARRP	19	2530C→T, R844C	Together with R722X and R865W	3
? only in patients	11	1628G→A, E540K	Uncommon missense substitution, compound in *cis* S661C	1
? only in patients	15	1982C→G, S661C	Uncommon missense substitution, compound in *cis* E540K, single	1
? only in patients	19	2612T→C, I871T	Uncommon missense substitution, heterozygous	1
Polymorphism	1	R20S	Equally found in patients and controls	1
Polymorphism	2	N118S	Equally found in patients and controls	1
Polymorphism	5/6	A282T	Equally found in patients and controls	1
Polymorphism	6	R293H	Equally found in patients and controls	
Polymorphism	9	R466K	Equally found in patients and controls	1
Polymorphism	10	N498S	Equally found in patients and controls	1
Polymorphism	10	I518V	Equally found in patients and controls	1
Polymorphism	19	2593C→T, R865W	Polymorphism	3
Polymorphism	19	V870I	Equally found in patients and controls	1

5.3 Results

5.3.1 Patient screen and sequencing

In a programme of work to identify patients and families with potentially treatable retinal degenerations, a panel of 96 unrelated probands with simplex and recessive rod-cone dystrophy were screened for mutations in *MERTK*. Patients were ascertained from the medical retinal clinics at Moorfields Eye Hospital and gave written informed consent to be included in the study and provided a blood sample for subsequent DNA extraction and DNA analysis. PCR primers were designed in a way that the entire coding sequence of all 19 exons and the intronic sequences important for splicing were covered. The primer sequences are listed in table 3 in chapter 2.8.3 (see also Appendix). The 19 coding exons of the *MERTK* gene were amplified and the PCR products were checked by gel electrophoresis. Figure 5.1 shows a picture of a DNA gel on which PCR products of exon 11 were loaded. After it was established that all samples showed a clean, specific single band of the predicted size, they were analysed by sequencing.

Figure 5.1: Gel electrophoresis. After amplification all samples were analysed by gel electrophoresis. As an example, PCR samples of exon 11 are shown. The primers were designed to cover the entire coding sequence as well as important intronic sequences. In case of exon 11 a fragment of ~ 200 bp was expected. (M=marker, 1- 18=patient samples)

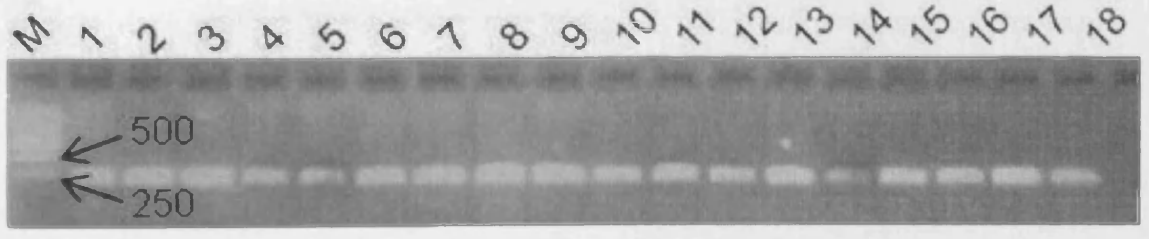

A total of 19 exons from 96 patients were screened for mutations in the coding and splice site sequences of the *MERTK* gene and 11 variants from the Genbank sequence (accession number NT022135 - build 35 version 1) were detected (summarised in table 5), including one mutation. This was a novel frameshifting single base deletion (2214delT) within exon 17. Both alleles contained the deletion. The sequence chromatograms of the patient, the unaffected mother and a control are shown in figure 5.2. The 2214delT sequence change cause a frameshift and a premature stop codon (TGA) 31 codons downstream of the mutation.

Figure 5.2: DNA sequence chromatograms. A novel mutation was identified in patients with severe retinal degeneration. The homozygous deletion 2214delT was found in affected individuals (top). The sequence of an unaffected carrier (middle) and an unaffected control are shown as well (bottom).

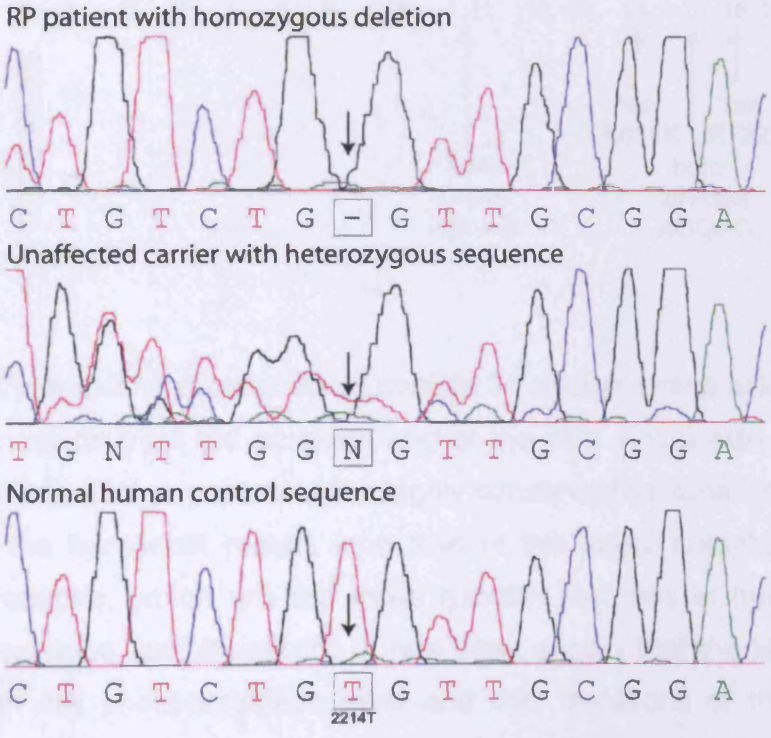

A schematic overview of the *MERTK* gene structure and the corresponding functional domains of the protein is given in figure 5.3. The mutation found in this study and mutations found in previous screens are indicated by arrows.

Figure 5.3: *MERTK* gene structure and mutations. The 19 coding exons and various encoded functional domains are shown (GenBank AF2605 14-529). Mutations identified in the present study (bold) and in previous studies are indicated by arrows. * compound heterozygous mutations found, hom = homozygous, het = heterozygous, Ig = immunoglobulin like, FN = fibronectin like, TM = transmembrane, TK= tyrosine kinase.

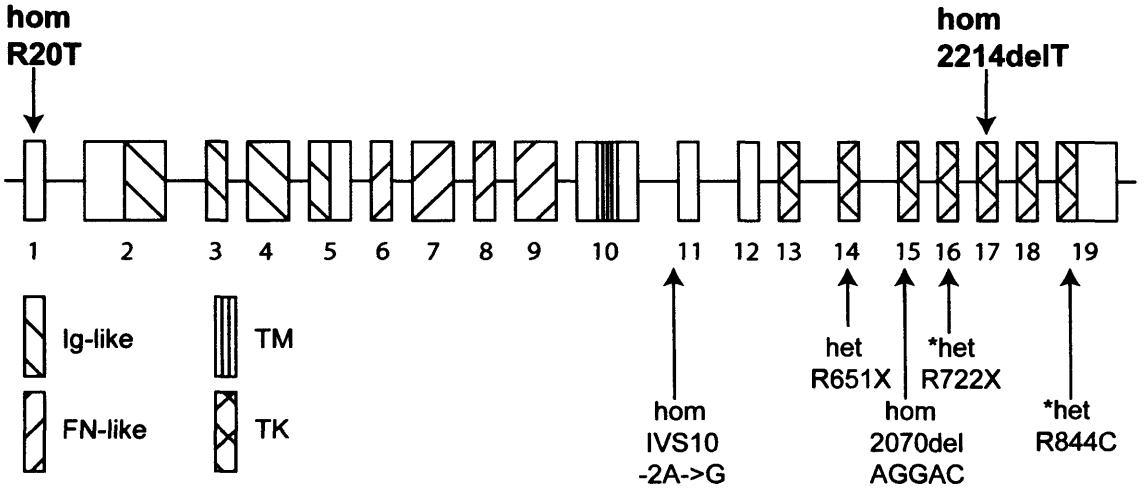

If translated, the resulting protein would contain 31 foreign amino acids and would lack 262 aminoacids from the carboxyl end of the 999 amino acid-long protein. This would include a large portion of the highly conserved tyrosine kinase domain. Furthermore, the frameshift results in a loss of the major autophosphorylation sites of the receptor, which are the three tyrosine residues in the IYSGDYYR amino acid sequence (aa748-aa755). It has been shown that the kinase activity correlates with the phosphorylation level and that mutations of these tyrosine residues significantly reduce the kinase activity [376]. Amino acid sequence alignment of MERTK shows, that the mutation is located in a region that is fully conserved between the human, chimpanzee, mouse, rat, and chicken proteins

(figure 5.4). The amino acid sequence of this region is also highly conserved between other members of the human axl subfamily of tyrosine receptor kinases, namely Axl and Tyro3.

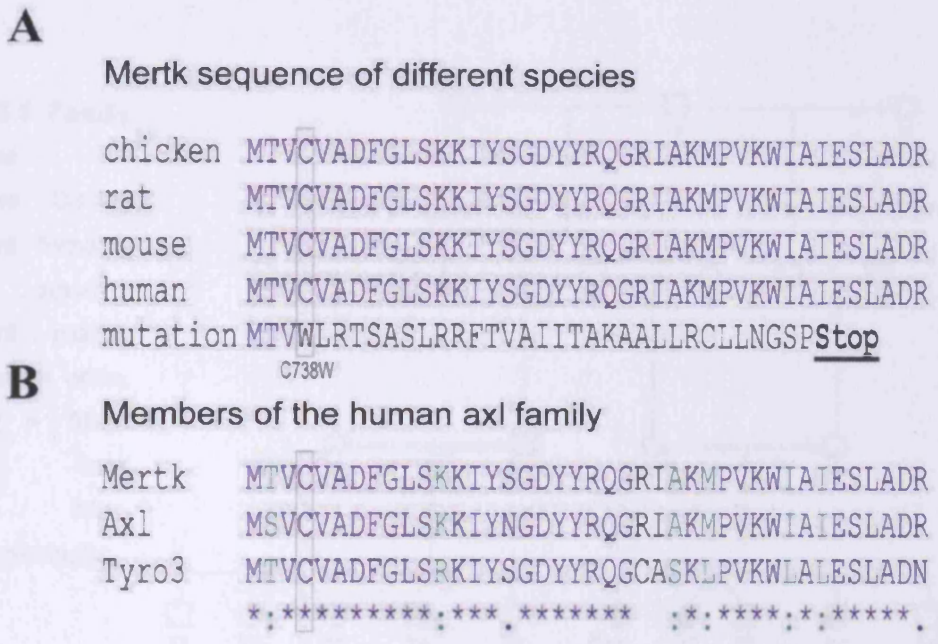

Figure 5.4: Amino acid sequences. Sequences were aligned using SDSC Biology WorkBench. **(A)** Amino acid alignments of different species show that the mutation occurred in a highly conserved domain of *MERTK*. The predicted sequence caused by a single base pair deletion of the affected probands is shown in the lowest line. The mutation leads to a frameshift and a premature translation termination signal within the tyrosine kinase domain of the protein. **(B)** Amino acid sequence comparison of different members of the human axl tyrosine kinase receptor family shows that the region, in which the mutation occurred, is highly conserved between all members. This suggests that the sequence is important for proper function.

The mutation segregated with disease in the family; all three affected siblings were homozygous for the deletion, as was the affected cousin; their unaffected mother and father were both heterozygotes. The pedigree structure is shown in figure 5.5.

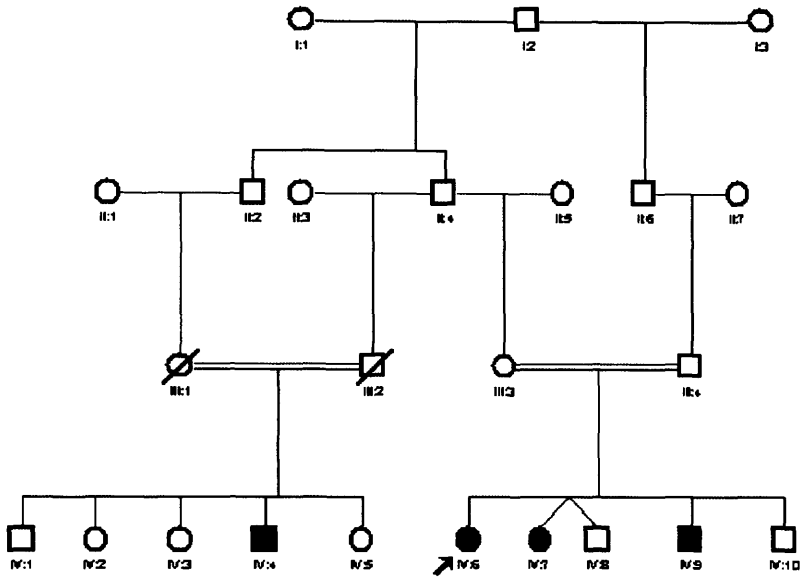

Figure 5.5: Family pedigree structure. Circles represent females and squares represent males: unaffected = open, affected = filled. Double lines indicate inter-related marriages.

The other sequence changes found in the screen include four variants that would not be expected to change the sequence of the encoded protein, being intronic or synonymous in nature. None of these, however, have been reported previously. Six base changes causing missense substitutions were found. Of these five had been reported previously; the prevalence in 96 control Caucasian samples was not significantly different to that of the 96 samples. The remaining missense change, R20T was detected in both *MERTK* alleles of a 54 year old patient with severe autosomal recessive RP. Sequence alignments show that at amino acid

position 20, arginine is a fully conserved residue in all members of the human axl protein subfamily but is not conserved between different species (figure 5.6). Furthermore, R20S is a known polymorphism in the human *MERTK* gene [122]. Since serine and threonine are structurally identical apart from a single methyl group, it is likely that this change is a rare polymorphism rather than a disease-causing change. However, the substitution was not found in 96 Caucasian and 41 Pakistani control DNA samples. Changes are summarised in table 5.

Figure 5.6: Missense change R20T. (A) DNA sequence chromatograms. The sequence of an autosomal recessive RP patient who carries the R20T change (top) and the control sequence (bottom) are shown. **(B)** Amino acid alignment. Comparison of the amino acid sequence of different species shows that the change did not occur in a conserved area. **(C)** Molecular structure of threonine and serine. The two amino acids are structurally similar apart from a single methyl group.

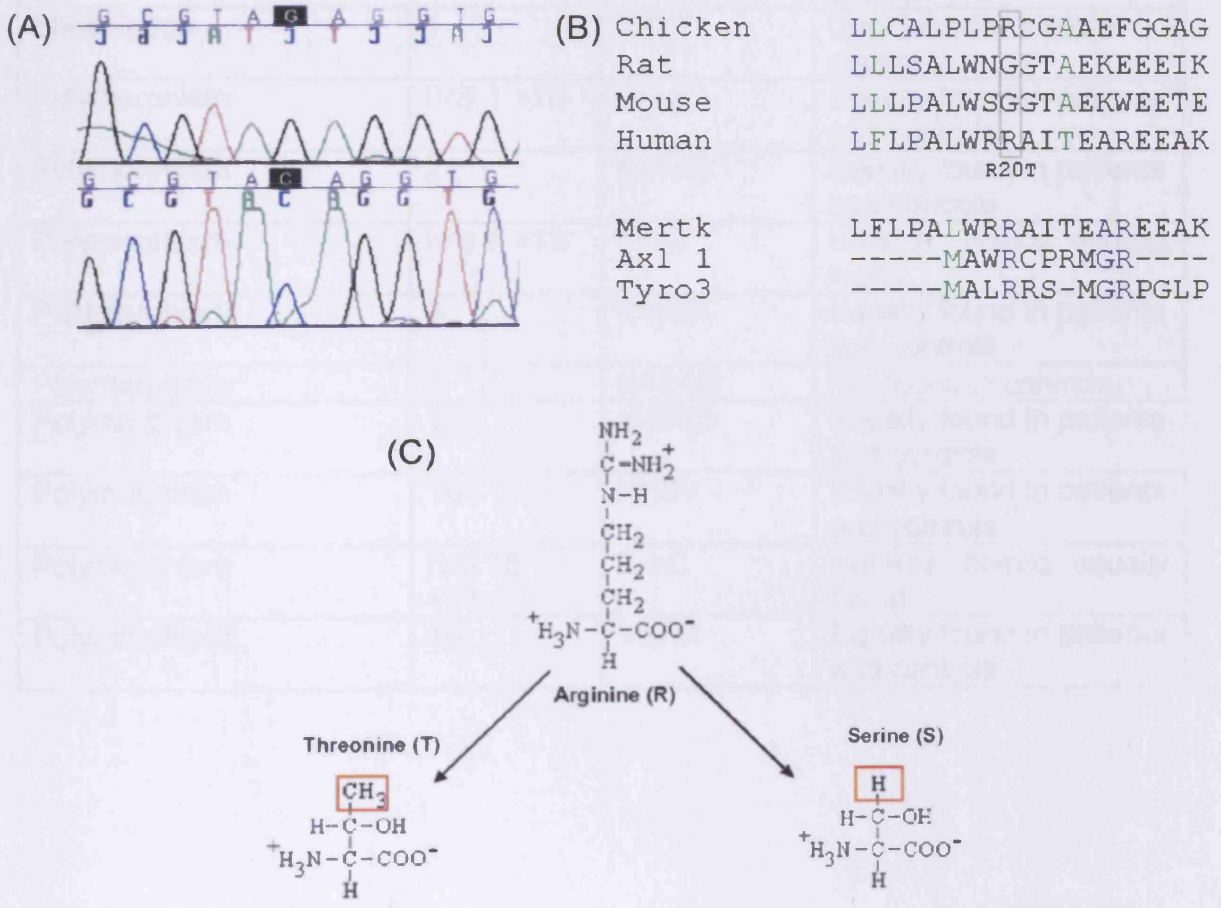

Table 5: *MERTK* sequence variants. Sequence variants in *MERTK* were identified by sequencing DNA from individuals affected by RP. The table summarises all changes found in the present study. Blue=identified in this screen, Black=known from previous screens.

Mutation/Polymorphism	Exon	Change	Remark
ARRP	17	2214delT, C738W	Frameshift, premature termination before position 770
Substitution	1	R20T	Only found in 1 ARRP patient
Polymorphism	IVS 1 +19	G→A	Equally found in patients and controls
Polymorphism*	2	N118S	Equally found in patients and controls
Polymorphism	IVS 3 +13	T→C	Heteroz., homoz. equally found
Polymorphism*	9	R466K	Equally found in patients and controls
Polymorphism	9	Q451Q	Not found in controls
Polymorphism*	10	N498S	Equally found in patients and controls
Polymorphism*	10	I518V	Equally found in patients and controls
Polymorphism	IVS 15 +11	T→C	Heteroz., homoz. equally found
Polymorphism*	19	V870I	Equally found in patients and controls

5.3.2 Clinical examination

The clinical characterisation of disease due to *MERTK* is important for assessment of any future therapies. Clinical assessment of affected individuals included fluorescein angiography, electrophysiology, Goldmann perimetry, OCT and autofluorescent imaging. Clinical examinations were conducted by A. Webster, G. Holder and colleagues at Moorfields Eye Hospital.

5.3.2.1 Visual acuity and visual fields

Visual acuity is the spatial resolving capacity of the visual system, which means it is a measure of the ability of the eyes to resolve details. Visual acuity is commonly examined by asking the patient to read a Snellen eye chart. The Snellen fractions, 20/20, 20/30, 20/40, etc., are measures of the sharpness of sight. They relate to the ability to identify a letter of a certain size at a specified distance. "Normal" vision is considered to be 20/20. Different factors including photoreceptor density throughout the eye limit visual acuity.

Patient IV:6 was first seen in 2001 at the age of 16 years. Her corrected visual acuities then were 20/30 OD (*oculus dexter*, right eye) and 20/40 OS (*oculus sinister*, left eye) and did not decline until the age of 19 years. The two younger siblings (IV:7 and IV:9) also showed well preserved visual acuities. The 2214delT deletion was also found in an older affected maternal half-cousin (IV:4). He was unavailable for examinations but gave a detailed history of the disease progress. His visual acuities were normal until the age of 15 years. From then onwards they started to decline until at the age of 46 years only his perception of light vision remained.

The term "visual field" refers to the total area in which objects can be seen in the peripheral vision while the eye is focused on a central point. Visual fields are commonly measured by using a Goldmann perimeter with the patient looking directly at a small spot in the center of the perimeter while an object is presented to the periphery. A normal field of vision is nearly 180° horizontally and about 120° in the vertical axis and the nasal fields of each eye show significant overlap. Visual field testing maps the visual field of each eye and can be used to detect pathological changes ([377], reviewed in [378]). The limits of the visual field depend on the intensity and the size of the target presented. In figure 5.7 the visual fields from patients are shown. Visual fields of patients were tested using Goldmann V4e and II4e targets, which differ in size, on a standard background. The expected normal visual field meassured with the target V4e is described as being 60° superiorly, 75° inferiorly, 60° nasally, and 95° temporally. In a visual field examination, the term isopter describes a line that connects all test locations from the same stimulus.The blue isopter reflects visual fields obtained by using the V4e target whereas the red isopter reflects the visual fields of the II4e target. The blind spot of the visual field is depicted by the red spot. The macula is thought to be the centre of each chart and each concentric circle on the graph represents 10°. With both targets, visual fields from patients were well preserved (figure 5.7).

Figure 5.7: Goldmann visual fields. Monocular Goldmann perimetry targets V4e (blue isopter) and II4e (red isopter) were used on standard background to obtain visual fields. With both targets visual fields from patients IV:6 **(A)**, IV:7 **(B)**, IV:9 **(C)** were well preserved.

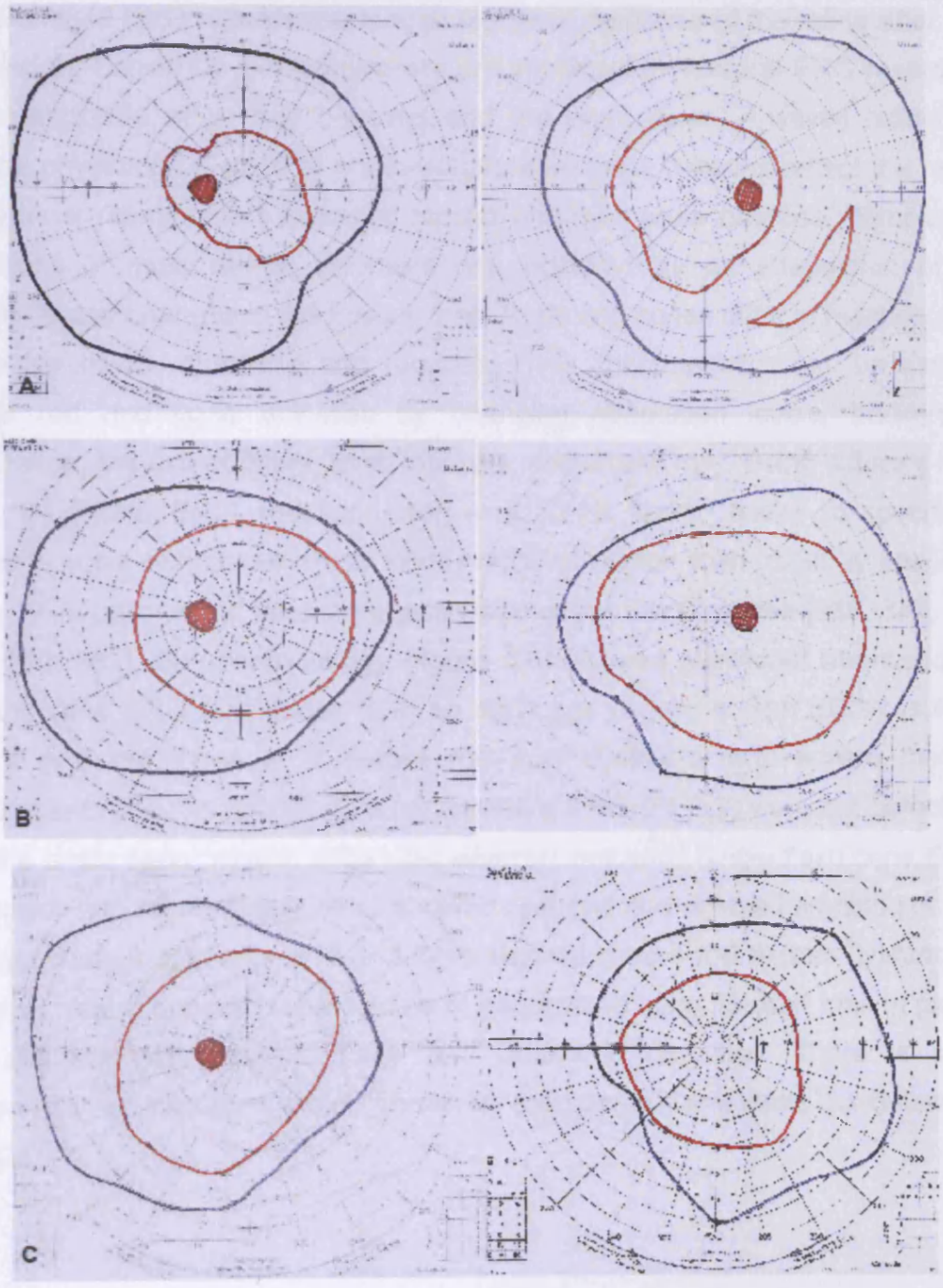

5.3.2.2 Clinical ERG

ERG records the light induced activity of the retina. It is used to assess the status of the retina and to precisely map regions of abnormally changed retinal activity. The Ganzfeld ERG records the overall electrical response of the retina after light stimulation. Principally two parameters are important to interpret ERG recordings – the amplitude of a- and b-waves and the peak times. A-waves reflect the general physiological state of photoreceptors whereas b-waves reflect the health of the inner retinal layers including bipolar and third order neurons. Pathological conditions in most retinal disorders are indicated by an attenuation of the amplitude and changes in the implicit time. Rods and cones differ in number, peak colour sensitivity, threshold and recovery. This characteristics can be used to isolate rod and cone activities by changing adaptation levels, background illumination, the use of filters, flash intensity, colour and rate. Using different rates of stimuli (flicker ERG, routinely used is a 30 Hz flicker) allows to specifically measure cone responses since cones recover faster than rods. A multifocal pattern ERG allows the detailed examination of the macular area [338, 377, 379, 337, 380, 381]. Electrophysiology (figure 5.8) showed significant attenuation of rod and cone ERG amplitudes from an early age (8 years). The ERG results of patient IV:6 are those of a severe rod-cone dystrophy with severe macular involvement. The rod-specific ERG and pattern ERG (PERG) were not detectable and the bright flash "mixed" ERG was severely reduced. Single flash cone ERGs (photopic) and 30 Hz flicker ERG showed reduced and delayed amplitudes. The younger siblings (patients IV:7 and IV:9) showed severe rod system dysfunction. However, there is better preservation of generalised cone function than in patient IV:6 but still with marked delay and amplitude reduction. There is some preservation of macular function shown by the very low amplitude but detectable PERGs.

Figure 5.8: Representative electrophysiological traces. ERGs from three patients showing a rod-cone pattern of abnormality. Patient IV:6 shows no detectable rod-specific ERG, a severely reduced bright flash "mixed" ERG, profoundly reduced and delayed 30Hz and single flash cone ERGs and an undetectable pattern ERG (PERG). Patients IV:7 and IV:9 also show no detectable rod-specific ERG. Mixed ERGs, 30 Hz flicker and photopic ERGs were better preserved than in patient IV:6 but still with marked delay and amplitude reduction. The PERGs were just detectable suggesting some degree of macular function preservation.

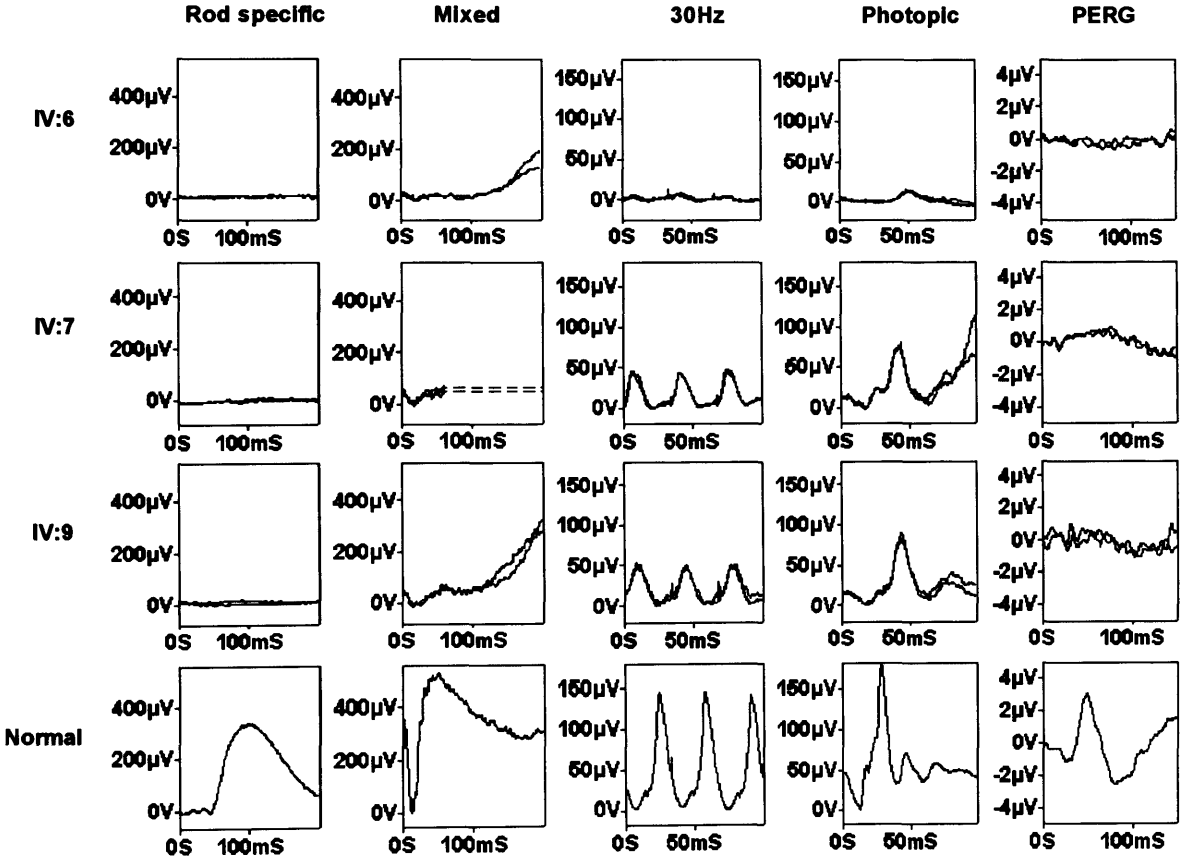

5.3.2.3 Fundus Imaging, Fluorescein Angiography and Scanning Laser Ophthalmoscopy (SLO)

Retinal blood vessel morphology is an important indicator for many diseases. The detection and measurement of blood vessels can be used to characterize and quantify the severity of disease. Retinal blood vessels have changes in diameter, branching angles, and length in different pathological conditions. Fluorescein angiography is an established technique for examining the circulation of the human retina. After colour images of the fundus have been taken, fluorescein is injected rapidly into a convenient vein to increase the contrast of blood vessels against the background and photographs are taken at different time points.

Fundus examination of patient IV:6 showed attenuated vessels as well as a pale reflex from the RPE. Furthermore, a bulls-eye lesion was seen at the macula. However, intraretinal pigmentation or bone spicules, which are typical characteristics of RP, could not be found in this patient. FFA from patient IV:6 was performed at the age of 16 years. A region of hypofluorescence could be seen throughout the central macula (figure 5.10b). Fundus examination of patients IV:7 and IV:9 showed a similar fundus appearance compared to IV:6. In addition, there were fine crystals present at the central macula present (figure 5.9).

Figure 5.9: Fundus photographs from the three affected siblings. **(A)** Fundus photograph of patient IV:6 showing attenuated vessels, a pale reflex form the RPE, and a bulls-eye lesion at the macula. **(B)** Fundus photograph of patient IV:7 showing fine crystals present at the central macula. **(C)** Fundus photograph of patient IV:9. IV:7 and IV:9 showing a similar appearance compared to IV:6, although with additional fine crystals present at the central macula.

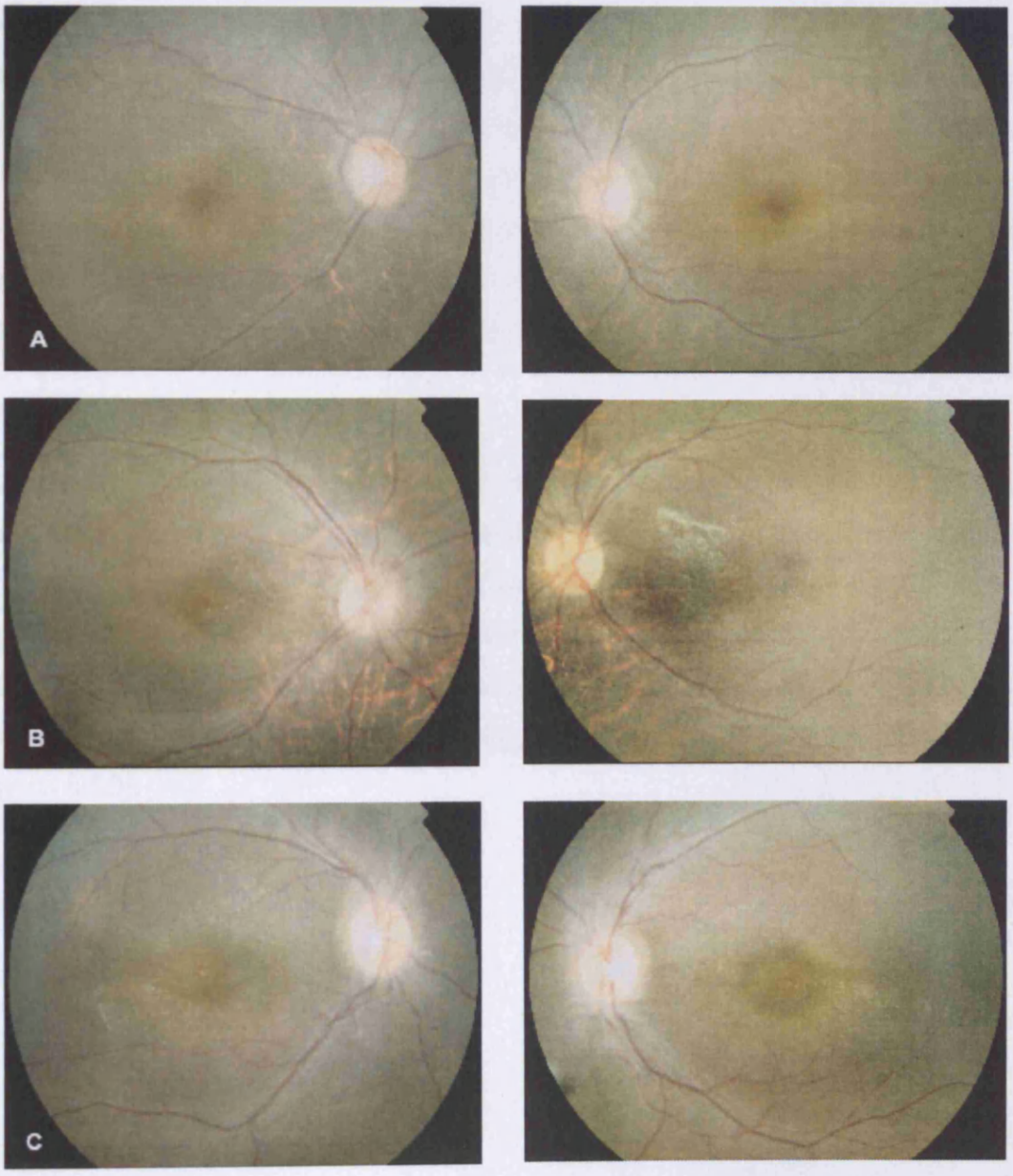

SLO is a routine technique for imaging of the fundus and has the advantages over conventional fundus imaging using a fundus camera of lower levels of light exposure, improved contrast by the selection of appropriate wavelength for the laser, and direct digital imaging. In SLOs a laser beam is scanned over the surface of the retina and a detector captures the reflected light. By using infra-red light visualisation of pathological conditions, such as choroidal neovascularisation and pigmentary changes in the RPE, which are often blocked by overlying haemorraghe, lipids, or pigments in normal fundus images otherwise, becomes possible [382-385]. In RPE cells autofluorescent lipofuscin granules accumulate with age in the lysosomal compartment as a waste product of phagocytosis of shed outer segments. The RPE plays a key role in the pathogenesis of different degenerative diseases. The confocal SLO (cSLO) can be used to examine and visualise topographical variations in the RPE autofluorescence [386].

Fundus autofluorescence imaging of patient IV:6 showed an area of hyper-autofluorescence surrounded by an area of hypo- autofluorescence in both eyes. This area is normally relatively hypofluorescent because of the presence of the pigment lutein which absorbs the incident blue light. The central macula lesion was seen in all three affected individuals, which masked choroidal fluorescence on angiography but appeared brightly hyperautofluorescent on SLO imaging (figure 5.10).

Figure 5.10: Fundus autofluorescence and FFA . (A) Fundus autofluorescence of patient IV:6 showing a bilateral area of increased autofluorescence encircled by an area of relative decreased signal. **(B)** FFA from patient IV:6 performed at the age of 16 years showing a region of hypofluorescence throughout the transit at the central macula. Fundus autofluorescence of patient IV:7 **(C)** and of patient IV:9 **(D)** were similar to patient IV:6 showing the central macula lesion which appeared hyperautofluorescent on SLO imaging.

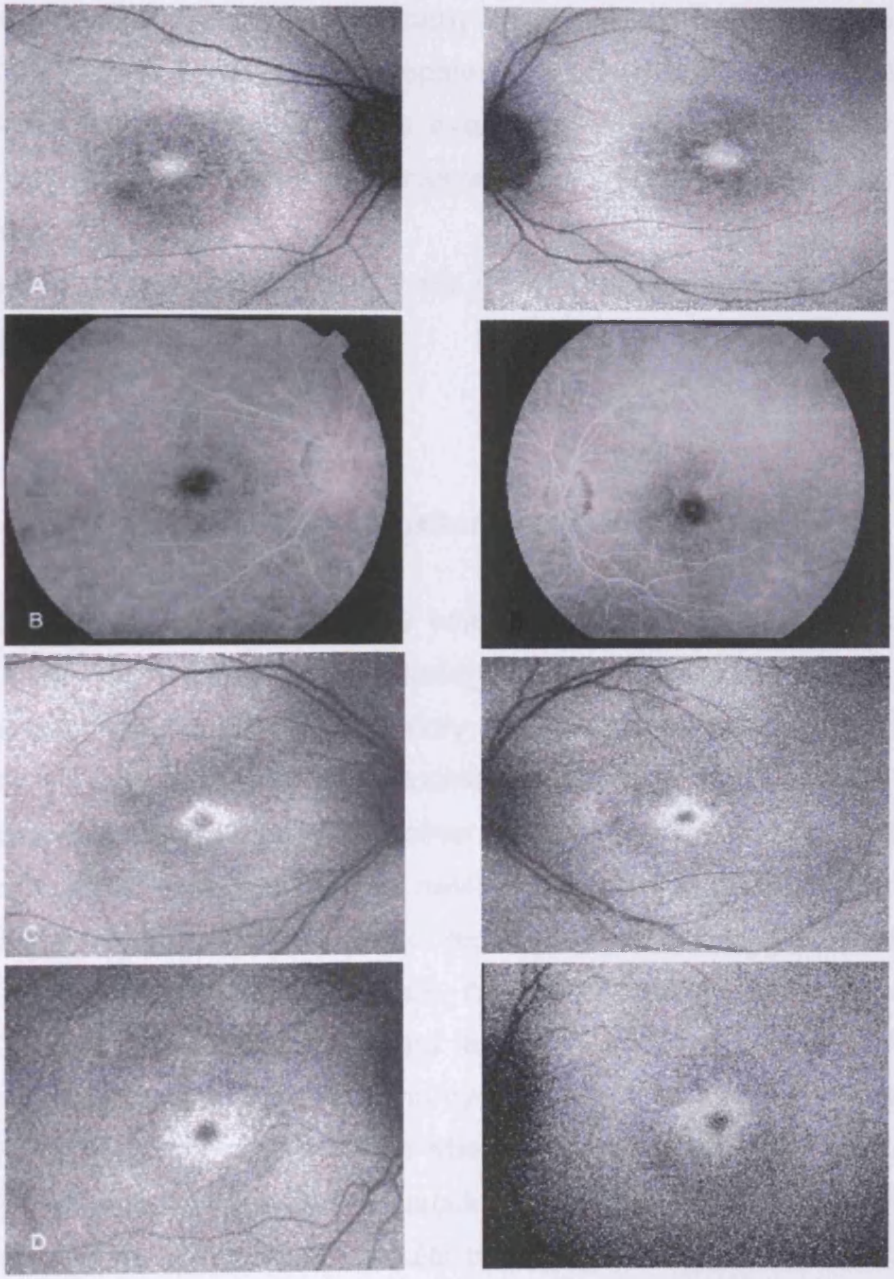

5.3.2.4 Optical Coherence Tomography (OCT)

OCT is an imaging technique that produces high resolution cross sectional imagines of optical reflectivity. Time delays in reflected signals are used to measure the distance between different ocular tissues. The high level of resolution achieved with OCT imaging is particularly suitable for retinal thickness measurements. Histological data of many human ocular disorders is rare and so far was only obtained from retinal biopsies and post-mortem tissues. OCT gives the possibility of in *vivo* histological examinations and can be either used to generate topographical maps or cross-sections through specific areas of the retina [381, 385].
OCT imaging did not demonstrate debris layer (The data could not be presented due to a technical failure of the OCT).

5.3.2.5 Summary of clinical examination and patients history

The proband (IV:6; figure 5.5), a 19 year old girl of Middle-Eastern origin, the oldest of 5 siblings of a first-cousin marriage, was diagnosed with RP at the age of 12 years. She had no significant history of systemic disease and no history of medication or drug use. She had become symptomatic at the time of diagnosis with nyctalopia but complained of no other symptoms by the age of 19 years. She did not experience any problems with navigation but found reading and discerning fine detail difficult, although she did not require the use of magnifying aids. When first examined at the age of 16 years, her best corrected visual acuities were 20/30 OD and 20/40 OS. Three years later, at the age of 19 years, her visual acuity had not changed. There was no nystagus and the anterior segments were normal. Fundus examination showed attenuated vessels, a pale reflex form the RPE, and a bulls-eye lesion at the macular (figure 5.9) There was no intraretinal pigmentation (bone spicules), or macular oedema evident on biomicroscopy.

Monocular perimetry (Goldman, V4e and II4e) showed well preserved visual fields (figure 5.7). Colour vision assessment with HRR plates showed both red-green and blue-yellow defects. Autofluorescent imaging of the RPE layer showed a relatively homogeneous signal from the posterior pole but was unusual in that it demonstrated a central area of hyper-autofluorescence of approximately 500 μm in diameter at the central macula (figure 5.10) encircled by an area of relative decreased autofluorescence. This region is usually relatively hypofluorescent due to the lutein pigment which absorbs the incident blue light. Fluorescein angiography, performed at the age of 16 years showed a region of hypofluorescence throughout the transit at the central macula (figure 5.10b). There was no retinal edema. OCT imaging did not demonstrate a debris layer, the central retina being of normal thickness. Electrophysiology performed at the age of 16 showed a significant reduction of both scotopic and photopic responses. The attenuated 30 Hz flicker showed significant delay. The pattern ERG was unrecordable (figure 5.8).

The proband's affected younger sister (IV:7) had been diagnosed with RP at the age of 10 years. By the age of 14 years, she experienced difficulty navigating and discerning colours in the dark but did not have problems reading. Her acuities were 20/30 OU best-corrected and she was mildly myopic (-2D spheres OU). Fundus examination revealed a similar appearance to her sister, although she had fine crystals present at the central macula (figure 5.9). Her visual fields were relatively well preserved. Colour vision assessment with HRR plates showed a marked red-green and blue-yellow defects. Autofluorescent imaging of the RPE showed a bilateral central area of increased autofluorescence at both maculae (figure 5.10). OCT imaging was unremarkable. ERG testing performed at the age of 10 years showed attenuation of rod and cone responses, delay of the cone implicit times and the pattern ERG was just recordable (figure 5.8).

The youngest affected sibling (IV:9) had noticed nyctalopia by the age of 10 years but otherwise had no symptoms. At age 7 years, when examined as part of a

family survey, his retinal examination was reportedly normal. At 10 years, his acuities were 20/20 OU (*oculi uterque*) unaided. Fundus examination revealed some pallor of the RPE in the peripheral retina and some fine crystalline deposits near the fovea. His visual fields (Goldman, V4e) were well preserved (figure 5.7). Colour vision testing with HRR plates showed moderate red-green and blue-yellow defects. Autofluorescent imaging of the RPE layer showed a similar appearance to his two older sisters, although the area of hyper-autofluorescence was larger (figure 5.10). OCT imaging was unremarkable. Electrophysiology showed an absent scoptic response, a severely attenuated maximal response, and delayed and attenuated reponses to photopic stimuli. The pattern ERG P50 was just recordable (figure 5.8).

An older affected maternal half-cousin of the proband (IV:4) was unavailable for examination. However, he was able to give a detailed history at the age of 46 years. He first started experiencing problems seeing in the dark at the age of 9 years. At that stage, his corrected visual acuities were normal. He was examined extensively in his early teens but was not diagnosed with RP until the age of 15 years. He learnt to drive, although he was advised to stop driving by the age of 18 years. For the next few years he managed well, attending University without assistance. At this stage, he began to find reading and writing challenging and by the age of 24 benefited from the use of a closed-circuit TV monitor. At the age of 34 years, he required a permanent guide for navigation. By the age of 38, he no longer found use for his monitor due to further deterioration of vision and presently, at the age of 46 years only has perception of light vision.

Retinal examinations of one other unaffected twin male sibling (IV:8) and the mother (III:3) were both normal.

5.4 Discussion

RP is highly heterogenous genetically, with at least 16 specific genes shown so far to cause autosomal recessive disease, 13 causing autosomal dominant disease and 5 genes causing X-linked disease (retnet September 2005). Many of these genes are specifically expressed in photoreceptors or RPE cells, whilst others have a ubiquitous expression pattern. The fundus appearance in RP is most typically characterised by a pigmentary degeneration of the retina indicated by the presence of bone spicules, attenuation and narrowing of the retinal blood vessels, and optic disc pallor (for a review see [387]). However, the presentation of RP is clinically variable; a factor that reflects the genetic heterogeneity. The onset of the symptoms of RP usually begins with a loss of dark adaptation (night blindness) followed by a progressive reduction in the mid-peripheral visual field. The primary pathological observation of the retina is degeneration of the rod photoreceptors, followed by secondary changes in cones, RPE cells and other cells of the neuronal retina.

Currently there are no effective treatments for patients suffering from retinal degeneration, although there has been much success with various therapeutic strategies using animal models. Current strategies include transplantation of normal photoreceptors and RPE cells [388], intravitreal injections of factors that prolong photoreceptor survival and promote function [182, 389], gene delivery to mutant photoreceptor and RPE cells using viral vectors [105, 228, 233] and liposomes [315]. The RCS rat has been widely used as a model for such strategies, including subretinal transplantation of RPE cells and cell lines [182, 390], treatment with growth factors such as bFGF [182], and gene replacement therapies [233]. The latter has also been successfully tested in another model for RP, the *rpe65*$^{-/-}$ dog [105]. The MERTK protein in the eye is predominately expressed in the RPE. Like *rpe65*, mutations in *MERTK* primarily cause RPE

defects whereas photoreceptor cell are inherited functional and morphological preserved.

Patients with autosomal recessive RP arising from mutations within genes expressed in the RPE may be predetermined to create a group that is a promising target for gene replacement approaches. However, in order to improve both the effectiveness of existing strategies and the development of novel therapies, it is crucial to understand and characterise the histopathological changes in individual patients with RP.

This study presents the first detailed clinical and molecular report of multiple family members affected by RP due to mutation in the *MERTK* gene and describes a novel mutation. Common to other reported surveys, the disorder is likely to be a rare cause of autosomal recessive RP (ARRP). Only one family was identified in a screen of 96 probands suggesting that mutations in *MERTK* count for approximately 1% of all ARRP. One previously unreported missense change, R20T was detected in this study on both alleles in one person of Pakistani origin with ARRP. The fact that this residue is polymorphic in the human population (R20S) and that it is not conserved in other species suggests that it is likely to be a non-disease causing variant although a rare one.

Childhood onset nyctalopia, preserved visual fields, relatively mild RPE changes with a bulls-eye lesion at the macula, absence of pigment migration to the RPE, and recordable autofluorescence within the RPE were all consistent and defining features of the disorder within the family. In addition, the age difference between the affected members enables some insight into the rate of visual decline of the disorder, at least in this particular family, which may prove useful when determining a time scale for preventative intervention. The time span of 10 years proved little in the way of detectable difference in fundus abnormalities, although functional decline was observed.

One clinical finding was a hyperfluorescent area, situated at the central macula, of up to half a disc area in size, in the three affected siblings. It was smaller in older individuals and showed hypofluorescence on fluorescein angiography. One possibility is that this represents debris from non-phagocytosed photoreceptor discs lying between the RPE and neurosensory retina with inherent autofluorescence but which masks choroidal fluorescence during angiography. In support, the debris characteristic of the degeneration in RCS rat retina is also autofluorescent to light of a comparable wavelength (figure 5.11). However, no such debris layer could be detected on OCT examination. This sign may be useful in the clinical identification of *MERTK*-deficient disease when examining families with RP. It should be emphasised that the appearance of this ring is much smaller than that reported by Robson *et al* and others [391] which can occurs in some patients with RP. The homogeneous autofluorescence elsewhere implies that phagocytosis of outer segments is not completely deficient and in this regard would be different from the RCS rat.

Figure 5.11: Fluorescence micrograph. The picture was taken of a 5 week old dystrophic RCS rat. Due to the phagocytotic defect of the RPE cells, a debris layer consisting of broken outer segment and membranous waste material has build up. Photoreceptor outer segments and RPE cells show strong autofluorescence, a characteristic feature of the degenerating retina. INL = inner nuclear layer, OPL = outer plexiform layer, ONL = outer nuclear layer, IS = inner segments, D = debris layer, RPE = retinal pigment epithelium, C = choroid

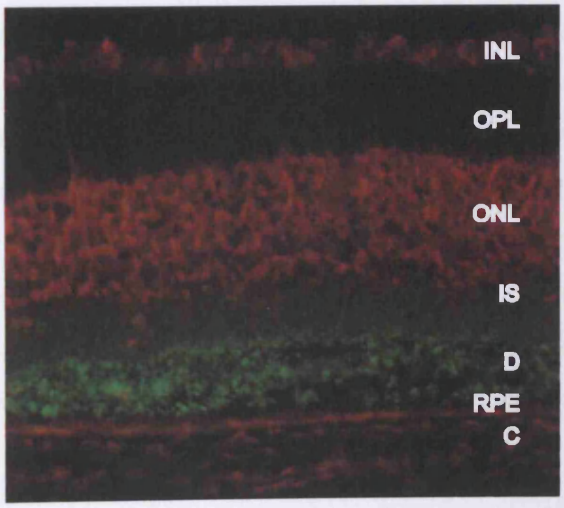

The decline of retinal function as measured by electrophysiology, appears at an early stage in this family with early loss of both macular and scotopic function at the age of 5 years (IV:9) and loss of photopic function soon after. By the age of 16 years all responses were severely attenuated and delayed. This early loss of the ERG, in which scotopic function is predominantly affected, is similar to that seen in the rat and mouse models. The preserved visual acuity and field into the second decade suggests that the visual system develops normally, an important consideration given the prospect of therapeutic intervention. The detailed description of the phenotype exhibited by the human *MERTK* mutation described here might assist the identification of eligible patients and families from amongst the many molecular types of RP.

The disease observed in the three affected members reported here, appear milder than those previously described for a patient of comparable age with a different *MERTK* genotype (R722X/R844C) who had vision reduced to 20/200 at 13 years and restricted visual fields [374]. In contrast the oldest member of the present sibship maintained acuites of 20/20 at the age of 18 years with more extensive visual fields. Interestingly, a common feature is the appearance of a ring of RPE depigmentation in a 'bull's eye' pattern on fundoscopy in all four photographed patients which in our family corresponded to the area of hyper-autofluorescence. The deletion 2214delT and the substitution R722X, result in premature termination signals. Whilst a proportion of the resulting mRNAs is likely to succumb to nonsense-mediated decay (NMD; for reviews see [392, 393]), the remaining mutant mRNAs would be expected to be translated into truncated proteins. Since the premature termination signal caused by the mutation R722X is located further up-stream to the deletion 2214delT, the truncated MERTK protein would lack a larger portion of its intracellular domain. This missing part might include recognition or binding sites for other proteins involved in the phagocytosis signaling pathway that are still present on the 2214delT truncated protein. In addition, the R722X substitution was found together with the missense

substitution R844C as compound heterozygeous. This substitution has been shown to be at a fully conserved position in different species, and has been shown to abolish MERTK tyrosine phosphorylation necessary for phagocytosis [374]. The presence of these two different mutant proteins might be one possible explanation for the difference in severity observed in the two *MERTK* genotypes, R722X/R844C and 2214delT/2214delT. Another explanation might be the influence of other genetic or environmental modifiers on the expression of *MERTK* deficiency.

The clinical characterisation of disease due to *MERTK* is important to allow the interpretation of any future therapies. The specific macular appearance may allow the identification of further patients through ophthalmic screening, and the rate of visual decline might allow preventative intervention.

6

6 Discussion

Inherited retinal degenerations, including RP, lead to a progressive loss of the visual field and in some cases finally to blindness. The last twenty years have seen enormous growth in the understanding of the molecular and histopathological changes that occur during retinal degeneration. The constantly improving knowledge and understanding of RP increases the prospects for developing new and effective strategies to delay photoreceptor cell death and prolong retinal function. With major advances in molecular-biological research, numerous retinal dystrophy genes have been identified. Thus, a fundamental requirement for the development of gene therapy for these type of diseases has been achieved. One recently identified gene is the receptor tyrosine kinase *MERTK* [122]. The resulting autosomal recessive disease in patients with a mutation in the *MERTK* gene is characterised by night blindness at a young age, with progressive loss of peripheral vision until only a small island of central vision remains [69]. The RCS rat provides a good animal model for this type of RP and has been used widely to test different therapeutic strategies, including subretinal transplantation of RPE cells and cell lines [182, 390], treatment with growth factors such as bFGF [182], and gene replacement therapies [233, 394, 395].

AAV-2-based vectors have already been tested in a wide range of tissues. Since AAV-2-mediated gene replacement had already been established as an efficient approach for a restoration of the *rpe65* defect in RPE65$^{-/-}$ dogs [105], we aimed to

evaluate its therapeutical potential in the RCS rat. In this study we demonstrated that subretinal injection of rAAV-2 expressing a functional copy of the *MERTK* gene can significantly slow retinal degeneration in the RCS rat. ERG analysis of treated eyes showed that functional photoreceptors were still present at 9 weeks, when there is virtually no activity in untreated control eyes. Histological analysis of treated eyes revealed a decrease in the amount of debris in the subretinal space, suggesting that RPE function was restored. Moreover, nine weeks after treatment the number of photoreceptors was 2.5 fold higher in treated compared with control eyes. Since AAV-2 transduces RPE and photoreceptor cells and the CMV promoter is ubiquitously active, the *rpe65* promoter was used to restrict transgene expression to the RPE. With both promoters comparable levels of rescue were achieved. This is important in view of future clinical trials, since gene expression should be limited to the cell type that carries the defect in order to avoid possible side effects induced by an additional expression of the transgene in other cell types.

Whilst AAV-based vectors are very effective, they do have some disadvantages. Firstly, they have a relatively small cloning capacity and therefore they cannot be used to deliver transgenes bigger than approximately 5 kb. Secondly, AAV-2 has a delay in onset of transgene expression of about 2 weeks and finally, they can evoke an immune response that renders re-administration difficult. It has been shown that infections by the non-pathogenic AAV-2 virus are common and lead to a pre-existing immunity against AAV-2 [396]. Different studies have suggested that anti-AAV antibodies have a neutralising effect that decreases the efficiency of in *vivo* vector delivery in different organs [397, 398]. However, the development of anti-AAV antibodies is minimal or not existent after dilivery of AAV to the brain or retina [399, 400]. Since other serotypes are less common than AAV-2, pre-existing immunity in humans is rare and pseudotyping would be an option to circumvent this problem. Although this is of minor importance for gene delivery to the eye because of its unique immunological environment, it is a major concern for other disorders. The delay in expression can be avoided by the use of chimeric

vectors. AAV-2 has been pseudotyped with AAV-1 and this chimeric vector has an onset of expression within 3 to 4 days after delivery. A fast onset of expression is particularly desirable in testing therapeutic approaches in models of disease with rapid retinal degeneration as is the case in the RCS rat. In consideration of the different life span and therefore the pace of photoreceptor loss of humans and rats, the delay in onset of AAV-2-mediated expression should not be a limiting factor for effective treatment of RP patients with *MERTK* mutations. Furthermore, AAV-2/1 and AAV-2/4 have been recently shown to specifically transduce RPE cells in different animal models including rats and dogs. Chimeric vectors are promising vehicles for targeted transgene expression, even though the therapeutical value of these vectors still needs to be evaluated [221, 343].

Lentiviral vectors have three outstanding features in regard to their use in human clinical trials: the ability to transduce non-dividing cells in *vivo*, the ability to efficiently deliver large genes (~8 kb) and the abilitiy to mediate long-term, high level transgene expression. In order to evaluate the efficacy of lentivirus-mediated gene replacement therapy in the RCS rat, we produced recombinant VSV-G pseudotyped HIV-1-based lentiviruses containing a *MERTK* cDNA driven by the ubiquiteous SFFV promoter. After subretinal delivery of the therapeutic construct animals were examined at various time points over a period of 7 months by light and electron microscopy, and electroretinography. A correction of the phagocytic defect, slowing of photoreceptor cell loss and preservation of retinal function for up to 7 months was observed. Comparing the different rates of degeneration of humans and rats a similar approach in patients might delay degeneration for years rather than months.

Lentiviral vectors based on HIV-1 have been used widely to develop efficient gene therapy protocols for a variety of disorders. A major concern of employing HIV-1-based vectors in clinical trials however is the possibility of generating recombination-competent viruses during vector production due to recombination events between vector plasmids or in *vivo* due to mobilisation of proviral DNA by

infectious retroviruses. Replication-competent viruses would be able to spread the therapeutic vector to non-target tissues. To address this concern, a class of vectors was designed to undergo self-inactivation. Self-inactivating vectors (SIN), which were also used in the experiments presented in this thesis [305, 349], will delete some of the *cis*-acting elements needed for replication upon delivery (see section 4.1). Therefore, even in the presence of a replication-competent virus, these vectors cannot be transferred to other target cells efficiently. The generation of a replication-competent virus involves either recombination between the defective helper plasmid and the vector encoding the gene of interest, or they can be produced through recombination between an endogenous retrovirus (present in the host genome) and the helper construct or the vector. SIN vectors efficiently infect and integrate into the target cell but generation of proviral transcripts is inhibited. Hence, they are less likely to be mobilised by other human retroviruses. However, the long-term persistence of viral DNA could result in the generation of recombination-competent viruses at any time after in *vivo* administration. Therefore, patients should be monitored for vector mobilisation and sensitive assays including PCR-based protocols to detect recombination competent lentiviruses are being developed.

Lentiviral vectors have the potential to infect both dividing and non-dividing cells and they have the ability of genome integration thereby ensuring long-term expression of the gene of interest. However, chromosomal integration occurs randomly and as a result the location of the inserted gene varies enormously (reviewed in [401]). It has been shown that random integration carries the risk of insertional mutagenesis [217, 358]. Studies of integration preferences of different viral systems provide new insight in the integration process. It has been demonstrated that differences exist between different types of retroviruses and that both vector and host factors are important for integration. Results suggest that integration preferences might be cell-type specific and different in dividing and non-dividing cells [402-404]. These problems can be circumvented by the use of non-integrating lentiviruses. As part of this project, the potential of non-

integrating HIV-1-based vectors for retinal degeneration has been investigated. We have shown that these integration-deficient vectors are effective templates for gene expression in *vivo* and that expression levels and the duration of transgene expression are similar to those achieved with integration proficient vectors. These results suggest that integration-deficient lentiviral vectors are attractive tools for human gene therapy approaches with increased biosafety features.

HIV-1 vectors have proven to mediate long-term and efficient transgene expression in *vivo*. However, HIV-1 is a lethal pathogenic virus that causes AIDS raising some safety concerns for the use of HIV-1-based vectors in clinical trials. Due to these biosafety issues, gene therapy vectors based on other lentiviruses have been developed. SIV [300], BIV [301] and FIV [295, 360, 361] based vectors have already been tested in the eye and show sustained expression in different ocular tissues after intraocular delivery. We aimed to assess the potential of another, non-primate lentivirus vector, namely an EIAV vector [345, 346]. The expression patterns and the duration of expression after different routes of intraocular delivery were evaluated and their utility as gene transfer vehicles for ocular gene therapy determined. Subretinal vector delivery resulted in efficient and stable transduction of RPE cells and variable transduction of photoreceptors up to 16 months post injection. Retinal trauma facilitated the local transduction of neurosensory retinal cells. Intracameral administration of VSV-G but not rabies-G pseudotyped vectors produced stable *gfp* expression in corneal endothelial cells and trabecular meshwork. These results suggest the potential of EIAV-based vectors as vehicles for delivering therapeutic genes in the management of inherited and acquired retinal and anterior segment disorders. Vectors based on non-primate lentiviruses have the advantage that they are only distantly related to HIV-1. This minimises the risk of recombination or other interactions between the vector and human endogenous retroviruses. Non-primate lentiviruses have no known human pathogenicity. However, they are also less well understood than HIV-1. Possible pathogenic features would probably only be revealed by clinical study. Other factors that should be considered are toxicities of viral gene products

and host immune responses to various lentiviral vectors, in particular in view of clinical applications.

The results presented in this study demonstrate the potential of gene therapy approaches for the treatment of retinal degenerations caused by defects specific to the RPE and support the use of lentiviral vectors and the development of AAV-mediated gene therapy for the treatment of such disorders. Pre-clinical trials of gene therapy for LCA due to mutations in the RPE-specific *rpe65* gene have been particularly successful [105, 290, 291] and highlight the utility of AAV-mediated gene therapy to target RPE-specific defects. RPE65 deficiency is characterised by an unusual feature, which is the dissociation of retinal function and structure. Despite the visual impairment, RPE65 deficient animals retain photoreceptor structure, which is normally lost in other types of retinal degeneration. It has been suggested that the relatively preserved retinal morphology is the main reason for the success of pre-clinical studies in RPE65 deficient animals and that the success rate is dependent on the level of preservation [405]. Clinical examinations of RPE65 patients show regional preservation of retinal structure similar to that observed in animal models. Therefore gene therapy might prove to be an adequate strategy to restore rod and cone function in such patients. In contrast, *MERTK* deficiency results in photoreceptor cell loss with disease progression. Gene therapy might be more efficient for RPE65 deficiencies rather than *MERTK* deficiencies as indicated by pre-clinical animal studies. However, the results presented in this thesis suggest that patients with *MERTK* mutation might still benefit. The necessity of structural preservation for efficient rescue levels also highlights the importance of treating patients at early stages of disease progress.

Theoretically, gene therapy targeted at the causal mutations represent the most promising approach to treat inherited retinal degeneration, especially for diseases in which photoreceptors are primarily healthy and their loss occurs as a secondary consequence. The assessment of risk to benefit ratio is the central

issue for human gene therapy approaches. Although over the last few years there have been major advances in lentiviral vector production with regard to purification and biosafety [406], the use of AAV vectors raises fewer concerns about safety. Recombinant AAV efficacy has been demonstrated in numerous gene therapy pre-clinical studies. As this vector is increasingly applied to human clinical trials, it is a priority to evaluate the risks of its use for workers involved in research and clinical trials as well as for the patients and their descendants. A critical aspect of in *vivo* gene delivery is the possible transmission of exogenous DNA to the germ line. Different studies that aimed to explore the risk of germ line transmission of rAAV have shown that there is a dose-dependent increase in the likelihood that vector sequences can be detected in gonadal DNA using a sensitive PCR technique in mice and rats (see [407] for a review). However, no vector sequences could be dedected in DNA extracted from semen saples of rabbits and dogs after intramuscular or hepatic atery delivery [408]. In clinical studies human subjects that received intramuscular injected of AAV vectors have shown no evidence of vector sequences in semen. In addition, direct exposure of mouse spermatozoa to AAV-2 vectors has shown no evidence of germ line transduction [409]. These results suggest that there is no significant risk of germ line transmission after different routes of delivery. Viral vectors that can integrate into the host genome have a potential higher risk of entering the germ line. Especially when using HIV-1-based vectors precautions must be taken since HIV-1 interacts with biological function of human endogenous retroviruses. Biodistribution studies of different rAAV serotypes, which were delivered intraocularly in rats and dogs, failed to detect vector sequences in liver or gonad samples. However, vector sequences were detected along the visual pathway after subretinal and intravitreal delivery of AAV-2. These findings raise safety concerns regarding intraocular delivery of AAV-2-based vectors and highlight the importance of tissue-specific transgene expression [410].

Whilst the results presented in this thesis of the rescue of the RCS rat are very encouraging, the potential for therapy in humans depends upon the identification

of patients. We therefore screened a panel of DNA from patients with autosomal recessive and sporadic forms of RP for mutations in the *MERTK* gene. A novel frame-shifting deletion and a number of polymorphisms within the gene were identified. The deletion allele was detected on both chromosomes of four affected members of a family with autosomal recessive RP. Patients with *MERTK* mutations suffered from early loss of scotopic and macular function on electrophysiology with later loss of photopic function. Acuities and fields were preserved into the second decade but only perception of light vision was present in the fourth decade. A 'bull's eye' appearance on funduscopy and an inherent hyper-autofluorescent lesion at the central macula were consistent clinical findings. These are distinctive clinical signs that may improve the chances of identifying further patients and families in the future and distinguishing this from the many other cause of human retinal degeneration. The study extends the phenotypic characteristics of retinal dystrophy associated with human *MERTK* mutation. However, the phenotype in these patients appears milder than that previously described for a patient of comparable age with a different *MERTK* genotype (R722X/R844C) suggesting variability in the degree of disease severity [374]. In order to develop an efficient therapeutic protocol, it is necessary to identify more patients with *MERTK* mutation and to gain a better knowledge of their clinical features.

The results presented in this study added weight to the prospect of applying gene therapy to the treatment of retinal degeneration. However, much research has to be done before gene therapy is routinely used in clinics. One of the main limiting factors for a fast progression into clinical trials is that any new therapeutical strategy must be shown to be efficient in an eye similar to that of humans. For several reasons, including that they are cheap and easy to keep, rodents are most commonly used. Nevertheless, fundamental differences between rodents and humans limit the rodent from being the best model for many human diseases. For instance, the rodent eye lacks specific characteristics of the human eye such as the macula (see section 1.2.6). The advantage of large animal models has also

become evident during this study. The RCS rat is a valuable animal model for retinal degeneration due to RPE-specific defects. The null mutation in the *MERTK* gene makes it an attractive model for early experiments [69]. Different from the RCS rat, the mutations identified in human patients are all located in the tyrosine kinase domain within the last third of the ORF [122, 374]. The resulting truncated protein is unlikely to lead to a complete loss of function as is the case in the RCS rat. The bulls-eye appearance on funduscopy and the hyperautofluorescent lesion at the central macula observed in patients with *MERTK* mutations are important clinical characteristics. Functional assessments and visual testing in these patients also showed an involvement of cone photoreceptors in the disease course. These findings differ from clinical findings in the RCS rat since rodents have no macula and a different cone distribution. Furthermore, the difference between the rate of degeneration between rat and human is significant. The differences may also be caused by genetic redundancy or altered biochemical pathways in rodents.

The availability of natural occurring large animal models is limited and their production difficult. Non-human primates closely parallel humans with regard to genetic, anatomic, and cognitive characteristics. Hence they are considered to be one of the best models for understanding human physiology and diseases. Transgenic technology in biomedicine has opened a new era for animal modeling, which accelerates model development and results in better understanding of diseases as well as development of therapies for patients. Over the last few years, transgenic animals with genetic alterations that lead to human genetic diseases have been created. This has a major impact on the understanding of disease development and the development of cures. In particular non-human primates mimic patient conditions. The major difficulty in producing transgenic non-human primates so far was the low efficiency of the gene transfer protocols. Apart from other designs, the development of replication defective retroviral and lentiviral vector systems [348, 411-413] have led animal biotechnology to broad applications and relatively high rate of efficiency. Recently the first transgenic

non-human primate animal has been created by using a retroviral vector [414]. These models will provide a more accurate representation of the human condition. However, the use of large animal models will increase the cost and the duration of experiments. Whilst large animal models for *MERTK* deficiency might help to better understand the pathways underlying the disease progress, they are not indispensable for future clinical gene therapy trials. Experience gained from pre-clinical studies for *rpe65* defects involving dogs and non-human primates have shown the potential of gene therapy for RPE-specific defects [105, 343, 415]. Taken together all results obtained from gene replacement studies on RPE specific defects, a benefit from this type of therapy for patients with *MERTK* mutations is suggested.

Reference List

1. Bessant, D.A., R.R. Ali, and S.S. Bhattacharya, *Molecular genetics and prospects for therapy of the inherited retinal dystrophies.* Curr Opin Genet Dev, 2001. **11**(3): p. 307-16.
2. Graw, J., *Genetic aspects of embryonic eye development in vertebrates.* Dev Genet, 1996. **18**(3): p. 181-97.
3. Fuhrmann, S., E.M. Levine, and T.A. Reh, *Extraocular mesenchyme patterns the optic vesicle during early eye development in the embryonic chick.* Development, 2000. **127**(21): p. 4599-609.
4. Kishi, H., H.K. Mishima, and U. Yamashita, *Growth regulation of retinal pigment epithelial (RPE) cells in vitro.* Curr Eye Res, 1994. **13**(9): p. 661-8.
5. Plaza, S., et al., *Identification and characterization of a neuroretina-specific enhancer element in the quail Pax-6 (Pax-QNR) gene.* Mol Cell Biol, 1995. **15**(2): p. 892-903.
6. Lee, C.S., N.R. May, and C.M. Fan, *Transdifferentiation of the ventral retinal pigmented epithelium to neural retina in the growth arrest specific gene 1 mutant.* Dev Biol, 2001. **236**(1): p. 17-29.
7. Levine, E.M., et al., *Sonic hedgehog promotes rod photoreceptor differentiation in mammalian retinal cells in vitro.* J Neurosci, 1997. **17**(16): p. 6277-88.
8. Pittack, C., G.B. Grunwald, and T.A. Reh, *Fibroblast growth factors are necessary for neural retina but not pigmented epithelium differentiation in chick embryos.* Development, 1997. **124**(4): p. 805-16.
9. Nguyen, M. and H. Arnheiter, *Signaling and transcriptional regulation in early mammalian eye development: a link between FGF and MITF.* Development, 2000. **127**(16): p. 3581-91.
10. Zhao, S., et al., *Patterning the optic neuroepithelium by FGF signaling and Ras activation.* Development, 2001. **128**(24): p. 5051-60.
11. Young, R.W., *Cell differentiation in the retina of the mouse.* Anat Rec, 1985. **212**(2): p. 199-205.
12. Kubota, R., et al., *Identification of ciliary epithelial-specific genes using subtractive libraries and cDNA arrays in the avian eye.* Dev Dyn, 2004. **229**(3): p. 529-40.
13. Wetts, R. and S.E. Fraser, *Multipotent precursors can give rise to all major cell types of the frog retina.* Science, 1988. **239**(4844): p. 1142-5.
14. Perron, M., et al., *The genetic sequence of retinal development in the ciliary margin of the Xenopus eye.* Dev Biol, 1998. **199**(2): p. 185-200.
15. Fischer, A.J. and T.A. Reh, *Identification of a proliferating marginal zone of retinal progenitors in postnatal chickens.* Dev Biol, 2000. **220**(2): p. 197-210.
16. Fischer, A.J., et al., *Insulin and fibroblast growth factor 2 activate a neurogenic program in Muller glia of the chicken retina.* J Neurosci, 2002. **22**(21): p. 9387-98.
17. Tropepe, V., et al., *Retinal stem cells in the adult mammalian eye.* Science, 2000. **287**(5460): p. 2032-6.
18. Moshiri, A. and T.A. Reh, *Persistent progenitors at the retinal margin of ptc+/- mice.* J Neurosci, 2004. **24**(1): p. 229-37.
19. Ahnelt, P.K., *The photoreceptor mosaic.* Eye, 1998. **12 (Pt 3b)**: p. 531-40.
20. Ahnelt, P.K. and H. Kolb, *The mammalian photoreceptor mosaic-adaptive design.* Prog Retin Eye Res, 2000. **19**(6): p. 711-77.
21. Masland, R.H., *The fundamental plan of the retina.* Nat Neurosci, 2001. **4**(9): p. 877-86.
22. Gouras, P., *Color Vision.* Prog. Ret. Res., 1984. **3**: p. 227-261.
23. Cooper, A. and C.A. Converse, *Energetics of primary processes in visula escitation: photocalorimetry of rhodopsin in rod outer segment membranes.* Biochemistry, 1976. **15**(14): p. 2970-8.
24. Baylor, D., *How photons start vision.* Proc Natl Acad Sci U S A, 1996. **93**(2): p. 560-5.

25. Grunwald, G.B., et al., *Detection of alpha-transducin in retinal rods but not cones.* Science, 1986. **231**(4740): p. 856-9.
26. Kawamura, S., *Light-sensitivity modulating protein in frog rods.* Photochem Photobiol, 1992. **56**(6): p. 1173-80.
27. Yau, K.W., *Cyclic nucleotide-gated channels: an expanding new family of ion channels.* Proc Natl Acad Sci U S A, 1994. **91**(9): p. 3481-3.
28. Fain, G.L., et al., *Adaptation in vertebrate photoreceptors.* Physiol Rev, 2001. **81**(1): p. 117-151.
29. Fain, G.L., H.R. Matthews, and M.C. Cornwall, *Dark adaptation in vertebrate photoreceptors.* Trends Neurosci, 1996. **19**(11): p. 502-7.
30. Moiseyev, G., et al., *RPE65 is the isomerohydrolase in the retinoid visual cycle.* Proc Natl Acad Sci U S A, 2005. **102**(35): p. 12413-8.
31. Redmond, T.M., et al., *Mutation of key residues of RPE65 abolishes its enzymatic role as isomerohydrolase in the visual cycle.* Proc Natl Acad Sci U S A, 2005.
32. Sun, H., R.S. Molday, and J. Nathans, *Retinal stimulates ATP hydrolysis by purified and reconstituted ABCR, the photoreceptor-specific ATP-binding cassette transporter responsible for Stargardt disease.* J Biol Chem, 1999. **274**(12): p. 8269-81.
33. Lin, Z.S., S.L. Fong, and C.D. Bridges, *Retinoids bound to interstitial retinol-binding protein during light and dark-adaptation.* Vision Res, 1989. **29**(12): p. 1699-709.
34. Stecher, H. and K. Palczewski, *Multienzyme analysis of visual cycle.* Methods Enzymol, 2000. **316**: p. 330-44.
35. Kim, T.S., et al., *Delayed dark adaptation in 11-cis-retinol dehydrogenase-deficient mice: a role of RDH11 in visual processes in vivo.* J Biol Chem, 2005. **280**(10): p. 8694-704.
36. Arshavsky, V., *Like night and day: rods and cones have different pigment regeneration pathways.* Neuron, 2002. **36**(1): p. 1-3.
37. Mata, N.L., et al., *Chicken retinas contain a retinoid isomerase activity that catalyzes the direct conversion of all-trans-retinol to 11-cis-retinol.* Biochemistry, 2005. **44**(35): p. 11715-21.
38. Daniele, S., et al., *Analysis of the rhodopsin and peripherin/RDS gene in two families with pattern dystrophy of the retinal pigment epithelium.* Eur J Ophthalmol, 1996. **6**(2): p. 197-200.
39. Strauss, O., *The retinal pigment epithelium in visual function.* Physiol Rev, 2005. **85**(3): p. 845-81.
40. Bok, D., *The retinal pigment epithelium: a versatile partner in vision.* J Cell Sci Suppl, 1993. **17**: p. 189-95.
41. Gonzalez-Fernandez, F., *Interphotoreceptor retinoid-binding protein--an old gene for new eyes.* Vision Res, 2003. **43**(28): p. 3021-36.
42. Alexander, J.P., et al., *Expression of matrix metalloproteinases and inhibitor by human retinal pigment epithelium.* Invest Ophthalmol Vis Sci, 1990. **31**(12): p. 2520-8.
43. Bost, L.M., A.E. Aotaki-Keen, and L.M. Hjelmeland, *Coexpression of FGF-5 and bFGF by the retinal pigment epithelium in vitro.* Exp Eye Res, 1992. **55**(5): p. 727-34.
44. Cao, W., et al., *Mechanical injury increases bFGF and CNTF mRNA expression in the mouse retina.* Exp Eye Res, 1997. **65**(2): p. 241-8.
45. Walsh, N., K. Valter, and J. Stone, *Cellular and subcellular patterns of expression of bFGF and CNTF in the normal and light stressed adult rat retina.* Exp Eye Res, 2001. **72**(5): p. 495-501.
46. Dawson, D.W., et al., *Pigment epithelium-derived factor: a potent inhibitor of angiogenesis.* Science, 1999. **285**(5425): p. 245-8.
47. Wenkel, H. and J.W. Streilein, *Evidence that retinal pigment epithelium functions as an immune-privileged tissue.* Invest Ophthalmol Vis Sci, 2000. **41**(11): p. 3467-73.
48. Rizzolo, L.J., *Polarity and the development of the outer blood-retinal barrier.* Histol Histopathol, 1997. **12**(4): p. 1057-67.
49. Alm, A. and A. Bill, *Ocular and optic nerve blood flow at normal and increased intraocular pressures in monkeys (Macaca irus): a study with radioactively labelled microspheres including flow determinations in brain and some other tissues.* Exp Eye Res, 1973. **15**(1): p. 15-29.

50. Miceli, M.V., M.R. Liles, and D.A. Newsome, *Evaluation of oxidative processes in human pigment epithelial cells associated with retinal outer segment phagocytosis.* Exp Cell Res, 1994. **214**(1): p. 242-9.
51. Beatty, S., et al., *Macular pigment and age related macular degeneration.* Br J Ophthalmol, 1999. **83**(7): p. 867-77.
52. Handelman, G.J., et al., *Carotenoids in the human macula and whole retina.* Invest Ophthalmol Vis Sci, 1988. **29**(6): p. 850-5.
53. Ben-Shabat, S., et al., *Biosynthetic studies of A2E, a major fluorophore of retinal pigment epithelial lipofuscin.* J Biol Chem, 2002. **277**(9): p. 7183-90.
54. Ban, Y. and L.J. Rizzolo, *Differential regulation of tight junction permeability during development of the retinal pigment epithelium.* Am J Physiol Cell Physiol, 2000. **279**(3): p. C744-50.
55. Adler, A.J. and R.E. Southwick, *Distribution of glucose and lactate in the interphotoreceptor matrix.* Ophthalmic Res, 1992. **24**(4): p. 243-52.
56. Nguyen-Legros, J. and D. Hicks, *Renewal of photoreceptor outer segments and their phagocytosis by the retinal pigment epithelium.* Int Rev Cytol, 2000. **196**: p. 245-313.
57. Weber, B.H., et al., *Mutations in the tissue inhibitor of metalloproteinases-3 (TIMP3) in patients with Sorsby's fundus dystrophy.* Nat Genet, 1994. **8**(4): p. 352-6.
58. Nagelhus, E.A., et al., *Immunogold evidence suggests that coupling of K+ siphoning and water transport in rat retinal Muller cells is mediated by a coenrichment of Kir4.1 and AQP4 in specific membrane domains.* Glia, 1999. **26**(1): p. 47-54.
59. Gundersen, D., J. Orlowski, and E. Rodriguez-Boulan, *Apical polarity of Na,K-ATPase in retinal pigment epithelium is linked to a reversal of the ankyrin-fodrin submembrane cytoskeleton.* J Cell Biol, 1991. **112**(5): p. 863-72.
60. Hamann, S., *Molecular mechanisms of water transport in the eye.* Int Rev Cytol, 2002. **215**: p. 395-431.
61. Lin, H. and S.S. Miller, *pHi-dependent Cl-HCO3 exchange at the basolateral membrane of frog retinal pigment epithelium.* Am J Physiol, 1994. **266**(4 Pt 1): p. C935-45.
62. Oakley, B., 2nd, *Potassium and the photoreceptor-dependent pigment epithelial hyperpolarization.* J Gen Physiol, 1977. **70**(4): p. 405-25.
63. la Cour, M., *The retinal pigment epithelium controls the potassium activity in the subretinal space.* Acta Ophthalmol Suppl, 1985. **173**: p. 9-10.
64. Bialek, S., D.P. Joseph, and S.S. Miller, *The delayed basolateral membrane hyperpolarization of the bovine retinal pigment epithelium: mechanism of generation.* J Physiol, 1995. **484 (Pt 1)**: p. 53-67.
65. la Cour, M., *Kinetic properties and Na+ dependence of rheogenic Na(+)-HCO3- co-transport in frog retinal pigment epithelium.* J Physiol, 1991. **439**: p. 59-72.
66. Ban, Y. and L.J. Rizzolo, *Regulation of glucose transporters during development of the retinal pigment epithelium.* Brain Res Dev Brain Res, 2000. **121**(1): p. 89-95.
67. Baehr, W., et al., *The retinoid cycle and retina disease.* Vision Res, 2003. **43**(28): p. 2957-8.
68. Young, R.W. and D. Bok, *Participation of the retinal pigment epithelium in the rod outer segment renewal process.* J Cell Biol, 1969. **42**(2): p. 392-403.
69. D'Cruz, P.M., et al., *Mutation of the receptor tyrosine kinase gene Mertk in the retinal dystrophic RCS rat.* Hum Mol Genet, 2000. **9**(4): p. 645-51.
70. Anderson, D.H., S.K. Fisher, and R.H. Steinberg, *Mammalian cones: disc shedding, phagocytosis, and renewal.* Invest Ophthalmol Vis Sci, 1978. **17**(2): p. 117-33.
71. LaVail, M.M., *Rod outer segment disk shedding in rat retina: relationship to cyclic lighting.* Science, 1976. **194**(4269): p. 1071-4.
72. LaVail, M.M., *Rod outer segment disc shedding in relation to cyclic lighting.* Exp Eye Res, 1976. **23**(2): p. 277-80.
73. Steinberg, R.H., I. Wood, and M.J. Hogan, *Pigment epithelial ensheathment and phagocytosis of extrafoveal cones in human retina.* Philos Trans R Soc Lond B Biol Sci, 1977. **277**(958): p. 459-74.

74. Besharse, J.C., D.A. Dunis, and B. Burnside, *Effects of cyclic adenosine 3',5'-monophosphate on photoreceptor disc shedding and retinomotor movement. Inhibition of rod shedding and stimulation of cone elongation.* J Gen Physiol, 1982. **79**(5): p. 775-90.
75. Albert, A.D., J.E. Young, and Z. Paw, *Phospholipid fatty acyl spatial distribution in bovine rod outer segment disk membranes.* Biochim Biophys Acta, 1998. **1368**(1): p. 52-60.
76. Feng, W., et al., *Mertk triggers uptake of photoreceptor outer segments during phagocytosis by cultured retinal pigment epithelial cells.* J Biol Chem, 2002. **277**(19): p. 17016-22.
77. Boyle, D., et al., *A mannose receptor is involved in retinal phagocytosis.* Invest Ophthalmol Vis Sci, 1991. **32**(5): p. 1464-70.
78. Finnemann, S.C., et al., *Phagocytosis of rod outer segments by retinal pigment epithelial cells requires alpha(v)beta5 integrin for binding but not for internalization.* Proc Natl Acad Sci U S A, 1997. **94**(24): p. 12932-7.
79. Miceli, M.V., D.A. Newsome, and D.J. Tate, Jr., *Vitronectin is responsible for serum-stimulated uptake of rod outer segments by cultured retinal pigment epithelial cells.* Invest Ophthalmol Vis Sci, 1997. **38**(8): p. 1588-97.
80. Lin, H. and D.O. Clegg, *Integrin alphavbeta5 participates in the binding of photoreceptor rod outer segments during phagocytosis by cultured human retinal pigment epithelium.* Invest Ophthalmol Vis Sci, 1998. **39**(9): p. 1703-12.
81. Ryeom, S.W., J.R. Sparrow, and R.L. Silverstein, *CD36 participates in the phagocytosis of rod outer segments by retinal pigment epithelium.* J Cell Sci, 1996. **109 (Pt 2)**: p. 387-95.
82. Duncan, J.L., et al., *An RCS-like retinal dystrophy phenotype in mer knockout mice.* Invest Ophthalmol Vis Sci, 2003. **44**(2): p. 826-38.
83. Finnemann, S.C., *Focal adhesion kinase signaling promotes phagocytosis of integrin-bound photoreceptors.* Embo J, 2003. **22**(16): p. 4143-54.
84. Hall, M.O., et al., *Outer segment phagocytosis by cultured retinal pigment epithelial cells requires Gas6.* Exp Eye Res, 2001. **73**(4): p. 509-20.
85. Patel, J.C., A. Hall, and E. Caron, *Vav regulates activation of Rac but not Cdc42 during FcgammaR-mediated phagocytosis.* Mol Biol Cell, 2002. **13**(4): p. 1215-26.
86. Heth, C.A. and P.A. Marescalchi, *Inositol triphosphate generation in cultured rat retinal pigment epithelium.* Invest Ophthalmol Vis Sci, 1994. **35**(2): p. 409-16.
87. Hall, M.O., T.A. Abrams, and T.W. Mittag, *The phagocytosis of rod outer segments is inhibited by drugs linked to cyclic adenosine monophosphate production.* Invest Ophthalmol Vis Sci, 1993. **34**(8): p. 2392-401.
88. Finnemann, S.C. and R.L. Silverstein, *Differential roles of CD36 and alphavbeta5 integrin in photoreceptor phagocytosis by the retinal pigment epithelium.* J Exp Med, 2001. **194**(9): p. 1289-98.
89. Nash, M.S., J.P. Wood, and N.N. Osborne, *Protein kinase C activation by serotonin potentiates agonist-induced stimulation of cAMP production in cultured rat retinal pigment epithelial cells.* Exp Eye Res, 1997. **64**(2): p. 249-55.
90. Cremers, F.P., J.A. van den Hurk, and A.I. den Hollander, *Molecular genetics of Leber congenital amaurosis.* Hum Mol Genet, 2002. **11**(10): p. 1169-76.
91. Molday, R.S., *Photoreceptor membrane proteins, phototransduction, and retinal degenerative diseases. The Friedenwald Lecture.* Invest Ophthalmol Vis Sci, 1998. **39**(13): p. 2491-513.
92. Allikmets, R., *Leber congenital amaurosis: a genetic paradigm.* Ophthalmic Genet, 2004. **25**(2): p. 67-79.
93. Inglehearn, C.F., *Molecular genetics of human retinal dystrophies.* Eye, 1998. **12 (Pt 3b)**: p. 571-9.
94. Kalloniatis, M. and E.L. Fletcher, *Retinitis pigmentosa: understanding the clinical presentation, mechanisms and treatment options.* Clin Exp Optom, 2004. **87**(2): p. 65-80.
95. Michaelides, M., D.M. Hunt, and A.T. Moore, *The genetics of inherited macular dystrophies.* J Med Genet, 2003. **40**(9): p. 641-50.
96. Travis, G.H., *Mechanisms of cell death in the inherited retinal degenerations.* Am J Hum Genet, 1998. **62**(3): p. 503-8.

97. Galvin, J.A., et al., *Clinical phenotypes in carriers of Leber congenital amaurosis mutations.* Ophthalmology, 2005. **112**(2): p. 349-56.
98. Perrault, I., et al., *Retinal dehydrogenase 12 (RDH12) mutations in leber congenital amaurosis.* Am J Hum Genet, 2004. **75**(4): p. 639-46.
99. Lewis, C.A., et al., *Tubby-like protein 1 homozygous splice-site mutation causes early-onset severe retinal degeneration.* Invest Ophthalmol Vis Sci, 1999. **40**(9): p. 2106-14.
100. Gu, S.M., et al., *Mutations in RPE65 cause autosomal recessive childhood-onset severe retinal dystrophy.* Nat Genet, 1997. **17**(2): p. 194-7.
101. Nicoletti, A., et al., *Molecular characterization of the human gene encoding an abundant 61 kDa protein specific to the retinal pigment epithelium.* Hum Mol Genet, 1995. **4**(4): p. 641-9.
102. Xue, L., et al., *A palmitoylation switch mechanism in the regulation of the visual cycle.* Cell, 2004. **117**(6): p. 761-71.
103. Hamel, C.P., et al., *Molecular cloning and expression of RPE65, a novel retinal pigment epithelium-specific microsomal protein that is post-transcriptionally regulated in vitro.* J Biol Chem, 1993. **268**(21): p. 15751-7.
104. Aguirre, G.D., et al., *Congenital stationary night blindness in the dog: common mutation in the RPE65 gene indicates founder effect.* Mol Vis, 1998. **4**: p. 23.
105. Acland, G.M., et al., *Gene therapy restores vision in a canine model of childhood blindness.* Nat Genet, 2001. **28**(1): p. 92-5.
106. Akey, D.T., et al., *The inherited blindness associated protein AIPL1 interacts with the cell cycle regulator protein NUB1.* Hum Mol Genet, 2002. **11**(22): p. 2723-33.
107. Shyjan, A.W., et al., *Molecular cloning of a retina-specific membrane guanylyl cyclase.* Neuron, 1992. **9**(4): p. 727-37.
108. Furukawa, T., E.M. Morrow, and C.L. Cepko, *Crx, a novel otx-like homeobox gene, shows photoreceptor-specific expression and regulates photoreceptor differentiation.* Cell, 1997. **91**(4): p. 531-41.
109. Allikmets, R., *A photoreceptor cell-specific ATP-binding transporter gene (ABCR) is mutated in recessive Stargardt macular dystrophy.* Nat Genet, 1997. **17**(1): p. 122.
110. Simon, A., et al., *The retinal pigment epithelial-specific 11-cis retinol dehydrogenase belongs to the family of short chain alcohol dehydrogenases.* J Biol Chem, 1995. **270**(3): p. 1107-12.
111. Wada, Y., et al., *A novel Gly35Ser mutation in the RDH5 gene in a Japanese family with fundus albipunctatus associated with cone dystrophy.* Arch Ophthalmol, 2001. **119**(7): p. 1059-63.
112. Yamamoto, H., et al., *Mutations in the gene encoding 11-cis retinol dehydrogenase cause delayed dark adaptation and fundus albipunctatus.* Nat Genet, 1999. **22**(2): p. 188-91.
113. Hims, M.M., S.P. Diager, and C.F. Inglehearn, *Retinitis pigmentosa: genes, proteins and prospects.* Dev Ophthalmol, 2003. **37**: p. 109-25.
114. Dryja, T.P., *Doyne Lecture. Rhodopsin and autosomal dominant retinitis pigmentosa.* Eye, 1992. **6 (Pt 1)**: p. 1-10.
115. Dryja, T.P., et al., *A point mutation of the rhodopsin gene in one form of retinitis pigmentosa.* Nature, 1990. **343**(6256): p. 364-6.
116. Phelan, J.K. and D. Bok, *A brief review of retinitis pigmentosa and the identified retinitis pigmentosa genes.* Mol Vis, 2000. **6**: p. 116-24.
117. Milam, A.H., Z.Y. Li, and R.N. Fariss, *Histopathology of the human retina in retinitis pigmentosa.* Prog Retin Eye Res, 1998. **17**(2): p. 175-205.
118. Berson, E.L., *Retinitis pigmentosa. The Friedenwald Lecture.* Invest Ophthalmol Vis Sci, 1993. **34**(5): p. 1659-76.
119. Marlhens, F., et al., *Mutations in RPE65 cause Leber's congenital amaurosis.* Nat Genet, 1997. **17**(2): p. 139-41.
120. Ruiz, A., et al., *Molecular and biochemical characterization of lecithin retinol acyltransferase.* J Biol Chem, 1999. **274**(6): p. 3834-41.
121. Thompson, D.A., et al., *Mutations in the gene encoding lecithin retinol acyltransferase are associated with early-onset severe retinal dystrophy.* Nat Genet, 2001. **28**(2): p. 123-4.

122. Gal, A., et al., *Mutations in MERTK, the human orthologue of the RCS rat retinal dystrophy gene, cause retinitis pigmentosa.* Nat Genet, 2000. **26**(3): p. 270-1.
123. Jiang, M., S. Pandey, and H.K. Fong, *An opsin homologue in the retina and pigment epithelium.* Invest Ophthalmol Vis Sci, 1993. **34**(13): p. 3669-78.
124. Morimura, H., E.L. Berson, and T.P. Dryja, *Recessive mutations in the RLBP1 gene encoding cellular retinaldehyde-binding protein in a form of retinitis punctata albescens.* Invest Ophthalmol Vis Sci, 1999. **40**(5): p. 1000-4.
125. den Hollander, A.I., et al., *Mutations in a human homologue of Drosophila crumbs cause retinitis pigmentosa (RP12).* Nat Genet, 1999. **23**(2): p. 217-21.
126. Musarella, M.A., *Molecular genetics of macular degeneration.* Doc Ophthalmol, 2001. **102**(3): p. 165-77.
127. Klein, R.J., et al., *Complement factor H polymorphism in age-related macular degeneration.* Science, 2005. **308**(5720): p. 385-9.
128. Hageman, G.S., et al., *A common haplotype in the complement regulatory gene factor H (HF1/CFH) predisposes individuals to age-related macular degeneration.* Proc Natl Acad Sci U S A, 2005. **102**(20): p. 7227-32.
129. Wilde, C.G., et al., *Cloning and characterization of human tissue inhibitor of metalloproteinases-3.* DNA Cell Biol, 1994. **13**(7): p. 711-8.
130. Langton, K.P., et al., *A novel tissue inhibitor of metalloproteinases-3 mutation reveals a common molecular phenotype in Sorsby's fundus dystrophy.* J Biol Chem, 2000. **275**(35): p. 27027-31.
131. Koenekoop, R.K., *The gene for Stargardt disease, ABCA4, is a major retinal gene: a mini-review.* Ophthalmic Genet, 2003. **24**(2): p. 75-80.
132. Sun, H. and J. Nathans, *Stargardt's ABCR is localized to the disc membrane of retinal rod outer segments.* Nat Genet, 1997. **17**(1): p. 15-6.
133. Birnbach, C.D., et al., *Histopathology and immunocytochemistry of the neurosensory retina in fundus flavimaculatus.* Ophthalmology, 1994. **101**(7): p. 1211-9.
134. Petrukhin, K., et al., *Identification of the gene responsible for Best macular dystrophy.* Nat Genet, 1998. **19**(3): p. 241-7.
135. Blodi, C.F. and E.M. Stone, *Best's vitelliform dystrophy.* Ophthalmic Paediatr Genet, 1990. **11**(1): p. 49-59.
136. Marmorstein, A.D., et al., *Bestrophin, the product of the Best vitelliform macular dystrophy gene (VMD2), localizes to the basolateral plasma membrane of the retinal pigment epithelium.* Proc Natl Acad Sci U S A, 2000. **97**(23): p. 12758-63.
137. De Laey, J.J., *Flecked retina disorders.* Bull Soc Belge Ophtalmol, 1993. **249**: p. 11-22.
138. Seeliger, M.W., et al., *Phenotype in retinol deficiency due to a hereditary defect in retinol binding protein synthesis.* Invest Ophthalmol Vis Sci, 1999. **40**(1): p. 3-11.
139. Intres, R., et al., *Molecular cloning and structural analysis of the human gene encoding cellular retinaldehyde-binding protein.* J Biol Chem, 1994. **269**(41): p. 25411-8.
140. Lamb, T.D. and E.N. Pugh, Jr., *Dark adaptation and the retinoid cycle of vision.* Prog Retin Eye Res, 2004. **23**(3): p. 307-80.
141. Crabb, J.W., et al., *Cloning of the cDNAs encoding the cellular retinaldehyde-binding protein from bovine and human retina and comparison of the protein structures.* J Biol Chem, 1988. **263**(35): p. 18688-92.
142. Sparkes, R.S., et al., *Assignment of the gene (RLBP1) for cellular retinaldehyde-binding protein (CRALBP) to human chromosome 15q26 and mouse chromosome 7.* Genomics, 1992. **12**(1): p. 58-62.
143. Besch, D., et al., *Inherited multifocal RPE-diseases: mechanisms for local dysfunction in global retinoid cycle gene defects.* Vision Res, 2003. **43**(28): p. 3095-108.
144. Schiaffino, M.V. and C. Tacchetti, *The ocular albinism type 1 (OA1) protein and the evidence for an intracellular signal transduction system involved in melanosome biogenesis.* Pigment Cell Res, 2005. **18**(4): p. 227-33.
145. Oetting, W.S., *New insights into ocular albinism type 1 (OA1): Mutations and polymorphisms of the OA1 gene.* Hum Mutat, 2002. **19**(2): p. 85-92.
146. Petit, C., *Usher syndrome: from genetics to pathogenesis.* Annu Rev Genomics Hum Genet, 2001. **2**: p. 271-97.

147. Ahmed, Z.M., S. Riazuddin, and E.R. Wilcox, *The molecular genetics of Usher syndrome.* Clin Genet, 2003. **63**(6): p. 431-44.
148. Gibbs, D., J. Kitamoto, and D.S. Williams, *Abnormal phagocytosis by retinal pigmented epithelium that lacks myosin VIIa, the Usher syndrome 1B protein.* Proc Natl Acad Sci U S A, 2003. **100**(11): p. 6481-6.
149. Rosenthal, R., et al., *Insulin-like growth factor-1 contributes to neovascularization in age-related macular degeneration.* Biochem Biophys Res Commun, 2004. **323**(4): p. 1203-8.
150. Seko, Y., et al., *Induction of vascular endothelial growth factor after application of mechanical stress to retinal pigment epithelium of the rat in vitro.* Invest Ophthalmol Vis Sci, 1999. **40**(13): p. 3287-91.
151. Petersen-Jones, S.M., *Animal models of human retinal dystrophies.* Eye, 1998. **12 (Pt 3b)**: p. 566-70.
152. Peichl, L., P. Nemec, and H. Burda, *Unusual cone and rod properties in subterranean African mole-rats (Rodentia, Bathyergidae).* Eur J Neurosci, 2004. **19**(6): p. 1545-58.
153. Fauser, S., J. Luberichs, and F. Schuttauf, *Genetic animal models for retinal degeneration.* Surv Ophthalmol, 2002. **47**(4): p. 357-67.
154. Chader, G.J., *Animal models in research on retinal degenerations: past progress and future hope.* Vision Res, 2002. **42**(4): p. 393-9.
155. Pittler, S.J., et al., *PCR analysis of DNA from 70-year-old sections of rodless retina demonstrates identity with the mouse rd defect.* Proc Natl Acad Sci U S A, 1993. **90**(20): p. 9616-9.
156. Pittler, S.J. and W. Baehr, *Identification of a nonsense mutation in the rod photoreceptor cGMP phosphodiesterase beta-subunit gene of the rd mouse.* Proc Natl Acad Sci U S A, 1991. **88**(19): p. 8322-6.
157. Travis, G.H., et al., *Identification of a photoreceptor-specific mRNA encoded by the gene responsible for retinal degeneration slow (rds).* Nature, 1989. **338**(6210): p. 70-3.
158. Bourne, M.C., *Hereditary degeneration of the rat retina.* Br. J. Ophthalmol, 1938. **22**: p. 613-622.
159. Nandrot, E., et al., *Homozygous deletion in the coding sequence of the c-mer gene in RCS rats unravels general mechanisms of physiological cell adhesion and apoptosis.* Neurobiol Dis, 2000. **7**(6 Pt B): p. 586-99.
160. Li, Z.Y., et al., *Rhodopsin transgenic pigs as a model for human retinitis pigmentosa.* Invest Ophthalmol Vis Sci, 1998. **39**(5): p. 808-19.
161. Petters, R.M., et al., *Genetically engineered large animal model for studying cone photoreceptor survival and degeneration in retinitis pigmentosa.* Nat Biotechnol, 1997. **15**(10): p. 965-70.
162. Veske, A., et al., *Retinal dystrophy of Swedish briard/briard-beagle dogs is due to a 4-bp deletion in RPE65.* Genomics, 1999. **57**(1): p. 57-61.
163. Saari, J.C., *The sights along route 65.* Nat Genet, 2001. **29**(1): p. 8-9.
164. Redmond, T.M., et al., *Rpe65 is necessary for production of 11-cis-vitamin A in the retinal visual cycle.* Nat Genet, 1998. **20**(4): p. 344-51.
165. Pang, J.J., et al., *Retinal degeneration 12 (rd12): a new, spontaneously arising mouse model for human Leber congenital amaurosis (LCA).* Mol Vis, 2005. **11**: p. 152-62.
166. LaVail, M.M., *Photoreceptor characteristics in congenic strains of RCS rats.* Invest Ophthalmol Vis Sci, 1981. **20**(5): p. 671-5.
167. LaVail, M.M. and B.A. Battelle, *Influence of eye pigmentation and light deprivation on inherited retinal dystrophy in the rat.* Exp Eye Res, 1975. **21**(2): p. 167-92.
168. Bok, D. and M.O. Hall, *The role of the pigment epithelium in the etiology of inherited retinal dystrophy in the rat.* J Cell Biol, 1971. **49**(3): p. 664-82.
169. Herron, W.L., et al., *Retinal dystrophy in the rat--a pigment epithelial disease.* Invest Ophthalmol, 1969. **8**(6): p. 595-604.
170. Liou, A.K., E.A. McCormack, and K.R. Willison, *The chaperonin containing TCP-1 (CCT) displays a single-ring mediated disassembly and reassembly cycle.* Biol Chem, 1998. **379**(3): p. 311-9.
171. Dowling, J.E. and R.L. Sidman, *Inherited retinal dystrophy in the rat.* J Cell Biol, 1962. **14**: p. 73-109.

172. Tso, M.O., et al., *Apoptosis leads to photoreceptor degeneration in inherited retinal dystrophy of RCS rats.* Invest Ophthalmol Vis Sci, 1994. **35**(6): p. 2693-9.
173. Crosier, K.E. and P.S. Crosier, *New insights into the control of cell growth; the role of the Axl family.* Pathology, 1997. **29**(2): p. 131-5.
174. Yamazaki, H., et al., *Preservation of retinal morphology and functions in royal college surgeons rat by nilvadipine, a Ca(2+) antagonist.* Invest Ophthalmol Vis Sci, 2002. **43**(4): p. 919-26.
175. Pearce-Kelling, S.E., et al., *Calcium channel blocker D-cis-diltiazem does not slow retinal degeneration in the PDE6B mutant rcd1 canine model of retinitis pigmentosa.* Mol Vis, 2001. **7**: p. 42-7.
176. Pawlyk, B.S., et al., *Absence of photoreceptor rescue with D-cis-diltiazem in the rd mouse.* Invest Ophthalmol Vis Sci, 2002. **43**(6): p. 1912-5.
177. Hoffmann, S., S. He, and P. Wiedemann, *[Carboxyamido-triazole inhibits substeps of choroidal neovascularization on retinal pigment epithelial cells and choroidal endothelial cells in vitro].* Ophthalmologe, 2004. **101**(10): p. 993-7.
178. Hoffmann, S., et al., *Carboxyamido-triazole modulates retinal pigment epithelial and choroidal endothelial cell attachment, migration, proliferation, and MMP-2 secretion of choroidal endothelial cells.* Curr Eye Res, 2005. **30**(2): p. 103-13.
179. Recchia, F., et al., *Beta-interferon, retinoids and tamoxifen as maintenance therapy in metastatic breast cancer. A pilot study.* Clin Ter, 1995. **146**(10): p. 603-10.
180. Berson, E.L., et al., *Vitamin A supplementation for retinitis pigmentosa.* Arch Ophthalmol, 1993. **111**(11): p. 1456-9.
181. Berson, E.L., et al., *Clinical trial of docosahexaenoic acid in patients with retinitis pigmentosa receiving vitamin A treatment.* Arch Ophthalmol, 2004. **122**(9): p. 1297-305.
182. Faktorovich, E.G., et al., *Photoreceptor degeneration in inherited retinal dystrophy delayed by basic fibroblast growth factor.* Nature, 1990. **347**(6288): p. 83-6.
183. Caffe, A.R., A. Soderpalm, and T. van Veen, *Photoreceptor-specific protein expression of mouse retina in organ culture and retardation of rd degeneration in vitro by a combination of basic fibroblast and nerve growth factors.* Curr Eye Res, 1993. **12**(8): p. 719-26.
184. Whiteley, S.J., et al., *Photoreceptor rescue after low-dose intravitreal IL-1beta injection in the RCS rat.* Exp Eye Res, 2001. **73**(4): p. 557-68.
185. Frasson, M., et al., *Glial cell line-derived neurotrophic factor induces histologic and functional protection of rod photoreceptors in the rd/rd mouse.* Invest Ophthalmol Vis Sci, 1999. **40**(11): p. 2724-34.
186. McGee Sanftner, L.H., et al., *Glial cell line derived neurotrophic factor delays photoreceptor degeneration in a transgenic rat model of retinitis pigmentosa.* Mol Ther, 2001. **4**(6): p. 622-9.
187. Tombran-Tink, J., et al., *Expression, secretion, and age-related downregulation of pigment epithelium-derived factor, a serpin with neurotrophic activity.* J Neurosci, 1995. **15**(7 Pt 1): p. 4992-5003.
188. Wu, Y.Q., et al., *Identification of pigment epithelium-derived factor in the interphotoreceptor matrix of bovine eyes.* Protein Expr Purif, 1995. **6**(4): p. 447-56.
189. Cayouette, M., et al., *Pigment epithelium-derived factor delays the death of photoreceptors in mouse models of inherited retinal degenerations.* Neurobiol Dis, 1999. **6**(6): p. 523-32.
190. Tansley, K., *The development of the rat eye in graft.* J Exp Biol., 1946. **22**: p. 221-223.
191. del Cerro, M., et al., *Intraocular retinal transplants.* Invest Ophthalmol Vis Sci, 1985. **26**(8): p. 1182-5.
192. del Cerro, M., et al., *Intraretinal grafting restores visual function in light-blinded rats.* Neuroreport, 1991. **2**(9): p. 529-32.
193. del Cerro, M., et al., *Intraretinal transplantation for rod-cell replacement in light-damaged retinas.* J Neural Transplant, 1989. **1**(1): p. 1-10.
194. McGill, T.J., et al., *Preservation of vision following cell-based therapies in a model of retinal degenerative disease.* Vision Res, 2004. **44**(22): p. 2559-66.

195. Sauve, Y., et al., *Preservation of visual responsiveness in the superior colliculus of RCS rats after retinal pigment epithelium cell transplantation.* Neuroscience, 2002. **114**(2): p. 389-401.
196. Grisanti, S., et al., *Xenotransplantation of retinal pigment epithelial cells into RCS rats.* Jpn J Ophthalmol, 2002. **46**(1): p. 36-44.
197. Weisz, J.M., et al., *Allogenic fetal retinal pigment epithelial cell transplant in a patient with geographic atrophy.* Retina, 1999. **19**(6): p. 540-5.
198. Humayun, M.S., et al., *Human neural retinal transplantation.* Invest Ophthalmol Vis Sci, 2000. **41**(10): p. 3100-6.
199. Mohand-Said, S., et al., *Photoreceptor transplants increase host cone survival in the retinal degeneration (rd) mouse.* Ophthalmic Res, 1997. **29**(5): p. 290-7.
200. Kwan, A.S., S. Wang, and R.D. Lund, *Photoreceptor layer reconstruction in a rodent model of retinal degeneration.* Exp Neurol, 1999. **159**(1): p. 21-33.
201. Klassen, H.J., et al., *Multipotent retinal progenitors express developmental markers, differentiate into retinal neurons, and preserve light-mediated behavior.* Invest Ophthalmol Vis Sci, 2004. **45**(11): p. 4167-73.
202. Pressmar, S., et al., *The fate of heterotopically grafted neural precursor cells in the normal and dystrophic adult mouse retina.* Invest Ophthalmol Vis Sci, 2001. **42**(13): p. 3311-9.
203. Meyer, J.S., M.L. Katz, and M.D. Kirk, *Stem cells for retinal degenerative disorders.* Ann N Y Acad Sci, 2005. **1049**: p. 135-45.
204. Schraermeyer, U., et al., *Subretinally transplanted embryonic stem cells rescue photoreceptor cells from degeneration in the RCS rats.* Cell Transplant, 2001. **10**(8): p. 673-80.
205. Boheler, K.R. and M.Y. Fiszman, *Can exogenous stem cells be used in transplantation?* Cells Tissues Organs, 1999. **165**(3-4): p. 237-45.
206. Wakitani, S., et al., *Embryonic stem cells form articular cartilage, not teratomas, in osteochondral defects of rat joints.* Cell Transplant, 2004. **13**(4): p. 331-6.
207. Moshiri, A., J. Close, and T.A. Reh, *Retinal stem cells and regeneration.* Int J Dev Biol, 2004. **48**(8-9): p. 1003-14.
208. Qiu, G., et al., *Photoreceptor differentiation and integration of retinal progenitor cells transplanted into transgenic rats.* Exp Eye Res, 2005. **80**(4): p. 515-25.
209. Blaese, R.M., et al., *T lymphocyte-directed gene therapy for ADA- SCID: initial trial results after 4 years.* Science, 1995. **270**(5235): p. 475-80.
210. Buckley, R.H., et al., *Human severe combined immunodeficiency: genetic, phenotypic, and functional diversity in one hundred eight infants.* J Pediatr, 1997. **130**(3): p. 378-87.
211. Hoogerbrugge, P.M., et al., *Bone marrow gene transfer in three patients with adenosine deaminase deficiency.* Gene Ther, 1996. **3**(2): p. 179-83.
212. Kohn, D.B., *Gene therapy for hematopoietic and immune disorders.* Bone Marrow Transplant, 1996. **18 Suppl 3**: p. S55-8.
213. Aiuti, A., et al., *Correction of ADA-SCID by stem cell gene therapy combined with nonmyeloablative conditioning.* Science, 2002. **296**(5577): p. 2410-3.
214. Hacein-Bey-Abina, S., A. Fischer, and M. Cavazzana-Calvo, *Gene therapy of X-linked severe combined immunodeficiency.* Int J Hematol, 2002. **76**(4): p. 295-8.
215. Cavazzana-Calvo, M., et al., *Gene therapy of human severe combined immunodeficiency (SCID)-X1 disease.* Science, 2000. **288**(5466): p. 669-72.
216. *French gene therapy group reports on the adverse event in a clinical trial of gene therapy for X-linked severe combined immune deficiency (X-SCID). Position statement from the European Society of Gene Therapy.* J Gene Med, 2003. **5**(1): p. 82-4.
217. Hacein-Bey-Abina, S., et al., *LMO2-associated clonal T cell proliferation in two patients after gene therapy for SCID-X1.* Science, 2003. **302**(5644): p. 415-9.
218. Couzin, J. and J. Kaiser, *Gene therapy. As Gelsinger case ends, gene therapy suffers another blow.* Science, 2005. **307**(5712): p. 1028.
219. Schwartz, R.H., *T cell anergy.* Annu Rev Immunol, 2003. **21**: p. 305-34.
220. Banchereau, J., et al., *Dendritic cells: controllers of the immune system and a new promise for immunotherapy.* Ann N Y Acad Sci, 2003. **987**: p. 180-7.

221. Rolling, F., *Recombinant AAV-mediated gene transfer to the retina: gene therapy perspectives.* Gene Ther, 2004. **11 Suppl 1**: p. S26-32.
222. Schauber, C.A., et al., *Lentiviral vectors pseudotyped with baculovirus gp64 efficiently transduce mouse cells in vivo and show tropism restriction against hematopoietic cell types in vitro.* Gene Ther, 2004. **11**(3): p. 266-75.
223. Schauber-Plewa, C., et al., *Complement regulatory proteins are incorporated into lentiviral vectors and protect particles against complement inactivation.* Gene Ther, 2005. **12**(3): p. 238-45.
224. Reyes-Sandoval, A. and H.C. Ertl, *CpG methylation of a plasmid vector results in extended transgene product expression by circumventing induction of immune responses.* Mol Ther, 2004. **9**(2): p. 249-61.
225. Chen, Y., et al., *Identification of methylated CpG motifs as inhibitors of the immune stimulatory CpG motifs.* Gene Ther, 2001. **8**(13): p. 1024-32.
226. Ali, R.R., et al., *Gene therapy for inherited retinal degeneration.* Br J Ophthalmol, 1997. **81**(9): p. 795-801.
227. Ali, R.R., et al., *Adeno-associated virus gene transfer to mouse retina.* Hum Gene Ther, 1998. **9**(1): p. 81-6.
228. Ali, R.R., et al., *Gene transfer into the mouse retina mediated by an adeno-associated viral vector.* Hum Mol Genet, 1996. **5**(5): p. 591-4.
229. Bennett, J., et al., *Photoreceptor cell rescue in retinal degeneration (rd) mice by in vivo gene therapy.* Nat Med, 1996. **2**(6): p. 649-54.
230. Ali, R.R., et al., *Restoration of photoreceptor ultrastructure and function in retinal degeneration slow mice by gene therapy.* Nat Genet, 2000. **25**(3): p. 306-10.
231. Schlichtenbrede, F.C., et al., *Intraocular gene delivery of ciliary neurotrophic factor results in significant loss of retinal function in normal mice and in the Prph2Rd2/Rd2 model of retinal degeneration*, in *Gene Ther.* 2003. p. 523-7.
232. Liang, F.Q., et al., *Long-term protection of retinal structure but not function using RAAV.CNTF in animal models of retinitis pigmentosa.* Mol Ther, 2001. **4**(5): p. 461-72.
233. Vollrath, D., et al., *Correction of the retinal dystrophy phenotype of the RCS rat by viral gene transfer of Mertk.* Proc Natl Acad Sci U S A, 2001. **98**(22): p. 12584-9.
234. Bhisitkul, R.B., et al., *An antisense oligodeoxynucleotide against vascular endothelial growth factor in a nonhuman primate model of iris neovascularization.* Arch Ophthalmol, 2005. **123**(2): p. 214-9.
235. Bantounas, I., et al., *Assessing adenoviral hammerhead ribozyme and small hairpin RNA cassettes in neurons: inhibition of endogenous caspase-3 activity and protection from apoptotic cell death.* J Neurosci Res, 2005. **79**(5): p. 661-9.
236. Lewin, A.S., et al., *Ribozyme rescue of photoreceptor cells in a transgenic rat model of autosomal dominant retinitis pigmentosa.* Nat Med, 1998. **4**(8): p. 967-71.
237. LaVail, M.M., et al., *Ribozyme rescue of photoreceptor cells in P23H transgenic rats: long-term survival and late-stage therapy.* Proc Natl Acad Sci U S A, 2000. **97**(21): p. 11488-93.
238. Reich, S.J., et al., *Small interfering RNA (siRNA) targeting VEGF effectively inhibits ocular neovascularization in a mouse model.* Mol Vis, 2003. **9**: p. 210-6.
239. Tolentino, M.J., et al., *Intravitreal injection of vascular endothelial growth factor small interfering RNA inhibits growth and leakage in a nonhuman primate, laser-induced model of choroidal neovascularization.* Retina, 2004. **24**(1): p. 132-8.
240. Maguire, M.G., S.L. Fine, and G.S. Ying, *Intravitreal injection of VEGF siRNA.* Retina, 2005. **25**(1): p. 101-2.
241. Cashman, S.M., E.A. Binkley, and R. Kumar-Singh, *Towards mutation-independent silencing of genes involved in retinal degeneration by RNA interference.* Gene Ther, 2005. **12**(15): p. 1223-8.
242. Kiang, A.S., et al., *Toward a gene therapy for dominant disease: validation of an RNA interference-based mutation-independent approach.* Mol Ther, 2005. **12**(3): p. 555-61.
243. Farrar, G.J., P.F. Kenna, and P. Humphries, *On the genetics of retinitis pigmentosa and on mutation-independent approaches to therapeutic intervention.* Embo J, 2002. **21**(5): p. 857-64.

244. Lau, D., et al., *Retinal degeneration is slowed in transgenic rats by AAV-mediated delivery of FGF-2.* Invest Ophthalmol Vis Sci, 2000. **41**(11): p. 3622-33.
245. Bok, D., et al., *Effects of adeno-associated virus-vectored ciliary neurotrophic factor on retinal structure and function in mice with a P216L rds/peripherin mutation.* Exp Eye Res, 2002. **74**(6): p. 719-35.
246. Miyazaki, M., et al., *Simian lentiviral vector-mediated retinal gene transfer of pigment epithelium-derived factor protects retinal degeneration and electrical defect in Royal College of Surgeons rats.* Gene Ther, 2003. **10**(17): p. 1503-11.
247. Qin, L., et al., *Promoter attenuation in gene therapy: interferon-gamma and tumor necrosis factor-alpha inhibit transgene expression.* Hum Gene Ther, 1997. **8**(17): p. 2019-29.
248. Ralph, G.S., et al., *Targeting of tetracycline-regulatable transgene expression specifically to neuronal and glial cell populations using adenoviral vectors.* Neuroreport, 2000. **11**(9): p. 2051-5.
249. Harding, T.C., et al., *Switching transgene expression in the brain using an adenoviral tetracycline-regulatable system.* Nat Biotechnol, 1998. **16**(6): p. 553-5.
250. Suzuki, M., R.N. Singh, and R.G. Crystal, *Regulatable promoters for use in gene therapy applications: modification of the 5'-flanking region of the CFTR gene with multiple cAMP response elements to support basal, low-level gene expression that can be upregulated by exogenous agents that raise intracellular levels of cAMP.* Hum Gene Ther, 1996. **7**(15): p. 1883-93.
251. Delyfer, M.N., et al., *Inherited retinal degenerations: therapeutic prospects.* Biol Cell, 2004. **96**(4): p. 261-9.
252. Howard, M.K., et al., *Gene delivery to rat enteric neurons using herpes simplex virus-based vectors.* J Mol Neurosci, 1997. **9**(2): p. 65-74.
253. Spencer, B., et al., *Herpes simplex virus-mediated gene delivery to the rodent visual system.* Invest Ophthalmol Vis Sci, 2000. **41**(6): p. 1392-401.
254. Liu, X., et al., *Herpes simplex virus mediated gene transfer to primate ocular tissues.* Exp Eye Res, 1999. **69**(4): p. 385-95.
255. Fraefel, C., et al., *In vivo gene transfer to the rat retina using herpes simplex virus type 1 (HSV-1)-based amplicon vectors.* Gene Ther, 2005. **12**(16): p. 1283-8.
256. Wang, Y., et al., *Herpes simplex virus type 1/adeno-associated virus rep(+) hybrid amplicon vector improves the stability of transgene expression in human cells by site-specific integration.* J Virol, 2002. **76**(14): p. 7150-62.
257. Heister, T., et al., *Herpes simplex virus type 1/adeno-associated virus hybrid vectors mediate site-specific integration at the adeno-associated virus preintegration site, AAVS1, on human chromosome 19.* J Virol, 2002. **76**(14): p. 7163-73.
258. Bakowska, J.C., et al., *Targeted transgene integration into transgenic mouse fibroblasts carrying the full-length human AAVS1 locus mediated by HSV/AAV rep(+) hybrid amplicon vector.* Gene Ther, 2003. **10**(19): p. 1691-702.
259. Cao, H., D.R. Koehler, and J. Hu, *Adenoviral vectors for gene replacement therapy.* Viral Immunol, 2004. **17**(3): p. 327-33.
260. Graham, F.L. and L. Prevec, *Adenovirus-based expression vectors and recombinant vaccines.* Biotechnology, 1992. **20**: p. 363-90.
261. Prevec, L., et al., *Immune response to HIV-1 gag antigens induced by recombinant adenovirus vectors in mice and rhesus macaque monkeys.* J Acquir Immune Defic Syndr, 1991. **4**(6): p. 568-76.
262. Amalfitano, A., C.R. Begy, and J.S. Chamberlain, *Improved adenovirus packaging cell lines to support the growth of replication-defective gene-delivery vectors.* Proc Natl Acad Sci U S A, 1996. **93**(8): p. 3352-6.
263. Wang, Q. and M.H. Finer, *Second-generation adenovirus vectors.* Nat Med, 1996. **2**(6): p. 714-6.
264. Dishart, K.L., et al., *Third-generation lentivirus vectors efficiently transduce and phenotypically modify vascular cells: implications for gene therapy.* J Mol Cell Cardiol, 2003. **35**(7): p. 739-48.

265. O'Neal, W.K., et al., *Toxicity associated with repeated administration of first-generation adenovirus vectors does not occur with a helper-dependent vector.* Mol Med, 2000. **6**(3): p. 179-95.
266. Kochanek, S., G. Schiedner, and C. Volpers, *High-capacity 'gutless' adenoviral vectors.* Curr Opin Mol Ther, 2001. **3**(5): p. 454-63.
267. Steinwaerder, D.S., C.A. Carlson, and A. Lieber, *Generation of adenovirus vectors devoid of all viral genes by recombination between inverted repeats.* J Virol, 1999. **73**(11): p. 9303-13.
268. Kochanek, S., et al., *A new adenoviral vector: Replacement of all viral coding sequences with 28 kb of DNA independently expressing both full-length dystrophin and beta-galactosidase.* Proc Natl Acad Sci U S A, 1996. **93**(12): p. 5731-6.
269. Kumar-Singh, R. and J.S. Chamberlain, *Encapsidated adenovirus minichromosomes allow delivery and expression of a 14 kb dystrophin cDNA to muscle cells.* Hum Mol Genet, 1996. **5**(7): p. 913-21.
270. Hartigan-O'Connor, D., et al., *Efficient rescue of gutted adenovirus genomes allows rapid production of concentrated stocks without negative selection.* Hum Gene Ther, 2002. **13**(4): p. 519-31.
271. Kumar-Singh, R. and D.B. Farber, *Encapsidated adenovirus mini-chromosome-mediated delivery of genes to the retina: application to the rescue of photoreceptor degeneration.* Hum Mol Genet, 1998. **7**(12): p. 1893-900.
272. Toietta, G., et al., *Lifelong elimination of hyperbilirubinemia in the Gunn rat with a single injection of helper-dependent adenoviral vector.* Proc Natl Acad Sci U S A, 2005. **102**(11): p. 3930-5.
273. Bennett, J., et al., *Adenovirus vector-mediated in vivo gene transfer into adult murine retina.* Invest Ophthalmol Vis Sci, 1994. **35**(5): p. 2535-42.
274. Reichel, M.B., et al., *Immune responses limit adenovirally mediated gene expression in the adult mouse eye.* Gene Ther, 1998. **5**(8): p. 1038-46.
275. Auricchio, A. and F. Rolling, *Adeno-associated viral vectors for retinal gene transfer and treatment of retinal diseases.* Curr Gene Ther, 2005. **5**(3): p. 339-48.
276. Zaiss, A.K., et al., *Differential activation of innate immune responses by adenovirus and adeno-associated virus vectors.* J Virol, 2002. **76**(9): p. 4580-90.
277. Inoue, N., et al., *Introduction of single base substitutions at homologous chromosomal sequences by adeno-associated virus vectors.* Mol Ther, 2001. **3**(4): p. 526-30.
278. Russell, D.W. and R.K. Hirata, *Human gene targeting by viral vectors.* Nat Genet, 1998. **18**(4): p. 325-30.
279. Russell, D.W., R.K. Hirata, and N. Inoue, *Validation of AAV-mediated gene targeting.* Nat Biotechnol, 2002. **20**(7): p. 658.
280. Hirata, R., et al., *Targeted transgene insertion into human chromosomes by adeno-associated virus vectors.* Nat Biotechnol, 2002. **20**(7): p. 735-8.
281. Hirata, R.K. and D.W. Russell, *Design and packaging of adeno-associated virus gene targeting vectors.* J Virol, 2000. **74**(10): p. 4612-20.
282. Flannery, J.G., et al., *Efficient photoreceptor-targeted gene expression in vivo by recombinant adeno-associated virus.* Proc Natl Acad Sci U S A, 1997. **94**(13): p. 6916-21.
283. Auricchio, A., et al., *Exchange of surface proteins impacts on viral vector cellular specificity and transduction characteristics: the retina as a model.* Hum Mol Genet, 2001. **10**(26): p. 3075-81.
284. Anand, V., et al., *Additional transduction events after subretinal readministration of recombinant adeno-associated virus.* Hum Gene Ther, 2000. **11**(3): p. 449-57.
285. Sarra, G.M., et al., *Gene replacement therapy in the retinal degeneration slow (rds) mouse: the effect on retinal degeneration following partial transduction of the retina.* Hum Mol Genet, 2001. **10**(21): p. 2353-61.
286. Boylan, J.P. and A.F. Wright, *Identification of a novel protein interacting with RPGR.* Hum Mol Genet, 2000. **9**(14): p. 2085-93.
287. Mavlyutov, T.A., H. Zhao, and P.A. Ferreira, *Species-specific subcellular localization of RPGR and RPGRIP isoforms: implications for the phenotypic variability of congenital retinopathies among species.* Hum Mol Genet, 2002. **11**(16): p. 1899-907.

288. Gerber, S., et al., *Complete exon-intron structure of the RPGR-interacting protein (RPGRIP1) gene allows the identification of mutations underlying Leber congenital amaurosis.* Eur J Hum Genet, 2001. **9**(8): p. 561-71.
289. Pawlyk, B.S., et al., *Gene Replacement Therapy Rescues Photoreceptor Degeneration in a Murine Model of Leber Congenital Amaurosis Lacking RPGRIP.* Invest Ophthalmol Vis Sci, 2005. **46**(9): p. 3039-45.
290. Narfstrom, K., et al., *Functional and structural recovery of the retina after gene therapy in the RPE65 null mutation dog.* Invest Ophthalmol Vis Sci, 2003. **44**(4): p. 1663-72.
291. Narfstrom, K., et al., *In vivo gene therapy in young and adult RPE65-/- dogs produces long-term visual improvement.* J Hered, 2003. **94**(1): p. 31-7.
292. Dejneka, N.S., et al., *In utero gene therapy rescues vision in a murine model of congenital blindness.* Mol Ther, 2004. **9**(2): p. 182-8.
293. Lai, C.M., et al., *Recombinant adeno-associated virus type 2-mediated gene delivery into the Rpe65-/- knockout mouse eye results in limited rescue.* Genet Vaccines Ther, 2004. **2**(1): p. 3.
294. Yi, Y., S.H. Hahm, and K.H. Lee, *Retroviral gene therapy: safety issues and possible solutions.* Curr Gene Ther, 2005. **5**(1): p. 25-35.
295. Loewen, N., et al., *Long-term retinal transgene expression with FIV versus adenoviral vectors.* Mol Vis, 2004. **10**: p. 272-80.
296. Cheng, L., et al., *Efficient gene transfer to retinal pigment epithelium cells with long-term expression.* Retina, 2005. **25**(2): p. 193-201.
297. Cheng, L., et al., *Human immunodeficiency virus type 2 (HIV-2) vector-mediated in vivo gene transfer into adult rabbit retina.* Curr Eye Res, 2002. **24**(3): p. 196-201.
298. Ikeda, Y., et al., *Gene transduction efficiency in cells of different species by HIV and EIAV vectors.* Gene Ther, 2002. **9**(14): p. 932-8.
299. Duisit, G., et al., *Five recombinant simian immunodeficiency virus pseudotypes lead to exclusive transduction of retinal pigmented epithelium in rat.* Mol Ther, 2002. **6**(4): p. 446-54.
300. Ikeda, Y., et al., *Simian immunodeficiency virus-based lentivirus vector for retinal gene transfer: a preclinical safety study in adult rats.* Gene Ther, 2003. **10**(14): p. 1161-9.
301. Takahashi, K., et al., *Sustained transduction of ocular cells with a bovine immunodeficiency viral vector.* Hum Gene Ther, 2002. **13**(11): p. 1305-16.
302. Beutelspacher, S.C., et al., *Comparison of HIV-1 and EIAV-based lentiviral vectors in corneal transduction.* Exp Eye Res, 2005. **80**(6): p. 787-94.
303. Naldini, L., et al., *In vivo gene delivery and stable transduction of nondividing cells by a lentiviral vector.* Science, 1996. **272**(5259): p. 263-7.
304. Naldini, L., et al., *Efficient transfer, integration, and sustained long-term expression of the transgene in adult rat brains injected with a lentiviral vector.* Proc Natl Acad Sci U S A, 1996. **93**(21): p. 11382-8.
305. Zufferey, R., et al., *Multiply attenuated lentiviral vector achieves efficient gene delivery in vivo.* Nat Biotechnol, 1997. **15**(9): p. 871-5.
306. Aldrovandi, G.M. and J.A. Zack, *Replication and pathogenicity of human immunodeficiency virus type 1 accessory gene mutants in SCID-hu mice.* J Virol, 1996. **70**(3): p. 1505-11.
307. Kaye, J.F., J.H. Richardson, and A.M. Lever, *cis-acting sequences involved in human immunodeficiency virus type 1 RNA packaging.* J Virol, 1995. **69**(10): p. 6588-92.
308. Lever, A., et al., *Identification of a sequence required for efficient packaging of human immunodeficiency virus type 1 RNA into virions.* J Virol, 1989. **63**(9): p. 4085-7.
309. McBride, M.S., M.D. Schwartz, and A.T. Panganiban, *Efficient encapsidation of human immunodeficiency virus type 1 vectors and further characterization of cis elements required for encapsidation.* J Virol, 1997. **71**(6): p. 4544-54.
310. Parolin, C., et al., *Analysis in human immunodeficiency virus type 1 vectors of cis-acting sequences that affect gene transfer into human lymphocytes.* J Virol, 1994. **68**(6): p. 3888-95.

311. Aldovini, A. and R.A. Young, *Mutations of RNA and protein sequences involved in human immunodeficiency virus type 1 packaging result in production of noninfectious virus.* J Virol, 1990. **64**(5): p. 1920-6.
312. Dull, T., et al., *A third-generation lentivirus vector with a conditional packaging system.* J Virol, 1998. **72**(11): p. 8463-71.
313. Bainbridge, J.W., et al., *In vivo gene transfer to the mouse eye using an HIV-based lentiviral vector; efficient long-term transduction of corneal endothelium and retinal pigment epithelium.* Gene Ther, 2001. **8**(21): p. 1665-8.
314. Miyoshi, H., et al., *Stable and efficient gene transfer into the retina using an HIV-based lentiviral vector.* Proc Natl Acad Sci U S A, 1997. **94**(19): p. 10319-23.
315. Hangai, M., et al., *In vivo gene transfer into the retina mediated by a novel liposome system.* Invest Ophthalmol Vis Sci, 1996. **37**(13): p. 2678-85.
316. Kachi, S., et al., *Nonviral ocular gene transfer.* Gene Ther, 2005. **12**(10): p. 843-51.
317. Matsuda, T. and C.L. Cepko, *Electroporation and RNA interference in the rodent retina in vivo and in vitro.* Proc Natl Acad Sci U S A, 2004. **101**(1): p. 16-22.
318. Olivares, E.C., et al., *Site-specific genomic integration produces therapeutic Factor IX levels in mice.* Nat Biotechnol, 2002. **20**(11): p. 1124-8.
319. Ortiz-Urda, S., et al., *PhiC31 integrase-mediated nonviral genetic correction of junctional epidermolysis bullosa.* Hum Gene Ther, 2003. **14**(9): p. 923-8.
320. Chalberg, T.W., et al., *{phi}C31 Integrase Confers Genomic Integration and Long-Term Transgene Expression in Rat Retina.* Invest Ophthalmol Vis Sci, 2005. **46**(6): p. 2140-6.
321. Ohlfest, J.R., et al., *Phenotypic correction and long-term expression of factor VIII in hemophilic mice by immunotolerization and nonviral gene transfer using the Sleeping Beauty transposon system.* Blood, 2005. **105**(7): p. 2691-8.
322. Fan, P.D. and J.Y. Dong, *Replication of rep-cap genes is essential for the high-efficiency production of recombinant AAV.* Hum Gene Ther, 1997. **8**(1): p. 87-98.
323. Zhang, X., et al., *High-titer recombinant adeno-associated virus production from replicating amplicons and herpes vectors deleted for glycoprotein H.* Hum Gene Ther, 1999. **10**(15): p. 2527-37.
324. Boulanger, A., et al., *The upstream region of the Rpe65 gene confers retinal pigment epithelium-specific expression in vivo and in vitro and contains critical octamer and E-box binding sites.* J Biol Chem, 2000. **275**(40): p. 31274-82.
325. Auricchio, A., et al., *Isolation of highly infectious and pure adeno-associated virus type 2 vectors with a single-step gravity-flow column.* Hum Gene Ther, 2001. **12**(1): p. 71-6.
326. Demaison, C., et al., *High-level transduction and gene expression in hematopoietic repopulating cells using a human immunodeficiency [correction of imunodeficiency] virus type 1-based lentiviral vector containing an internal spleen focus forming virus promoter.* Hum Gene Ther, 2002. **13**(7): p. 803-13.
327. Ruther, K. and E. Zrenner, *[Developments in ophthalmologic electrophysiology].* Klin Monatsbl Augenheilkd, 1993. **202**(2): p. 140-5.
328. Marmor, M.F. and E. Zrenner, *Standard for clinical electro-oculography. International Society for Clinical Electrophysiology of Vision.* Arch Ophthalmol, 1993. **111**(5): p. 601-4.
329. Marmor, M.F. and E. Zrenner, *Standard for clinical electroretinography (1999 update). International Society for Clinical Electrophysiology of Vision.* Doc Ophthalmol, 1998. **97**(2): p. 143-56.
330. Bach, M., et al., *Standard for pattern electroretinography. International Society for Clinical Electrophysiology of Vision.* Doc Ophthalmol, 2000. **101**(1): p. 11-8.
331. Grant, C.A., et al., *Evaluation of recombinant adeno-associated virus as a gene transfer vector for the retina.* Curr Eye Res, 1997. **16**(9): p. 949-56.
332. Bainbridge, J.W., et al., *Stable rAAV-mediated transduction of rod and cone photoreceptors in the canine retina.* Gene Ther, 2003. **10**(16): p. 1336-44.
333. Rolling, F., et al., *Evaluation of adeno-associated virus-mediated gene transfer into the rat retina by clinical fluorescence photography.* Hum Gene Ther, 1999. **10**(4): p. 641-8.
334. Sarra, G.M., et al., *Kinetics of transgene expression in mouse retina following sub-retinal injection of recombinant adeno-associated virus.* Vision Res, 2002. **42**(4): p. 541-9.

335. LaVail, M.M. and R.J. Mullen, *Role of the pigment epithelium in inherited retinal degeneration analyzed with experimental mouse chimeras.* Exp Eye Res, 1976. **23**(2): p. 227-45.
336. Celesia, G.G., *Anatomy and physiology of visual evoked potentials and electroretinograms.* Neurol Clin, 1988. **6**(4): p. 657-79.
337. Wachtmeister, L., *Oscillatory potentials in the retina: what do they reveal.* Prog Retin Eye Res, 1998. **17**(4): p. 485-521.
338. Holder, G.E., *Pattern electroretinography (PERG) and an integrated approach to visual pathway diagnosis.* Prog Retin Eye Res, 2001. **20**(4): p. 531-61.
339. Li, T., et al., *In vivo transfer of a reporter gene to the retina mediated by an adenoviral vector.* Invest Ophthalmol Vis Sci, 1994. **35**(5): p. 2543-9.
340. Xiao, X., J. Li, and R.J. Samulski, *Efficient long-term gene transfer into muscle tissue of immunocompetent mice by adeno-associated virus vector.* J Virol, 1996. **70**(11): p. 8098-108.
341. Bennett, J., et al., *Stable transgene expression in rod photoreceptors after recombinant adeno-associated virus-mediated gene transfer to monkey retina.* Proc Natl Acad Sci U S A, 1999. **96**(17): p. 9920-5.
342. Huang, P.C., et al., *Cellular interactions implicated in the mechanism of photoreceptor degeneration in transgenic mice expressing a mutant rhodopsin gene.* Proc Natl Acad Sci U S A, 1993. **90**(18): p. 8484-8.
343. Weber, M., et al., *Recombinant adeno-associated virus serotype 4 mediates unique and exclusive long-term transduction of retinal pigmented epithelium in rat, dog, and nonhuman primate after subretinal delivery.* Mol Ther, 2003. **7**(6): p. 774-81.
344. Mitta, B., et al., *Design and in vivo characterization of self-inactivating human and non-human lentiviral expression vectors engineered for streptogramin-adjustable transgene expression.* Nucleic Acids Res, 2004. **32**(12): p. e106.
345. Mitrophanous, K., et al., *Stable gene transfer to the nervous system using a non-primate lentiviral vector.* Gene Ther, 1999. **6**(11): p. 1808-18.
346. O'Rourke, J.P., et al., *Comparison of gene transfer efficiencies and gene expression levels achieved with equine infectious anemia virus- and human immunodeficiency virus type 1-derived lentivirus vectors.* J Virol, 2002. **76**(3): p. 1510-5.
347. Bai, Y., et al., *Effective transduction and stable transgene expression in human blood cells by a third-generation lentiviral vector.* Gene Ther, 2003. **10**(17): p. 1446-57.
348. Miyoshi, H., et al., *Development of a self-inactivating lentivirus vector.* J Virol, 1998. **72**(10): p. 8150-7.
349. Zufferey, R., et al., *Self-inactivating lentivirus vector for safe and efficient in vivo gene delivery.* J Virol, 1998. **72**(12): p. 9873-80.
350. Bukovsky, A.A., J.P. Song, and L. Naldini, *Interaction of human immunodeficiency virus-derived vectors with wild-type virus in transduced cells.* J Virol, 1999. **73**(8): p. 7087-92.
351. Quinonez, R. and R.E. Sutton, *Lentiviral vectors for gene delivery into cells.* DNA Cell Biol, 2002. **21**(12): p. 937-51.
352. Zufferey, R., et al., *Woodchuck hepatitis virus posttranscriptional regulatory element enhances expression of transgenes delivered by retroviral vectors.* J Virol, 1999. **73**(4): p. 2886-92.
353. Yam, P.Y., et al., *Design of HIV vectors for efficient gene delivery into human hematopoietic cells.* Mol Ther, 2002. **5**(4): p. 479-84.
354. Park, F. and M.A. Kay, *Modified HIV-1 based lentiviral vectors have an effect on viral transduction efficiency and gene expression in vitro and in vivo.* Mol Ther, 2001. **4**(3): p. 164-73.
355. Kim, H., H. Lee, and Y. Yun, *X-gene product of hepatitis B virus induces apoptosis in liver cells.* J Biol Chem, 1998. **273**(1): p. 381-5.
356. Schuster, R., W.H. Gerlich, and S. Schaefer, *Induction of apoptosis by the transactivating domains of the hepatitis B virus X gene leads to suppression of oncogenic transformation of primary rat embryo fibroblasts.* Oncogene, 2000. **19**(9): p. 1173-80.

357. Mullen, R.J. and M.M. LaVail, *Inherited retinal dystrophy: primary defect in pigment epithelium determined with experimental rat chimeras.* Science, 1976. **192**(4241): p. 799-801.
358. Li, Z., et al., *Murine leukemia induced by retroviral gene marking.* Science, 2002. **296**(5567): p. 497.
359. Vargas, J., Jr., et al., *Novel integrase-defective lentiviral episomal vectors for gene transfer.* Hum Gene Ther, 2004. **15**(4): p. 361-72.
360. Lotery, A.J., et al., *Gene transfer to the nonhuman primate retina with recombinant feline immunodeficiency virus vectors.* Hum Gene Ther, 2002. **13**(6): p. 689-96.
361. Loewen, N., et al., *Comparison of wild-type and class I integrase mutant-FIV vectors in retina demonstrates sustained expression of integrated transgenes in retinal pigment epithelium.* J Gene Med, 2003. **5**(12): p. 1009-17.
362. Kostic, C., et al., *Activity analysis of housekeeping promoters using self-inactivating lentiviral vector delivery into the mouse retina.* Gene Ther, 2003. **10**(9): p. 818-21.
363. Sellon, D.C., F.J. Fuller, and T.C. McGuire, *The immunopathogenesis of equine infectious anemia virus.* Virus Res, 1994. **32**(2): p. 111-38.
364. Wong, L.F., et al., *Transduction patterns of pseudotyped lentiviral vectors in the nervous system.* Mol Ther, 2004. **9**(1): p. 101-11.
365. Mazarakis, N.D., et al., *Rabies virus glycoprotein pseudotyping of lentiviral vectors enables retrograde axonal transport and access to the nervous system after peripheral delivery.* Hum Mol Genet, 2001. **10**(19): p. 2109-21.
366. Yamada, K., et al., *Functional correction of fanconi anemia group C hematopoietic cells by the use of a novel lentiviral vector.* Mol Ther, 2001. **3**(4): p. 485-90.
367. Bienemann, A.S., et al., *Long-term replacement of a mutated nonfunctional CNS gene: reversal of hypothalamic diabetes insipidus using an EIAV-based lentiviral vector expressing arginine vasopressin.* Mol Ther, 2003. **7**(5 Pt 1): p. 588-96.
368. Azzouz, M., et al., *VEGF delivery with retrogradely transported lentivector prolongs survival in a mouse ALS model.* Nature, 2004. **429**(6990): p. 413-7.
369. Ralph, G.S., et al., *Silencing mutant SOD1 using RNAi protects against neurodegeneration and extends survival in an ALS model.* Nat Med, 2005. **11**(4): p. 429-33.
370. Reading, H.W. and A. Sorsby, *The metabolism of the dystrophic retina. II. Amino acid transport and protein synthesis in the developing rat retina, normal and dystrophic.* Vision Res, 1964. **4**(3): p. 209-20.
371. Walters, P.T., *Anaerobic glycolysis in rats affected with retinitis pigmentosa. Its significance in relation to various forms of primary pigmentary degeneration of the retina.* Br J Ophthalmol, 1959. **43**: p. 686-96.
372. Fletcher, E.L. and M. Kalloniatis, *Neurochemical development of the degenerating rat retina.* J Comp Neurol, 1997. **388**(1): p. 1-22.
373. Fletcher, E.L., *Alterations in neurochemistry during retinal degeneration.* Microsc Res Tech, 2000. **50**(2): p. 89-102.
374. McHenry, C.L., et al., *MERTK arginine-844-cysteine in a patient with severe rod-cone dystrophy: loss of mutant protein function in transfected cells.* Invest Ophthalmol Vis Sci, 2004. **45**(5): p. 1456-63.
375. McHenry, C.L., *MERTK R844C Mutant Shows Reduced Phosphorylation Activity in Transfected Cells and is Associated with Severe Rod-Cone Dystrophy.* ARVO abstract, 2003: p. 3566/B269.
376. Ling, L., D. Templeton, and H.J. Kung, *Identification of the major autophosphorylation sites of Nyk/Mer, an NCAM-related receptor tyrosine kinase.* J Biol Chem, 1996. **271**(31): p. 18355-62.
377. Sandberg, M.A., et al., *The relationship between visual field size and electroretinogram amplitude in retinitis pigmentosa.* Invest Ophthalmol Vis Sci, 1996. **37**(8): p. 1693-8.
378. Cohen, S. and A. Kawasaki, *Introduction to formal visual field testing: Goldmann and Humphrey perimetry.* J Ophthalmic Nurs Technol, 1999. **18**(1): p. 7-11; quiz 35-6.

379. Holder, G.E., et al., *Pattern ERG: clinical overview, and some observations on associated fundus autofluorescence imaging in inherited maculopathy.* Doc Ophthalmol, 2003. **106**(1): p. 17-23.
380. Palmowski, A.M., *Multifocal stimulation techniques in ophthalmology -- Current knowledge and perspectives.* Strabismus, 2003. **11**(4): p. 229-37.
381. Hedges, T.R., 3rd and M.L. Quireza, *Multifocal visual evoked potential, multifocal electroretinography, and optical coherence tomography in the diagnosis of subclinical loss of vision.* Ophthalmol Clin North Am, 2004. **17**(1): p. 89-105.
382. Melamed, S. and H. Levkovitch-Verbin, *Laser scanning tomography and angiography of the optic nerve head for the diagnosis and follow-up of glaucoma.* Curr Opin Ophthalmol, 1997. **8**(2): p. 7-12.
383. von Ruckmann, A., F.W. Fitzke, and A.C. Bird, *Distribution of pigment epithelium autofluorescence in retinal disease state recorded in vivo and its change over time.* Graefes Arch Clin Exp Ophthalmol, 1999. **237**(1): p. 1-9.
384. von Ruckmann, A., F.W. Fitzke, and A.C. Bird, *Distribution of fundus autofluorescence with a scanning laser ophthalmoscope.* Br J Ophthalmol, 1995. **79**(5): p. 407-12.
385. Sharp, P.F., et al., *The scanning laser ophthalmoscope--a review of its role in bioscience and medicine.* Phys Med Biol, 2004. **49**(7): p. 1085-96.
386. Delori, F.C., et al., *In vivo fluorescence of the ocular fundus exhibits retinal pigment epithelium lipofuscin characteristics.* Invest Ophthalmol Vis Sci, 1995. **36**(3): p. 718-29.
387. Pagon, R.A., *Retinitis pigmentosa.* Surv Ophthalmol, 1988. **33**(3): p. 137-77.
388. Bok, D., G.S. Hageman, and R.H. Steinberg, *Repair and replacement to restore sight. Report from the Panel on Photoreceptor/Retinal Pigment Epithelium.* Arch Ophthalmol, 1993. **111**(4): p. 463-71.
389. Lin, N., et al., *Basic fibroblast growth factor treatment delays age-related photoreceptor degeneration in Fischer 344 rats.* Exp Eye Res, 1997. **64**(2): p. 239-48.
390. Li, L.X. and J.E. Turner, *Transplantation of retinal pigment epithelial cells to immature and adult rat hosts: short- and long-term survival characteristics.* Exp Eye Res, 1988. **47**(5): p. 771-85.
391. Robson, A.G., et al., *Comparison of fundus autofluorescence with photopic and scotopic fine-matrix mapping in patients with retinitis pigmentosa and normal visual acuity.* Invest Ophthalmol Vis Sci, 2004. **45**(11): p. 4119-25.
392. Holbrook, J.A., et al., *Nonsense-mediated decay approaches the clinic.* Nat Genet, 2004. **36**(8): p. 801-8.
393. Wilkinson, M.F., *A new function for nonsense-mediated mRNA-decay factors.* Trends Genet, 2005. **21**(3): p. 143-8.
394. Smith, A.J., et al., *AAV-Mediated gene transfer slows photoreceptor loss in the RCS rat model of retinitis pigmentosa.* Mol Ther, 2003. **8**(2): p. 188-95.
395. Tschernutter, M., et al., *Long-term preservation of retinal function in the RCS rat model of retinitis pigmentosa following lentivirus-mediated gene therapy.* Gene Ther, 2005. **12**(8): p. 694-701.
396. Chirmule, N., et al., *Immune responses to adenovirus and adeno-associated virus in humans.* Gene Ther, 1999. **6**(9): p. 1574-83.
397. Moskalenko, M., et al., *Epitope mapping of human anti-adeno-associated virus type 2 neutralizing antibodies: implications for gene therapy and virus structure.* J Virol, 2000. **74**(4): p. 1761-6.
398. Halbert, C.L., et al., *Transduction by adeno-associated virus vectors in the rabbit airway: efficiency, persistence, and readministration.* J Virol, 1997. **71**(8): p. 5932-41.
399. Lo, W.D., et al., *Adeno-associated virus-mediated gene transfer to the brain: duration and modulation of expression.* Hum Gene Ther, 1999. **10**(2): p. 201-13.
400. Anand, V., et al., *A deviant immune response to viral proteins and transgene product is generated on subretinal administration of adenovirus and adeno-associated virus.* Mol Ther, 2002. **5**(2): p. 125-32.
401. Bushman, F.D., *Integration site selection by lentiviruses: biology and possible control.* Curr Top Microbiol Immunol, 2002. **261**: p. 165-77.

402. Holman, A.G. and J.M. Coffin, *Symmetrical base preferences surrounding HIV-1, avian sarcoma/leukosis virus, and murine leukemia virus integration sites.* Proc Natl Acad Sci U S A, 2005. **102**(17): p. 6103-7.
403. Crise, B., et al., *Simian immunodeficiency virus integration preference is similar to that of human immunodeficiency virus type 1.* J Virol, 2005. **79**(19): p. 12199-204.
404. Maxfield, L.F., C.D. Fraize, and J.M. Coffin, *Relationship between retroviral DNA-integration-site selection and host cell transcription.* Proc Natl Acad Sci U S A, 2005. **102**(5): p. 1436-41.
405. Jacobson, S.G., et al., *Identifying photoreceptors in blind eyes caused by RPE65 mutations: Prerequisite for human gene therapy success.* Proc Natl Acad Sci U S A, 2005. **102**(17): p. 6177-82.
406. Reiser, J., *Production and concentration of pseudotyped HIV-1-based gene transfer vectors.* Gene Ther, 2000. **7**(11): p. 910-3.
407. Tenenbaum, L., E. Lehtonen, and P.E. Monahan, *Evaluation of risks related to the use of adeno-associated virus-based vectors.* Curr Gene Ther, 2003. **3**(6): p. 545-65.
408. Arruda, V.R., et al., *Lack of germline transmission of vector sequences following systemic administration of recombinant AAV-2 vector in males.* Mol Ther, 2001. **4**(6): p. 586-92.
409. Couto, L., A. Parker, and J.W. Gordon, *Direct exposure of mouse spermatozoa to very high concentrations of a serotype-2 adeno-associated virus gene therapy vector fails to lead to germ cell transduction.* Hum Gene Ther, 2004. **15**(3): p. 287-91.
410. Provost, N., et al., *Biodistribution of rAAV vectors following intraocular administration: evidence for the presence and persistence of vector DNA in the optic nerve and in the brain.* Mol Ther, 2005. **11**(2): p. 275-83.
411. Soriano, P., et al., *Tissue-specific and ectopic expression of genes introduced into transgenic mice by retroviruses.* Science, 1986. **234**(4782): p. 1409-13.
412. Powell, S.K., et al., *Breeding of retroviruses by DNA shuffling for improved stability and processing yields.* Nat Biotechnol, 2000. **18**(12): p. 1279-82.
413. Lois, C., et al., *Germline transmission and tissue-specific expression of transgenes delivered by lentiviral vectors.* Science, 2002. **295**(5556): p. 868-72.
414. Chan, A.W., et al., *Transgenic monkeys produced by retroviral gene transfer into mature oocytes.* Science, 2001. **291**(5502): p. 309-12.
415. Le Meur, G., et al., *Postsurgical assessment and long-term safety of recombinant adeno-associated virus-mediated gene transfer into the retinas of dogs and primates.* Arch Ophthalmol, 2005. **123**(4): p. 500-6.
416. Reichel, M.B., et al., *An immune response after intraocular administration of an adenoviral vector containing a beta galactosidase reporter gene slows retinal degeneration in the rd mouse.* Br J Ophthalmol, 2001. **85**(3): p. 341-4.
417. Xiao, W., et al., *Gene therapy vectors based on adeno-associated virus type 1.* J Virol, 1999. **73**(5): p. 3994-4003.
418. Ritter, T., et al., *Stimulatory and inhibitory action of cytokines on the regulation of hCMV-IE promoter activity in human endothelial cells.* Cytokine, 2000. **12**(8): p. 1163-70.
419. Harms, J.S. and G.A. Splitter, *Interferon-gamma inhibits transgene expression driven by SV40 or CMV promoters but augments expression driven by the mammalian MHC I promoter.* Hum Gene Ther, 1995. **6**(10): p. 1291-7.
420. Vigna, E., et al., *Efficient Tet-dependent expression of human factor IX in vivo by a new self-regulating lentiviral vector.* Mol Ther, 2005. **11**(5): p. 763-75.
421. Auricchio, A., et al., *Pharmacological regulation of protein expression from adeno-associated viral vectors in the eye.* Mol Ther, 2002. **6**(2): p. 238-42.
422. Lebherz, C., et al., *Long-term inducible gene expression in the eye via adeno-associated virus gene transfer in nonhuman primates.* Hum Gene Ther, 2005. **16**(2): p. 178-86.

Abbreviations

aa	amino acid
AAV	adeno-associated virus
AB	antibody
ABCA4, ABCR	ATP-binding cassette transporter
Ad	adenovirus
ADA	adenosine deaminase
ADP	adenosine-5'-diphosphate
AMD	age related macular degeneration
AMP	adenosine-5'-monophosphate
APC	antigen-presenting cell
ATP	adenosine-5'-triphosphate
β-PDE	β subunit of the rod cGMP phosphodiesterase
BHK cells	baby hamster kidney cells
BIV	bovine immunodeficiency virus
bp	base pair
cAMP	cyclic AMP
cDNA	complementary DNA
CFH	complement factor H
cGMP	cyclic GMP
CMV	cytomegalovirus
CMZ	ciliary margin zone
CNS	central nervous system
CNTF	ciliary neurotrophic factor
CNV	choroidal neovascularisation
CORD	cone–rod dystrophy
cPPT	central polypurine tract element
CRALBP	cellular retinaldehyde binding protein
CRBP	cellular retinol-binding protein
DNA	deoxyribo-nucleic acid
EIAV	equine infectious anemia virus
ELM	external limiting membrane
ERG	electroretinography
ES	embryonic stem cell
FGF	fibroblast growth factor
FIV	feline immunodeficiency virus
Gas6	Growth arrest specific factor 6
GC	ganglion cell layer
GDNF	glia cell line derived neurotrophic factors
GDP	guanosine- 5'-diphosphate
GFP	green fluorescent protein
GLUT	glucose transporter
GMP	guanosine 5'-monophosphate

GTP	guanosine-5'-triphosphate
HIV	human immunodeficiency virus
HMG1	high mobility group 1
hr	hour
HSV	herpesvirus
IGF-1	insulin-like growth factor 1
IL	interleukin
ILM	internal limiting membrane
INL	inner nuclear layer
$InsP_3$	inositol-triphosphate
IPL	inner plexiform layer
IPM	interphotoreceptor matrix
IRBP	interphotoreceptor retinoid-binding protein
IS	inner segments
ITR	inverted terminal repeats
iu	infectouse units
kb	kilobases
kDa	kilodalton
l	litre
lacZ	E. coli lactose operon gene Z = β-galactosidase
LCA	Leber's congenital amaurosis
LRAT	lecithin-retinol acyltransferase
LTR	long terminal repeat
μ-	micro-
m	metre
m-	milli-
MAP	mitogen-activated protein
MD	macular degeneration
Mertk	mer-receptor tyrosine kinase
min	minute
MiTF	micropthalmia transcription factor
MLV	molony murine leukemia virus
MOI	multiplicity of infection
mRNA	messenger ribonucleic acid
MV	microvilli
myo	myosin
n-	nano-
NAD^+, NADH	oxidized and reduced nicotinamide–adenine dinucleotide
$NADP^+$, NADPH	oxidized and reduced nicotinamide–adenine dinucleotide phosphate
NF	nerve fibre layer
nt	nucleotide
ONL	outer nuclear layer
OP	oscillatory potential
OPL	outer plexiform layer
ORF	open reading frame

OS	outer segments
P	postnatal day
Pax	paired-box transcription factors
PCR	polymerase chain reaction
PDE	phosphodiesterase
PEDF	pigment epithelium derived factor
PEG	polyethylene glycol
Ph	phagosome
pi	post injection
PS	phosphatidylserine
rAAV	recombinant AAV
RBP	retinol binding protein
RCS rat	Royal College of Surgeon rat
rd	retinal degeneration
RDH	retinal dehydrogenase
rds	retinal degeneration slow
RNA	ribonucleic acid
RNAi	RNA interference
RP	Retinitis pigmentosa
RPE	retinal pigment epithelium
RPGR	retinitis pigmentosa GTPase regulator
RPGRIP	RPGR-interacting protein
RT	reverse transcription
SCID	Severe combined immune deficiency
SFD	Sorsby's fundus dystrophy
SFFV	spleen focus forming virus
SIN	self inactivating vector
siRNA	small interfering RNA
SIV	semian immunodeficiency virus
SRBP	serum retinol-binding protein
TGF	transforming growth factor
TIMP3	tissue inhibitor of metalloproteinase 3
TNF	tumor necrosis factor
U	unit
USH1	Usher syndrome type 1
V	volt
VEGF	vascular endothelial growth factor
VSV-G	vesicular stomatitis virus G-protein
WPRE	Woodchuck hepatitis virus post-transcriptional element
w/v	weight/volume percent or mass/volume percent

Publications arising from this project

AAV-mediated gene transfer slows photoreceptor loss in the RCS rat model of retinitis pigmentosa. Smith AJ, Schlichtenbrede FC, Tschernutter M, Bainbridge JW, Thrasher AJ, Ali RR. *Mol Ther. 2003 Aug;8(2):188-95.*

Long-term preservation of retinal function in the RCS rat model of retinitis pigmentosa following lentivirus-mediated gene therapy. Tschernutter M, Frank C. Schlichtenbrede FC, Howe S, Bainbridge JW, Thrasher AJ, Smith AJ, Ali RR. *Gene Ther. 2005 Jan 20.*

Stable and efficient intraocular gene transfer using pseudotyped EIAV lentiviral vectors. Balaggan KS, Binley K, Esapa M, Iqball S, Askham Z, Kan O, Tschernutter M, Bainbridge JW, Naylor S, Ali RR. *J Gene Med. 2006 Mar;8(3):275-85.*

Clinical characterisation of a family with retinal dystrophy due to a mutation in the *Mertk* gene. Tschernutter M, Jenkins SA, Waseem NH, Saihan Z, Holder GE, Bird AC, Bhattacharya SS, Ali RR, Webster AR. *Br J Ophthalmol 2006:1-6*

Appendix

Murine *MERTK* mRNA sequence (NM_ 008587)

```
   1 tggatacgtg catctgtccg gagagaactg ccagatccgc ggccccgcga tggttctggc
  61 cccactgcta ctggggctgc tgctgctacc cgcgctctgg agtggaggca ctgccgagaa
 121 gtgggaagag accgagctag atcagctatt ttcagggcct ttaccaggga gactcccagt
 181 caaccacagg ccattctctg ctcctcactc cagccgggac cagctgccac caccccagac
 241 tggaagatca catccagcac acacagccgc tccccaggtg acctccacag catcaaagct
 301 cctacctcct gttgcgttta atcacaccat tggacacata gtactgtcgg aacataaaaa
 361 tgtcaaattt aattgctcca tcaatattcc taacacatac caagaaacag ctggcatttc
 421 atggtggaaa gatggaaagg aattgctcgg ggcacatcat tcaatcacac agttttatcc
 481 tgatgaggaa ggggtatcaa taattgcatt gttcagcata gccagtgtgc agcgctcaga
 541 caatgggtcg tacttctgta agatgaaggt gaacaataga gagattgtat ctgatcccat
 601 atacgtggaa gttcaaggac tcccttactt tattaagcag cctgagagtg tgaatgtcac
 661 cagaaacaca gccttcaacc tcacctgcca ggccgtgggc cctcctgagc ccgtcaatat
 721 cttctgggtt caaaatagca gccgtgttaa tgaaaaaccg gaaaggtccc cgtctgtcct
 781 aaccgtacct ggtctgacag agacagcagt cttcagctgt gaggcccaca atgacaaagg
 841 actgacggtg tccaagggtg tacatatcaa catcaaagta atcccctccc cgcccactga
 901 agtccatatc ctcaacagta cagcacacag catcctggtc tcctgggtcc ctggttttga
 961 tggctactcc ccacttcaga actgcagcat tcaggtcaag gaagctgacc ggctgagtaa
1021 tggctcagtc atggttttta atacctctgc ttcgccacat ctgtatgaga tccagcagct
1081 gcaagccctg gctaattaca gcatcgctgt gtcctgtcgg aatgagattg gctggtctgc
1141 agtaagccct tggattctgg ccagcacaac agaaggagct ccatctgtag caccttttaaa
1201 catcactgtg tttctgaacg aatctaacaa tatcctggat attagatgga cgaagcctcc
1261 aattaagcgg caggatgggg aactggtggg ctaccggata tctcacgtgt gggaaagcgc
1321 agggacttac aaagagcttt ctgaagaagt cagccagaat ggcagctggg ctcagattcc
1381 tgtccaaatc cacaatgcca cctgcacagt gagaatcgcg gccattacta aaggggcat
1441 cgggcccttc agtgagccag tgaatatcat cattcctgaa cacagtaagg tagattacgc
1501 accctcgtca accccagccc ctggcaacac cgactctatg ttcatcatcc tcggctgctt
1561 ctgtggattc attttaatcg ggttaatttt gtgtatttct ctggccctca gaaggagagt
1621 ccaggaaaca aagtttgggg gagcattctc tgaggaggat tcccaactgg tcgtaaatta
1681 tagagcgaag aagtccttct gccggcgagc catcgagctt accttgcaga gcctgggagt
1741 gagcgaggag ctgcagaata agctggaaga tgttgtgatt gacagaaacc ttctggttct
1801 cggcaaagtt ctgggtgaag gagagtttgg gtctgtaatg gaaggaaatt tgaagcaaga
1861 agatgggact tctcagaagg tggcagtgaa gaccatgaag ttggacaact tttctcaacg
1921 ggagatcgag gagtttctca gcgaagcagc atgcatgaaa gacttcaacc acccaaatgt
1981 catccgactt ctaggcgtgt gtatagaact gagctctcaa ggcatcccga agcccatggt
2041 gattttaccc ttcatgaaat acggagacct ccacaccttc ctgttatatt cccgattaaa
2101 cacaggaccc aagtacattc acctgcagac actactgaag ttcatgatgg acattgccca
2161 gggaatggag tatctgagca acaggaattt tcttcatagg gatttggcag ctcgaaactg
2221 catgttgcgg gatgacatga ctgtctgcgt ggcagacttt ggcctctcaa agaagattta
2281 cagtggtgat tattaccgcc aaggccgcat tgccaaaatg cctgtgaagt ggatcgccat
2341 cgagagcctg gcggaccgag tctacacaag caaaagtgac gtgtgggctt ttggcgtgac
2401 catgtgggaa ataacaacac ggggaatgac tccctatccc ggagttcaga accatgagat
2461 gtacgactac cttctccacg gccacaggct gaagcagcct gaggactgct tggatgaact
2521 gtatgacatc atgtactctt gctggagtgc tgatcccttg gatcgaccca ccttctctgt
2581 gttgaggctg cagctggaaa agctctccga gagtttgcct gatgcgcagg acaaagaatc
2641 catcatctac atcaataccc agttgctaga gagctgcgag ggcatagcca atgggccctc
2701 actcacgggg ctagacatga acattgaccc tgactccatc attgcctctt gcacaccagg
2761 cgctgccgtc agcgtggtca cggcagaagt tcacgagaac aaccttcgtg aggaaagata
2821 catcttgaat gggggcaatg aggaatggga agatgtgtcc tccactcctt ttgctgcagt
2881 cacacctgaa aaggatggtg tcttaccgga ggacagactc accaaaaatg gcgtctcctg
2941 gtctcaccat agtacactac ccttggggag cccatcacca gatgaacttt tatttgtaga
3001 tgactccttg gaagactctg aagttctgat gtgaagccag ctgagaggag gcatgagaga
3061 accaagcaaa tacagcttcc tgggatctgg tggtcttaga tactttgtta ttgctctgat
3121 aaaacatcat gaccaaggca atcttcaaga gaaagtgttt aactaggttt actgtttcag
3181 ggggttagag tctatgattg cagaaggaag ttatgatggc aggaacagct gagtgcttat
3241 atctttaaga gcaagcagga gacagagagc actctgggaa atggcaccta tcttttgaaa
3301 cctcaaagcc tgctcccagt gacaaaagtc cttcaacagg ccatacctcc taatccttcc
3361 caaacaattc caccaactgg agaccaaaca ttcaaatgta tgcgcgtatt ggggccattc
3421 ttaagcaaac cactacactg gttatacctg aggttttggt acttgttttc cttaccaagt
3481 agagttcatg gccggacagc accaggtgaa agctgtcaag tcaggtttgc aaatacataa
3541 ccaaggtctt gagagctcgt gccg
```

MERTK amino acid sequence alignment (Biology WorkBench)

BWB1040 human
BWB1104 mouse
BWB1148 rat

* - single, fully conserved residue
: - conservation of strong groups
. - conservation of weak groups
 - no consensus

```
BWB1148         MVLAPLLLGL-LLLSALWNGGTAEKEEEIKPDQPFSGPLPGSLPADHRPFF-APHSSGDQ
BWB1104         MVLAPLLLGL-LLLPALWSGGTAEKWEETELDQLFSGPLPGRLPVNHRPFS-APHSSRDQ
BWB1040         MGPAPLPLLLGLFLPALWRRAITEAREEAKPYPLFPGPFPGSLQTDHTPLLSLPHASGYQ
                *  *** * * *:*.***  . :*  ** :    *.**:** * .:* *:   **:*  *

BWB1148         ----LSPSQTGRSHPAHTATPQMTSAASNLLPPVAFKNTIGRIVLSEHKSVKFNCSINIP
BWB1104         ----LPPPQTGRSHPAHTAAPQVTSTASKLLPPVAFNHTIGHIVLSEHKNVKFNCSINIP
BWB1040         PALMFSPTQPGRPHTGNVAIPQVTSVESKPLPPLAFKHTVGHIILSEHKGVKFNCSISVP
                    :.*.*.**.*..:.* **:**. *: ***:**::*:*:*:*****.*******.:*

BWB1148         NVYQETAGISWWKDGKELLGAHHSITQFYPDEEGVSIIALFSITSVQRSDNGSYICKMKV
BWB1104         NTYQETAGISWWKDGKELLGAHHSITQFYPDEEGVSIIALFSIASVQRSDNGSYFCKMKV
BWB1040         NIYQDTT-ISWWKDGKELLGAHHAITQFYPDDEVTAIIASFSITSVQRSDNGSYICKMKI
                * **:*: ***************:*******:* .:*** ***:**********:****:

BWB1148         NDREVVSDPIYVEVQGLPYFTKQPESVNVTRNTAFNLTCQAVGPPEPVNIFWVQNSSRVN
BWB1104         NNREIVSDPIYVEVQGLPYFIKQPESVNVTRNTAFNLTCQAVGPPEPVNIFWVQNSSRVN
BWB1040         NNEEIVSDPIYIEVQGLPHFTKQPESMNVTRNTAFNLTCQAVGPPEPVNIFWVQNSSRVN
                *:.*:******:******:* ******:**********************************

BWB1148         ENPERSPSVLTVAGLTETAVFSCEAHNDKGLTVSKGVQINIKVIPSPPTEVHILNSTAHS
BWB1104         EKPERSPSVLTVPGLTETAVFSCEAHNDKGLTVSKGVHINIKVIPSPPTEVHILNSTAHS
BWB1040         EQPEKSPSVLTVPGLTEMAVFSCEAHNDKGLTVSKGVQINIKAIPSPPTEVSIRNSTAHS
                *:**:********.**** ********************:****.******** * ******

BWB1148         ILVSWVPGFDGYSPLQNCSIQVKEADQLSNGSVMVFNTSASPHLYEVQQLQALANYSVTV
BWB1104         ILVSWVPGFDGYSPLQNCSIQVKEADRLSNGSVMVFNTSASPHLYEIQQLQALANYSIAV
BWB1040         ILISWVPGFDGYSPFRNCSIQVKEADPLSNGSVMIFNTSALPHLYQIKQLQALANYSIGV
                **:************::********** ******:***** ****:::*********: *

BWB1148         SCRNEIGWSAVSPWILASTTEGAPAVAPLNITVFLNESSNNLEIRWTKPPIKRQDGELVG
BWB1104         SCRNEIGWSAVSPWILASTTEGAPSVAPLNITVFLNESNNILDIRWTKPPIKRQDGELVG
BWB1040         SCMNEIGWSAVSPWILASTTEGAPSVAPLNVTVFLNESSDNVDIRWMKPPTKQQDGELVG
                ** ********************:*****:*******.: ::*** *** *:*******

BWB1148         YRISHVWESAGTSKELSEEVSQNGSWAQVPVQMHNATCTVRIAVITKGGIGPFSEPVDVA
BWB1104         YRISHVWESAGTYKELSEEVSQNGSWAQIPVQIHNATCTVRIAAITKGGIGPFSEPVNII
BWB1040         YRISHVWQSAGISKELLEEVGQNGSRARISVQVHNATCTVRIAAVTRGGVGPFSDPVKIF
                *******:***  *** ***.**** *::.**:**********.:*:**:****:**.:

BWB1148         IPEHSRVDYAPSSTPAPGNTESMLIILGCFCGFVLMGLILYLSLAIKRRVQETKFGGAFS
BWB1104         IPEHSKVDYAPSSTPAPGNTDSMFIILGCFCGFILIGLILCISLALRRRVQETKFGGAFS
BWB1040         IPAHGWVDYAPSSTPAPGNADPVLIIFGCFCGFILIGLILYISLAIRKRVQETKFGNAFT
                ** *. ************:::.::**:******:*:**** :***:::********.**:

BWB1148         EEDSQLVVNYRAKKSFCRRAIELTLQSLGVSEELQNKLEDVVVDRNLLILGKVLGEGEFG
BWB1104         EEDSQLVVNYRAKKSFCRRAIELTLQSLGVSEELQNKLEDVVIDRNLLVLGKVLGEGEFG
BWB1040         EEDSELVVNYIAKKSFCRRAIELTLHSLGVSEELQNKLEDVVIDRNLLILGKILGEGEFG
                ****:***** **************:****************:*****:***:********
```

```
BWB1148         SVMEGNLKQEDGTSQKVAVKTMKLDNFSLREIEEFLSEAACMKDFNHPNVIRLLGVCIEL
BWB1104         SVMEGNLKQEDGTSQKVAVKTMKLDNFSQREIEEFLSEAACMKDFNHPNVIRLLGVCIEL
BWB1040         SVMEGNLKQEDGTSLKVAVKTMKLDNSSQREIEEFLSEAACMKDFSHPNVIRLLGVCIEM
                ********************** *********** * ***************.*************:

BWB1148         SSQGIPKPMVILPFMKYGDLHTFLLYSRIESVPKSIPLQTLLKFMVDIAQGMEYLSSRNF
BWB1104         SSQGIPKPMVILPFMKYGDLHTFLLYSRLNTGPKYIHLQTLLKFMMDIAQGMEYLSNRNF
BWB1040         SSQGIPKPMVILPFMKYGDLHTYLLYSRLETGPKHIPLQTLLKFMVDIALGMEYLSNRNF
                ************************:******::: ** * ********:*** ******.***

BWB1148         LHRDLAARNCMLRDDMTVCVADFGLSKKIYSGDYYRQGRIAKMPVKWIAIESLADRVYTS
BWB1104         LHRDLAARNCMLRDDMTVCVADFGLSKKIYSGDYYRQGRIAKMPVKWIAIESLADRVYTS
BWB1040         LHRDLAARNCMLRDDMTVCVADFGLSKKIYSGDYYRQGRIAKMPVKWIAIESLADRVYTS
                ************************************************************

BWB1148         KSDVWAFGVTMWEIATRGMTPYPGVQNHEMYDYLLHGHRLKQPEDCLDDLYEIMYSCWSA
BWB1104         KSDVWAFGVTMWEITTRGMTPYPGVQNHEMYDYLLHGHRLKQPEDCLDELYDIMYSCWSA
BWB1040         KSDVWAFGVTMWEIATRGMTPYPGVQNHEMYDYLLHGHRLKQPEDCLDELYEIMYSCWRT
                **************:************************************:**:****** :

BWB1148         DPLDRPTFSVLRLQLEKLSESLPDAQDKESIIYINTQLLESCEGLANRSSLAGLDMNIDP
BWB1104         DPLDRPTFSVLRLQLEKLSESLPDAQDKESIIYINTQLLESCEGIANGPSLTGLDMNIDP
BWB1040         DPLDRPTFSVLRLQLEKLLESLPDVRNQADVIYVNTQLLESSEGLAQGSTLAPLDLNIDP
                ****************** *****.::: .:**:*******.**:*: .:*: **:*****

BWB1148         DSIIASCTAGAAVSVVMAEVHENNLHEERYILNGGNEEWEDVASTPFATVTAGKDGVLPE
BWB1104         DSIIASCTPGAAVSVVTAEVHENNLREERYILNGGNEEWEDVSSTPFAAVTPEKDGVLPE
BWB1040         DSIIASCTPRAAISVVTAEVHDSKPHEGRYILNGGSEEWEDLTSAPSAAVTAEKNSVLPG
                ********. **:*** ****:.: :* *******.******::*:* *:**. *:.***

BWB1148         DRLTKNGISWSHHSTLPLGSPSPDELLFADDSSGDSEVLM
BWB1104         DRLTKNGVSWSHHSTLPLGSPSPDELLFVDDSLEDSEVLM
BWB1040         ERLVRNGVSWSHSSMLPLGSSLPDELLFADDSSEGSEVLM
                :**.:**:**** * *****. ******.***  .*****
```

Human *MERTK* exon 1-19 nucleotide sequence

AF260514-AF260529, AF3666903

Coding sequences: bold
Primer binding site: underlined

Exon 1 (<142..202)

```
1   cttggctccg ccactcggca ctcactgccc gggccgcccg gacagggagc ttcgctggcg
61  cgcttggccg gcgacaggac aggttcggga cgtccatctg tccatccgtc cggagagaaa
121 ttacagatcc gcagccccgg gatggggccg gccccgctgc cgctgctgct gggcctcttc
181 ctccccgcgc tctggcgtag aggtgagtgc gcccggctgg gggccaggcg agggggtggg
241 ggctcccagg aggaagcagg ggcctctggg gagggagcgc gtccacaggg gcgcgcctgg
301 ctgctggaca agtttgcaaa caccctccac ccactgcggt gccagaggag ggggcgtagg
361 cgaacctacc
```

Exon 2 (179..599)

```
1   acgaatgaac tggtgaataa gaatatgtcc agatgtgtgt gttaatgaat tctgcttatc
61  ttttcctggg gcacagagga caccccagtg ctctctcttc ttggcctaag aagttgggaa
121 cctacttggg aaactcttct tatttaaaag gctaaaattt ggatgttttt ttttacagct
181 atcactgagg caagggaaga agccaagcct tacccgctat tcccgggacc ttttccaggg
241 agcctgcaaa ctgaccacac accgctgtta tcccttcctc acgccagtgg gtaccagcct
301 gccttgatgt tttcaccaac ccagcctgga agaccacata caggaaacgt agccattccc
361 caggtgacct ctgtcgaatc aaagccccta ccgcctcttg ccttcaaaca cacagttgga
421 cacataatac tttctgaaca taaaggtgtc aaatttaatt gctcaatcag tgtacctaat
481 atataccagg acaccacaat ttcttggtgg aaagatggga aggaattgct tggggcacat
541 catgcaatta cacagtttta tccagatgat gaagttacag caataatcgc ttccttcagg
601 tatgtgttct ttcttccttt tttatttttt tagttttaat atttatttat ttatttactt
661 attgagacag agtatcattc tgtagcccag
```

Exon 3 (183..283)

```
1   gtaccttcac agcaacatct aggctagggt ttgaccaaac aactgcgtac aatggcctag
61  ccaagctgac atataaaatt aactatcaca gcatatgaca aagaagttga agaagtttcc
121 atcctataat aggaactcaa agggtagtca ctgtaaatat cttcatgtgt ttttctttgc
181 agcataacca gtgtgcagcg ttcagacaat gggtcgtata tctgtaagat gaaaataaac
241 aatgaagaga tcgtgtctga tcccatctac atcgaagtac aaggtaagtc cacagaccag
301 agtcccattg ccagagaact gtttgtttta gggcctgtgt taaatgtttt gtgtataata
361 ctctagagtt ttgcctgcct atttataact ctgtatgcaa accttgcaaa tctatcagca
421 ctgaaatttt acaaggtact ccactttgta gtctataagt aataatgaaa tgaattcaat
481 tcctgaagtt tgagctctat tataggcatt acaggtgaga taaaaagaga ttttggactt
541 ccttgtccac agattattga c
```

Exon 4 (96..269)

```
1   ctattgccaa gttctagtcc agtttccatt ccccttttggg ctctgtctct gttttcagat
61  ctgaaacatt cttttgtgta acgttttctc cgcaggactt cctcacttta ctaagcagcc
121 tgagagcatg aatgtcacca gaaacacagc cttcaacctc acctgtcagg ctgtgggccc
181 gcctgagccc gtcaacattt tctgggttca aaacagtagc cgtgttaacg aacagcctga
241 aaaatccccc tccgtgctaa ctgttccagg taagtccgag ctgtgggctt attgatttat
301 tctctaatag cggacaggat caaaagtttg gcgacccttg ctgtgcacca ctagcaggca
361 gtggagacag atgaaaatac aggtgtggca gcaaagttat gggaccaggt agac
```

Exon 5 (180..266)

```
1   ccttgggttt aatcccaggt ttgtttctcc atagctagca cacctttaa attaactttg
61  cactaatgcc caaaagccat gaaccaagaa ataaaataat acaaagacaa ccatagaatt
121 gtagtgaaca gcagcctgtt tctctgctgc tggtctcatg agtctccttc cattccagag
181 cctgacggag atggcggtct tcagttgtga ggcccacaat gacaaagggc tgaccgtgtc
241 aaagggagtg cagatcaaca tcaaaggtaa gcagcaaggc taggctcccc atgcatgttc
301 tgggagctgg tgagggtaca gcatgagctt gcagctggct gcctgggtgt ggatcctggc
361 tttctcactg tctcaaggtt ctttgtgacc ttggacaact cacttctcct ctttggtgtc
421 agggttc
```

Exon 6 (71..186)

```
1   gtagctgtag cctgtcatct ataattgtgt ttgtgtgtgt atgtgtgtgt gtgtgttttg
61  ttttatgcag caattccctc cccaccaact gaagtcagca tccgtaacag cactgcacac
121 agcattctga tctcctgggt tcctggtttt gatggatact ccccgttcag gaattgcagc
181 attcaggtaa agttccaggg tgaagaggga agtagctgtt tggtgctctc tgtgggttta
241 aggatttttc ttccttccaa ggatgggcat ggagggcatt tctccatctc tgtacagagt
301 cccctgacct ccctgcttca gtgtccagca tgcatgcact attccatgtc catgc
```

Exon 7 (88..271)

```
1   ccacgtgcac cgaatgcaca caggccccgt gcctgacatt cccaccacct tactaatgcc
61  cggtcctcat gtttactctt cgtttaggtc aaggaagctg atccgctgag taatggctca
121 gtcatgattt ttaacacctc tgccttacca catctgtacc aaatcaagca gctgcaagcc
181 ctggctaatt acagcattgg tgtttcctgc atgaatgaaa taggctggtc tgcagtgagc
241 ccttggattc tagccagcac gactgaagga ggtaattcct ggggttcaga atgtatattg
301 cccccaatga catgtgattc aacaaaccct tcccagtggc ctgactgaga gttgaaactt
361 tgctttgttt ggactttgtc tctggaggag aaaattattg aggcgactga tgaaaatggg
421 aaagatattt cctccatact gtaaaagcat tcagtgacaa aacttagccg tgttatgtat
481 agg
```

Exon 8 (134..285)

```
1   gtgctataag tcttggtctc atttgagtgc ttttcataga gcatttgaaa accaaacact
61  tgaaaaccca gatgagaata catctgtgtg tgctttgtgg ttcttcattc ttctctcctt
121 ttttcttttg tagccccatc agtagcacct ttaaatgtca ctgtgtttct gaatgaatct
181 agtgataatg tggacatcag atggatgaag cctccgacta agcagcagga tggagaactg
241 gtgggctacc ggatatccca cgtgtggcag agtgcaggga tttccgtaag tctaaaccct
301 agaagagcac gattagtcat ctcctttcaa cttgctggtt tacttcagtt ttagaagctt
361 tcatttggtt ttgaaaagac ctggtgtgat tgagttaggc aaggcacc
```

Exon 9 (293..446)

```
1   gtgcatctgc tacgtgctcc ctctcttcca gaagcttctt taggaccact ctaagtgcca
61  tgccctcatg gccctagctt gccaatgccc cccaaaactt gatgttacat cctgtcccta
121 cctgactttt ggttccattg gccatggcct gagtgacaaa ggaatgctgt ggaagtgtgg
181 cttctggcct cggacgtggg cgggatggct tccctcagaa ggaactgtag atgcacctgc
241 agtttgccca gacctcagtg ttttcatttc ctctcttcct ctctgtctcc agaaaagagct
301 cttggaggaa gttggccaga atggcagccg agctcggatc tctgttcaag tccacaatgc
361 tacgtgcaca gtgaggattg cagccgtcac cagaggggga gttgggccct tcagtgatcc
421 agtgaaaata tttatccctg cacacggtga gagctatacc cagtaagggc tgataggatg
481 tgatggtcca ggcagtgcac agattgccag aaagt
```

Exon 10 (146..299)

```
1   tacacaaagt gagacctgcc tatatttgta gattataaaa gatttaactg agttctgaaa
61  gctttgacta tttgttcttc cctgttacaa gccagtgttt ctcatatatt tcaaacccat
121 gactggtcta ttggtatctc accaggttgg gtagattatg ccccctcttc aactccggcg
181 cctggcaacg cagatcctgt gctcatcatc tttggctgct tttgtggatt tattttgatt
241 gggttgattt tatacatctc cttggccatc agaaaaagag tccaggagac aaagtttggg
301 taagtctccc agctaaaaat gtttgcccac tggtattgac aaggttgtta taccaagtga
361 ttatgccttt cctgttgggc cagctgctta cattgctccc agatggctgc cctgccttat
421 gcataccctg ggctcaggca gcttcctgac ttacgccatg gtctacagaa gcagctgcca
481 gcaaaagcca ggcctgaaaa gggttccttt acagagaaga gtatcagtag gcctttgct
```

Exon 11(182..267)

```
1   caatattgcc aagtaagtct aaaataaatc aaaggaaaga aacacgtttc ttctaggggg
61  aaagcttttg ttgtagaaga gcccattgaa aagcggaagc tctgtagcat ccttgtggaa
121 tcagtgcctg ccccagtagc cctgttttta tagtgaagta tctttgtttt cattcaccca
181 ggaatgcatt cacagaggag gattctgaat tagtggtgaa ttatatagca aagaaatcct
241 tctgtcggcg agccattgaa cttacctgta agttgacttt catttccctt tttggcaaaa
301 gttaaaatag ttgagaacaa agaaggatca atagacagat ttctaacaaa agccaaagat
361 gtcgaagaag aatggatatt tttaatgtac aaaatgtctt taaaagcagc aagtagatag
421 ccag
```

Exon 12 (99..194) and 13 (911..991)

```
1    ggaatgtttt attatacagg actttatttc attttaatta tcaagtgaaa gaaaacacgc
61   tgacaatttt tgtacatact atgttactcc tttttcagta catagcttgg gagtcagtga
121  ggaactacaa aataaactag aagatgttgt gattgacagg aatcttctaa ttcttggaaa
181  aattctgggt gaaggtaagc aatttaaagt aattctttta aaatgtggga taagaaggta
241  gcagtttaga ataattcttt aacatatatt tattaaataa aatagcatct caggactctg
301  agttatacta tggatagtta tattttatta tttaaaatga tagactattg atttttgaaa
361  ctcagatctg gcacatgaaa agattctctt caatgcctag cacatacagg tccttgaaaa
421  atattaattt tctttcttca ttgaaaagca tgtaattcat tgagtagttt cctatgtact
481  ttaagtttat tcctctagtt cttaagttca ttgttcttgg caccttttcta attaggaaca
541  aaaatgaaaa tacgtattta acttgttaag ttgttcttag gatgaatgat aatggtatta
601  aaagtttgtg ctttaaaaac ttcaataata tttttcatgt tctcttctaa gtgtcttgga
661  ttggttataa tgcttaataa agtgatgagc aaaggtaggc ccaagccacc caagctcgtg
721  acaagcagga gactagagcg tggcgcatca ccctggtttg cgatgtgggt ggcctgggca
781  ggctctgcct ggctgcccgt gggtgagttg ctctcatacc acatgaaacc agcagctctg
841  gcactgtagc atttctgtgg tcagggaaga gtttgcacag tgtccataca ggtgttcttt
```

901 cacttcacag **gagagtttgg gtctgtaatg gaaggaaatc ttaagcagga agatgggacc**
961 **tctctgaaag tggcagtgaa gaccatgaag** tgtgagttat cagtgatgaa tcccattctt
1021 ctagggtggg cagttgcttc agtattgggt gctccatgag gccatatgtc acaatctcag
1081 ttcccagtgg gccagaaggc aatgtggaac a

Exon 14 (184..276)

1 ctgtttgccc ctctcttatc tcccctagcc ctactagccc ctgacaacca ctcatctgtt
61 tcctgtctct atactttcat ctcttcctga cctgggtttt agagaacaga actgctgttg
121 cccacccact ccccttaatt gagtaaatta tccatactta acctttttcta ttttctcctc
181 tag**tggacaa ctcttcacag cgggagatcg aggagtttct cagtgaggca gcgtgcatga**
241 **aagacttcag ccacccaaat gtcattcgac ttctag**gtac ttccgagaaa tgcaggagtg
301 ggtggccaag agggctctgc tgatctgctc tgtgccaaag gaaaaaatct ctggtgtaga
361 taagtttac

Exon 15 (144..262)

1 cagagtgtga gttaggcgct cttgattttt tcaaactgtt aacttggtaa cacacggctt
61 cagtttttcc agtggtccac gagggctttt ctggtcacag taacaaggac tctttgtaat
121 tgatgctgtg tttgtaattt cag**gtgtgtg tatagaaatg agctctcaag gcatcccaaa**
181 **gcccatggta attttaccct tcatgaaata cggggacctg catacttact tactttattc**
241 **ccgattggag acaggaccaa ag**gtaatgat ctccttgtgt taccctgaa cacttctcag
301 ggcttatgtg acttagccag gacaaccaaa tcatctaatc ttgaaagtga agccaggaag
361 gagaggacgt tgacttttgt tcagtgctcc ctgtgtg

Exon 16 (292..401)

1 ggatcacgtt tgacctcata ccttctaaaa agaaacaatg tcattcactg taaatacttt
61 taaagatggg gaaaagagaa tatgatgttt gccaagaagt ttaaggtttt tctcattcct
121 ttttaaaaac cttatttgtg atattagtga tagggaaata aaagatttgt ttccttattt
181 catcactaca ctgtaataaa ttaaagcatc ctaaaccccc cccggcagaa actgcttgca
241 agttttcctt tttaaaagat agtctttctt cttgtttcct ctatcatcta g**catattcct**
301 **ctgcagacac tattgaagtt catggtggat attgccctgg gaatggagta tctgagcaac**
361 **aggaattttc ttcatcgaga tttagctgct cgaaactgca t**gtaagagtc ctcggctatc
421 ctggaagggt ttggacctca tggtgtttgg tctttgcagg gttagtgaga ggacctgttc
481 ctgtttagat aggcaaggaa gctgcagtca gcgggggatg gtgtggcttg ctccgaagat
541 ggaaat

Exon 17 (159..318) and 18 (995..1131)

1 gctctgccat tggtcccaat gcagcatgct cacaggctgg tggtgtctct gtgttctttt
61 ggtcaattat cataagtgtt ttcacctgtg tctgatacag accagtaatt taaggcattg
121 cctctgacgc tgctgaagac gtaacctgct ctctgtag**gt tgcgagatga catgactgtc**
181 **tgtgttgcgg acttcggcct ctctaagaag atttacagtg gcgattatta ccgccaaggc**
241 **cgcattgcta agatgcctgt taaatggatc gccatagaaa gtcttgcaga ccgagtctac**
301 **acaagtaaaa gtgatgtg**gt atgtacacag ctttgattca ggggtcccac agcacaaaga
361 ggagggcata ttgaaagaaa tgacctcagc tggtatggca agacatttta ctctttgata
421 aactgagggt tggcagcttg ctcagatctc ttttatatct taccatcaga tactttaatt
481 caagtggaac agtagattct gatgaagtgt cctgacattc agaagatgtg tgctttgcaa
541 aagcccttaa tttcttccca tttttccttg ccgtcaaagg atgactcatt gcccacaact
601 aggatatttc atagtcacat taaattgaat gagttcatcc actggctctt ggaacctaga
661 tgctatatga aaggtgctgt gtaattacgc ccttgacccg agataaggaa aaaaaagcac

721 ctcacagcaa cagtggagga gagcactaag cagatgtgtg acgaggctgt ttctgccttt
781 gccagatttc ccagaacagc ttttgtagaa gtggggaact gtgacactcc aaccccacgt
841 tattgccgcg ttgggagagc agtgcgtctc acacataatt gccagctttg tgcatgatca
901 tcagtgttta aggaaatgac ctttcccagt gaaaaagtcc attcaggctt tgtggaaagg
961 cttgcatcct aacttgttgt tgctttgttc ccag**tgggca tttggcgtga ccatgtggga**
1021 **aatagctacg cggggaatga ctccctatcc tggggtccag aaccatgaga tgtatgacta**
1081 **tcttctccat ggccacaggt tgaagcagcc cgaagactgc ctggatgaac** tgtgagtggg
1141 cttctctgtc tcccttccat actctgcatg gggcagccac ctggctctgc actgacctcg
1201 gaaacacagc catgggaggg gaaagggact gctgttagcc angtgggcat gtgcagaggg
1261 gtggaaccca cagacacccc agcccaggag ccattcctga tgtgggagat agtgtgtggt
1321 atctccagtg ag

Exon 19 (234..>747)

1 actgccacat atgtgctctt cctagaaaca gaatcacttt tttgtcaaat accatggaac
61 atttacaaaa gttgtataaa tattaggcca ccaaaaaagt ctcaataatt tttataaaaa
121 gtagaatgaa tgctgattaa aatgtgataa agattctgta aaaacaaagg catggattgc
181 acaaagagat gggtgccatg ctgggagaca atccacttct ttttaacttt cag**gtatgaa**
241 **ataatgtact cttgctggag aaccgatccc ttagaccgcc ccacctttc agtattgagg**
301 **ctgcagctag aaaaactctt agaaagtttg cctgacgttc ggaaccaagc agacgttatt**
361 **tacgtcaata cacagttgct ggagagctct gagggcctgg cccagggctc caccttgct**
421 **ccactggact tgaacatcga ccctgactct ataattgcct cctgcactcc ccgcgctgcc**
481 **atcagtgtgg tcacagcaga agttcatgac agcaaacctc atgaaggacg gtacatcctg**
541 **aatgggggca gtgaggaatg ggaagatctg acttctgccc cctctgctgc agtcacagct**
601 **gaaaagaaca gtgttttacc gggggagaga cttgttagga atggggtctc ctggtcccat**
661 **tcgagcatgc tgcccttggg aagctcattg cccgatgaac ttttgtttgc tgacgactcc**
721 **tcagaaggct cagaagtcct gatgtga**gga gaggtgcggg gagacattcc aaaaatcaag
781 ccaattcttc tgctgtagga gaatccaatt gtacctgatg tttttggtat ttgtcttcct
841 taccaagtga actccatggc